

**Photochemistry of ( $\mu_2$ -alkyne)cobaltcarbonyl Complexes  
and their Role in the Pauson - Khand Reaction**



---

**DUBLIN CITY  
UNIVERSITY**

---

**Ollscoil Chathair Bhaile Átha Cliath**

**A Thesis presented for the degree of Doctor of Philosophy**

**by**

**Bronagh Myers B.Sc. (Hons.)**

**under the supervision of Dr. Conor Long**

**at**

**DUBLIN CITY UNIVERSITY  
School of Chemical Sciences**

**MAY 2000**

"The story of the prancing horse is simple and fascinating. The horse was painted on the fuselage of the fighter plane flown by Francesco Baracca, a heroic Italian pilot who died on Mount Montello: the Italian ace of aces of first World War.

In 1923, when I won the first Savio circuit, which was run in Ravenna, I met count Enrico Baracca, the pilot's father, and subsequently his mother, Countess Paolina.

One day she said to me, "Ferrari, why don't you put my son's prancing horse on your cars; it would bring you luck." I still have Baracca's photograph with the dedication by his parents, in which they entrusted the emblem to me. The horse was black and has remained so; I added the canary yellow background because it is the colour of Modena"

*Enzo Ferrari*

### ***Declaration***

I hereby certify that this material, which I now submit for assessment on the programme of study leading to the award of Ph.D. is entirely my own work and has not been taken from the work of others save to the extent that such work has been cited and acknowledged within the text of my own work.

Signed : Bronagh Myers

Date : 11/07/00.

**Bronagh Myers B.Sc.(Hons)**

## ***Dedication***

**To my Family**

## ***Acknowledgements***

First and foremost, I would like to thank my supervisor Dr. Conor Long for providing me with the opportunity for carrying out this research, for his advice, helpful discussions and support during my time at DCU. I also thank Dr. Sylvia Draper from Trinity College Dublin for her input into this work.

With sincere gratitude, I thank Dr. Mary Pryce for her guidance, help and useful discussions. I thank Dr. Siobhán O' Keeffe for all the training, advice and particularly for her friendship over the last few years.

I would like to thank the technical staff in particular the most obliging Mick Burke. I also had a lot of help from Veronica, Ambrose (an absolute star), Maurice, Damien and Vinny. I thank my project students Fiona, Peter and Wesley for all the work they have done, Paddy for the help with Hyperchem and Ben for everything - NMR, advice and friendship.

For the fellow members of the CLRG research group thanks to Davnat, Peter, Deirdre, Kevin K., Kieran and the new team Jennifer, Karl, and Kevin M. Keep up the good work. (Peter - we'll get the Nobel prize yet!) In the past thanks to the original AG07 gang including Ollie, Ben, Orla and Collette. Let me not forget AG12 (the girls and Luke - how things change!) Christy, Kierse (sure we'll have another one), Miriam, Karen, Frances, Anthea (ginger spice), Helen, Tia, Benedicte (rrrabbitte) and Eva. I thank more of the originals Joe, Theresa, Michaela, Nick, Tim, Johanne, Darren, Sven, Astrid and Dominic (where are you living next?). I would also like to thank Scott (for the lab dances - even if they were upside down), Adrian (fellow Grand Prix enthusiast), mad Marco (for introducing me to the best Lasange in the world and Ferarra) and Conor Hogan (for rasher Thursday - may it always stay

a tradition). Thanks guys for all the laughs, the friendship and the sessions . Thanks to Frank, Mike Sheehy, Jenny and Declan, Mairead, Colm, Carol and James Delaney.

From home thanks to Michelle and Maura, Fiona and Brendan, especially for *not* stopping the taxi outside my house but instead at a niteclub 12 miles away! Thanks to Brigid (remember I knew him first!), Michelle and Holly. A big thanks is due to Sharon. Thanks to James and Jude (Hey Jude) for the craic.

From the early days I thank Miriam O' Shea, and particularly Marie Migraine and Enda for all the holidays in the back of de van. Sandra your a star. Thanks for all the girly chats, the nights out and your ongoing friendship. Remember don't sleep too close to the edge of the bed you might fall out!

To Luke O'Brien, the first boy I met in AS in college (sure I'd no chance!), we started together and we'll finish together. The biggest thanks for all the sneaky pints, the matches (Kerry will make it yet) and particularly thanks for the treasured friendship. To P.J. thanks for your continuing love and remember if I'd been put in a kart at five I would be driving Formula 1 now!

I would like to thank especially Sarah Keegans (Dr. K.) for your guidance and friendship over the years and how could I forget the 600 miles in the Fiesta!

I express sincere gratitude to my family for their love, support and encouragement they have given me throughout my lifetime. Thanks to Sr. Patricia, Brigid, Mary - K and Margaret, Fidelma, Angela and Patricia Buller (the Derry years!) Thanks especially to my Mum and Dad. Thanks to my siblings Orla (and extended family Pat, Lauren (Beanie), Rachel and Ciara), Sean, Keith, Clodagh, Rowena and how could I forget trendy Brian. I dedicate this thesis to you all.

## **Abbreviations**

1,2 DME	1,2 dimethoxyethane
achc	acetylenedicobalthexacarbonyl (acetylene hexacarbonyldicobalt(0))
cat	catalyst
cco	<i>cis</i> -cyclooctene
cod	cyclooctadiene
Cy	cyclohexylamine
$\delta$	chemical shift (NMR)
dcm	dichloromethane
DMAc	<i>N, N</i> -dimethylacetamide
dpachc	diphenylacetylenedicobalthexacarbonyl (diphenylacetylenehexacarbonyldicobalt(0))
dec	decomposes
dmso	dimethylsulphoxide
$\epsilon$	extinction coefficient
equivs	equivalents
hrs	hours
IR	infrared
min.	minutes
m.p.	melting point ( $^{\circ}\text{C}$ )
nbn	norbornene
nbd	norbornadiene
Nd-YAG	neodymium yttrium aluminium garnet
NMO	<i>N</i> -methylmorpholine <i>N</i> -oxide
NMR	nuclear magnetic resonance
pachc	phenylacetylenedicobalthexacarbonyl (phenylacetylenehexacarbonyl- dicobalt(0))

PG	prostaglandin
PK	Pauson - Khand
tcne	tetracyanoethylene
tco	<i>trans</i> -cyclooctene
THF	tetrahydrofuran
TLC	thin layer chromatography
TMO	trimethylamine <i>N</i> -oxide
TRIR	time resolved infra - red
UV	ultraviolet
$\nu$	stretching frequency ( $\text{cm}^{-1}$ )



## Table of Contents

Contents	Page
Title Page	i
Declaration	ii
Dedication	iii
Acknowledgments	iv
Abbreviations	vi
Table of contents	viii
Abstract	xviii
<b>CHAPTER 1</b>	
<b>Introduction</b>	<b>1</b>
<b>1.1 Introduction</b>	<b>2</b>
<b>1.2 Bonding in Organometallic Complexes</b>	<b>2</b>
1.2.1 Metal - metal bonding	3
1.2.2 Bonding in metal - carbonyl complexes	4
1.2.3 Bonding in metal - acetylene complexes	5
1.2.4 Bonding effects with ligand substitution	7
<b>1.3 Product Analysis in Chemical Reactions</b>	<b>8</b>
1.3.1 Reaction mechanisms	9
1.3.2 Steady - state product analysis	9
1.3.3 Transient methods of product analysis	9
1.3.3.1 Laser Flash Photolysis	10
1.3.3.2 Operation of the flash photolysis apparatus	10

<b>1.4 Photochemical Processes</b>	<b>13</b>
1.4.1 Thermal v Photochemical processes	13
1.4.2 Photochemistry of metal carbonyls	14
1.4.3 Photochemistry of bimetallic carbonyl complexes	15
1.4.4 PK-like cyclisations of metal carbonyl complexes involving photochemical CO insertion	16
<b>1.5 The Pauson - Khand Reaction</b>	<b>18</b>
1.5.1 Origins of the Pauson - Khand Reaction	18
1.5.2 Scope of the PK reaction	20
1.5.3 The Catalyst System	21
1.5.3.1 Dicobalt octacarbonyl	21
1.5.3.2 Thermal studies of cobalt - carbonyl systems	23
1.5.4 Mechanism of the Pauson - Khand Reaction	25
1.5.4.1 Trapping of an Intermediate	27
1.5.5 Reaction Promoters	28
1.5.6 Pauson - Khand reactions with Electron Deficient Groups	29
1.5.7 Alternative Pauson - Khand Catalytic Systems	33
1.5.7.1 Intramolecular Pauson - Khand reactions involving non cobalt catalysts	34
1.5.7.2 Iron carbonyl catalysts	34
1.5.7.3 Tungsten carbonyl catalysts	37
1.5.7.4 Titanium and Zirconium catalysts	37
1.5.7.5 Palladium and Molybdenum catalysts	39
1.5.7.6 Rhodium and Ruthenium catalysts	39
1.5.7.7 Intermolecular Pauson -Khand reactions involving (indenyl)Co(I) and Mo catalysts	40
1.5.8 Photochemistry and the Pauson - Khand Reaction	41
1.5.9 Synthetic Applications	43
1.5.9.1 Prostaglandin History	43
1.5.9.2 Triquinanes	44

1.5.9.3 Bicyclo[3.3.0]octenones and terpenes	45
1.5.9.4 Chiral complexes	47
1.5.9.5 Perfumes and fenestranes	48
<b>1.6 References</b>	<b>51</b>

## CHAPTER 2

<b>The Photochemistry of (<math>\mu_2</math>-Alkyne)Co<sub>2</sub>(CO)<sub>6</sub> complexes</b>	<b>58</b>
<b>2.1 Introduction</b>	<b>58</b>
<b>2.2 Photolysis of (<math>\mu_2</math>-C<sub>6</sub>H<sub>5</sub>C<sub>2</sub>H)Co<sub>2</sub>(CO)<sub>6</sub></b>	<b>61</b>
2.2.1 Molecular modeling of ( $\mu_2$ -C <sub>6</sub> H <sub>5</sub> C <sub>2</sub> H)Co <sub>2</sub> (CO) <sub>6</sub>	61
2.2.2 Synthesis and Spectroscopic Characterisation of ( $\mu_2$ -C <sub>6</sub> H <sub>5</sub> C <sub>2</sub> H)Co <sub>2</sub> (CO) <sub>6</sub>	62
2.2.2.1. Preparation and IR spectrum of ( $\mu_2$ -C <sub>6</sub> H <sub>5</sub> C <sub>2</sub> H)Co <sub>2</sub> (CO) <sub>6</sub>	62
2.2.2.2. NMR characterisation of ( $\mu_2$ -C <sub>6</sub> H <sub>5</sub> C <sub>2</sub> H)Co <sub>2</sub> (CO) <sub>6</sub>	64
2.2.2.3. Electronic absorbance spectrum of ( $\mu_2$ -C <sub>6</sub> H <sub>5</sub> C <sub>2</sub> H)Co <sub>2</sub> (CO) <sub>6</sub>	66
2.2.3 Steady-state photolysis experiments	67
2.2.3.1. Photolysis of ( $\mu_2$ -C <sub>6</sub> H <sub>5</sub> C <sub>2</sub> H)Co <sub>2</sub> (CO) <sub>6</sub> in the presence of trapping ligands	67
2.2.3.2. Steady-state UV/Vis monitored photolysis of ( $\mu_2$ -C <sub>6</sub> H <sub>5</sub> C <sub>2</sub> H)Co <sub>2</sub> (CO) <sub>6</sub> for $\lambda_{exc} > 400$ and 340 nm	71
2.2.4 Laser flash photolysis of ( $\mu_2$ -C <sub>6</sub> H <sub>5</sub> C <sub>2</sub> H)Co <sub>2</sub> (CO) <sub>6</sub> at $\lambda_{exc} = 355$ nm	73
2.2.4.1. Flash photolysis under varying atmospheres	73
2.2.4.2. Flash photolysis in different solvents	75
2.2.4.3. Flash photolysis in the presence of pyridine trapping ligand	76
2.2.5 Summary of Results for photolysis experiments using $\lambda_{exc} = 355$ nm	79

2.2.6	Laser flash photolysis of $(\mu_2\text{-C}_6\text{H}_5\text{C}_2\text{H})\text{Co}_2(\text{CO})_6$ at $\lambda_{\text{exc}} = 266$ nm	80
2.2.7	Laser flash photolysis of $(\mu_2\text{-C}_6\text{H}_5\text{C}_2\text{H})\text{Co}_2(\text{CO})_6$ at $\lambda_{\text{exc}} = 532$ nm	80
2.2.8	Steady-state photolysis of $(\mu_2\text{-C}_6\text{H}_5\text{C}_2\text{H})\text{Co}_2(\text{CO})_6$ for $\lambda_{\text{exc}} > 500$ nm.	85
2.2.9	Summary for low energy photolysis ( $\lambda_{\text{exc}} = 532$ nm)	86
<b>2.3</b>	<b>Photolysis of <math>(\mu_2\text{-C}_2\text{H}_2)\text{Co}_2(\text{CO})_6</math></b>	<b>88</b>
2.3.1	Molecular modeling of $(\mu_2\text{-C}_2\text{H}_2)\text{Co}_2(\text{CO})_6$	88
2.3.2	Synthesis and Spectroscopic Characterisation of $(\mu_2\text{-C}_2\text{H}_2)\text{Co}_2(\text{CO})_6$	88
2.3.2.1.	Preparation and IR spectrum of $(\mu_2\text{-C}_2\text{H}_2)\text{Co}_2(\text{CO})_6$	88
2.3.2.2.	NMR characterisation of $(\mu_2\text{-C}_2\text{H}_2)\text{Co}_2(\text{CO})_6$	90
2.3.2.3.	Electronic absorbance spectrum of $(\mu_2\text{-C}_2\text{H}_2)\text{Co}_2(\text{CO})_6$	91
2.3.3	Steady-state Photolysis Experiments	92
2.3.3.1.	Photolysis of $(\mu_2\text{-C}_2\text{H}_2)\text{Co}_2(\text{CO})_6$ in the presence of trapping ligands	92
2.3.3.2.	$^1\text{H}$ NMR monitored steady-state photolysis of $(\mu_2\text{-C}_2\text{H}_2)\text{Co}_2(\text{CO})_6$ in $\text{d}_5\text{-pyridine}$ .	95
2.3.3.3.	UV/Vis monitored steady-state photolysis of <b>achc</b> and $(\mu_2\text{-C}_2\text{H}_2)\text{Co}_2(\text{CO})_5(\text{PPh}_3)$	95
2.3.3.4.	Summary of Results for broad band photolysis experiments ( $\lambda_{\text{exc}} > 340$ and $> 400$ nm)	97
2.3.4	Laser flash photolysis of $(\mu_2\text{-C}_2\text{H}_2)\text{Co}_2(\text{CO})_6$ at $\lambda_{\text{exc}} = 355$ nm	98
2.3.5	Laser flash photolysis of $(\mu_2\text{-C}_2\text{H}_2)\text{Co}_2(\text{CO})_6$ at $\lambda_{\text{exc}} = 532$ nm	101
2.3.6	IR monitored steady-state photolysis of $(\mu_2\text{-C}_2\text{H}_2)\text{Co}_2(\text{CO})_6$ for $\lambda > 500$ nm	105

2.3.7 Explanation of results for photolysis of <b>achc</b>	105
<b>2.4 Photolysis of <math>(\mu_2-(C_6H_5C)_2)Co_2(CO)_6</math></b>	<b>107</b>
2.4.1 Molecular modeling of $(\mu_2-(C_6H_5C)_2)Co_2(CO)_6$	107
2.4.2 Synthesis and Spectroscopic Characterisation of $(\mu_2-(C_6H_5C)_2)Co_2(CO)_6$	107
2.4.2.1. Preparation and IR spectrum of $(\mu_2-(C_6H_5C)_2)Co_2(CO)_6$	107
2.4.2.2. NMR characterisation of $(\mu_2-(C_6H_5C)_2)Co_2(CO)_6$	109
2.4.2.3. Electronic absorbance spectrum of $(\mu_2-(C_6H_5C)_2)Co_2(CO)_6$	110
2.4.3 Steady-state Photolysis Experiments	111
2.4.3.1. Photolysis of $(\mu_2-(C_6H_5C)_2)Co_2(CO)_6$ in the presence of trapping ligands	111
2.4.4 Laser flash photolysis of $(\mu_2-(C_6H_5C)_2)Co_2(CO)_6$ at $\lambda_{exc} = 355$ nm	117
2.4.5 Laser flash photolysis of $(\mu_2-(C_6H_5C)_2)Co_2(CO)_6$ at $\lambda_{exc} = 532$ nm	120
2.4.6 Irradiation of $(\mu_2-(C_6H_5C)_2)Co_2(CO)_6$ with monochromatic light ( $\lambda_{exc} = 532$ nm)	122
2.4.7 Laser flash photolysis of $(\mu_2-(C_6H_5C)_2)Co_2(CO)_6$ at $\lambda_{exc} = 266$ nm	122
2.4.8 Discussion of results for photolysis of <b>dpachc</b>	123
<b>2.5 Conclusions</b>	<b>126</b>
<b>2.6. References</b>	<b>126</b>

## CHAPTER 3

<b>Reaction of (<math>\mu_2</math>-alkyne-<math>\text{Co}_2(\text{CO})_6</math>) Complexes with Alkenes</b>	<b>129</b>
<b>3.1 Introduction</b>	<b>130</b>
<b>3.2 Thermal Preparation of Cyclopentenone complexes</b>	<b>135</b>
3.2.1. Thermal cyclisation of 2-phenyl-3a,4,5,6,7,7a-hexahydro-4,7-methanoinden-1-one	135
3.2.1. Thermal preparation of 2-phenyl-3a,4,5,6,7,7a-hexahydroinden-1-one	141
3.2.3. Thermal synthesis of 3a,4,7,7a-Tetrahydro-4,7-methanoinden-1-one	142
<b>3.3 Steady-state Photolysis Experiments</b>	<b>144</b>
3.3.1. IR monitored steady-state photolysis of ( $\mu_2\text{-C}_2\text{H}_2$ ) $\text{Co}_2(\text{CO})_6$ in the presence of alkenes	144
3.3.2. UV/Vis. monitored photolysis of ( $\mu_2\text{-C}_2\text{H}_2$ ) $\text{Co}_2(\text{CO})_6$ and alkenes <b>nbn</b> and <b>nbd</b>	149
3.3.3. IR monitored steady-state photolysis of ( $\mu_2\text{-C}_6\text{H}_5\text{C}_2\text{H}$ ) $\text{Co}_2(\text{CO})_6$ in the presence of alkenes	150
<b>3.4. Photolytic reaction of (<math>\mu_2</math>-alkyne)dicobalthexacarbonyl complexes with alkenes</b>	<b>153</b>
3.4.1. Reaction of <b>pachc</b> with norbornene	153
3.4.2. Reaction of <b>pachc</b> with cyclohexene	154
3.4.4. Reaction of <b>dpachc</b> with cis-cyclooctene (cco) and norbornene	155
<b>3.5. Preparation of (<math>\mu_2</math>-alkyne)<math>\text{Co}_2(\text{CO})_5(\text{alkene})</math> Complexes at Low Temperature</b>	<b>156</b>
<b>3.6. Conclusions</b>	<b>158</b>
<b>3.7. References</b>	<b>161</b>

## CHAPTER 4

<b>Experimental Procedures</b>	<b>163</b>
<b>4 Experimental</b>	<b>164</b>
<b>4.1 Reagents</b>	<b>164</b>
<b>4.2 Equipment</b>	<b>164</b>
<b>4.3 Sample preparation for Laser Flash Photolysis Experiments</b>	<b>165</b>
<b>4.4 General experimental details for the preparation of acetylene cobalt carbonyl complexes</b>	<b>166</b>
<b>4.5 Synthesis of (<math>\mu_2</math>-alkyne)hexacarbonyldicobalt Complexes. Reaction of <math>\text{Co}_2(\text{CO})_8</math> with alkynes</b>	<b>166</b>
4.5.1 ( $\mu_2$ - $\text{C}_2\text{H}_2$ ) $\text{Co}_2(\text{CO})_6$ - Acetylene hexacarbonyldicobalt	166
4.5.2 ( $\mu_2$ - $\text{C}_6\text{H}_5\text{C}_2\text{H}$ ) $\text{Co}_2(\text{CO})_6$ - Phenylacetylene hexacarbonyldicobalt	167
4.5.3 ( $\mu_2$ -( $\text{C}_6\text{H}_5\text{C}$ ) $_2$ ) $\text{Co}_2(\text{CO})_6$ - Diphenylacetylene hexacarbonyldicobalt	168
<b>4.6 Synthesis of the Ligand Substituted Pentacarbonyl Complexes. Reaction of (<math>\mu_2</math>-alkyne)<math>\text{Co}_2(\text{CO})_6</math> with ligands triphenylphosphine and pyridine</b>	<b>169</b>
4.6.1 Thermal Synthesis of ( $\mu_2$ - $\text{RC}_2\text{R}'$ ) $\text{Co}_2(\text{CO})_5(\text{PPh}_3)$ - Acetylenedicobaltpentacarbonyl Triphenylphosphine complexes	169
4.6.2 Thermal Synthesis of ( $\mu_2$ - $\text{RC}_2\text{H}$ ) $\text{Co}_2(\text{CO})_5(\text{C}_5\text{H}_5\text{N})$ - Acetylenedicobaltpentacarbonyl Pyridine complexes	170
<b>4.7 Synthesis of the (<math>\mu_2</math>-<math>\text{R}_2\text{C}_2\text{H}</math>)<math>\text{Co}_2(\text{CO})_4(\text{L})_2</math> Tetracarbonyl Complexes (<math>\text{L} = \text{C}_5\text{H}_5\text{N}</math> or <math>\text{PPh}_3</math>).</b>	<b>171</b>
4.7.1 Synthesis of ( $\mu_2$ - $\text{R}_2\text{C}_2\text{H}$ ) $\text{Co}_2(\text{CO})_4(\text{C}_5\text{H}_5\text{N})_2$ complexes	171
4.7.2 Synthesis of ( $\mu_2$ - $\text{R}_2\text{C}_2\text{H}$ ) $\text{Co}_2(\text{CO})_4(\text{PPh}_3)_2$ complexes	171
<b>4.8 Steady-state photochemical experiments. Photochemical synthesis of (<math>\mu_2</math>-<math>\text{RC}_2\text{H}</math>)<math>\text{Co}_2(\text{CO})_5(\text{L})</math> (<math>\text{L} = \text{C}_5\text{H}_5\text{N}</math> or <math>\text{PPh}_3</math>)</b>	<b>172</b>

4.8.1	Photochemical synthesis of $(\mu_2\text{-RC}_2\text{H})\text{Co}_2(\text{CO})_5(\text{C}_5\text{H}_5\text{N})$ complexes	172
4.8.2	Photochemical synthesis of $(\mu_2\text{-RC}_2\text{H})\text{Co}_2(\text{CO})_5(\text{PPh}_3)$ complexes	173
<b>4.9</b>	<b>Preparation of <math>(\mu_2\text{-C}_2\text{H}_2)\text{Co}_2(\text{CO})_6</math> for <math>^1\text{H}</math> NMR monitored steady-state photolysis</b>	<b>174</b>
<b>4.10</b>	<b>Cyclopentenone Synthesis</b>	<b>174</b>
4.10.1	Thermal synthesis of 2-Phenyl-3a,4,5,6,7,7a-Hexahydro-4,7-methanoinden-1-one	175
4.10.2	Thermal synthesis of 2-Phenyl-3a,4,5,6,7,7a-hexahydroinden-1-one	176
4.10.3	Thermal synthesis of 3a,4,7,7a-Tetrahydro-4,7-methanoinden-1-one	177
4.10.4	Thermal synthesis of 3a,4,5,6,7a-Hexahydro-4,7-methanoinden-1-one	177
<b>4.11</b>	<b>Photochemical synthesis of norbornene derived cyclopentenones</b>	<b>178</b>
4.11.1	Reaction of phenylacetylene dicobalthexacarbonyl with norbornene	178
4.11.2	Reaction of phenylacetylene dicobalthexacarbonyl with cyclohexene	179
4.11.3	Reaction of phenylacetylene dicobalthexacarbonyl with norbornadiene	179
4.11.4	Reaction of phenylacetylene dicobalthexacarbonyl with hept-1-ene	180
4.11.5	Reaction of phenylacetylene dicobalthexacarbonyl with cis-cyclooctene	180
<b>4.12</b>	<b>Photolytic synthesis of olefin substituted <math>(\mu_2\text{-alkyne})\text{dicobaltcarbonyl}</math> complexes</b>	<b>181</b>
4.12.1	Photolysis apparatus	181
4.12.2	Attempted synthesis of $(\mu_2\text{-C}_6\text{H}_5\text{C}_2\text{H})\text{Co}_2(\text{CO})_5(\text{cis-cyclooctene})$	182
4.12.3	Attempted synthesis of $(\mu_2\text{-C}_6\text{H}_5\text{C}_2\text{H})\text{Co}_2(\text{CO})_5(\text{THF})$	182
<b>4.13</b>	<b>Purification Procedures</b>	<b>182</b>
4.13.1	Purification of Norbornadiene	182
4.13.2	Purification of Hept-1-ene	183



4.13.3	Purification of Hexene	183
4.13.4	Purification of Tetrahydrofuran	184
4.14	References	185
 <b>CHAPTER 5</b>		 <b>188</b>
5.0	Conclusions	187
 <b>APPENDICES</b>		 <b>190</b>
A	Presentations and Publications	
B	Paper	
C	Calculations for the determination of extinction coefficients	
	Peakfit Analysis of UV spectra	
	Calculated rate of reaction from rate equations	
D	Data for the determination of extinction coefficients	

## *Abstract*

An important method for the production of cyclopentenones is the Pauson - Khand reaction. First reported in 1973, the reactions most important aspect is carbonyl insertion, obtained by reacting an alkene, an alkyne and carbon monoxide which is most often supplied by octacarbonyl dicobalt. However, for many reasons the investigation of the corresponding mechanism is difficult, so that it has remained a subject of intense discussion. This report outlines an investigation of the use of photochemical techniques to generate possible intermediates in order to elucidate the mechanism of the reaction.

We have shown that the early stages of such processes can be investigated with the aid of the laser flash photolysis technique, which allows the UV spectroscopic identification of intermediates. Studies on various alkyne dicobalthexacarbonyl complexes have revealed a wavelength dependent photochemistry. Results following high energy photolysis ( $\lambda_{\text{exc}} = 355\text{nm}$ ) have been interpreted in terms of a reversible homolytic cleavage of the Co - Co bond while low energy photolysis ( $\lambda_{\text{exc}} = 532\text{nm}$ ) produces CO loss. Primary photoproducts involved in the reaction of these complexes with coordinating ligands were identified and characterised. Kinetic data for the reaction of these complexes with CO and ligands were obtained.

Time resolved IR has been used to investigate the photochemical reactions of alkyne hexacarbonyldicobalt complexes with various olefins. Visible light irradiation and 1 atmosphere of CO has been shown to be sufficient to generate cyclopentenones in a photolytic Pauson - Khand reaction from these alkyne hexacarbonyldicobalt complexes and olefins. This work demonstrates the need for correct selection of excitation wavelength in photo-induced Pauson - Khand reactions.

# **CHAPTER 1**

## **Introduction**

## 1.1 Introduction

Over the last forty years, complexes of metals have been utilised as catalysts in the conversion of many raw materials to commercially important products. Developments are still being carried out up to the present day in the search for new and more highly active selective catalysts which will save energy and materials. A catalyst acts by producing an alternative low energy pathway which speeds up a reaction without losing its chemical identity. The exact mechanisms of many of the catalytic reactions remain unknown but as the processes involve coordination of a substrate to the metal, the initial steps involved must be the generation of a vacant site at the metal centre.

In metal carbonyl complexes the principal process involving the displacement of a carbonyl group by a nucleophilic ligand can occur thermally or photochemically. From the initial stages to generation of final product many intermediates are involved in the reaction. A number of techniques have been employed to aid in the elucidation of the identity, structure and reaction kinetics of these intermediate species. Low temperature isolation and flash photolysis have been most successful in this regard. In order to obtain a greater understanding of these processes, kinetic studies of ligand substitution reactions of  $(\mu_2\text{-alkyne})\text{Co}_2(\text{CO})_6$  were undertaken as the basis for this study. As an introduction to these systems the nature of bonding in organometallic complexes will be discussed.

## 1.2 Bonding in Organometallic Complexes

Transition metals are characterised by the fact that the  $(n-1)d$  orbitals have energies similar to those of the  $ns$  and  $np$  orbitals of the valence shell, and so participate in bond formation. The special symmetry of these  $d$  - orbitals is responsible for a particular type of bond between the transition-metal and the ligand,

which facilitates unique bonding types particularly for low valent metals.<sup>1</sup> The reactivity of metal carbonyl complexes cannot be explained without understanding the nature of the metal - carbonyl bond. Different types of bonding modes which are encountered in the following work will be considered:

- i. metal - metal bonding,
- ii. bonding in metal - carbonyl complexes,
- iii. bonding in metal - acetylene complexes,
- iv. bonding effects with ligand substitution,

### 1.2.1 *Metal - metal bonding*

In transition-metal complexes only a limited number of combinations of metal and ligand will give an 18 electron count. The first row carbonyls mostly follow the 18 electron rule with each metal contributing the same number of electrons as its group number and each CO contributes two electrons. The even electron metals are able to attain 18 electrons without M - M bond formation. They do so by binding the appropriate number of carbonyls. In  $\text{V}(\text{CO})_6$ , the complex is 17 electron, but is easily reduced to the 18 electron configuration for each metal. For the first transition series, the d - orbitals are relatively small and even in moderately low oxidation states (+ 2 and + 3) they apparently do not extend sufficiently for good overlap. Odd electron metals however, need to form M - M bonds in order to satisfy the 18 electron rule. Low oxidation states favour the occurrence of metal - metal bonds. In the 17 electron fragment  $\text{Co}(\text{CO})_4$ , dimerisation takes place via a metal - metal bond.

### 1.2.2 Bonding in metal - carbonyl complexes

Metal carbonyl bonds can be (a) terminal or (b) bridging in nature. Terminal carbonyl groups resemble a carbonyl moiety relatively unchanged from free CO i.e. the bond between the carbon and oxygen can best be approximated as a triple bond. The bond order is reflected in the C - O stretching frequencies,  $2143\text{ cm}^{-1}$  for free CO and  $2000 \pm 100\text{ cm}^{-1}$  for terminal CO groups in  $\text{Co}_2(\text{CO})_8$  complexes. Bridging carbonyls resemble carbonyl groups in organic chemistry, such as unsaturated ketones exhibiting C - O stretching frequencies at  $1800 \pm 75\text{ cm}^{-1}$  compared with  $1715 \pm 10\text{ cm}^{-1}$  for saturated ketones. The IR spectrum of a metal carbonyl compound thus can provide important information on the nature of the CO groups and may allow the distinction between a structure with only terminal carbonyls and one containing one or more bridging CO groups.

It has widely been accepted that the photochemical dissociation of metal - ligand bonds stems from ligand - field excitations. In octahedral complexes, ligand field splitting involving d - molecular orbitals arise from an electron in the  $t_{2g}$  orbital ( $\pi$  - bonding) being excited into the  $e_g^*$  orbital (strongly antibonding) (Figure 1.1). The result of this promotion of electrons is heterolytic dissociation leading to labilisation of a CO ligand. Baerends *et al.* have recently shown that the relation between the lowest excited state at equilibrium geometry and the photochemistry is less direct than assumed in the standard model.<sup>2</sup> The calculated orbital energies suggested that the ligand field states are not the accessible excited states and that the lowest excited states are in fact metal to ligand charge transfer in character. However, the dissociation is still driven by the presence of a strongly dissociative LF state, which is at high energy at  $R_e$ , but rapidly lowers in energy upon M - C bond lengthening. Upon metal - CO bond lengthening the antibonding character present in the  $e_g^*$  orbital rapidly diminishes and may eventually become the lowest excited state. The photochemical metal - CO dissociation takes place regardless of the nature of the initially populated excited state.

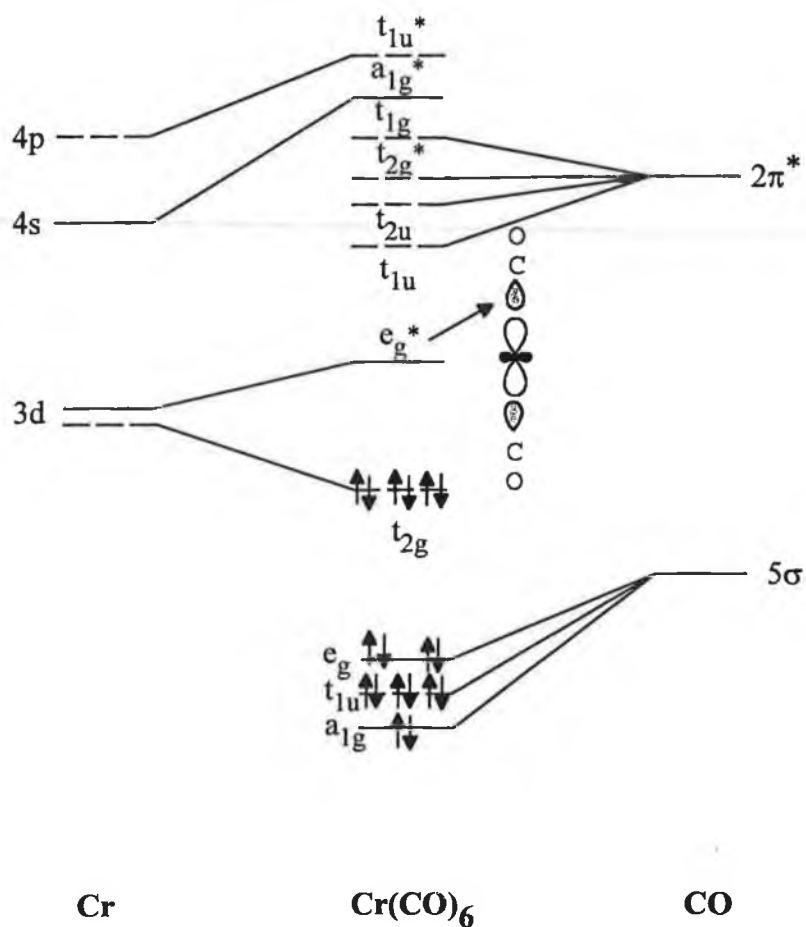
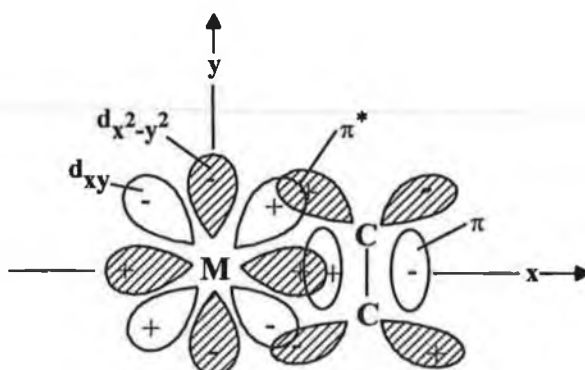


Figure 1.1

### 1.2.3 Bonding in metal - acetylene complexes

Acetylenes have two mutually exclusive perpendicular sets of  $\pi$  orbitals which can be employed in a  $\sigma$ ,  $\pi$  - bond formation. They can act as monodentate ligands binding exclusively to one metal, or as bidentate ligands bridging two metals. Since the two  $\pi$  clouds lie in planes perpendicular to each other, it is impossible to get efficient overlap of both  $\pi$  systems with one metal's orbitals at the same time. Orbitals on metals can combine with empty antibonding orbitals of suitable

symmetry. This bonding scheme is represented by the well known Dewar Chatt - Duncanson model of metal - acetylene bond (Figure 1.2).<sup>3</sup>



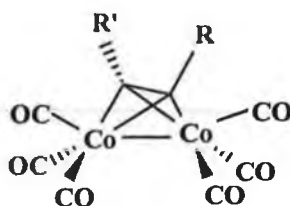
**Figure 1.2** *Dewar Chatt - Duncanson model for bonding between a metal atom and an acetylene.*

In most polynuclear metal complexes alkyne ligands adopt a bridging coordination and serve as four - electron donors to the metal atoms. In binuclear metal complexes alkynes usually coordinate in the  $\mu\text{-}\perp$  coordination mode although  $\mu\text{-}\parallel$  coordination modes are possible.

When acetylene reacts with  $\text{Co}_2(\text{CO})_8$ , two molecules of CO are eliminated. The acetylene is therefore acting as a four electron donor (two electrons donated to each Co atom replacing the two carbonyl ligands which have been displaced). The position of the two Co atoms is such as to allow efficient overlap from both  $\pi$  orbitals of the  $\text{C}\equiv\text{C}$  triple bond. Thus the carbon centres on the acetylene approximate  $\text{sp}^3$  hybridization (1). The stability of alkyne complexes increases with increasing electron - withdrawing character of X in the complexes of  $\text{XC}\equiv\text{CX}$ . Thus, halogen - substituted acetylenes, which are highly explosive compounds in the uncomplexed state, may be stabilised by complex formation. Also, cyclohexyne which is unstable as a free molecule can be stabilised as a metal complex.<sup>4</sup> Alkyne ligands bearing



more electronegative substituents can therefore exchange at a faster rate at room temperature e.g.  $(\text{CF}_3)_2 > \text{C}_2(\text{CO}_2\text{Me})_2 > \text{C}_2\text{Ph}_2 > \text{PhC}_2\text{H} > \text{C}_2\text{H}_2 > \text{C}_2(\text{CH}_2\text{NEt})_2$ .



(1)

The acetylenic  $\text{C}_1 - \text{C}_2$  distance of  $1.46 \text{ \AA}$  in complexed acetylene is  $0.27 \text{ \AA}$  larger than the  $\text{C}_1 - \text{C}_2$  distance in uncomplexed acetylene. This indicates a significant modification to the bond order in the acetylene. The acetylenic proton resonances in the NMR spectra are shifted to low field relative to the uncomplexed ligand ( $\delta 1.8\text{--}3.3$ ); they are thus located in the region more associated with olefinic protons ( $\delta 4.5\text{--}6.8$ ).

#### 1.2.4 Bonding effects with ligand substitution

Formation of ligand substituted metal carbonyl complexes may occur if orbitals of suitable symmetry are available (e.g.  $d$ -orbitals of phosphorus in  $\text{PPh}_3$ ).  $\text{AM}_2(\text{CO})_{6-n}\text{L}_n$  type complexes, where A = alkyne, L = ligand e.g.  $\text{PPh}_3$ ,  $\text{POPh}_3$ , solvent etc., are formed from  $\text{M}_2(\text{CO})_8$  when overlap of ligand L orbitals with the metal M orbitals is efficient and subsequent loss of one carbonyl occurs. The carbonyl stretching frequency of carbonyl complexes depends on how much electron density passes into antibonding  $\pi^*$  orbital of the CO by retrodonative  $\pi$ -bonding from the metal; the larger this density the weaker the bond between the carbon and oxygen and hence the lower its  $\nu_{\text{CO}}$ . Alternatively if electron density is withdrawn from  $\pi^*$  (CO) by a  $\pi$  acceptor  $\nu_{\text{CO}}$  is increased. A ligand L which can act as a  $\pi$  acceptor can withdraw

electrons from the  $\pi$  bonds of other ligands; the  $d\pi$  orbitals of the metal act as a “conductor” for the electrons, thus the  $\pi$  bond to the CO is weakened by the presence of the incoming ligand (Figure 1.3).

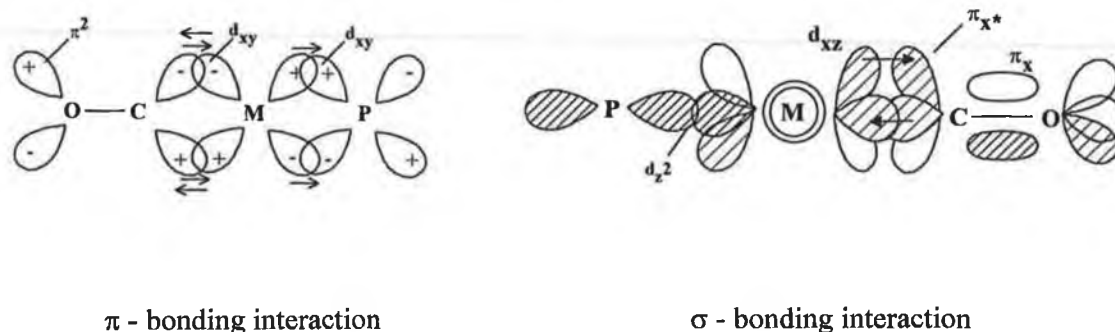


**Figure 1.3** Bonding effects with ligand substitution ( $L = \text{phosphine}$ ).

A lone pair of electrons on the C supplies the  $\sigma$  bond, while the retrodonative  $\pi$  bond is formed with the aid of an antibonding  $\pi^*$  orbital.

### 1.3 Product Analysis in Chemical Reactions

Reaction kinetics is the study of the speed of chemical reactions and is important for describing the rates of forward and reverse chemical processes. For reactions involving entering or leaving groups, the nature of these groups (e.g.  $\sigma$  - donor,  $\pi$  - acceptor character, bond strength, concentration etc.) will affect the rate of reaction. The type of technique which can be employed for product analysis depends on whether a reaction has a rate convenient for measurement.

- (i) static methods ( $t_{1/2} \geq 1 \text{ min}$ ) - steady state photolysis,
- (ii) relaxation methods ( $t_{1/2} \leq 1 \text{ sec}$ ) - laser flash photolysis.

### 1.3.1 Reaction mechanisms

A major problem in elucidating the detailed mechanism of a reaction is to characterise the structures and reactivities of intermediates formed along the reaction coordinates. Such species are elusive under thermal catalytic (or stoichiometric) conditions owing to the low steady - state concentrations which impede direct spectroscopic observation. Other conditions and methods must be used to ensure that the high energy species studied are those of interest in the thermal reaction schemes. In this respect, flash photolysis can be a good tool for preparing high, non - steady - state concentrations of reaction intermediates.

### 1.3.2 Steady - state product analysis

Steady - state methods of product analysis, for our studies, were made by IR and UV/Vis spectroscopic monitoring. Owing to their strong IR chromophores and experimentally convenient monitoring frequencies, metal - carbonyl complexes are ideal candidates to be studied in the steady - state. Typically a light source (Xe arc lamp) is used to irradiate the sample. The energy absorbed from the incoming light, controlled by means of absorption filters, may be enough to produce excited states in the molecule and initiate a photochemical reaction. The product is formed in real time ( $t_{1/2} \geq 1$  minute or less) and is stable enough for analysis by IR or UV measurements to be taken.

### 1.3.3 Transient methods of product analysis

An early method for studying the photochemistry of transient photochemical intermediates was to induce photochemistry using a low intensity light source and stabilise the intermediates produced in low temperature matrices. Thus their lifetimes are increased to the point where kinetic measurement is possible.<sup>5</sup> Pulsed laser

sources have made it possible to study the photochemistry of transient intermediates under ambient conditions. The development of flash lamps and lasers as sources of pulsed excitation has allowed the study of excited states and transient intermediates whose lifetimes are exceedingly short.<sup>6</sup> Very large amounts of structural and kinetic information can be obtained from TRIR.

#### 1.3.3.1 *Laser Flash Photolysis*

Laser flash photolysis was developed by Norrish and Porter,<sup>7</sup> in the 1950s, who subsequently won the Nobel prize for chemistry in 1967 for their contribution to the studies of extremely fast chemical reactions. Flash spectroscopy uses a short intense pulse of light, for example, a discharge tube or laser, which produces transient species, radicals or excited molecules in concentrations many thousand times greater than in previous systems. By very quickly analysing the time evolution of the system by absorbance or emission spectroscopy, the decay of concentration with time is measured. If new products are formed the rates of formation of such species can also be monitored. Advances in laser technology have allowed the time resolution of photolysis studies to increase from milliseconds in the 1960s to nanoseconds in the 1970s to femtoseconds in the 1980s.

#### 1.3.3.2 *Operation of the flash photolysis apparatus*

An intense light source (the pump source) excites the sample inducing a change in electronic state and initiates a photochemical process. The absorbance changes induced by the excitation pulse are monitored by a second light source (the probe source (Xe arc lamp)). The intensity of monitoring beam being transmitted through the solution before the laser flash,  $I_0$ , is initially recorded. This corresponds to the voltage generated by the photomultiplier when the monitoring source (Xe arc lamp) shutter is open, less the voltage generated by stray light. The intensity of the monitoring beam is measured in real time ( $I_t$ ). Since  $I_0/I_t = \text{absorbance}$  the change in

intensity of the probe beam transmitted through the sample is measured as a function of time and or wavelength. Changes in absorbance in the sample solution reflect the formation of intermediates or depletion of the parent compound or both.

The excitation source used in this thesis is a neodymium yttrium aluminium garnet (Nd - YAG) laser which operates at 1064 nm. Nd atoms are implanted in the host YAG crystals of approximately one part per hundred. The YAG host material has the advantage of having a relatively high thermal conductivity to remove heat, thus allowing these crystals to be operated at high repetition rates. The pulse frequency can be doubled, tripled or quadrupled with nonlinear optical components to generate a second, third or fourth harmonic at 532, 355 or 266 nm respectively. The pulse time is approximately 10 ns. The energy generated for 532, 355 and 266 nm frequencies is typically 150 mJ, 30 mJ and 45 mJ per pulse respectively. The apparatus has been described in detail elsewhere with the excitation and monitoring beams arranged in a cross - beam configuration.<sup>8</sup>

By recording transient signals sequentially over a range of monitoring wavelengths, absorbance readings can be calculated at any time after the flash to generate a time - resolved difference absorption spectrum of the transient species. Spectra are obtained as a result of point by point build up by optically changing the wavelength of the monochromator. It is necessary that the solution be optically transparent for the monitoring light beam and hence solvents of spectroscopic transparency are required. Metal carbonyl compounds are suitable because their moderate solubility in non polar solvents and their UV/Vis absorptions are intense.

A schematic of the laser flash photolysis instrument is shown in Figure 1.4. The laser is directed through a power meter, triggering the oscilloscope<sup>9</sup> and onto a sample cuvette by a series of prisms. The UV/Vis monitoring light source is a cooled 275 Watt Xenon arc lamp arranged at right angles to the laser beam. The beam passes

through the sample cell and is focused into monochromator slits and the light is detected by a photomultiplier which is interfaced to a computer.

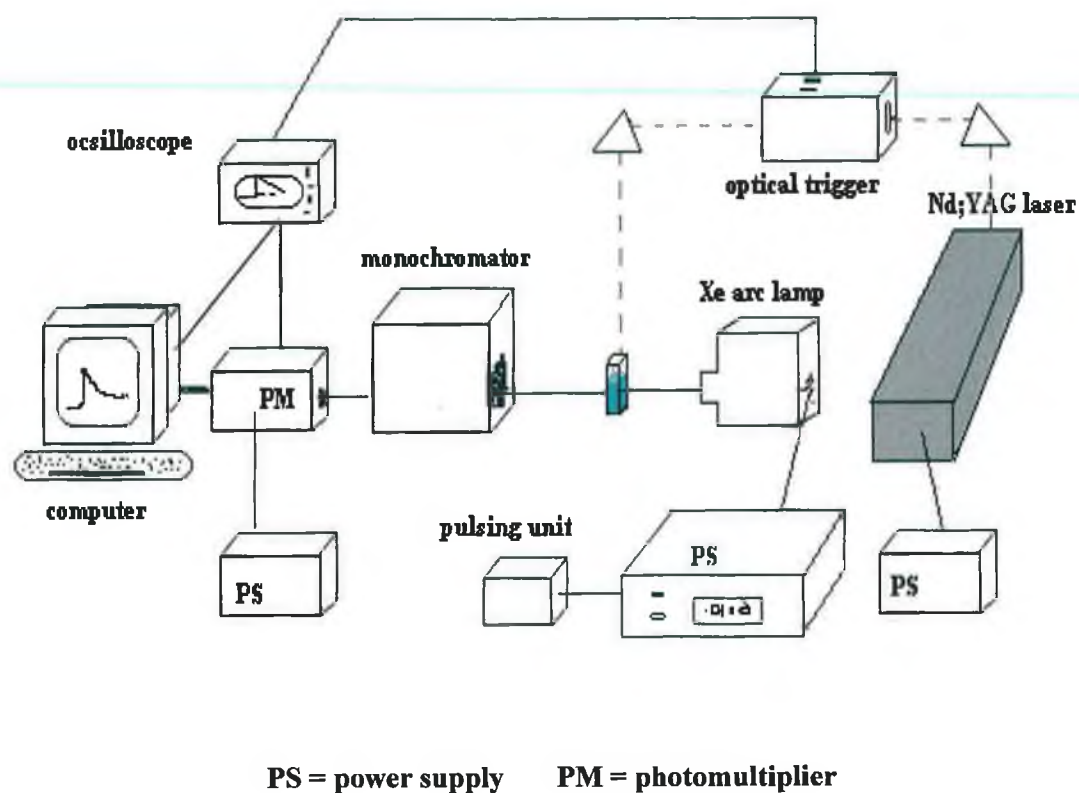


**Figure 1.4**    *Schematic diagram of the laser flash photolysis system*

## 1.4 Photochemical Processes

### 1.4.1 Thermal v Photochemical processes

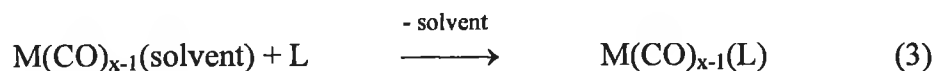
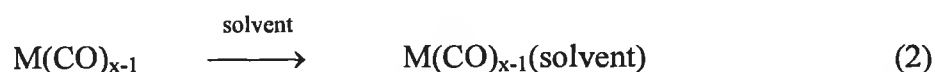
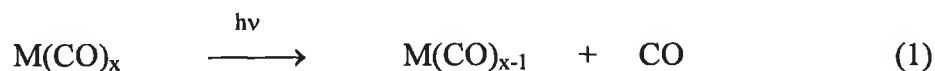
Photochemical processes can occur when light is absorbed by a compound. In this process, an electron is promoted from the ground state configuration into the excited state configuration. If any photochemistry is to occur, the excited state must react very quickly, since the lifetime of an electron in an excited state is of the order  $10^{-6}$  to  $10^{-9}$  seconds. Chemical change can follow production of electronically excited species and ultimately bond rupture can occur. Ideally a molecule of product is formed for each photon absorbed, giving a quantum yield,  $\Phi$ , of unity. However, in some cases, no chemistry occurs and the electron falls back to the ground state and the compound either emits light or is heated up thermally. In this case the quantum yield is less than unity.

In contrast, thermal energy may be distributed about all modes of excitation in a species including translational, rotational and vibrational. For a species in equilibrium and obeying Boltzman's Law of distribution, a typical energy of electronic excited state =  $250 \text{ KJmol}^{-1}$  in thermal units, at room temperature ( $\sim 2500 \text{ Jmol}^{-1}$ ) the population in the excited state can be calculated to be  $\sim 4 \times 10^{-46}$  i.e. negligible. To induce a 1 % population of excited species would require temperatures greater than  $6800^\circ\text{C}$ . Most molecular species would rapidly thermally decompose from the ground electronic state and it would not be possible to produce enough electronically excited molecules.

In essence more thermodynamic products are accessible to a photoexcited molecule than to a ground state molecule. Selectivity of activation, by light rather than heat, of a photoreaction is allowed. Some reactions are initiated at low temperatures.

### 1.4.2 Photochemistry of metal carbonyls

The photochemistry of metal carbonyl complexes has become of increasing importance in recent years. The potential uses of these compounds in synthetic and catalytic applications has been known for many years. The reactions involve photolysis of the metal carbonyl compound in a solvent medium. The solvent can range from donor solvents, for example, alcohol, ether, or cycloalkene to an inert solvent such as an alkane. The function of the solvent is to occupy the vacant site created by ejection of a CO molecule(s) upon photolysis (eq 1-2) but it can also assist in the dissipation of excess vibrational energy. In the presence of a stronger  $\sigma$  - donor ligand, for example pyridine or  $\text{PPh}_3$ , the coordinated solvent is easily displaced, yielding  $\text{M}(\text{CO})_{x-1}(\text{L})$  complex, ( $\text{M} = \text{Cr}, \text{Mo}$  or  $\text{W}$ ) (eq 3).



Further reactions with molecules in the medium can lead to additional ligand substitution (eq 4).



Photolysis reactions are usually carried out under argon or nitrogen atmospheres to prevent reaction with oxygen which would result in decomposition. Also, by maintaining a constant stream of argon or nitrogen throughout the reaction process, ensures that any liberated CO is expelled, thus preventing the unproductive back reaction.



The products of most photochemical and thermal reactions are often identical. As well as increasing accessibility to certain reactions, the rate of reactions has been increased by photochemical means. The use of photochemical methods to study catalytic processes can therefore provide valuable information about the nature of these reactions. Thus reactions which may have taken days under thermal conditions proceed in hours or even minutes photochemically.

#### 1.4.3 Photochemistry of bimetallic carbonyl complexes

The photochemistry of bimetallic complexes derived from  $\text{Co}_2(\text{CO})_8$ ,  $\text{Mn}_2(\text{CO})_{10}$ ,  $\text{Re}_2(\text{CO})_{10}$  and  $\text{Fe}_2(\text{CO})_8$  has often been compared due to the similarity in their molecular structures and also to determine if the complexes exhibit related photochemistry. Ragni and Trogu have reported the ultraviolet irradiation of acetylene<sup>10</sup> and  $\text{Hg}[\text{Co}(\text{CO})_4]_2$  in ether solution yielding  $[(\mu_2\text{-C}_2\text{H}_2)\text{Co}_2(\text{CO})_6]$  as well as trace quantities of  $[(\mu_2\text{-C}_2\text{H}_2)\text{Co}_4(\text{CO})_{10}]$  and  $[\text{HgCo}_2(\text{CO})_6(\mu_2\text{-C}_2\text{H}_2)]_2$ . A similar reaction of diacetylene(butadiyne) with  $\text{Hg}[\text{Co}(\text{CO})_4]_2$ , but under photochemical conditions, gives trace quantities of the corresponding dark red butadiyne complex  $[\text{Co}_2(\text{CO})_6]_2\text{C}_4\text{H}_2$  in which each of the triple bonds of the butadiyne system bonds to a  $\text{Co}_2(\text{CO})_6$  group.

The photochemistry of metal-metal bonded complexes has been extensively studied by Wrighton. Near UV photoexcitation of  $\text{Mn}_2(\text{CO})_{10}$ ,  $\text{Re}_2(\text{CO})_{10}$ ,  $\text{MnRe}(\text{CO})_{10}$  amongst others has resulted in homolytic cleavage of the metal-metal bond as the primary photoprocess. Cleavage of metal-metal bonds in complexes can potentially lead to two paramagnetic centers, of increased reactivity, each with an odd number of electrons. This is important both stoichiometrically and catalytically in reactions of metal carbonyls with organic substrates.

Wrighton and Ginley<sup>11</sup> reported photolysis of  $\text{Mn}_2(\text{CO})_{10}$  in degassed isooctane solutions of  $\text{PPh}_3$  yielding  $\text{Mn}_2(\text{CO})_8(\text{PPh}_3)_2$  as the principal primary

photoproduct upon flash photolysis. While formation of  $\text{Mn}_2(\text{CO})_9(\text{PPh}_3)$  was as only a very minor component (< 5 %) of the reaction, no homolytic cleavage product was observed. Photoreactions of  $\text{Mn}_2(\text{CO})_{10}$ <sup>12</sup> in rigid matrices at low temperature yields only net loss of CO, and not  $\text{Mn}(\text{CO})_5$  radicals which dominate the photoproducts in fluid solution at 298 K.

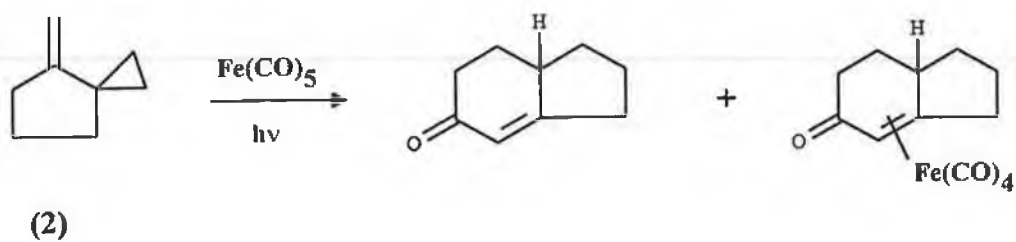
For matrix photochemistry, reported by Rest<sup>13</sup>, of dinuclear metal species  $[\text{Cr}_2(\mu\text{-}\eta^6\text{:}\eta^6\text{-C}_{12}\text{H}_{10})(\text{CO})_6]$  and  $[\text{Mn}_2(\mu\text{-}\eta^5\text{:}\eta^5\text{-C}_{10}\text{H}_8)(\text{CO})_6]$ , for each species photolysis resulted in photochemical ejection of a CO ligand to produce coordinately unsaturated metal dicarbonyl centers. The electronic transitions, into which the irradiation took place, all involved some metal to carbonyl charge transfer and therefore excited state species formed can lose a carbonyl ligand. Wrighton also reported that *trans*  $(\eta^5\text{-C}_5\text{H}_5)_2\text{Fe}_2(\text{CO})_4$  and related complexes upon photoexcitation in rigid media at low temperatures yield triply CO bridged  $(\eta^5\text{-C}_5\text{H}_5)\text{Fe}_2(\text{CO})_3$  with dissociative loss of CO.<sup>14</sup>

#### 1.4.4 PK-like cyclisations of metal carbonyl complexes involving photochemical CO insertion

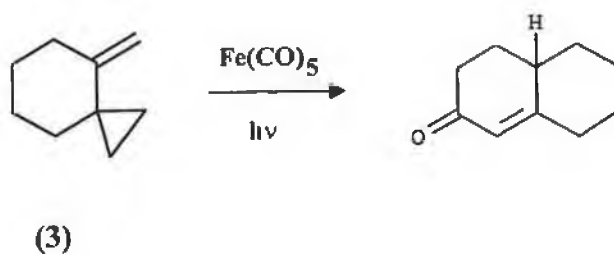
Photochemical reactions involving CO insertion by a metal carbonyl catalyst producing PK-like cyclic products have been frequently reported. Sarel *et al.*<sup>15</sup> reported photoreactions of  $\text{Fe}(\text{CO})_5$  with dicyclopropylethylene, giving rise predominantly to cyclohexenone products. Two olefinic monospiranes 4-methylenspiro[2,4]-decane (**2**) (Reaction 1.1(a)), and 4-methylenspiro[2,5]-octene (**3**) (Reaction 1.1(b)), were photoreacted with  $\text{Fe}(\text{CO})_5$  producing bicyclic enones. The corresponding dispiro-olefin yielded a tricarbonyl iron  $\sigma,\pi$  complex.

Casey, Haller *et al.*<sup>16</sup> photolysed  $[(\text{C}_5\text{H}_5)\text{COFe}]_2(\mu\text{-CO})(\mu\text{-C=CH}_2)$  with diphenylacetylene for two hours under CO (Reaction 1.2) leading to the formation of a metallocyclopentalenone (**4**).

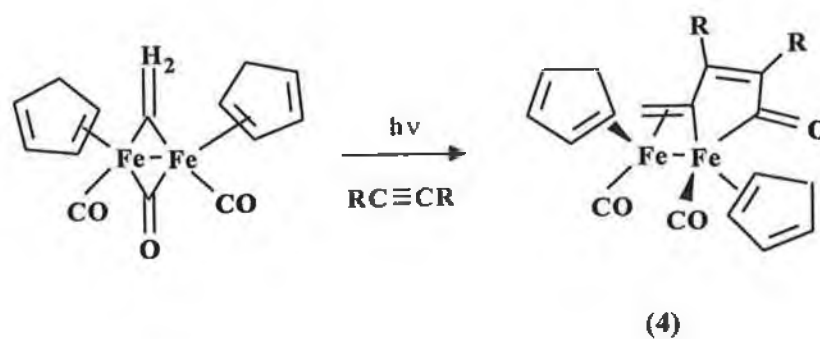
(a)



(b)



## Reaction 1.1(a-b)

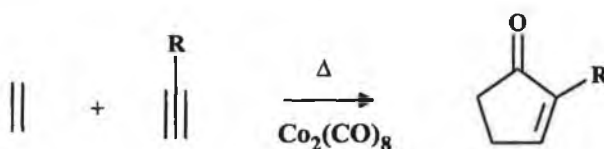


## Reaction 1.2

## 1.5 The Pauson - Khand Reaction

### 1.5.1 Origins of the Pauson - Khand Reaction

The convergent assembly of cyclopentenones from an alkene and an acetylene hexacarbonyldicobalt complex is known as the Pauson - Khand (PK) reaction (Reaction 1.3) and is widely used in the synthesis of biological compounds.<sup>17</sup> R groups on the alkyne can be functionalised organics, such as  $\text{NEt}_2$  or organometallics e.g. ferrocene. The variety of alkyne ligands that can be used is continually being explored. A number of reviews of the literature have appeared over the years outlining the progress and the limitations of the reaction.<sup>18</sup> This method of cyclisation is growing in popularity and developments are continually being reported on ways to improve its yield and utility.



**Reaction 1.3**

The development of this reaction has included many variations in the reaction conditions. Application of the Pauson - Khand (PK) reaction is often limited because of the need for high reaction temperatures and long reaction times. This restricts the range of organic substrates to those which demonstrate thermal stability. Mostly, yields are low for many intramolecular processes. The use of promoters has helped to improve this problem. Several substrates that are otherwise not reactive under normal conditions can be used. The viability of the reaction is strongly dependent on the substitution pattern and best results are achieved with unsubstituted and gem - disubstituted enynes at position 4 (Figure 1.5). Great reduction in yield is observed

for substituted alkenes, the exception being strained cyclic systems. Controlling the stereochemistry is also an important consideration as is the development of catalytic systems. Work has also concentrated on methods of extending the range of useful olefin and alkyne substrates.

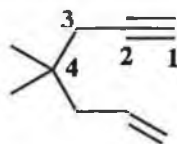


Figure 1.5

Most of the initial applications required a stoichiometric ratio of octacarbonyl dicobalt to alkyne and olefin. However, higher yields can be achieved using a catalytic amount of cobalt carbonyl in some systems. General procedures in the PK reaction include the initial formation of alkyne hexacarbonyl cobalt complexes by reaction of the alkyne of choice with octacarbonyl dicobalt. This complex then reacts with the alkene ultimately forming a cyclopentenone. Sometimes mixing alkene, alkyne and cobalt carbonyl in a “one pot” synthesis produces the cyclopentenone without need for isolation of the hexacarbonyl intermediate.

Of late, procedures using promoters such as N-oxide and alkyne bearing heteroatoms (see later section) have shown improved yields and reaction rates. Another procedure which is described in detail in a later section involves the use of dry adsorbates. Typically the work up is carried out using flash chromatography techniques.

### 1.5.2 Scope of the PK reaction

It is important to consider the different types of substrate alkynes and alkenes which can be used in the reaction. All alkynes with the exception of derivatives of propynoic acid can be used. If either R or R' groups of the acetylene are electron donors (e.g. alkyl group) such a group will tend to render the acetylene  $\pi$  orbitals more readily available for the formation of a  $\sigma$  bond to the metal. If the groups are electronegative (e.g.  $\text{CF}_3$ ) then back donation of electrons by the metal atom to the absorbing  $\pi^*$  orbitals of the acetylene will be facilitated. Electron withdrawing groups (see later section) on alkenes render them unsuitable for the PK reaction. However, when using tungsten complexes as catalysts in the PK reaction some electron withdrawing groups can be tolerated.<sup>19</sup> Unstrained cyclic alkenes are generally less reactive, giving usable yields only in a few cases. Cyclopentene and dihydrofuran are the exception.

In most cases, only intramolecular reactions achieved good control of regioselectivity. However, by correct selection of substituents on the alkyne ligand and on the alkene reactant, satisfactory regiocontrol can be achieved in intermolecular reactions. Terminal alkenes give poor yields and poor regioselectivity. One major problem associated with the intermolecular reaction is the formation of regioisomeric cyclopentenones when unsymmetrical substituted olefins are used, although unsymmetrically substituted acetylenes favour an orientation which places the larger substituent in the  $\alpha$  - position of the cyclopentenone. Three substituted positional isomers can be obtained by placing a large protecting group on the hexacarbonyl acetylene initially e.g.  $\text{Si}(\text{CH}_3)_3$ . After cyclopentenone formation, the protecting group can be easily removed. Krafft has more recently shown that reactions of terminal alkenes and internal alkynes are highly selective.<sup>20</sup>

Intramolecular cycloadditions occur upon complexation of derivatives of hept-en-6-yne and oct-1-en-7-yne to octacarbonyl dicobalt and subsequent heating

giving bicyclic enones. Intramolecular reactions give satisfactory results with terminal, internal and even trisubstituted alkenes while terminal alkynes are most favored. Steric hindrance plays an important role in the latter case where reactions with terminal alkynes are most favoured.

### 1.5.3 The Catalyst System

#### 1.5.3.1 Dicobalt octacarbonyl

The first and most widely used catalyst in the Pauson - Khand reaction was  $\text{Co}_2(\text{CO})_8$ .<sup>21</sup> Containing only cobalt metal and carbonyl groups it was amongst the earliest metal carbonyls to be isolated and characterised by Mond *et al.*<sup>22</sup> It was prepared from finely divided metal in a Cu lined autoclave made from Ni steel at 150 °C and a CO pressure of 30 - 40 bar. Current preparations employ reductive carbonylation of Co salts such as  $\text{CoCO}_3$ ,  $\text{CoO}$ ,  $\text{Co}(\text{OAc})_2$  and  $\text{Co}(\text{NO}_3)_2$  at elevated temperatures and a high pressure of hydrogen and carbon monoxide.<sup>23</sup> Among the reactions noted at the time was the slow air oxidation to give a violet basic carbonate. Consequently  $\text{Co}_2(\text{CO})_8$  is air sensitive both in the solid state and in solution. The bimetallic complex was also found to decompose in reactions with halides and at higher temperatures.<sup>24</sup> Cobalt sources such as cobalt clusters and cobalt metal can be used to generate  $\text{Co}_2(\text{CO})_8$ .<sup>25</sup> A decomposition product of the cobalt carbonyl,  $\text{Co}_4(\text{CO})_{12}$  will also revert back to  $\text{Co}_2(\text{CO})_8$  at high pressures of CO.

$\text{Co}_2(\text{CO})_8$  contains a Co - Co bond with bridging carbonyl groups ( $>\text{C}=\text{O}$ ) in addition to terminal carbonyl groups ( $-\text{C}\equiv\text{O}$ ). The bond order is reflected in the carbonyl stretching frequency, 2143  $\text{cm}^{-1}$  for free CO and  $1950 \pm 100 \text{ cm}^{-1}$  for terminal carbonyl groups. The bond order may again be inferred from the IR frequency which is  $1800 \pm 50 \text{ cm}^{-1}$  for the bridging carbonyl groups compared with  $1715 \pm 10 \text{ cm}^{-1}$  for saturated ketones for example.

The IR spectrum of a metal carbonyl thus provides important information on the nature of the carbonyl groups present and may allow one to distinguish between structures with only terminal carbonyl groups or structures containing one or more bridging carbonyl groups e.g. 2 isomers of  $\text{Co}_2(\text{CO})_8$ . The metal atoms are zerovalent and are formally  $d^9$  but diamagnetic because of the Co - Co bond. Three structures have been observed by combining a single crystal X-ray structural determination of the orange crystals<sup>26, 27</sup> at higher temperatures and by IR investigation<sup>28</sup> of  $\text{Co}_2(\text{CO})_8$  in solution, a  $C_{2v}$  isomer **5a** with two bridging carbonyl groups in the solid, a  $D_{3d}$  isomer **5b** as well as a second non-bridged isomer **5c** of unknown structure in solution (Figure 1.6).

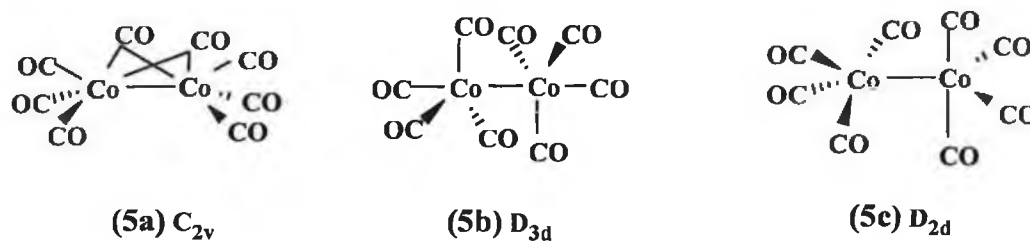
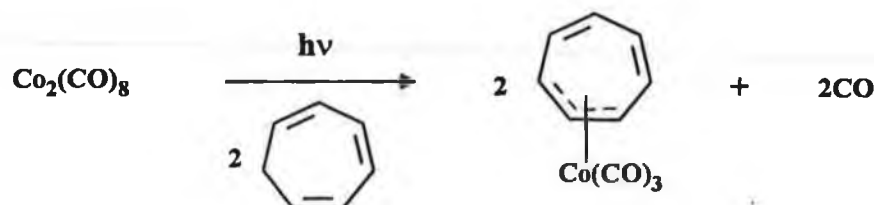


**Figure 1.6** The 3 isomers of octacarbonyl dicobalt:- (5a) predominates at  $T < 0^\circ\text{C}$ , (5b) exists at  $0 > T < 100^\circ\text{C}$ , (5c) exists at  $T > 100^\circ\text{C}$ .

At very low temperatures the bridged form  $C_{2v}$  predominates and as the temperature is raised the second isomer  $D_{3d}$  appears while temperatures greater than  $100^\circ\text{C}$  gives rise to the third isomer  $D_{2d}$ . Further evidence was supported by the electronic spectra produced by Wrighton *et al.*<sup>29</sup> At room temperature there exists a strong band at 350 nm with a shoulder on the higher energy side. Upon cooling, the lower energy band reduces in intensity and a well defined intense band at 280 nm appears. Assignment of these bands is to the  $\sigma - \sigma^*$  transition of the non-bridged species at 350 nm, while the band at 280 nm has been attributed to the  $d\pi - \sigma^*$  transition in the cobalt bridged dimer.



Simple photosubstitution of CO is an important photoreaction of  $\text{Co}_2(\text{CO})_8$  and some photoinduced metal - metal bond cleavage has been reported<sup>30</sup> as exemplified by Reaction 1.4.



**Reaction 1.4**

Matrix studies of the photochemistry of  $\text{Co}_2(\text{CO})_8$  have showed CO loss to be the dominant photoprocess in an inert matrix giving  $\text{Co}_2(\text{CO})_7$ .<sup>31</sup> Other evidence for Co - Co bond cleavage in CO matrices giving  $\text{Co}(\text{CO})_4^-$  has also been reported.<sup>32</sup>

#### 1.5.3.2 Thermal studies of cobalt - carbonyl systems

In 1954 Sternberg, Wender *et al.*<sup>1</sup> showed that  $\text{RC}\equiv\text{CR}'$ , readily displaced the two bridging carbonyl groups in octacarbonyl dicobalt  $\text{Co}_2(\text{CO})_8$  yielding  $(\text{RC}_2\text{R}')\text{Co}_2(\text{CO})_6$ , two carbon, two cobalt tetrahedranes type complexes. Sly<sup>33</sup> using single crystal X-Ray diffraction techniques determined the molecular structure of diphenylacetylene cobalt hexacarbonyl. Later Bonnet<sup>34</sup> determined the structure of  $(\mu_2\text{-C}_6\text{H}_5\text{C}_2\text{H})\text{Co}_2(\text{CO})_4(\text{PMe}_3)_2$  demonstrating the localised  $\text{C}_{2v}$  symmetry about the cobalt center. The metal - metal distance of 2.47 Å is consistent with the presence of a metal - metal bond. The arrangement of CO groups in  $(\mu_2\text{-alkyne})\text{dicobalthexacarbonyl}$  compounds represents a distorted octahedral arrangement of six bonds about each metal atom (provided each metal - acetylene C atom interaction is described as a discrete bond). This results in the two pairs of CO groups being directly trans to each other.

Bower and Stiddard<sup>35</sup> had assigned a  $D_{3d}$  structure to  $\text{Co}_2(\text{CO})_6(\text{PR}_3)_2$ . Bor and Kettle<sup>36</sup> assigned  $C_s$  symmetry and observed five IR active bands. Later, based on studies using isotopic substituted molecules by Iwashita,<sup>37</sup> an assignment of the infrared absorption bands of the coordinated acetylene complex  $(\mu_2\text{-C}_2\text{H}_2)\text{Co}_2(\text{CO})_6$  was proposed; 3116 and 3086  $\text{cm}^{-1}$ ,  $\nu(\text{CH})$ ; 2098, 2051, 2034, 2028 and 2016  $\text{cm}^{-1}$ ,  $\nu(\text{CO})$ ; 1403  $\text{cm}^{-1}$ ,  $\nu(\text{CC})$ ; 894 and 768  $\text{cm}^{-1}$ ,  $\nu(\text{CH deformations})$ ; 605 and 551  $\text{cm}^{-1}$ ,  $\nu(\text{Co - acetylene})$ . In the free acetylene the  $\nu(\text{CC})$  band appears at  $\sim 1974 \text{ cm}^{-1}$ . A strong metal - acetylene interaction is also indicated by the high frequencies of the cobalt-acetylene stretching vibrations. Varadi & Palyi<sup>38</sup> showed how the influence of the electronic structure of R and R' in cobalt complexes provided an assignment for CO stretching bands.

One or two carbonyl ligands in  $(\mu_2\text{-RCCR}')\text{Co}_2(\text{CO})_6$  compounds can be replaced by phosphines as demonstrated by the synthesis of acetylene and diphenylacetylene - $\text{Co}_2(\text{CO})_5\text{PPh}_3$  and - $\text{Co}_2(\text{CO})_4(\text{PPh}_3)_2$  complexes.<sup>39</sup> An increase in electron donor character of both the phosphine and the bridging ligand makes substitution more efficient. Steric factors are also important. Larger aromatic substituents on the phosphine make preparation of these derivatives more difficult. Varadi and Palyi<sup>38</sup> have shown that phosphine substitution occurs in all cases in the axial rather than equatorial position, (Figure 1.7) based on IR spectroscopy.

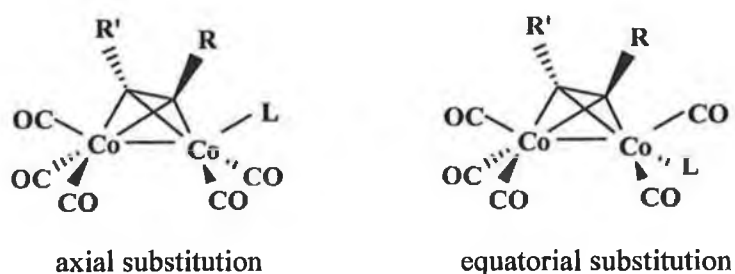
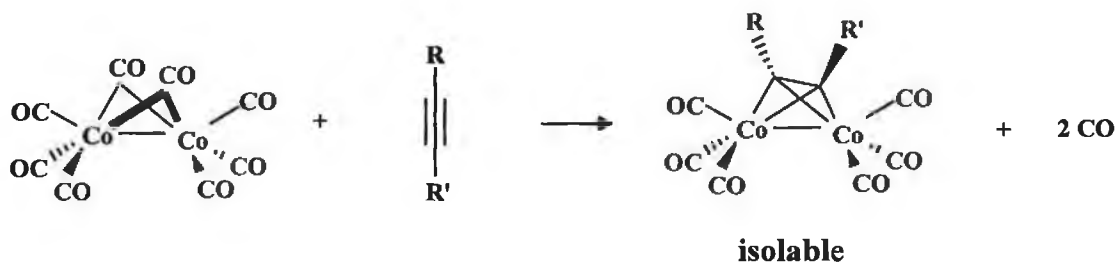


**Figure 1.7** Axial and equatorial substitution of ligand L ( $L = \text{phosphine}$ ) in dicobalt hexacarbonyl complexes.

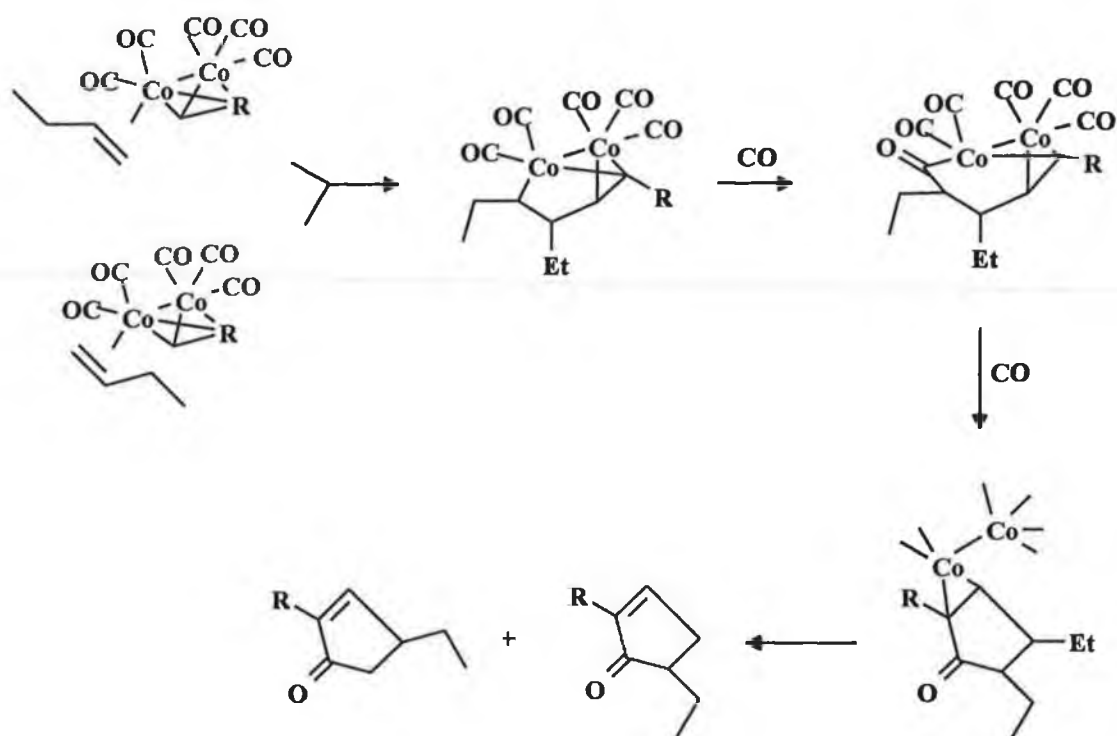
### 1.5.4 Mechanism of the Pauson - Khand Reaction

The initial step in the reaction of an alkyne with cobalt carbonyl is the substitution of two bridging carbonyl ligands by one acetylene with the liberation of two molecules of CO giving rise to a  $(\mu_2\text{-alkyne})\text{Co}_2(\text{CO})_6$  complex. The alkyne ligand is placed at right angles to the Co - Co bond (Reaction 1.5). Alkynes with bulky substituents tend to react more slowly. Once generated, this alkyne hexacarbonyl dicobalt forming step is irreversible and in many cases the complex thus formed has been isolated. It is beyond this point in the reaction scheme that evidence to support a reaction mechanism is lacking. The current level of mechanistic understanding is inferred from observations of regio- and stereochemistry in a large number of examples. The actual path of the reaction depends mainly on the substitution of the acetylene used.



#### Reaction 1.5

It is assumed that the complexation of the alkene to one Co atom occurs in a reversible process via a dissociative loss of one carbonyl ligand. Irreversible insertion of the complexed face of the alkene  $\pi$  bond into one of the formal Co - CO bonds of the alkyne complex occurs. This is followed by CO addition to the coordinately unsaturated cobalt atom. Migratory insertion of a cobalt bound carbonyl, addition of another CO molecule and reductive elimination of the  $\{\text{Co}(\text{CO})_3\}$  moiety occurs. Loss of the  $\text{Co}_2(\text{CO})_6$  fragment either before or after attachment of an additional ligand completes the process (Scheme 1.1).



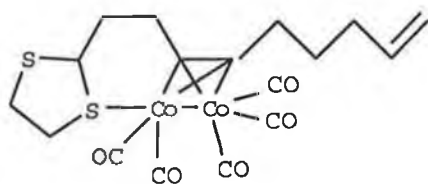
**Scheme 1.1** *Proposed mechanism of the Pauson - Khand reaction.*

While alkene regiochemistry is not easily predictable, alkyne regiochemistry is governed mainly by steric crowding and is determined during the insertion into the cobalt - carbon bond. If the alkyne is unsymmetrical, insertion and carbon - carbon bond formation proceed exclusively at the alkyne carbon possessing the smaller substituent.

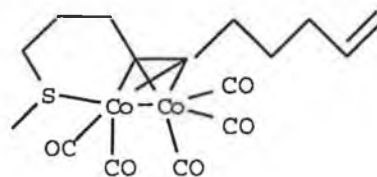
#### 1.5.4.1 Trapping of an Intermediate

The instability of intermediate complexes has thus far prevented their isolation in the PK reaction, with the exception of a propargylic sulfide complex isolated by Krafft *et al.*<sup>40</sup> Structure determination of intermediates would undoubtedly shed significant light on the reaction pathway of the PK reaction.

During a course of study where heteroatom - substituted substrates containing S, N, or O were shown to enhance the reactivity of the PK reaction<sup>41</sup>, Krafft showed that the greatest effect on the reaction rate was observed with S and N ligands. In further studies on similar *N* - methylmorpholine - *N* - oxide (NMO) promoted reactions with complexes containing S - substituted substrates,<sup>40</sup> TLC analysis revealed complexes (6) and (7). These were then converted to the respective bicyclic cyclopentenones. NMR investigation of these two complexes indicated the presence of coordinated S through the chemical shift of protons adjacent to the S and a non - equivalence of the methylene protons on the tether between the alkyne and sulfide. Decomposition of (6) and (7) generated paramagnetic impurities which prevented further NMR studies. The trapping of the pentacarbonyl complex provides direct experimental evidence for removal of CO from the alkyne hexacarbonyl complex by amine oxides. This is the most important second step in the PK reaction.



(6)



(7)

### 1.5.5 Reaction Promoters

The PK reaction often involves the use of high reaction temperatures and high pressures of CO. Thermal degradation can limit the number of organic substrates which can be employed. It was discovered unexpectedly by Smit *et al.*<sup>42</sup> that reaction on dry adsorbent (silica or alumina) in an *oxygen* atmosphere promotes the intramolecular PK reaction at a rate faster than when the reaction is carried out in solution. In an *argon* atmosphere, monocyclic products were obtained rather than the bicyclic enones. Optimum water content for reaction lies between 10 - 20 %.

Table 1.1 lists other promoters which have been used in accelerating the PK reaction. Most of the recent reports concentrate on specific reactions but all have a critical limitation of their reactivities toward the intermolecular PK reaction.

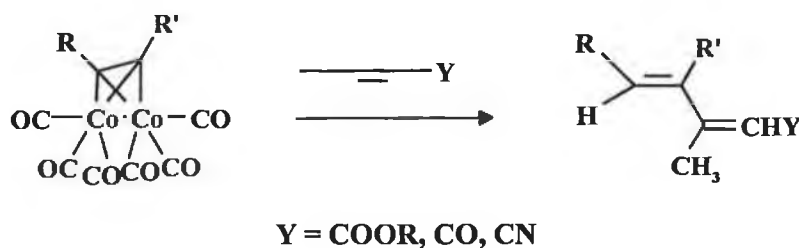
**Table 1.1 Promoters of the Pauson - Khand reaction.**

Entry	Promoter	Reference
1.	Adsorbates Silica gel Alumina	42, 43
2.	Ultrasound	44
3.	<i>tert</i> -amine <i>N</i> -Oxides:- <i>N</i> -methylnmorpholine <i>N</i> -oxide (NMO) trimethylamine <i>N</i> -oxide (TMO)	45, 46
4.	Dimethyl sulfoxide (DMSO)	47
5.	Amines <sup>a</sup> :- tetramethylenediamine $\alpha$ - methylbenzylamine dimethylformamide (DMF)	48

<sup>a</sup>DCM/t-BuOH using CoBr<sub>2</sub>/Zn/CO

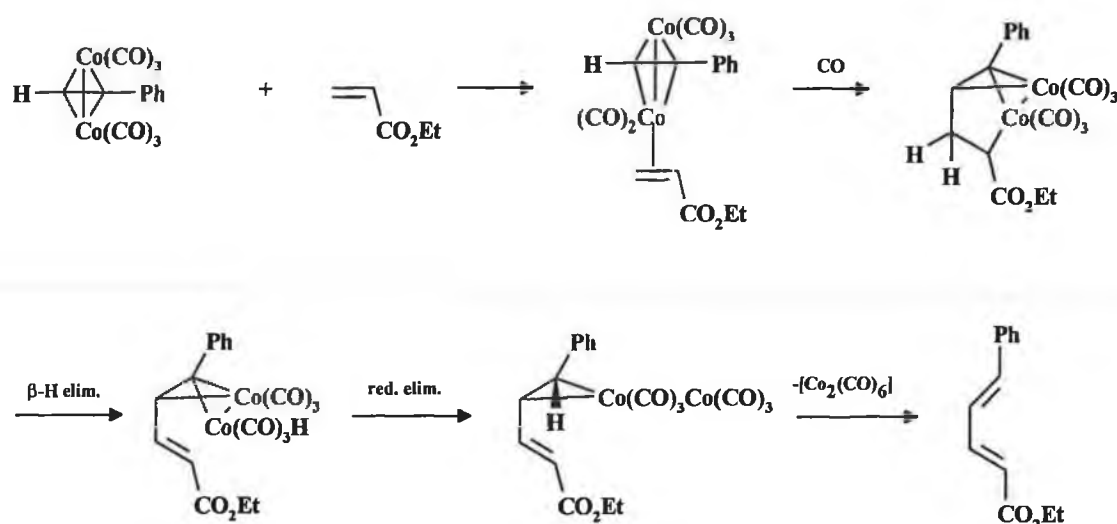
### 1.5.6 Pauson - Khand reactions with Electron Deficient Groups

A variation of the reaction was encountered when alkenes bearing strongly electron withdrawing groups (CN, CO<sub>2</sub>R, SO<sub>2</sub>R etc.) were examined.<sup>19</sup> Reacting with terminal acetylene complexes, the alkenes produced linear coupling products rather than cyclopentenones (Reaction 1.6).



**Reaction 1.6**

The proposed mechanism involves the insertion of the alkene into the cobalt alkyne complex and hydrogen migration yielding the diene product. The reaction is completely regioselective, the new C - C bond forming between the less hindered alkyne C and the less hindered electropositive polarised alkene C. The electron withdrawing group in every example of the reactions reported is  $\pi$ -conjugating. It has been suggested<sup>26</sup> that the  $\beta$ -hydrogen elimination/ reductive elimination sequence competes with CO insertion, by providing a driving force for regeneration of the alkene (Scheme 1.2).



Scheme 1.2

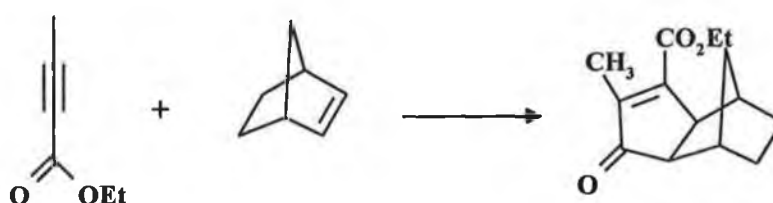
When styrene and substituted styrenes are used both cyclopentenones and dienes are formed. No consistent pattern with different substituents on styrene has been observed. In particular, no consistent enhancement of diene yield results from attachment of either the electron withdrawing *p*-halogen or the more electron withdrawing  $\{\text{Cr}(\text{CO})_3\}$  group on the arene. When diolefins were used both dienes and cyclopentenone products were observed. 2-vinylfuran and vinylferrocene, regarded as being electron rich systems, yielded dienes with only trace quantities of ketones. With respect to alkynes ethoxyacetylene and similar electron poor substituents gave low yields and propargyl alcohol failed to react.

Electron deficient alkenes yielded only dienes in the PK reaction. However, recently Krafft has observed that electron deficient alkynes can undergo cycloaddition to give pentenones for both intra- and intermolecular reactions on the absence of any diene products.<sup>49</sup>

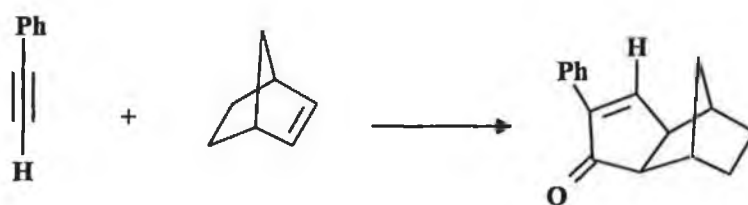


In early reports reaction with only methyl propynoate were observed.<sup>50</sup> Using NMO as a promoter<sup>46,51</sup> at ambient temperature the best results were obtained for the intramolecular cycloaddition. Alkyne dicobalthexacarbonyl complexes were prepared initially, purified and isolated. Redissolution in solvent (usually  $\text{CH}_2\text{Cl}_2$ ) followed by sequential addition of solid NMO monohydrate at 0 °C and stirring for two hours usually gave the cyclopentenones which were then purified by conventional methods. Solvent mixtures THF/ $\text{CH}_2\text{Cl}_2$  caused substantial decomplexation of the alkyne moiety from the dicobalthexacarbonyl core. Unsubstituted terminal alkynoates usually failed to undergo cycloaddition and in a few cases where the reaction occurred, the yields were low.

For intermolecular cycloaddition reactions, cobalt alkynoates complexed with alkenes gave moderate to excellent yields. Previous reactions with terminal alkenes and internal alkynes suggest that steric interactions between alkene and alkyne substituents are responsible for formation of 2,3,5-trisubstituted cyclopentenone rather than 2,3,4-trisubstituted enones. In the majority of cases with asymmetrical alkynes the larger substituent is  $\alpha$  to the carbonyl in the product. This larger substituent was placed at the 1,4 position (Reaction 1.7) instead of the usual 1,3 (Reaction 1.8). Utilisation of 1,6-enynes containing a double bond bearing an electron withdrawing group as substrates, which were previously found unable to undergo intermolecular PK reaction, has also been reported by Smit and Caple.<sup>52</sup>

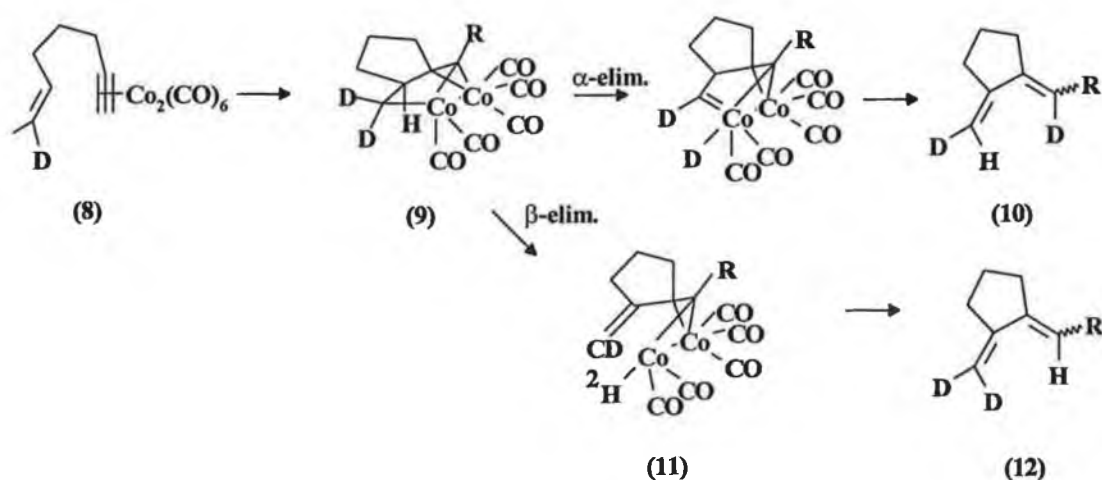


**Reaction 1.7**



### Reaction 1.8

Very recently<sup>53</sup> Krafft has shown that thermolysis of unactivated hexacarbonyldicobalt complexes of 1,6- or 1,7- enynes under a nitrogen atmosphere predominantly yields monocyclic 1,3 - dienes. The mechanism was investigated by isotope enrichment studies.  $\alpha$  - elimination of enyne (8) would give rise to diene (10) whereas  $\beta$  - elimination would give rise to diene (12) (Scheme 1.3).



**Scheme 1.3**

The  $\alpha$  - elimination pathway was insignificant because of the lack of deuterium scrambling in the cycloaddition of a variety of enynes. However, allylic C-H coupling was implicated rather than a formal  $\beta$  - elimination step based on the observed diene product. A formal  $\beta$  - elimination from (9) to (11) should prefer a transition state in which the M-C and C-H bonds are approximately *syn* and parallel. Since the relevant metal center is in the five - membered metallacyclic ring, this alignment would be difficult to achieve with that metal.

#### 1.5.7 Alternative Pauson - Khand Catalytic Systems

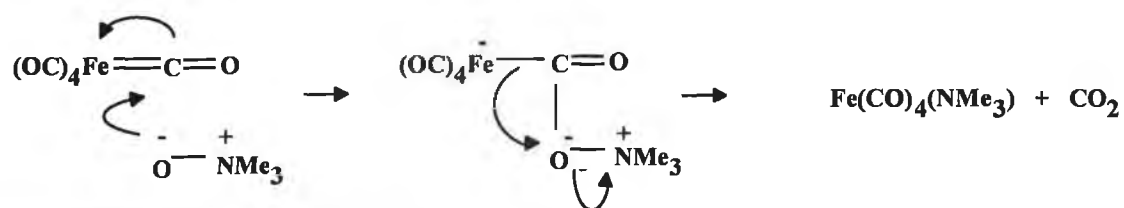
While cobalt carbonyl is the most widely used metal complex to induce conversion of enynes to bicyclic cyclopentenones interest is growing in relation to the use of alternative metal complex catalysts which have the advantage of being more cost efficient. Another factor is that these 'alternative' PK promoters are shown to promote some cyclisations that have not been accessible using the traditional cobalt catalyst. These alternative systems involve iron, molybdenum, tungsten, titanium, nickel, rhodium, ruthenium, palladium and zirconium complexes as well as other cobalt systems such as (indenyl)Co(cod) and Co(acac)<sub>2</sub>.<sup>54</sup>

### 1.5.7.1 Intramolecular Pauson - Khand reactions involving non cobalt catalysts

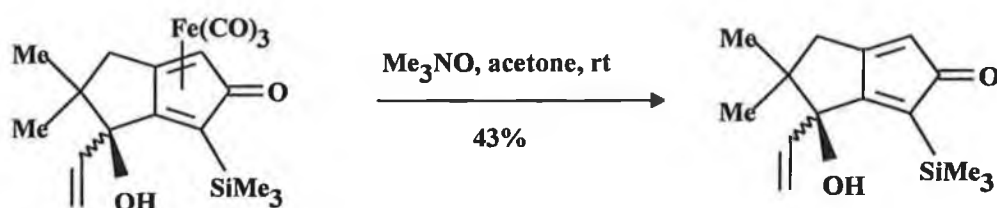
### 1.5.7.2 Iron carbonyl catalysts

Pearson reported that iron carbonyl complexes can promote the PK reaction in 1991.<sup>55</sup> By modification of a method whereby nona-2,7,diyne was converted to a cyclopentadienone-Fe(CO)<sub>3</sub> by reaction with Fe(CO)<sub>5</sub>,<sup>56</sup> the yield was increased from the original 14 % to 87 % by increasing reaction temperature from 110 °C to 135 - 145 °C. The reactions were carried out in sealed tubes charged with 50 - 60 psi of CO. Overall reaction times were found to be long, in some cases taking up to 60 hours to reach completion. When alkenes containing gem dimethyl groups were used, cyclic dienes were obtained, a product formed usually in the intramolecular ene reaction.

Hydroxy-substituted diynes which previously had presented problems with cobalt carbonyl promoted PK reactions were later shown to cyclise, forming bicyclopentadienone Fe(CO)<sub>3</sub> complexes.<sup>57</sup> In order to be synthetically useful, decomposition of the product must be efficient. In some cases demetalation of complexes was achieved using trimethylamine N-oxide. Although yields were moderate to high for most of the substrates tried, no diastereoselectivity was obtained during the reactions, with equimolar amounts of *syn* and *anti* alcohols being formed in each case. A mechanism was proposed to account for the demetallation reaction based on the common assumption that amine oxide promoted removal of a carbonyl ligand from all transition-metal carbonyls proceeds according to the mechanism shown in Scheme 1.4.<sup>58</sup> Five, six and seven membered fused rings were formed in these reactions. Trimethylsilyl functional groups were included as terminal groups on the starting alkynes with the intention that these could be removed from the cyclopentadienones formed giving rise to less highly substituted molecules (Scheme 1.5). This scenario has been used in traditional PK reactions.

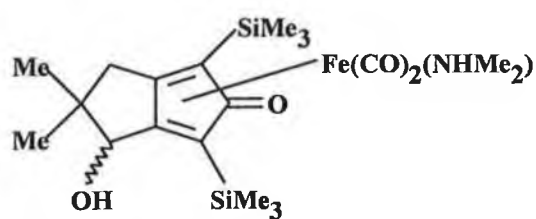


Scheme 1.4

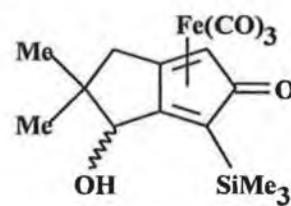


Scheme 1.5

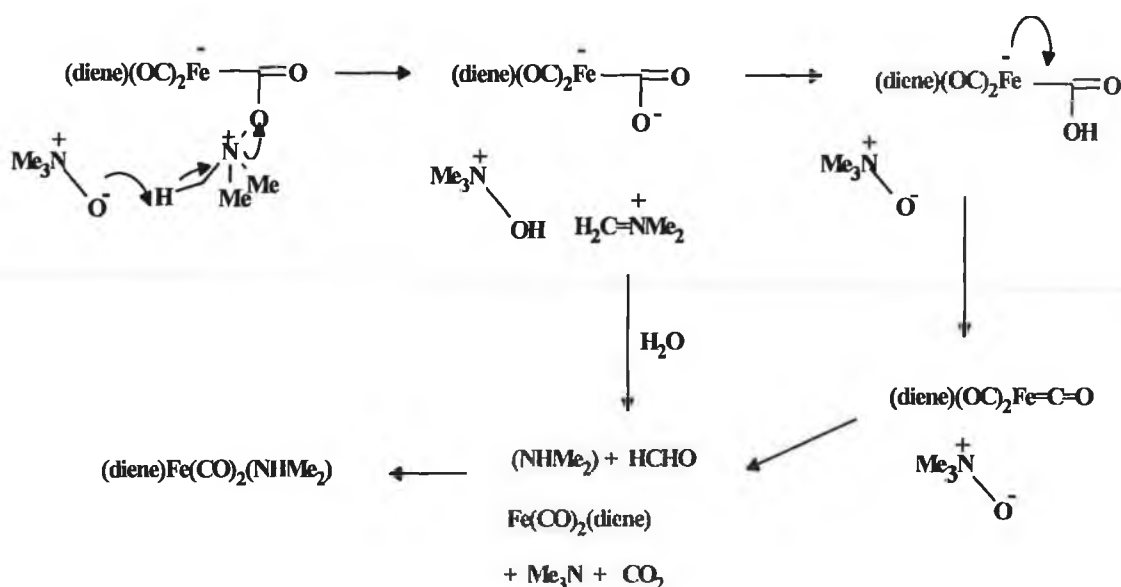
The diene- $\text{Fe(CO)}_2(\text{NHMe}_2)$  complex (**13**) was isolated in attempts to demetallate complex (**14**) using trimethylamine N-Oxide. The mechanism as presented in Scheme 1.6 was proposed to account for the demethylation reaction. Further treatment of (**13**) with  $\text{Me}_3\text{NO}$  effected its conversion to the corresponding cyclopentenone.



(13)



(14)



Scheme 1.6

Pearson<sup>59</sup> also reported the iron carbonyl promoted cyclocarbonylation of 1,6 enynes to give bicyclo[3.3.0]octenones which is essentially equivalent to the intramolecular PK reaction. The yields of reaction promoted by  $\text{Fe}(\text{CO})_5$  are similar to  $\text{Co}_2(\text{CO})_8$  promoted reactions. Enyne ethers undergo cyclisation most readily. Cyclisation of terminal alkynes could not be achieved with ether derivatives, however, all other internal alkynes (with  $\text{SiMe}_3$ , Ph, Et, Me terminal groups) used were successful. An 8-oxabicyclooctenone cyclisation however was unsuccessful.

A coordinately unsaturated  $\{\text{Fe}(\text{CO})_4\}$ , which is presumed to be an involved intermediate in iron carbonyl promoted PK reactions, was sought by means other than by thermal dissociation of a CO ligand from  $\text{Fe}(\text{CO})_5$ .  $\text{Fe}(\text{CO})_4(\text{acetone})$  is formed from the reaction of acetone and  $\text{Fe}_2(\text{CO})_9$ . Analogous complexes prepared respectively from mecn or  $\text{NMe}_3$  gave  $\text{Fe}(\text{CO})_4(\text{mecn})$  or  $\text{Fe}(\text{CO})_4(\text{NMe}_3)$ . Yields of cyclocarbonylation with these  $\text{Fe}(\text{CO})_4\text{L}$  complexes were generally higher than those obtained using iron pentacarbonyl in mecn. However, the pregeneration of  $\text{Fe}(\text{CO})_4\text{L}$  complexes requires higher temperatures and also involves synthesis and handling of

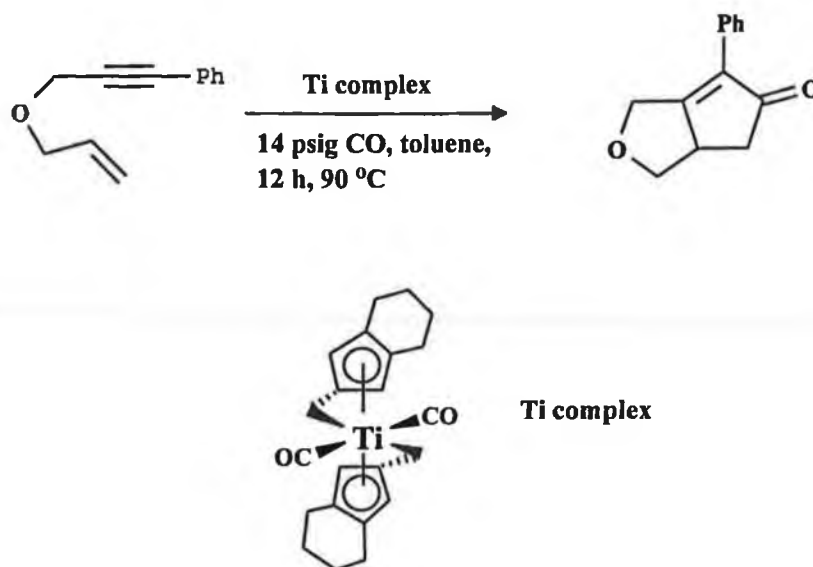
air-sensitive intermediates.<sup>60</sup> Also a major drawback was that the 5-en-1-yne isomer of the starting material was obtained as a major byproduct from these reactions.

#### 1.5.7.3 Tungsten carbonyl catalysts

Tungsten pentacarbonyl has been shown to promote “PK like” cyclisation with substrates including electron deficient -alkene or -alkyne moieties.<sup>19</sup> As previously, use is made of  $M(CO)_{n-1}(\text{solvent})$  complexes where typically 10 mol %  $W(CO)_5(\text{THF})$  was used as the catalyst. In this case however  $W(CO)_5(\text{THF})$  is generated by irradiation of  $W(CO)_6$  in dry THF. Advantages to this procedure include the air stability of  $W(CO)_6$  as well as its relative less toxicity in comparison to other metal carbonyls. Use was also made of the promoter DMSO with  $W(CO)_6$  again cyclising electron deficient alkynes.<sup>61</sup>

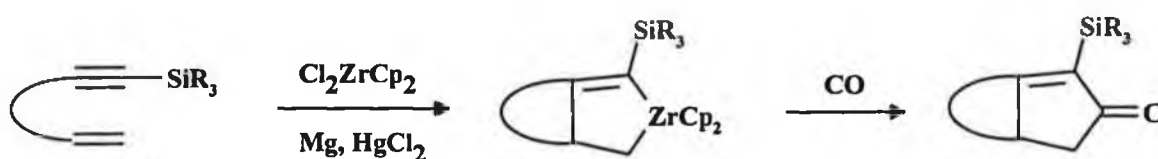
#### 1.5.7.4 Titanium and Zirconium catalysts

Titanium catalysed enyne cyclisation/isocyanide insertions are also known.<sup>25</sup> Usually iminocyclopentenones are formed from the use of 10 mol % of  $CpTi(PMe_3)_2$  when an isocyanide is used instead of a CO and a subsequent hydrolysis step gives the corresponding bicyclic cyclopentenones (Reaction 1.9). One drawback is the lengthy procedure required but the reaction tolerates the presence of polar functional groups such as ethers, N - containing compounds and esters, as well as chiral enynes. In general, reactions promoted by  $CpTi(PMe_3)_2$  give poor yields.



Reaction 1.9

$\text{Cp}_2\text{TiCl}_2$  and  $\text{Cp}_2\text{ZrCl}_2$  metallocenes in the presence of CO can cyclise enynes by initially forming metallacycles. They are subsequently converted into enones by carbonylation (Scheme 1.7).<sup>62</sup> Terminal alkynes are unsuitable substrates but may be used if a suitable protecting group is used. Generally the range of substrates which are suitable for reaction is limited by the basic, highly reducing conditions.

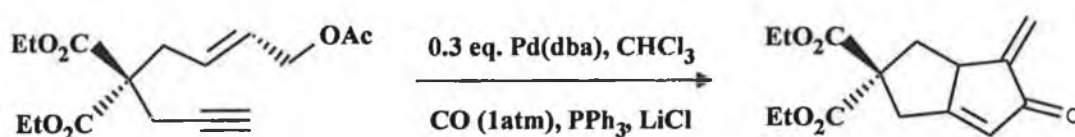


Scheme 1.7



## 1.5.7.5 Palladium and Molybdenum catalysts

Heathcock *et al.*<sup>63</sup> reported the use of a palladium catalyst in the synthesis of an  $\alpha$ -methylene cyclopentenone fused to a five membered ring (Reaction 1.10). Heating (alkyne)Mo<sub>2</sub>Cp<sub>2</sub>(CO)<sub>4</sub> complexes<sup>64</sup> with the commonly studied alkenes norbornadiene and norbornene surprisingly gave rise to the cyclopentenones in Reaction 1.11.



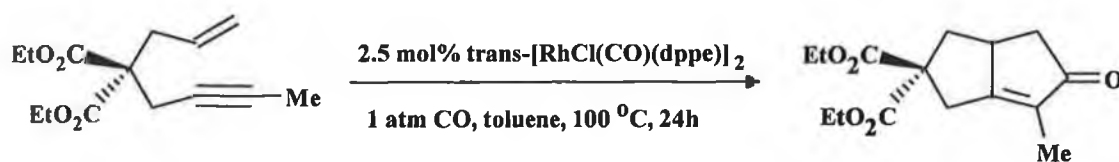
Reaction 1.10



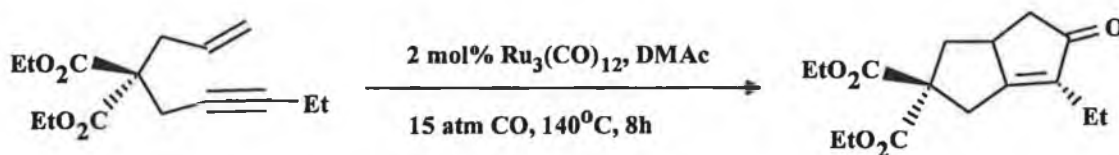
Reaction 1.11

## 1.5.7.6 Rhodium and Ruthenium catalysts

Rhodium catalysts such as [RhCl(CO)<sub>2</sub>]<sub>2</sub> and RhCl(CO)(PPh<sub>3</sub>) have also been used to convert enynes to bicyclic enones.<sup>65</sup> Jeong *et al.*<sup>66</sup> reported a catalytic intramolecular PK reaction using *trans*-RhCl(CO)(dppe) as a Rh(I) catalyst in the presence of an atmosphere of CO (Reaction 1.12). Using PPh<sub>3</sub> substituted analogues required the use of AgOTf for initial activation.

**Reaction 1.12**

Mitsudo *et al.* reported the first ruthenium-catalyzed intramolecular reaction. *N,N*-dimethylacetamide (DMAc) was the promoter under 15 atmospheres of CO (Reaction 1.13).<sup>67</sup>

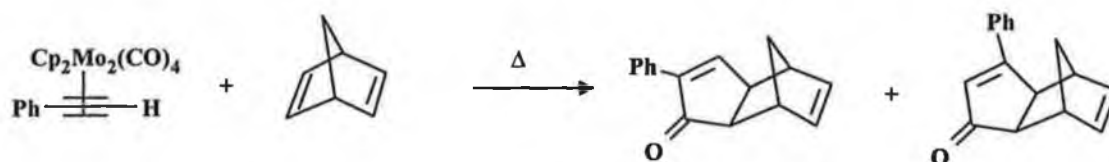
**Reaction 1.13**

#### 1.5.7.7 Intermolecular Pauson-Khand reactions involving (indenyl)Co(I) and Mo catalysts

All metal promoters discussed previously are involved in catalytic *intramolecular* PK like cyclisations. Chung,<sup>68</sup> however, reported the first practically useful catalytic system for the formation of cyclopentenones *intermolecularly* using 1,4-cyclooctadiene(indenyl)cobalt(I) as catalyst. In addition some intramolecular substrates were also used effectively. Norbornadiene or norbornene substrates, terminal alkynes and 1 mol % of catalyst was sufficient to effect cyclisation. 1,7-octadiyne and propargyl alcohol, which usually give low yields with the  $\text{Co}_2(\text{CO})_8$  catalyst, were obtained in excellent yield. Disubstituted alkynes diphenylacetylene

and methylphenylacetylene proceeded less efficiently. In all cases the oxo isomer was formed.

The molybdenum - alkyne complex mentioned earlier was also found to be effective for intermolecular cycloaddition.<sup>64</sup> Heating a phenylacetylene- $\text{Mo}_2\text{Cp}_2(\text{CO})_4$  complex with the strained alkene norbornadiene produced the corresponding cyclopentenones substituted at both the 2 and 3 position in 45 and 32 % yield respectively (Reaction 1.14).



**Reaction 1.14**

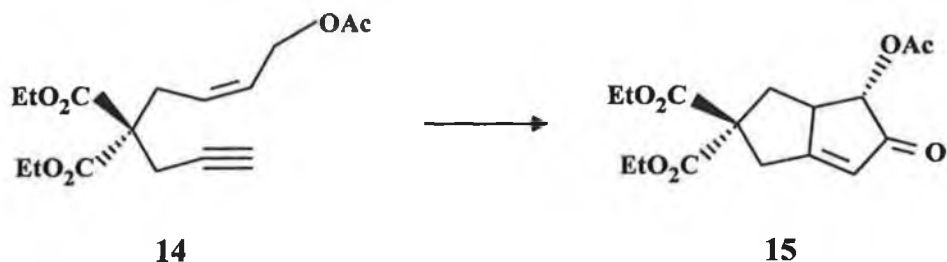
As with  $\text{Co}_2(\text{CO})_8$ , alternative PK promoters have problems in relation to substrates and reaction conditions. Most importantly, however, they do provide access to compounds not accessible by traditional means.

#### 1.5.8 Photochemistry and the Pauson - Khand Reaction

Many PK reactions to date require that the metal carbonyl fragment be supplied in stoichiometric quantities, which is a significant problem for commercialisation of the PK process. There has been considerable interest in the development of systems which use only catalytic amounts of the metal carbonyl. However, only a few examples of catalytic reactions have appeared in the literature.<sup>68</sup> Those that have, tend to require lengthy procedures but recently Livinghouse<sup>69</sup> and Pauson<sup>70</sup> have investigated a number of systems of a photochemically driven

stoichiometric PK reaction which proceeded in very low yields. Using a Q-beam MAX MILLION spotlight as the visible light source, Livinghouse showed the intramolecular PK reaction proceeded catalytically at 50 - 55 °C under 1 atmosphere of CO pressure, typically for 4 - 12 hours. The precise role the photon plays in the reaction however, remains uncertain. In the past thermal reactions with enynes have been formed mainly on cyclisation of 1,6, enynes. Reactions 1.15(a-c) shows a selection of substrates which have been used including the 1,7 enyne (14). Selective cyclisation was also observed with (18) yielding (19).

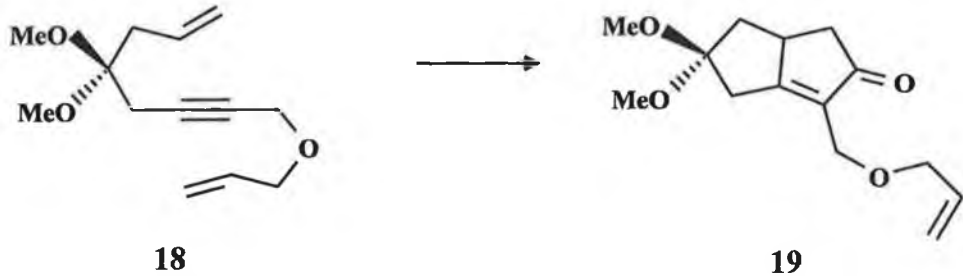
(a)



(b)



(c)



Reactions 1.15(a-c)

In general low concentrations of substrate inhibited the photochemical PK reaction. Choice of light source and purity of  $\text{Co}_2(\text{CO})_8$  were found to be critical. Solvent systems hexane, THF and acetonitrile were found to be inferior to ethyl acetate, 1,2-dimethoxyethane (1,2-DME) and diglyme, the most efficient being 1,2 DME.

### 1.5.9 Synthetic Applications

#### 1.5.9.1 Prostaglandin History

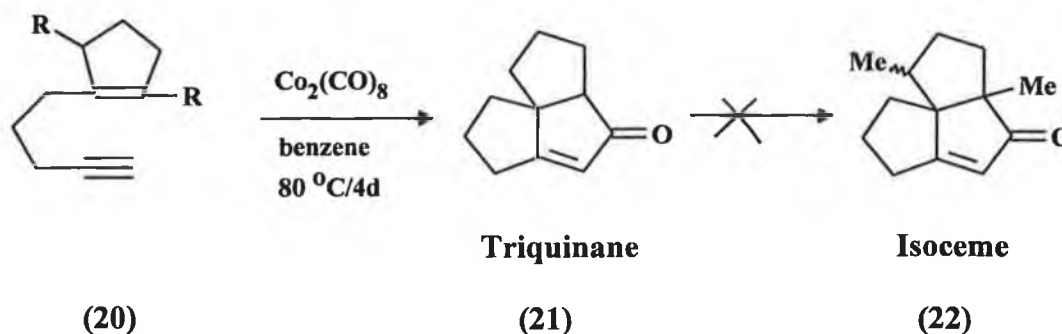
Seventy years ago scientists in Europe and the USA observed that lipid fractions isolated from human semen induced contraction and relaxation of the human uterus. The active component, prostaglandin (PG), was named by Van Euler who believed that the substance was produced in the prostate gland. In fact, prostaglandin is widely distributed in mammalian tissue. Onions contain appreciable quantities of PG  $\text{A}_1$  while PG  $\text{A}_2$ -15 acetate has been obtained from coral found in the Caribbean. Thirty years later Bergstrom *et al.* isolated the first prostaglandins in pure form and determined their structure.

In general they exhibit a wide range of biological activity. Rheumatoid arthritis is probably caused by overproduction of PG in the diseased joint. Aggregation of blood platelets in humans and induction of labour are also promoted by the presence of PG's. Under production of a particular PG could be corrected by the administration of a suitable prostanoid (agonist) which binds specifically to the appropriate biological receptor and elicits the same response as that given by the naturally produced substance.

Prior to the development of the Pauson - Khand cyclisation reactions lengthy synthesis were required to obtain prostaglandin analogues.<sup>71, 72</sup> New analogue designs were sought to avoid intermediates which take numerous steps to prepare. Pauson and Khand have provided a cyclopentenone synthesis which offers improvements in both efficiency and ease of use.

### 1.5.9.2 Triquinanes

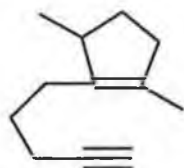
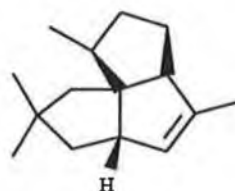
Magnus used intramolecular  $\text{Co}_2(\text{CO})_8$  promoted cyclopentenone preparation for the total synthesis of corolin, a linear fused triquinane.<sup>73</sup> Bicyclo[4.3.0] nonanes and bicyclo[3.3.0] octanes<sup>74</sup> were previously reported as precursors for the synthesis of corolin and hirsutic acid. The first attempts to produce angularly fused triquinanes (tricyclo[6.3.0] undecanes) avoiding the use of carbocyclic starting materials was suggested by Schore.<sup>75</sup> Treating enyne (20) with  $\text{Co}_2(\text{CO})_8$  produced triquinane (21) - the first example of the generation of a quaternary carbon at multiple ring fusion. Attempted methylation of the triquinane, however, could not produce isoceme (22).



In a later report Schore showed two approaches towards cyclisation precursors for angularly fused triquinanes. One involves producing the unsubstituted ring system in only four steps from acyclic precursors. The second is a regiochemically controlled construction of more highly substituted derivatives. A tetrasubstituted alkene substrate (23) was tested for compatibility to undergo intramolecular PK reaction in

an attempt to find the fate of the allylic methyl group, an important stereochemical question. All attempts failed to produce the cyclised product, demonstrating the limitations of tolerance for alkene substitution.

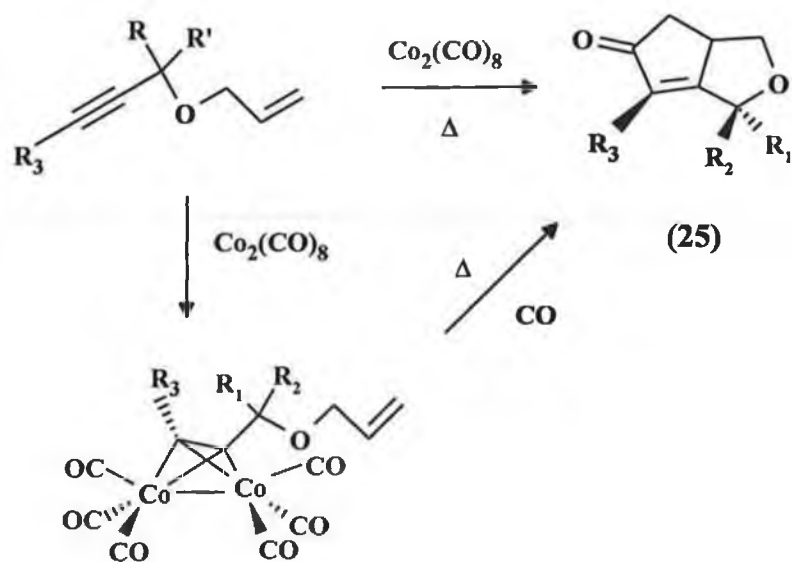
The synthesis of ( $\pm$ )-pentalenene (**24**) was also reported by Schore<sup>74</sup> on continuation of his study on triquinanes. Only the methyl group at the lone stereoisomer in the precursor enyne was used to direct ring closure in the required direction.

**(23)****(24)**

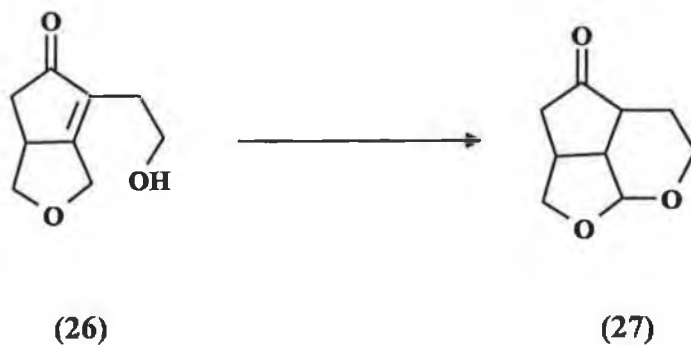
#### 1.5.9.3 Bicyclo[3.3.0]octenones and terpenes

The bicyclo[3.3.0]octenones (**25**), a class of compounds not accessible by conventional routes, have been useful intermediates in natural product synthesis. They have potential as intermediates for preparation of iridoid monoterpenes. Billington<sup>76</sup> prepared a series of cyclopentenones derived from allyl-propargyl ethers cyclised with  $\text{Co}_2(\text{CO})_8$ . Heating the formed hexacarbonyldicobalt ether complex in an atmosphere of CO gave the desired product (Scheme 1.8). It is the first reported synthetic example of heterocyclic synthesis by this manner. Syntheses of the ethers are reported from the treatment of the alcohol with allyl bromide in the presence of KOH.

(a)



(b)

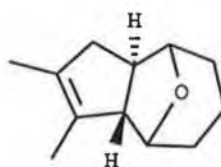


Scheme 1.8

Hydrogenation and deprotection for  $R_1=R_2=\text{H}$ ,  $R_3=\text{CH}_2\text{CH}_2\text{OTHP}$  gives (26) the penultimate intermediate in the synthesis of ( $\pm$ ) - tetrahydroanhydro aucubigenone (27). The potential of this class of compounds to partake in the synthesis of both Japanese hop ether and iridoid monoterpenes in general is being investigated.



The three natural products, the algae terpene dictyoxide, the furanosequiterpenoid fungal metabolites furanether A and furanether B, all contain the 11-oxatricyclo[5.3.1.0]undecane ring system (28). Derivatives of this ring system has been reported by Schore<sup>77</sup> to emerge from the corresponding 8-oxabicyclo[3.2.1]oct-6-ene ring system participating to varying extents in the  $\text{Co}_2(\text{CO})_8$  promoted cyclopentenone synthesis producing moderate yields and predictable regiochemistry.



(28)

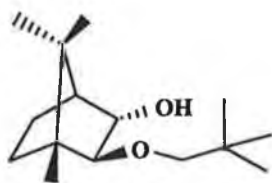
#### 1.5.9.4 Chiral complexes

Chiral cluster complexes have been prepared by Nicholas<sup>78</sup> following an interest in cluster promoted asymmetric reactions and catalysts. A series of diastereomeric monosubstituted phosphine cobalt *pentacarbonyl* acetylene complexes were prepared with formula  $(\text{R}^1\text{C}\equiv\text{CCH}(\text{OH})\text{R}^2)\text{Co}_2(\text{CO})_5\text{PPh}_3$  from chiral (propargyl alcohol) $\text{Co}_2(\text{CO})_6$ . Flash chromatography separated the diastereoisomers. The complexes possess the typical pseudotetrahedral core, characteristic of cobalt hexacarbonyl complexes, with the  $\text{PPh}_3$  ligand occupying an axial position *trans* to the Co - Co bond. It was suggested that the enantioselection does not arise from the influence of the chiral glyphos ligand but from the chiral  $\text{Co}_2\text{C}_2$  core. Exploitation of this novel type of asymmetric induction in effecting stereocontrolled coupling reactions of the extremely stable propargylium complexes derived from protonation of the phosphine substituted complexes is being exploited.

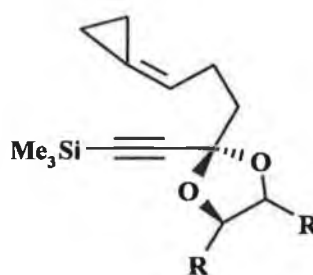
While inducing asymmetry as above, is one way of producing chiral compounds, another method employed involves use of chiral auxiliary. These may be bound to either the alkene or the alkyne moiety. Greene *et al.*<sup>79</sup> most widely studied PK reactions of alkoxy enynes derived from chiral alcohols (29, 30). The stereochemical outcomes of the reactions were explained based on chiral auxiliary - directed  $\pi$  - face discrimination. De Meijere *et al.*<sup>80</sup> reported the use of a chiral acetal adjacent to the triple bond in 1,6 - enynes (31).



(29)



(30)



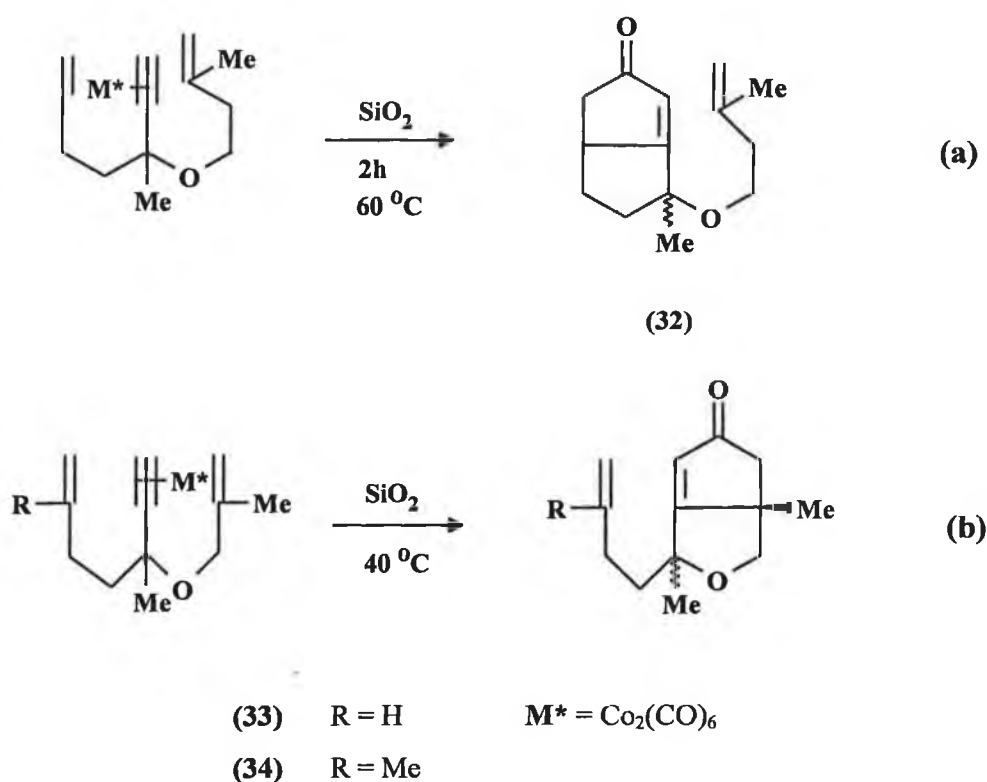
R = Me, Ph, c-Hex

(31)

#### 1.5.9.5 Perfumes and fenestranes

An important perfumery chemical precursor 2-pentylcyclopent-2-en-1-one, a *trans* -hydrojasmonate has been prepared from hept-1-yne ethylene and CO by catalytic PK reaction.<sup>75</sup> Aphidicolin and stemodin are diterpenes with a unique spirocyclic constitution containing numerous stereo centers and are known for their high biological activity. Vollhardt<sup>81</sup> reported their synthesis in 1991 presenting the first cyclisation involving an exocyclic alkene.

Several fenestrane derivatives have been prepared by Smit and Caple<sup>82</sup> (32) cutting down from the usual multi-step and tedious procedure to operationally simple steps based on etherification of  $\mu$ -cobalt carbonyl complexes of 1,6 enyn-5-ols with unsaturated alcohols and intramolecular PK reaction and [2 + 2] photocyclisation. Dry state adsorption conditions were used for the intramolecular PK reaction. Substrates containing several competing double bonds in the dienyne were used and demonstrated the regioselectivity of the intramolecular reaction (Reaction 1.16(a)).



### Reaction 1.16

In Reaction 1.16(b) substrates (33) and (34) contain two double bonds similarly positioned with respect to the triple bond. In both cases the intramolecular PK reaction proceeds with predominant participation of the double bond of allyoxy moiety leading to 5 - oxabicyclo[3.3.0]octane derivatives in both cases. Also geminal substitutions on one of the double bonds prevents it from participation in the

intramolecular PK reaction. Other uses of the PK reaction can be obtained from references.<sup>83</sup>

## 1.6 References

---

1. H.W. Sternberg, H. Greenfield, R.A. Friedel, J. Wotiz, R. Markby, L. Wender, *J. Am. Chem. Soc.*, **76** (1954) 1457.
2. E.J. Bearends, A. Roas, C. Pollak, *J. Am. Chem. Soc.*, **119** (1997) 7324.
3. *Inorganic Chemistry*, 3<sup>rd</sup> Edn; J.E. Huheey, Harper International Edition, (1983).
4. P.O. Whimp, *J. Organomet. Chem.*, **32** (1971) C 69.
5. (a) E. Whittle, D. A. Dows, G.C. Pimentel, *J. Phys. Chem.*, **22** (1954) 1953; (b) G.C. Pimentel, *Agnew. Chem. Int. Ed. Engl.* **14** (1975) 199; (c) R. N. Perutz, in *Chemistry and Physics of Matrix-Isolated Species*; Chpt. 9, L. Andrews, M. Moskovits, eds., Elsevier Science (1989).
6. For examples see (a) G.K. Yang, K.S. Peters, V. Vaida, *J. Am. Chem. Soc.*, **108** (1986) 2511; (b) J. Nasielski, A. Colas, *J. Organomet. Chem.*, **101** (1975) 215; (c) R.L. Whetten, K. J. Fu, E. Grant, *J. Am. Chem. Soc.*, **104** (1982) 4270.
7. Norrish R.G., Porter G., *Nature*, **164** (1950) 615.
8. C.M. Gordon, M. Kiszka, I.R. Dunkin, W.J. Kerr, J.S. Scott, J. Gebicki, *J. Organomet. Chem.*, **554** (1998) 147.
9. (a) K. Shimoda in 'Introduction to Laser Physics' - Springer Series in Optical Physics (1984) Vol. 44 - Verlag, Berlin; (b) A. Ben Shaul, Y Haas, K.L. Kompa, R.D. Levine in 'Lasers in Chemical Change' - Vol. 10 Springer Verlag, Berlin.
10. G. Peyronel, A. Ragnu, E.F. Trognu, *Gazz. Chim Ital.*, **97** (1967) 327
11. M.S. Wrighton, D.S. Ginley, *J. Am. Chem. Soc.*, **97** (1975) 2065.
12. A.F. Hepp, M.S. Wrighton, *J. Am. Chem. Soc.*, (1983) **105** 5934.
13. P.E. Bloyce, R.H. Hooker, A.J. Rest, T.E. Bitterwolf, N.J. Fitzpatrick, J.E. Shade, *J. Chem. Soc. Dalton Trans.*, (1990) 833.

- 
14. A.F. Hepp, J. Paw Blaha, C. Lewis, M.S. Wrighton, *Organometallics*, **3** (1984) 174.
  15. S. Sarel, A. Felzenstrin, R. Vixtor, J. Yovell, *J. Chem. Soc. Chem. Commun.*, (1974) 1025.
  16. C.P. Casey, W.H. Miles, P. J. Fagan, K.J. Haller, *Organometallics*, **4** (1985) 559.
  17. (a) I.U. Khand, G. R. Knox, P.L. Pauson, W.E. Watts, *J. Chem. Soc. Chem. Commun.*, (1971) 36; (b) I.U. Khand, G. R. Knox, P.L. Pauson, W.E. Watts, *J. Chem. Soc. Perkin Trans. 1*, (1973) 975; (c) I.U. Khand, G. R. Knox, P.L. Pauson, W.E. Watts, *J. Chem. Soc. Perkin Trans. 1*, (1973) 977.
  17. (a) O. Geis, H.G. Schmalz, *Angew. Chem. Int. Ed.*, **37** (1998), 911; (b) P.L. Pauson in *Organometallics in Organic Synthesis 2* A. de Meijere, H. tom Dieck, Eds.; Springer -Verlag Berlin Hiedelberg, (1987) 234; (c) P.L. Pauson, *Tetrahedron*, **41** (1985) 5855; (d) N.E. Schore in *Organic Reactions*, L.A. Paquette Ed., **40** (1991) (e) P.L. Pauson, I.U. Khand, *Ann. N. Y. Acad. Sci.*, **295** (1977) 2; (f) F.L. Bowden, A.B.P. Lever, *Organomet. Chem. Rev.*, **3** (1968) 227; (g) M.E. Krafft, I.L. Scott, R.H. Romero, S. Feilbelmann, C.E. Van Pelt, *J. Am. Chem. Soc.*, **115** (1993) 7199.
  19. T. Hoye, J.A. Suriano, *J. Am. Chem. Soc.*, **115** (1993) 1154.
  20. M.E. Krafft, *Tetrahedron Lett.*, **29** (1988) 999.
  21. (a) M.S. Wrighton, D.S. Ginley, *J. Am. Chem. Soc.*, **97** (1975) 2065; (b) R. Markby, I. Wender, R.A. Freidel, F.A. Cotton, H.W. Sternberg, *J. Am. Chem. Soc.*, **80** (1958) 6529.
  22. L. Mond, C. Langer, F. Quincke, *J. Chem. Soc.*, **57** (1890) 749.
  23. (a) G.L. Rochfort, R.D. Rieke, *Inorg. Chem.*, **23** (1984) 787; (b) G.L. Rochfort, R.D. Rieke, *Inorg. Chem.*, **25** (1986) 348.
  24. R. Tannenbaum, *Inorg. Chim. Acta*, **227** (1994) 223.

- 
25. For examples of catalytic PK reactions see (a) N.Y. Lee, Y.K. Chung, *Tetrahedron Lett.*, **37** (1996) 3145; (b) S.C. Berk, R. B. Grossman, S.L. Buchwald, *J. Am. Chem. Soc.*, **116** (1994) 8593; (c) B. M. Trost, *Science*, **254** (1991) 1471; (d) B. M. Trost, *Angew. Chem. Int. Ed. Engl.*, **34** (1995) 259.
  26. N.E. Schore, *Comprehensive Organic Synthesis*, P.M. Trost, Ed.; Pergamon: Oxford, **5** (1991) 1037.
  27. I.U. Khand, P.L. Pauson, *J. Chem. Soc. Perkin I*, (1976) 30.
  28. G. Bor, U.K. Dietler, K. Noack, *J. Chem. Soc. Chem. Comm.*, (1976) 914.
  29. H.B. Abrahamson, C.C. Frazier, D.S. Ginley, H.B. Gray, M.R. Wrighton, *Inorg. Chem.*, **16** (1977) 1554.
  30. R.B. King, M.B. Bisnette, *Inorg. Chem.*, **3** (1964) 785.
  31. R. L. Sweanay, T. L. Brown, *Inorg. Chem.*, **16** (1977) 415.
  32. O. Crichton, A. J. Rest, *J. Chem. Soc., Dalton Trans.*, (1978) 208.
  33. W.G. Sly, *Inorg. Chem.*, **81** (1959) 18.
  34. J.J. Bonnet, R. Mattieu, *Inorg. Chem.*, **17** (1978) 1973.
  35. L.M. Bower, M. H. B. Stiddard, *J. Organomet. Chem.*, **13** (1968) 235.
  36. G. Bor, S.F.A. Kettle, P.L. Stanghellini, *Inorg. Chim. Acta*, **18** (1976) L18.
  37. Y. Iwashita, T. Fumihide, A. Nakamura, *Inorg. Chem.*, **8** (1969) 1179.
  38. G. Varadi, A. Vizi-Orosz, S. Vastag, G. Palyi, *J. Organomet. Chem.*, **108** (1976) 225.
  39. (a) L.S. Chia, W.R. Cullen, M. Franklin, A.R. Manning, *Inorg. Chem.*, **14** (1975) 2521; (b) A. Avey, G.F. Nieckarz, D.R. Tyler, *Organometallics*, **14** (1995) 2790.
  40. M.E. Krafft, I.L. Scott, R.H. Romero, S. Feilbelmann, C.E. Van Pelt, *J. Am. Chem. Soc.*, **115** (1993) 7199.
  41. M.E. Krafft, I.L. Scott, *Tetrahedron Lett.*, **33** (1992) 3839.

- 
42. S.O. Simonian, W.A. Smit, A.S. Gybin, A.S. Shashkov, G.S. Mikaelian, V.A. Tarasov, I.I. Ibragimov, R. Caple, D.E. Froen, *Tetrahedron Lett.*, **27** (1986) 1245.
  43. A.S. Gybin, W.A. Smit, R. Caple, A.L. Veretenov, A.S. Shashkov, L.G. Vorontsova, M.G. Kurella, V.S. Chertkov, A.A. Carapetyan, A.Y. Kosnikov, M.S. Alexanyan, S.V. Lindeman, V.N. Panov, A.V. Maleev, Y.T. Struchkov, S.M. Sharpe, *J. Am. Chem. Soc.*, **114** (1992) 711.
  44. D.C. Billington, I.M. Helps, P. L. Pauson, W. Thomson, D. Willison, *J. Organometal. Chem.*, **354** (1988) 233.
  45. (a) H. Alper, J.T. Edward, *Can. J. Chem.*, **48** (1970) 1543; (b) J.K. Shen, Y.C. Gao, Q Zhen, F. Basolo, *Organometallics*, **8** (1989) 2144.
  46. S. Shambayati, W.E. Crowe, S.L. Schreiber, *Tetrahedron. Lett.*, **31** (1990) 5289.
  47. Y.K. Chung, B.Y. Lee, N. Jeong, M. Hedecek, P.L. Pauson, *Organometallics*, **12** (1993) 220.
  48. T. Sugihara, M. Yamada, H. Ban, M. Yamaguchi, C. Kaneto, *Angew. Chem. Int. Ed. Engl.*, **36** (1997) 2801.
  49. M.E. Krafft, H. Romero, I.L. Scott, *J. Org. Chem.*, **31** (1992) 5277.
  50. F.L. Bowden, A.B.P. Lever, *Organometallics. Chem. Rev.*, **3** (1968) 227.
  51. N. Jeong, Y.K. Chung, B.Y. Lee, H.L. Lee, S.E. Loo, *Synlett*, (1991) 204.
  52. A.L. Veretenov., W.A. Smit, L.G. Vorontsova, M.G. Kurella, R. Caple, A.S. Gybin, *Tetrahedron. Lett.*, **32** (1991) 2109.
  53. M.E. Krafft, A.M. Wilson, O.A. Dasse, L. V.R. Bonaga, Y.Y. Cheung, Z. Fu, B. Shao, I. L. Scott, *Tetrahedron Lett.*, **39** (1998) 5911.
  54. N.Y. Yee, Y.K. Chung, *Tetrahedron Lett.*, **37** (1996) 3145.
  55. A.J. Pearson, R.A. Dubbert, *J. Chem. Soc., Chem. Commun.*, (1991) 202.
  56. R.S. Dickson, C. Mok, G. Connor, *Aust. J. Chem*, **30** (1977) 2143.
  57. A.J. Pearson, R.J. Shively Jr., *Organometallics*, **13** (1994) 578.



- 
58. H. Alper, J.T. Edward, *J. Chem. Soc. Chem. Comm.*, (1920) 1543.
  59. A.J. Pearson, R.A. Dubbert, *Organometallics*, **13** (1994) 1656.
  60. A.J. Pearson, A. Perosa, *Organometallics*, **14** (1995) 5178.
  61. N. Jeong, S.J. Lee, B.Y. Lee, Y.K. Chung, *Tetrahedron Lett.*, **34** (1993) 4027.
  62. E.I. Negishi, S.J. Holmes, J.M. Tour, J.A. Miller, *J. Am. Chem. Soc.*, **107** (1985) 2568.
  63. N.C. Ihle, C.H. Heathcock, *J. Org. Chem.*, **58** (1993) 560.
  64. C. Mukai, M. Uchiyama, M. Hanaoka, *J. Chem. Soc. Chem. Commun.*, (1992) 1014.
  65. Y. Koga, T. Kobayashi, K. Narasaka, *Chem. Lett.*, (1998) 249.
  66. N. Jeong, S. Lee, B. Sung, *Organometallics*, **17** (1998) 1154.
  67. T. Kondo, N. Suzuki, T. Okada, T. Mitsudo, *J. Am. Chem. Soc.*, **119** (1997) 6187.
  68. (a) N. Jeong, S. Yoo, B.Y. Lee, Y. Lee, S.H. Lee, Y.K. Chung, *Tetrahedron Lett.*, **32** (1991) 2137 (b) L. Jordi, M. Moreto, S. Ricart, J.M. Vinas, M. Mejias, E. Molins, *Organometallics*, **11** (1992) 3507.
  69. T. Livinghouse, L. Pagenkopft, *J. Amer. Chem. Soc.*, **118** (1996) 2285.
  70. S.W. Brown, P.L. Pauson, *J. Chem. Soc. Chem. Comm.*, (1990) 1205.
  71. D. Nicholls in 'Comprehensive Inorganic Chemistry' Ch. 41, Review, 1053.
  72. S. Shambayati, W.E. Crowe, S.L. Schreiber, *Tetrahedron. Lett.*, **31** (1990) 5289.
  73. P. Magnus, C. Exon, *J. Am. Chem. Soc.*, **105** (1983) 2477.
  74. N.E. Schore, E.G. Rowley, *J. Am. Chem. Soc.*, **110** (1988) 5224.
  75. M.J. Knudsen, N.E. Schore, *Org. Chem.*, **49** (1984) 5025.
  76. D.C. Billington, D. Willison, *Tetrahedron. Lett.*, **25** (1984) 4041.
  77. B.E. La Belle, M.J. Knudsen, M.M. Olnstead, H. Hope, M.D. Yanuck, N.E. Schore, *Org. Chem.*, **50** (1985) 5215.
  78. D.H. Bradley, M.A. Khan, K.M. Nicholas, *Organometallics*, **8** (1989) 554.

- 
79. (a) M. Poch, E. Valenti, A. Moyano, M.A. Pericàs, J. Castro, A. De Nicola, A.E. Greene, *Tetrahedron Lett.*, **31** (1990) 7505; (b) V. Bernardes, N. Kann, A. Riera, A. Moyano, M.A. Pericàs, A. E. Greene, *J. Org. Chem.*, **60** (1995) 6670.
80. A. Stolle, H. Becker, J. Salaun, A. de Meijere, *Tetrahedron Lett.*, **35** (1994) 3521.
81. J. Germanas, C. Aubert, K.P.C. Vollhardt, *J. Am. Chem. Soc.*, **113** (1991) 4006.
82. W.A. Smit, S.M. Buhanjuk, S.O. Simonyan, Shashkov, Y.T. Struchkov, A.I. Yanovsky, R. Caple, A.S. Gybun, L.G. Anderson, J.A. Whiteford, *Tetrahedron Lett.*, **32** (1991) 2105.
83. (a) T. Kuhnen, M. Stradiotto, R. Ruffolo, D. Ulbrich, M.J. McGlinchey, M.A. Brook, *Organometallics*, **16** (1997) 5048; (b) S. Fonquera, A. Moyan, M.A. Percias, A. Riera, *J. Am. Chem. Soc.*, **119** (1997) 10225.

## **CHAPTER 2**

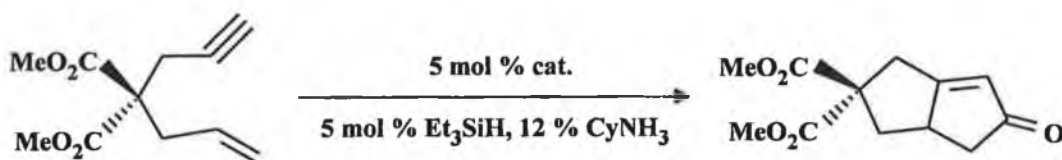
### **The Photochemistry of ( $\mu_2$ -Alkyne) $\text{Co}_2(\text{CO})_6$ Complexes**

## 2.1 Introduction

Investigations into the Pauson - Khand reaction have shown that  $(\mu_2\text{-alkyne})\text{Co}_2(\text{CO})_6$  complexes can be conveniently isolated from the reaction of  $\text{Co}_2(\text{CO})_8$  and alkynes (Scheme 2.1).<sup>1</sup> Studies on these  $(\mu_2\text{-alkyne})\text{Co}_2(\text{CO})_6$  complexes by Livinghouse and Belanger<sup>2</sup> have shown that in some cases they can serve as sources of an active catalyst for carbonylative enyne cyclisations (Scheme 2.2). A series of  $(\mu_2\text{-alkyne})\text{Co}_2(\text{CO})_6$  complexes were screened in combination with  $\text{Et}_3\text{SiH}$  in the catalytic Pauson - Khand reaction (PKR).



Scheme 2.1



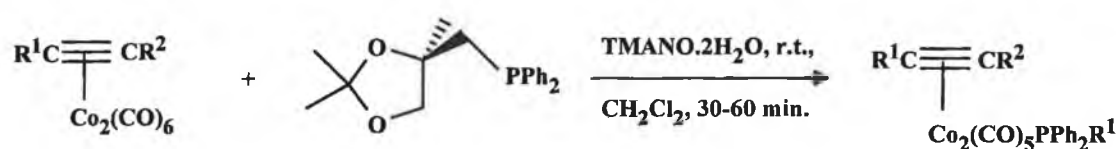
cat. =  $[\text{HO}(\text{CH}_3)_2\text{CC}\equiv\text{CH}]\text{Co}_2(\text{CO})_6$

Cy = cyclohexylamine

Scheme 2.2

A reaction mechanism has been proposed for the Pauson - Khand reaction based on the regio- and stereochemical outcome of a vast number of thermal reactions. It is widely believed that decarbonylation of the  $(\mu_2\text{-alkyne})\text{Co}_2(\text{CO})_6$  species is a prerequisite for the overall reaction sequence. Krafft and co-workers<sup>3</sup> have successfully trapped such a CO-loss species by a sulphur atom of a thio-substituent on the alkyne, yielding an isolable pentacarbonyl complex amenable to spectroscopic and structural analysis.

A variety of complexes where L is a simple phosphine or phosphite ligand (e.g.  $\text{L} = \text{PPh}_3$ ,  $\text{P(OMe)}_3$ ,  $\text{PCy}_3$  and  $\text{P}^n\text{Bu}_3$ ) are known. Manning and co-workers<sup>4</sup> have thermally prepared penta- and tetracarbonyl derivatives of  $(\mu_2\text{-alkyne})\text{Co}_2(\text{CO})_6$  complexes by replacement of one or both axial CO groups with monodentate phosphines, phosphites and arsines. Kerr<sup>5</sup> has shown that alkyne pentacarbonyldicobalt complexes containing the chiral ligand (R)-(+)-Glyphos can be readily synthesised in moderate to good yields under standard thermal reaction conditions. Additionally, novel tertiary amine N-oxide promoted reactions have been developed which allow the rapid formation of the same mono-(R)-(+)-Glyphos complexes in consistently good yields under mild conditions (Scheme 2.3). Separation of the diastereoisomers produces complexes which are optically pure and can then be used in enantioselective versions of the Pauson - Khand reaction.



$\text{PPh}_2\text{R}^1 = (\text{R})\text{-(+)-Glyphos}$

$\text{TMANO}\cdot 2\text{H}_2\text{O} = \text{Trimethylamine N-oxide}\cdot\text{dihydrate}$

Scheme 2. 3

While the thermal chemistry of cobalt carbonyl complexes has received widespread attention the photochemistry of such complexes has remained relatively unknown. The high temperature required for the Pauson - Khand process is a considerable disadvantage, particularly if olefin substrates undergo thermally induced rearrangements. Thus, the types of olefins which can be used is limited. Taylor and Viney<sup>6</sup> have generated  $(\mu_2\text{-C}_6\text{H}_5\text{C}_2\text{H})\text{Co}_2(\text{CO})_5(\text{PPh}_3)$  photochemically by utilising irradiation with linearly polarised laser light on a preparative scale. Livinghouse and Pagenkopf<sup>7</sup> reported the photochemical promotion of the intramolecular PKR. High intensity visible light effectively promoted an intramolecular catalytic PKR at 50 to 55 °C and 1 atmosphere of CO. However, the precise role the photon plays in the reaction remains uncertain. Although turnover numbers were not high (max. 60), the choice of the appropriate light source, the purity of  $\text{Co}_2(\text{CO})_8$  and the reaction temperature were all reported to be critically important for successful catalytic reactions.

Recently, a matrix isolation study demonstrated that CO-loss occurs following short - wavelength ( $\lambda_{\text{exc}} = 250$  nm) photolysis of  $(\mu_2\text{-C}_6\text{H}_5\text{C}_2\text{H})\text{Co}_2(\text{CO})_6$ .<sup>8</sup> This work demonstrated that  $(\mu_2\text{-C}_6\text{H}_5\text{C}_2\text{H})\text{Co}_2(\text{CO})_6$  is photochemically inert when irradiated with  $\lambda_{\text{exc}} = 350$  nm. However it would not be feasible to use photons of wavelengths less than 300 nm in the Pauson - Khand reaction because of risk of photochemical damage to the unsaturated substrates.

The possibility of using photochemical techniques to promote the Pauson - Khand reaction has been investigated and is detailed in this chapter. A study of the wavelength dependent nature of the photochemistry of cobalt hexacarbonyl complexes has not been studied previously. A fuller investigation will provide further evidence for the importance of the CO-loss process to the Pauson - Khand reaction, and present an alternative and more attractive means of promoting the reaction particularly when thermally sensitive substrates are required.

To assist with a fuller understanding of the mechanistic pathways of the PKR a series of experiments have been conducted using phenylacetylene hexacarbonyldicobalt (**pachc**) as a model complex. Preliminary experiments were undertaken to identify the photoproducts generated. Both photochemical and thermal derivatisation followed by spectroscopic and structural analysis of the products confirmed the primary photoproduct to contain the  $(\mu_2\text{-alkyne})\text{Co}_2(\text{CO})_5$  fragment. Both steady-state and laser flash photolysis techniques were used in this study. The investigation was extended to include the photochemistry of acetylene hexacarbonyldicobalt (**achc**) and diphenylacetylene hexacarbonyldicobalt (**dpachc**) complexes. This work reveals for the first time a wavelength dependent photochemistry of the  $(\mu_2\text{-alkyne})\text{Co}_2(\text{CO})_6$  complex and demonstrates the importance of correct selection of excitation wavelengths in promoting the desired CO-loss process.

## 2.2 Photolysis of $(\mu_2\text{-C}_6\text{H}_5\text{C}_2\text{H})\text{Co}_2(\text{CO})_6$

### 2.2.1 Molecular modeling of $(\mu_2\text{-C}_6\text{H}_5\text{C}_2\text{H})\text{Co}_2(\text{CO})_6$

The molecular model of **pachc** is shown in Figure 2.1. The bonding between the alkyne carbon - carbon bond and the  $\{\text{Co}_2(\text{CO})_6\}$  moiety is described by the  $\sigma$  - donation of  $\pi$  - electrons from the alkyne group to an empty orbital on the metal and the formation of a  $\pi$  - bond by the back donation from a filled  $d$  - orbital on the metal into the  $\pi^*$  - orbital of the triple bond. This back bonding contributes to the stabilisation of the alkyne - metal linkage. Therefore, the alkyne acts as a four electron donor, with each cobalt atom receiving two electrons in place of the two carbonyls which have been displaced from  $\text{Co}_2(\text{CO})_8$ . The position of the cobalt atom is such to allow efficient overlap from both  $\pi$  - orbitals of the acetylene  $\text{C}\equiv\text{C}$  triple bond. Thus the acetylene bridges the cobalt - cobalt bond at right angles and the carbon centers approximate  $\text{sp}^3$  hybridization.

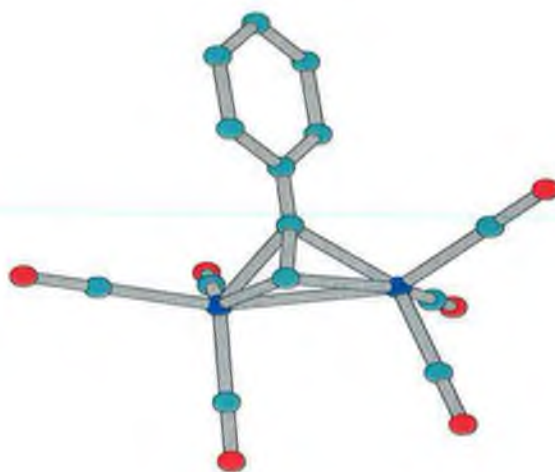


**Figure 2.1**    *Molecular model of pachc*

## 2.2.2 Synthesis and Spectroscopic Characterisation of $(\mu_2\text{-C}_6\text{H}_5\text{C}_2\text{H})\text{Co}_2(\text{CO})_6$

### 2.2.2.1. Preparation and IR spectrum of $(\mu_2\text{-C}_6\text{H}_5\text{C}_2\text{H})\text{Co}_2(\text{CO})_6$

The synthesis of phenylacetylene hexacarbonyldicobalt (**pachc**) was carried out according to the method of Sternberg and Greenfield.<sup>9,10</sup> Formation of the **pachc** complex results from simple replacement of the two bridging carbonyls in  $\text{Co}_2(\text{CO})_8$  by phenylacetylene. The reaction was monitored by IR spectroscopy which indicated the disappearance of parent bands and the formation of a product which was identified as  $(\mu_2\text{-C}_6\text{H}_5\text{C}_2\text{H})\text{Co}_2(\text{CO})_6$ . The product was isolated by flash chromatography elution on silica gel using pentane as eluent and characterised by IR and  $^1\text{H}$  NMR spectroscopy and elemental analysis.  $\text{Co}_2(\text{CO})_8$  has  $\text{C}_{2v}$  symmetry and the observed IR spectrum showed five terminal bands at 2095, 2064, 2042, 2032 and 2028  $\text{cm}^{-1}$  and two bridging bands at 1867 and 1859  $\text{cm}^{-1}$  (Figure 2.2(a)). The IR spectrum of **pachc** (Figure 2.2(b)) shows in particular the absence of bridging CO



bands and the presence of new terminal CO bands at 2094, 2055.9, 2033, 2028.6  $\text{cm}^{-1}$  and a shoulder at 2018  $\text{cm}^{-1}$ .

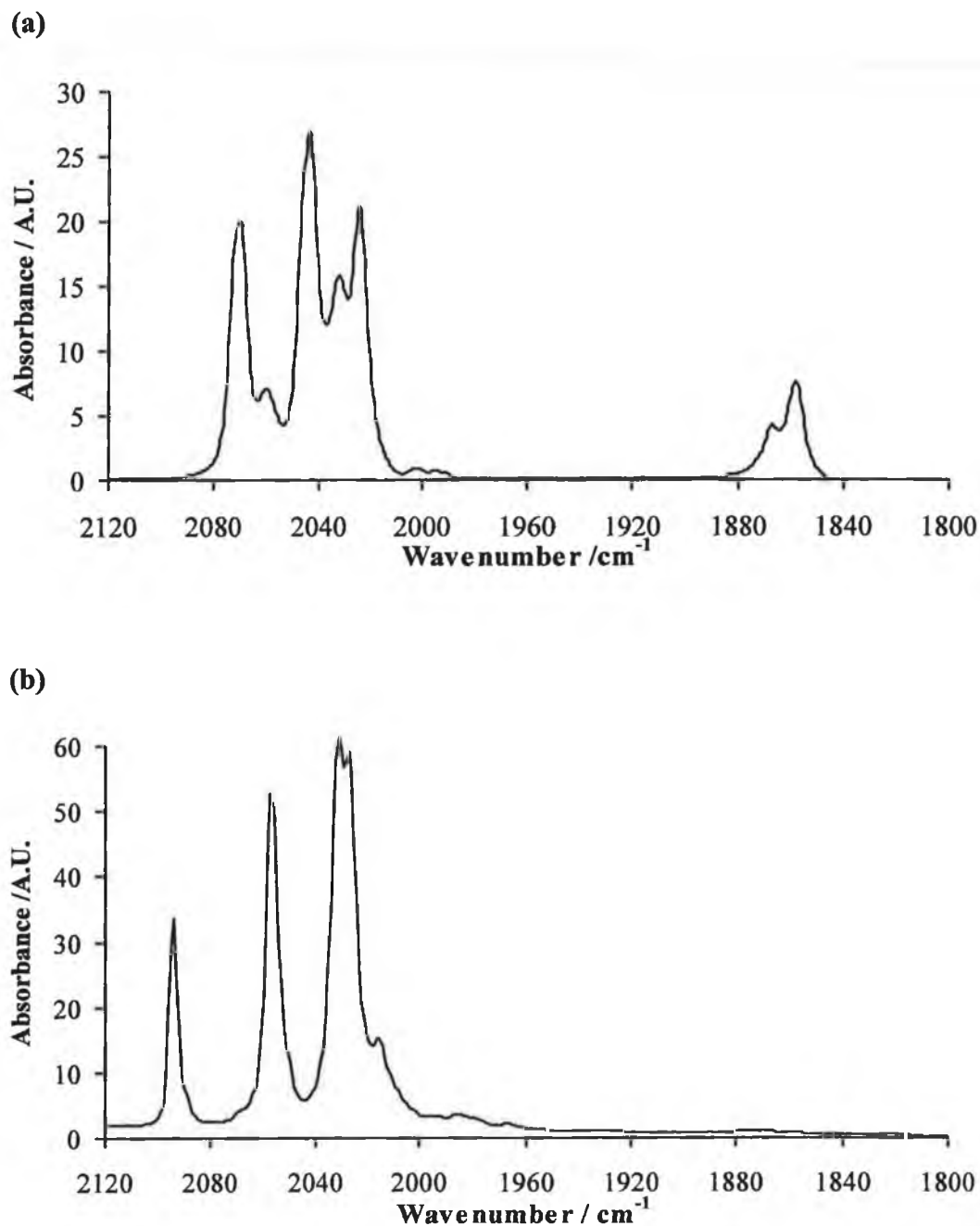


**Figure 2.2** IR spectrum in the CO stretching region of (a)  $\text{Co}_2(\text{CO})_8$  (b)  $(\mu_2\text{-C}_6\text{H}_5\text{C}_2\text{H})\text{Co}_2(\text{CO})_6$  at 298 K (cyclohexane;  $\text{cm}^{-1}$ ,  $\pm 1 \text{ cm}^{-1}$ ).

#### 2.2.2.2. NMR characterisation of $(\mu_2\text{-C}_6\text{H}_5\text{C}_2\text{H})\text{Co}_2(\text{CO})_6$

The proton  $^1\text{H}$  NMR spectrum of uncoordinated phenylacetylene and the **pachc** complex are presented in Figure 2.3. A shift of the free ligand protons upon complexation is observed. Resonances observed at 3.1 (s, 1H) ppm in uncoordinated phenylacetylene, assigned to the acetylene  $\equiv\text{C}\text{-}\underline{\text{H}}$  proton, have shifted to 6.3 (s, 1H) ppm. Because of the electronic delocalisation onto the  $\text{C}_2\text{Co}_2$  core and the reduction of the alkyne character of the carbon - carbon bond upon complexation, the terminal proton is deshielded and appears at lower field. In the aromatic region resonances at 7.19-7.27 (m, 3H, Ar-CH,  $J = 1.7$  Hz) ppm and 7.4 (m, 2H, Ar-CH,  $J = 1.7$  Hz) ppm are assigned to the complexed protons in the phenyl ring. These bands have shifted upfield upon complexation.

The  $^{13}\text{C}$  NMR spectrum of **pachc** is presented in Figure 2.4. Upon coordination, the acetylenic carbon atoms that originally appear at 77.9 and 84.1 ppm ( $\text{CDCl}_3$ ) are observed at 72.9 and 89.7 ppm respectively. Upon coordination of the alkyne to the  $\{\text{Co}_2(\text{CO})_6\}$  moiety, the position of the terminal carbon atom  $^{13}\text{C}_1$  is shifted by *ca.* 6 ppm upfield of TMS, and the resonance of the carbon atom  $^{13}\text{C}_2$  close to the phenyl ring is shifted by *ca.* 6 ppm downfield. The  $\pi$  - electron density of the carbon - carbon bond has decreased and is now localised on the ' $\text{C}_2\text{Co}_2$ ' core. Since the  $^{13}\text{C}_2$  is close to the electron withdrawing phenyl ring, this carbon is deshielded and thus appears downfield.

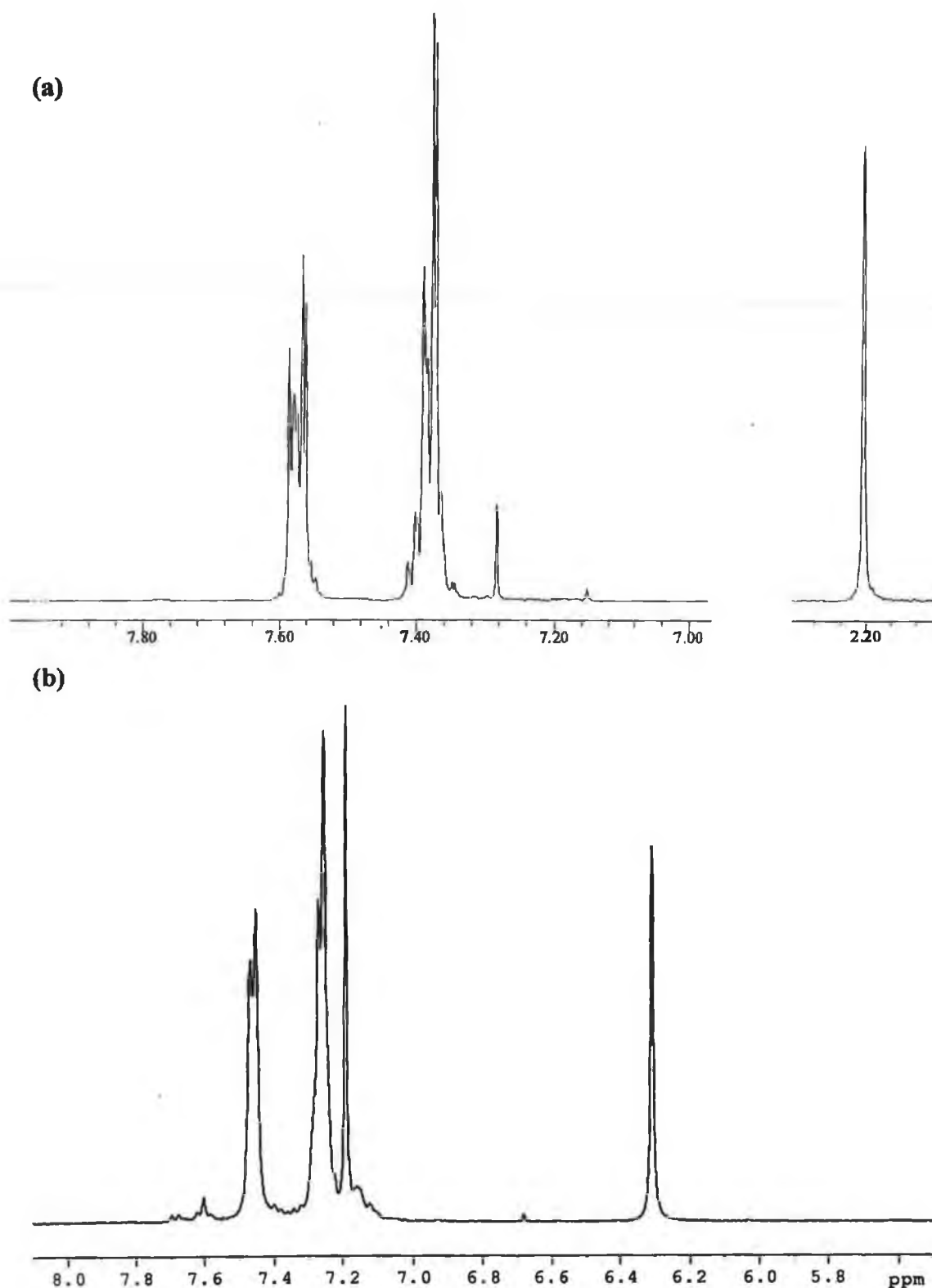


**Figure 2.3**  $^1\text{H}$  NMR spectrum of (a) uncoordinated phenylacetylene (b)  $(\mu_2\text{-C}_6\text{H}_5\text{C}_2\text{H})\text{Co}_2(\text{CO})_6$  at 298 K in  $\text{CDCl}_3$ .

The aromatic carbon atom attached to the dimetallatetrahedrane core undergoes a dramatic shift. The electron density on the phenyl ring is delocalised on the ring, therefore the closest aromatic carbon atom to the core will be mostly sensitive to the deshielding effect of this unit and its position will be strongly shifted downfield. The  $^{13}\text{C}$  chemical shifts of the carbonyl ligands in the  $(\mu_2\text{-C}_6\text{H}_5\text{C}_2\text{H})\text{Co}_2(\text{CO})_6$  complex appear as a broad signal at around 201 ppm, suggesting that the carbonyls are rapidly interchanging on an NMR timescale.

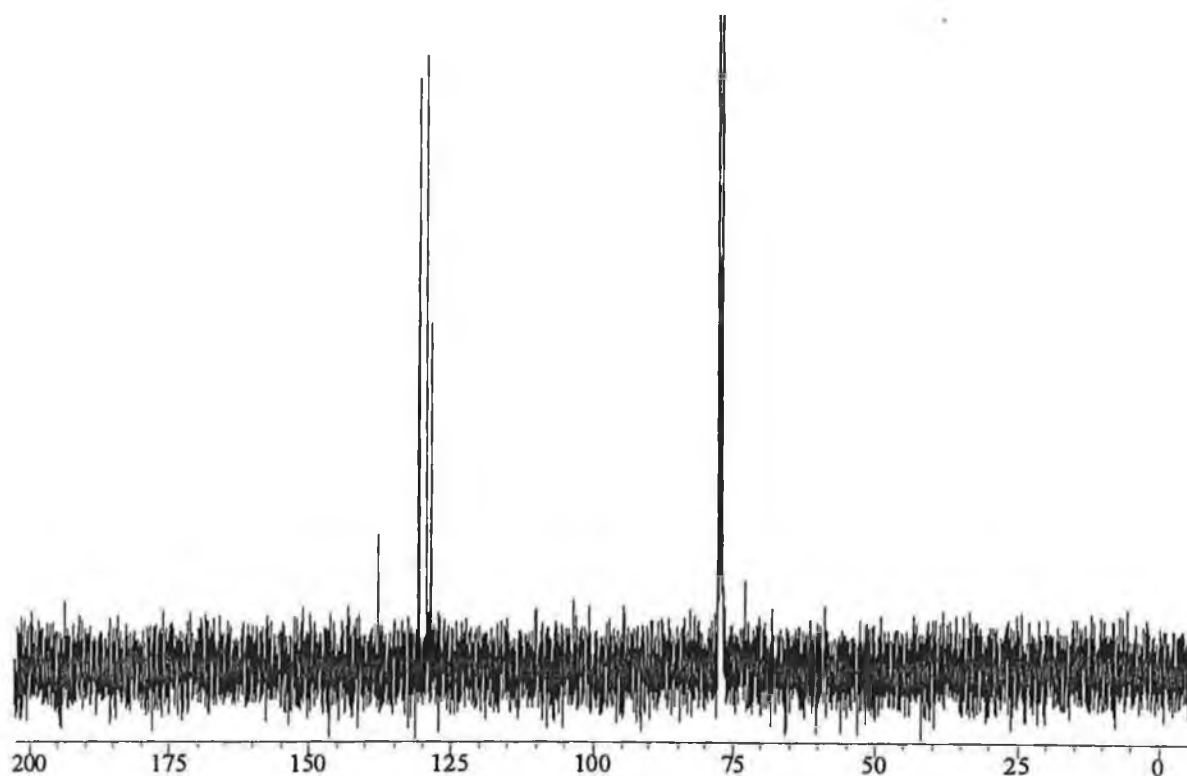


**Figure 2.4**  $^{13}\text{C}$  NMR spectrum of *pache* at 298 K in  $\text{CDCl}_3$ .

#### 2.2.2.3. Electronic absorbance spectrum of $(\mu_2\text{-C}_6\text{H}_5\text{C}_2\text{H})\text{Co}_2(\text{CO})_6$

The UV/Vis spectrum of *pache* is presented in Figure 2.5. Generally this type of complex absorbs across a broad range of wavelengths up to 630 nm. The  $\lambda_{\text{max}}$  at 352 nm ( $\epsilon = 7.35 \times 10^6 \text{ mol}^{-1} \text{ dm}^3 \text{ cm}^{-1}$ ) has been assigned to a  $\sigma\text{-}\sigma^*$  transition associated with the M - M bond according to Manning based on studies of  $\text{Co}_2(\text{CO})_8$ <sup>11</sup> and is shifted to lower energy upon complexation. They attribute the

bands at lower energy (422 ( $\epsilon = 2.23 \times 10^6 \text{ mol}^{-1} \text{ dm}^3 \text{ cm}^{-1}$ ) and 536 ( $\epsilon = 1.13 \times 10^6 \text{ mol}^{-1} \text{ dm}^3 \text{ cm}^{-1}$ ) nm to  $\pi\text{-}\pi^*$  transitions. The absorbance of the complex stretches well into the visible region of the spectrum, a characteristic which will become important for selective photolysis of the complex.

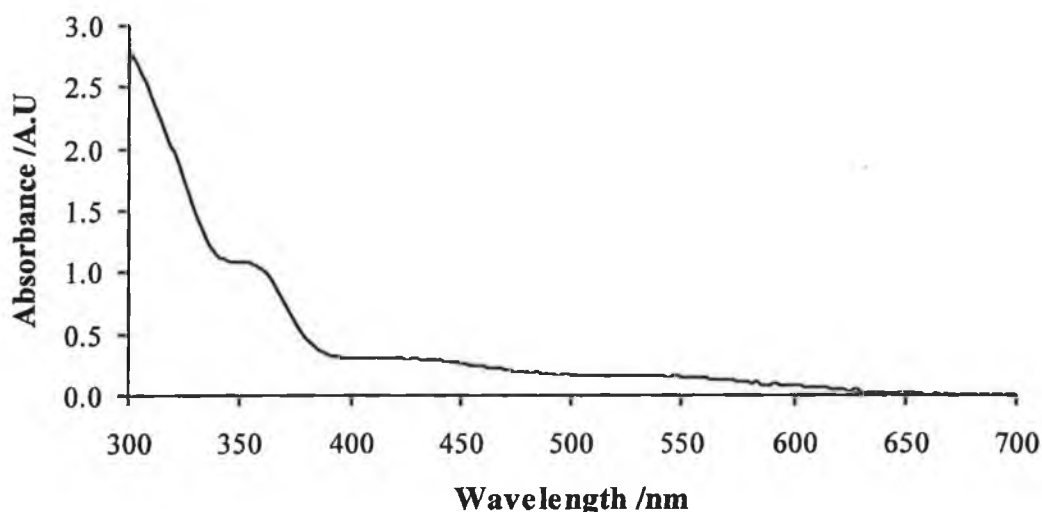


**Figure 2.5** UV/Vis spectrum of *pachc* (conc. =  $3.2 \times 10^{-4} \text{ M}$ ) in pentane solution at 298 K.

### 2.2.3 Steady-state Photolysis Experiments

#### 2.2.3.1. Photolysis of $(\mu_2\text{-C}_6\text{H}_5\text{C}_2\text{H})\text{Co}_2(\text{CO})_6$ in the presence of trapping ligands

Preliminary experiments were conducted on **pachc** using broad band photolysis techniques in order to identify any products which arise as a result of photolysis of the  $(\mu_2\text{-alkyne})\text{Co}_2(\text{CO})_6$  complex. Once this was established it was important to identify which spectral region produced the desired CO-loss process.

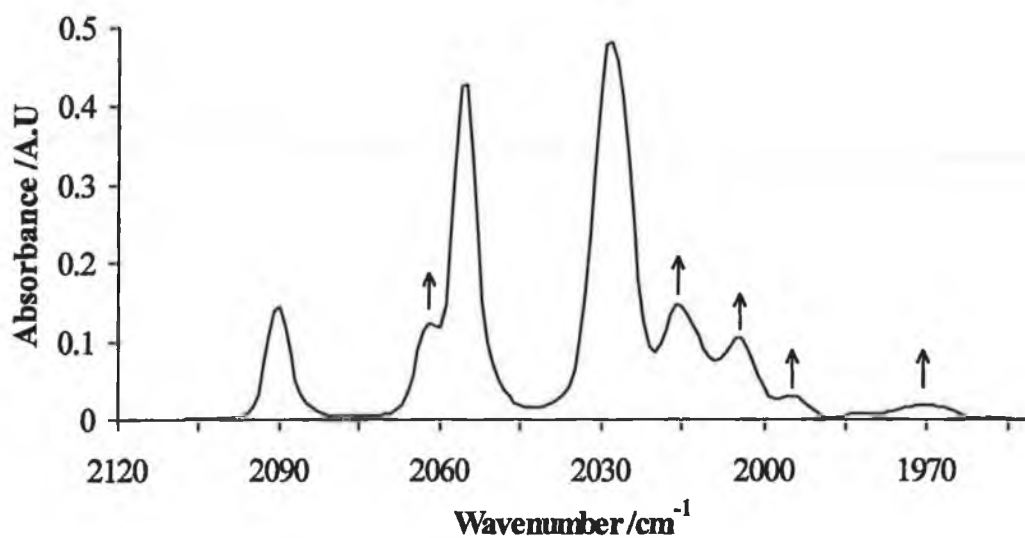
Initially, **pachc** was photolysed in the neat degassed alkane solvents (cyclohexane or pentane) at  $\lambda_{\text{exc}} > 340 \text{ nm}$ . No changes were observed in the IR

spectra monitored at  $t = 0, 0.5, 1, 2, 3, 5, 10, 15$  and  $20$  minutes. However, if a photoreaction is taking place any products formed would not be visible in a steady-state in neat solvents as ligand loss would be reversible in solution. By employing a trapping ligand such as  $\text{PPh}_3$  or  $\text{C}_5\text{H}_5\text{N}$ , which are two electron donors, the CO-loss product could be trapped. Any photoproducts which arise can then be identified by IR spectroscopy.

Photolysis in pentane containing a 4-fold excess of  $\text{C}_5\text{H}_5\text{N}$ , after argon purging (20 min) and irradiation with  $\lambda_{\text{exc}} > 340$  nm produced new bands accompanied by the depletion of parent bands. The IR combination and difference spectrum for the photoreaction are given in Figure 2.6 for  $t = 15$  minutes. Arrows indicate the direction of band increase or decrease. The new bands are identified as  $(\mu_2\text{-C}_6\text{H}_5\text{C}_2\text{H})\text{Co}_2(\text{CO})_5(\text{C}_5\text{H}_5\text{N})$ . Substitution of the  $\text{C}_5\text{H}_5\text{N}$  ligand for CO was accompanied by a change of photolysed solution to a darker red colour. After irradiation for 20 minutes the concentration of the newly formed pentacarbonyl complex was higher than that of the starting complex  $(\mu_2\text{-C}_6\text{H}_5\text{C}_2\text{H})\text{Co}_2(\text{CO})_6$ . Some bi-substituted product  $(\mu_2\text{-C}_6\text{H}_5\text{C}_2\text{H})\text{Co}_2(\text{CO})_4(\text{C}_5\text{H}_5\text{N})_2$  also formed upon continued photolysis.

Similar results were obtained with  $\text{PPh}_3$  for photochemical experiments resulting in substitution of either one or two CO ligands by  $\text{PPh}_3$  (see Table 2.1). Unlike the photoreaction of **pache** with  $\text{C}_5\text{H}_5\text{N}$ , the reaction with  $\text{PPh}_3$  does not go to completion. The yield of photoproduct  $(\mu_2\text{-C}_6\text{H}_5\text{C}_2\text{H})\text{Co}_2(\text{CO})_5(\text{PPh}_3)$  was 70%, based on the intensity of  $\nu_{\text{CO}}$  bands, compared to 98% for  $(\mu_2\text{-C}_6\text{H}_5\text{C}_2\text{H})\text{Co}_2(\text{CO})_5(\text{C}_5\text{H}_5\text{N})$ . As well as the assigned bands for mono- and bi-substitution a band is occasionally observed at  $1981.2\text{ cm}^{-1}$  the origin of which is uncertain.

(a)



(b)

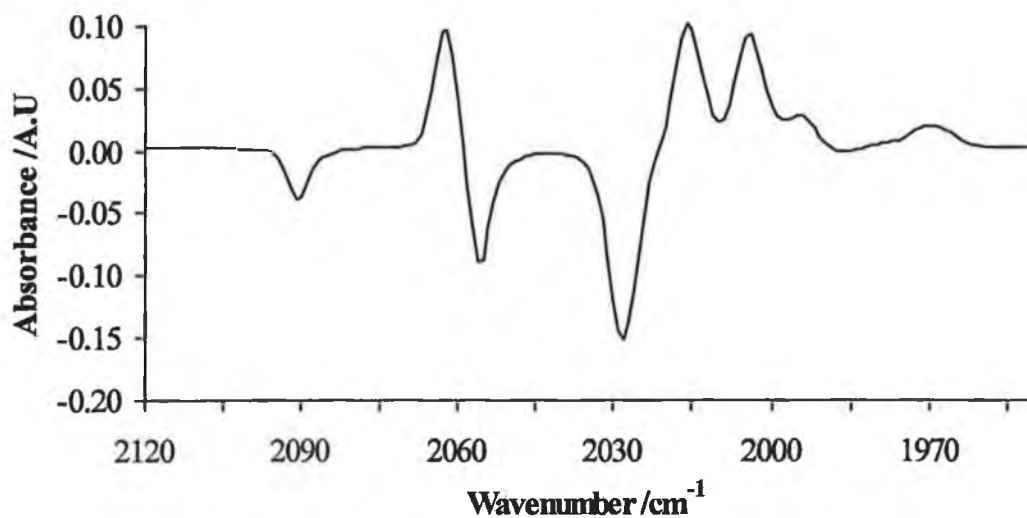


**Figure 2.6** IR spectrum in the CO stretching region following broad band photolysis of *pachc* after 15 minutes irradiation in the presence of pyridine ( $\lambda_{\text{exc}} > 340$  nm) (a) combination spectrum showing new photoproduct and parent bands (b) difference spectrum. The positive bands are identified as  $(\mu_2\text{-C}_6\text{H}_5\text{C}_2\text{H})\text{Co}_2(\text{CO})_5(\text{C}_5\text{H}_5\text{N})$ .

The characterisation of product was achieved by comparison of observed  $\nu_{\text{CO}}$  bands with published data for  $\text{PPh}_3$  derivatisation by Manning<sup>4</sup> and Bonnet.<sup>12</sup> The synthesis of mono- and disubstituted complexes by thermal methods was reproduced for comparison of  $\nu_{\text{CO}}$  bands and confirmation of results (Figure 2.7). Comparison of photochemical and thermal results show the formation of  $(\mu_2\text{-C}_6\text{H}_5\text{C}_2\text{H})\text{Co}_2(\text{CO})_5(\text{PPh}_3)$  after 20-30 minutes photolysis time compared with 3 hours using thermal methods. Thus photochemical methods are more efficient for the preparation of these compounds.

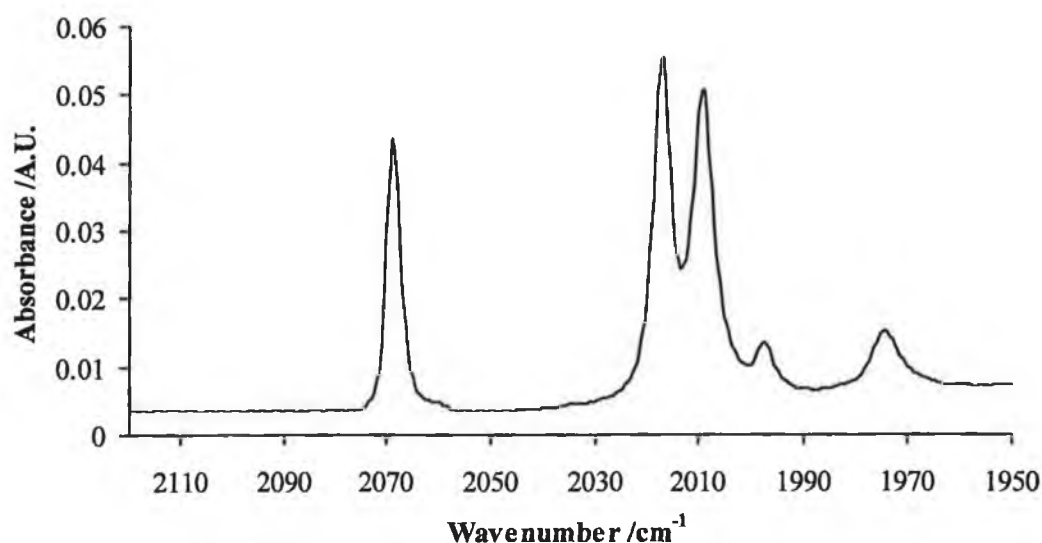


**Figure 2.7** IR spectrum in the CO stretching region for  $(\mu_2\text{-C}_6\text{H}_5\text{C}_2\text{H})\text{Co}_2(\text{CO})_5(\text{PPh}_3)$  synthesised by thermal methods (cyclohexane,  $\text{cm}^{-1}$ ,  $\pm 1 \text{ cm}^{-1}$ ).

All experiments carried out at  $\lambda_{\text{exc}} > 340 \text{ nm}$  were repeated at  $\lambda_{\text{exc}} > 400 \text{ nm}$ . Comparison of changes in band formation for direct photolysis at  $\lambda_{\text{exc}} > 340 \text{ nm}$  to that at  $\lambda_{\text{exc}} > 400 \text{ nm}$  showed the yield of photoproducts was greater at  $\lambda_{\text{exc}} > 340 \text{ nm}$ . This is possibly due to the absorption characteristics of **pachc** which absorbs more in the region at 340 nm. In order to rule out the possibility that reactions may be thermal and not photochemical, experiments were set up in duplicate. One of the solutions



was photolysed in front of an IR sink while the other was stored in the dark for the corresponding amount of time. Spectroscopic analysis of the control solution showed no changes had occurred during the time span of the experiment.

**Table 2.1** The  $\nu_{\text{CO}}$  band positions observed following steady-state photolysis of *pachc*.

Compound	$\nu_{\text{CO}}$
$(\mu_2\text{-C}_6\text{H}_5\text{C}_2\text{H})\text{Co}_2(\text{CO})_6^{\text{a}}$	2094, 2056, 2033, 2029, 2014(sh)
$(\mu_2\text{-C}_6\text{H}_5\text{C}_2\text{H})\text{Co}_2(\text{CO})_5(\text{C}_5\text{H}_5\text{N})^{\text{b}}$	2069, 2018, 2005, 1994, 1966
$(\mu_2\text{-C}_6\text{H}_5\text{C}_2\text{H})\text{Co}_2(\text{CO})_4(\text{C}_5\text{H}_5\text{N})_2^{\text{b}}$	2021, 2018, 1967, 1942
$(\mu_2\text{-C}_6\text{H}_5\text{C}_2\text{H})\text{Co}_2(\text{CO})_5(\text{PPh}_3)^{\text{b}}$	2065, 2016, 2006, 1997, 1972
$(\mu_2\text{-C}_6\text{H}_5\text{C}_2\text{H})\text{Co}_2(\text{CO})_4(\text{PPh}_3)_2^{\text{b}}$	2021, 2004, 1972, 1942

Cyclohexane solution at 298 K ( $\text{cm}^{-1}$ ;  $\pm 1 \text{ cm}^{-1}$ ); <sup>a</sup> complex prepared by thermal methods; <sup>b</sup> complexes generated by steady-state photolysis experiments.

#### 2.2.3.2. Steady-state UV/Vis monitored photolysis of $(\mu_2\text{-C}_6\text{H}_5\text{C}_2\text{H})\text{Co}_2(\text{CO})_6$ for $\lambda_{\text{exc}} > 400$ and 340 nm

**Pachc** was photolysed in a cyclohexane solution with added  $\text{PPh}_3$  and outgassed by flushing with argon. The reaction was followed by steady-state UV/Vis spectroscopy (Figure 2.8) and showed a depletion in bands at 352, 422 and 536 nm while a band at  $\sim 382$  nm was observed. After further photolysis this new band depletes, indicating the degradation of the newly formed species. The photoproduct was identified as  $(\mu_2\text{-C}_6\text{H}_5\text{C}_2\text{H})\text{Co}_2(\text{CO})_5(\text{PPh}_3)$  by comparison with the  $\nu_{\text{CO}}$  bands of an authentic sample prepared by thermal methods.<sup>4</sup> Upon photolysis in the presence of pyridine under the same conditions, the steady-state UV/Vis spectrum shows a similar decrease in bands at 352, 422 and 536 nm while a new band again appears at 396 nm. These spectral changes suggest the formation of  $(\mu_2\text{-C}_6\text{H}_5\text{C}_2\text{H})\text{Co}_2(\text{CO})_5(\text{C}_5\text{H}_5\text{N})$ .

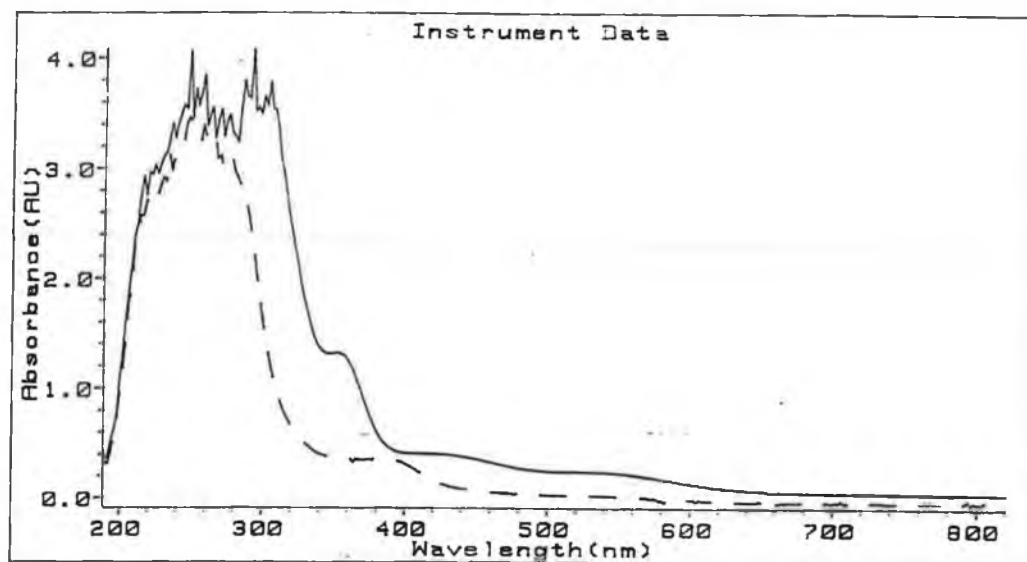
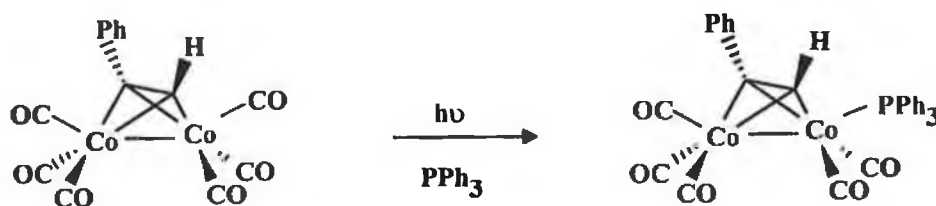


**Figure 2.8** Steady-state UV/Vis spectral changes upon photolysis of *pachc* in the presence of  $\text{PPh}_3$  ( $10^{-4} \text{ M}$ ) at 298 K (cyclohexane solvent);  $\lambda_{\text{exc}} > 340 \text{ nm}$ ; — pre-photolysis, - - - after photolysis.

Broad band photolysis of *pachc* in degassed alkane solutions containing  $\text{C}_5\text{H}_5\text{N}$  or  $\text{PPh}_3$  proceeds according to Reaction 2.1. The unique ligand occupies the axial position as observed by Manning for the thermal products. The results so far demonstrate that the photoprocess that occurs following broad band photolysis is CO-loss rather than alkyne loss. This prompted a fuller investigation of this system using monochromatic irradiation.



**Reaction 2.1**

## 2.2.4 Laser flash photolysis of $(\mu_2\text{-C}_6\text{H}_5\text{C}_2\text{H})\text{Co}_2(\text{CO})_6$ at $\lambda_{\text{exc}} = 355\text{ nm}$

### 2.2.4.1 Flash photolysis under varying atmospheres

The pulse excitation ( $\lambda_{\text{exc}} = 355\text{ nm}$ ) of a solution of **pachc** in cyclohexane under 1 atmosphere of argon resulted in depletion and rapid recovery of the absorption as represented in Figure 2.9(a). This behaviour was observed at all monitoring wavelengths where the parent hexacarbonyl has significant absorption. The rate of recovery was found to follow first order kinetics with  $k_{\text{obs}} = 3.14 \times 10^7\text{ s}^{-1}$  at 298 K. The steady-state UV/Vis spectrum recorded throughout photolysis showed a slight depletion of all bands of the starting solution however (Figure 2.9 (b)).

An experiment carried out under 1 atmosphere of CO, exhibited a similar transient signal with a similar rate of recovery of  $3.5 \times 10^7\text{ s}^{-1}$ . No evidence for a CO-loss intermediate was observed in either case. Under 0.5 atmosphere of CO ( $[\text{CO}] = 4.5 \times 10^{-3}\text{ M}$ ) the observed rate was  $4.3 \times 10^7\text{ s}^{-1}$ . This is strong evidence that the primary photochemical reaction observed in these experiments was not the result of CO-loss.

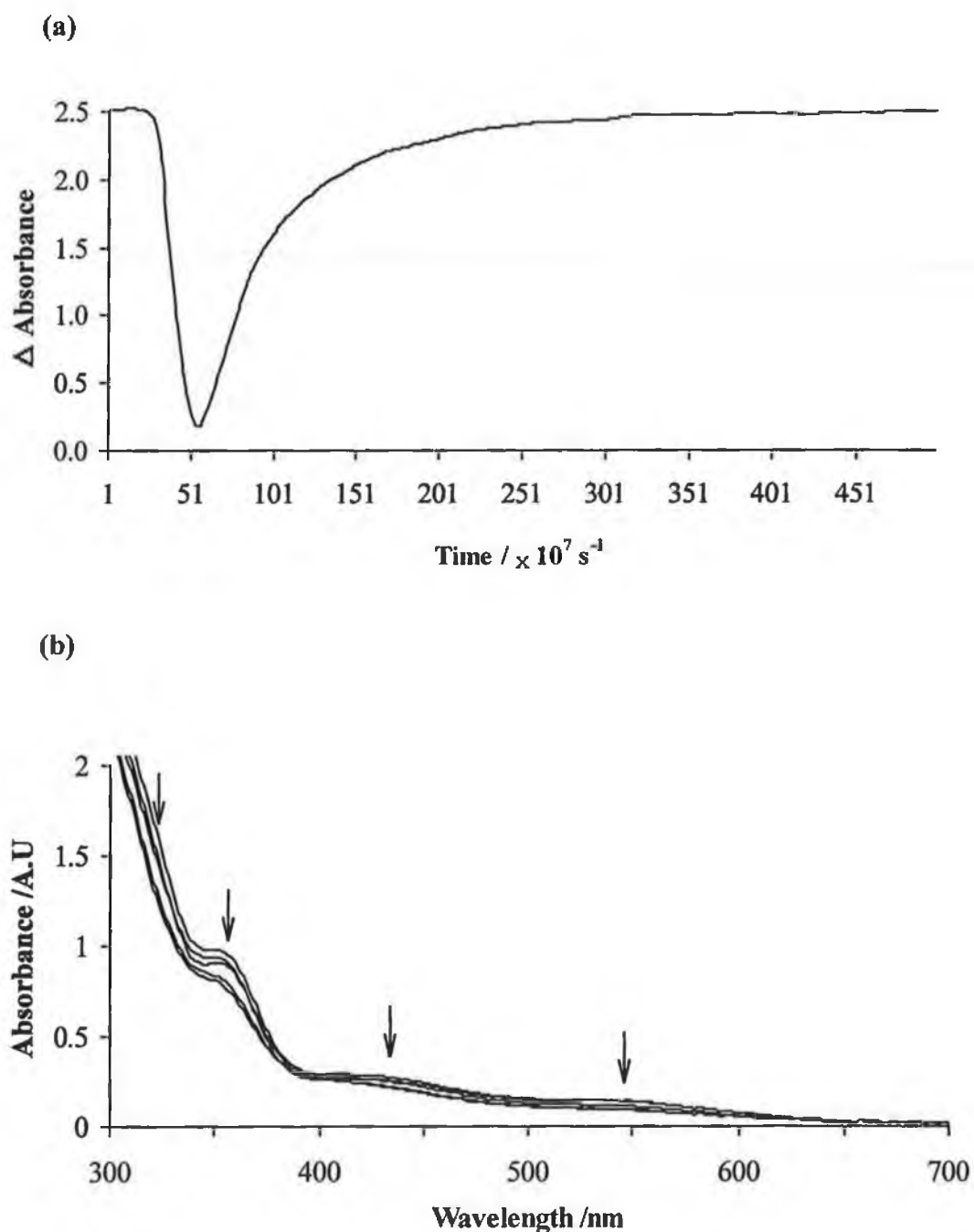


**Figure 2.9** (a) Typical transient signal observed at 400 nm following laser flash photolysis of *pachc* in cyclohexane solution at 298 K under 1 atmosphere of argon ( $\lambda_{\text{exc}} = 355 \text{ nm}$ ) (b) the steady-state UV/Vis spectrum monitored during photolysis. Note the slight depletion of parent bands with no obvious product bands.

## 2.2.4.2. Flash photolysis in different solvents

In these experiments acetonitrile was used as solvent because this solvent can act as a two electron donor. **Pachc** was flash photolysed under 1 atmosphere of argon. If CO-loss were to occur an acetonitrile molecule would occupy the vacant coordination site. However, the transient signal observed showed a depletion of parent followed by a rapid recovery. The rate of recovery was measured to be  $5.34 \times 10^7 \text{ s}^{-1}$  (Table 2.2). A sample of **pachc** prepared in cyclohexane gave a similar transient with  $k_{\text{obs}} = 3.14 \times 10^7 \text{ s}^{-1}$ . The steady-state UV/Vis spectrum showed a slight depletion of all parent bands following these experiments indicating degradation.

**Table 2.2** The observed rate of recovery ( $k_{\text{obs}}$ ) of parent absorption measured for laser flash photolysis of *pachc* at  $\lambda_{\text{exc}} = 355 \text{ nm}$ .

Atmosphere	Solvent	$k_{\text{obs}} / \text{s}^{-1}$
1 atm Ar	cyclohexane	$3.14 \times 10^7$
1 atm CO	cyclohexane	$3.50 \times 10^7$
1 atm Ar	acetonitrile	$5.34 \times 10^7$
0.5 atm CO	cyclohexane	$4.30 \times 10^7$

When samples prepared in mecn were photolysed under 1 atmosphere of CO ( $[\text{CO}] = 9 \times 10^{-3} \text{ M}$ ), light scattering, possibly due to localised heating effects, was observed in laser signals which masked the transient recovery. No correlation of results for first and second order rate equations was obtained. To ensure that the reactions being carried out were generated as a result of photochemistry and not because of thermal reactions, a control experiment was set up. Solutions were prepared as in the photochemical experiments. This control sample in a sealed cuvette was left in the dark and spectra were recorded for the same duration as the

photochemical experiments. Both IR and steady-state UV/Vis spectrum did not show any change under these conditions.

#### 2.2.4.3. Flash photolysis in the presence of pyridine trapping ligand

Solutions of **pachc** were prepared in pentane containing 50, 10 and 5 equivalents of pyridine. Each sample was placed under 1 atmosphere of argon after three freeze-pump-thaw cycles procedure to  $10^{-2}$  Torr. The solution, at room temperature was then subjected to a dynamic vacuum, a process which has been shown to remove traces of water, and a liquid pumping.<sup>13</sup> A typical steady-state UV/Vis spectrum recorded throughout photolysis is shown in Figure 2.10. An absorbance *increase* centered at 352 and 386 nm was observed. However, only bleaching of parent species was observed as previously. No apparent differences were observed for solutions containing different concentrations of pyridine (Table 2.3).

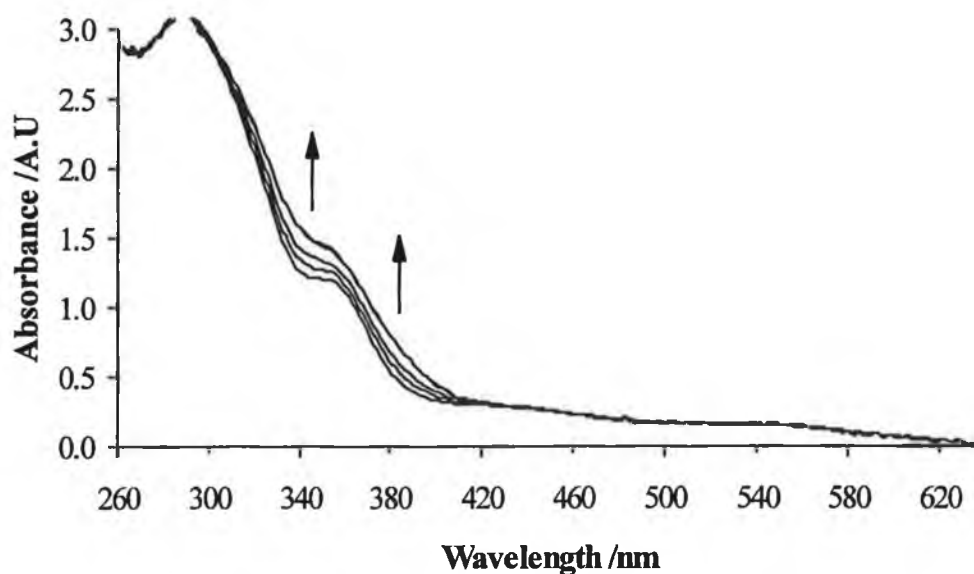


**Figure 2.10** Steady-state UV/Vis monitoring of laser flash photolysis of **pachc** in pyridine ( $1 \times 10^{-6}$  M) in pentane,  $\lambda_{\text{exc}} = 355$  nm, 1 atmosphere argon. Note that the new bands indicated by the arrows increase throughout photolysis.

**Table 2.3** Transient signal changes observed during flash photolysis of *pachc* containing varying concentrations of  $\text{C}_5\text{H}_5\text{N}$  at 298 K.

$[\text{C}_5\text{H}_5\text{N}]$ (M)	Laser Changes <sup>o</sup>	$k_{\text{obs}}$ ( $\times 10^7 \text{s}^{-1}$ )
$1.06 \times 10^{-5}$	depletion and recovery	8.9
$1.79 \times 10^{-5}$	depletion and recovery	4.8
$3.15 \times 10^{-2}$	depletion and recovery	7.4
10% solution	depletion and recovery	2.6
Neat $\text{C}_5\text{H}_5\text{N}$	depletion and recovery	1.8

$\lambda_{\text{exc}} = 355 \text{ nm}$ ; cyclohexane solution; 1 atmosphere argon; <sup>o</sup> steady-state UV/Vis. spectra showed an increase in absorbance between 340 and 420 nm for all experiments.

The intensity of the transient signal decreased on changing monitoring wavelengths from 380 to 590 nm. The experiment was repeated for 10% pyridine solutions with the same result as above. IR spectral changes were recorded immediately after laser flash photolysis of the sample containing 10 molar equivalents of pyridine. The parent bands at 2094, 2056, 2032, and 2028  $\text{cm}^{-1}$  depleted while new bands at 2066, 2021, 2006, 1996(vs) and 1967  $\text{cm}^{-1}$  were observed indicating the formation of  $(\mu_2\text{-C}_6\text{H}_5\text{C}_2\text{H})\text{Co}_2(\text{CO})_5(\text{C}_5\text{H}_5\text{N})$ . This was based on the results of steady-state photolysis of *pachc* in the presence of pyridine and the similarity of the product spectrum to that of other monosubstituted species.

Crystals of this product were grown and examination of these by IR spectroscopy showed bands at 2065, 2016, 2005, 1996 (vs) and 1970, which are identified as newly formed  $(\mu_2\text{-C}_6\text{H}_5\text{C}_2\text{H})\text{Co}_2(\text{CO})_5(\text{C}_5\text{H}_5\text{N})$ , while bands at 2094, 2055, 2032, 2026  $\text{cm}^{-1}$  have been identified as  $(\mu_2\text{-C}_6\text{H}_5\text{C}_2\text{H})\text{Co}_2(\text{CO})_6$ . A fifth band for this complex which usually appears as a shoulder on the band at 2026  $\text{cm}^{-1}$  is probably obscured by the band at 2016  $\text{cm}^{-1}$ . (Figure 2.11(a)). This compound was found to be very air

sensitive which prevented further examination. The UV/Vis spectrum of these crystals are given in Fig 2.11(b).

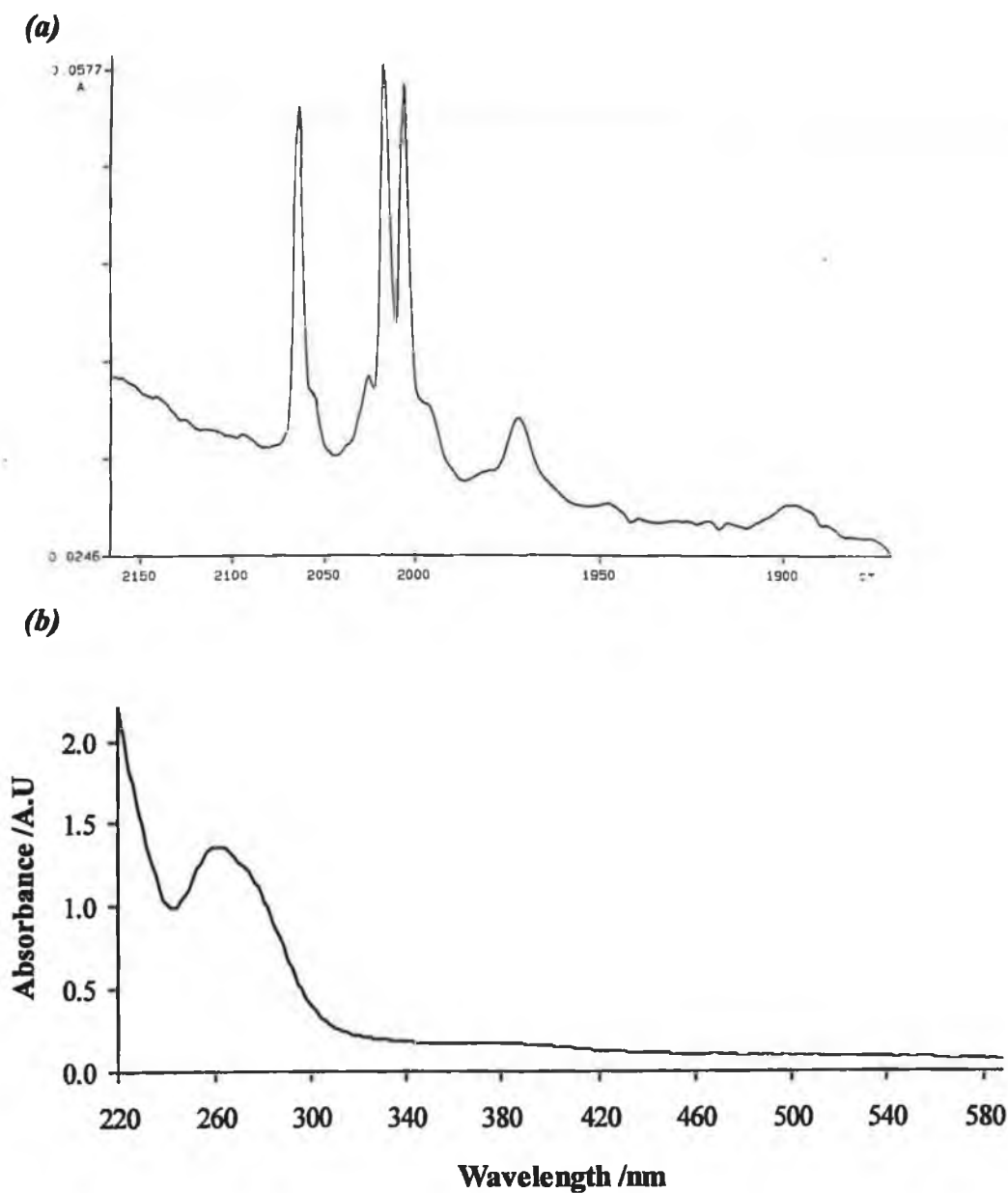


**Figure 2.11** Spectroscopic preparation of crystals formed following photolysis of *pachc* in 10% pyridine (a) IR spectrum in the CO stretching region ( $\text{cm}^{-1}$ ,  $\pm 1 \text{ cm}^{-1}$ ) and (b) UV/Vis spectrum in cyclohexane.



### 2.2.5 Summary of Results for Photolysis Experiments using $\lambda_{\text{exc}} = 355 \text{ nm}$

The five new bands in the IR spectrum following steady-state photolysis of **pachc** in the presence of either  $\text{PPh}_3$  or  $\text{C}_5\text{H}_5\text{N}$  confirm the products to be the appropriate substituted species  $(\mu_2\text{-C}_6\text{H}_5\text{C}_2\text{H})\text{Co}_2(\text{CO})_5(\text{C}_5\text{H}_5\text{N})$  or  $(\mu_2\text{-C}_6\text{H}_5\text{C}_2\text{H})\text{Co}_2(\text{CO})_5(\text{PPh}_3)$ . Steady-state UV/Vis spectral monitoring throughout photolysis also showed the two parent bands at 352 and 422 nm decreased with the simultaneous increase in a new band at 416 nm when  $\text{C}_5\text{H}_5\text{N}$  was added suggesting the formation of  $(\mu_2\text{-C}_6\text{H}_5\text{C}_2\text{H})\text{Co}_2(\text{CO})_5(\text{C}_5\text{H}_5\text{N})$ .

Pulsed photolysis experiments conducted in the presence of trapping ligands such as  $\text{C}_5\text{H}_5\text{N}$ ,  $\text{PPh}_3$  or  $\text{CO}$  resulted in transient signals showing the depletion of parent absorption followed by a rapid recovery to pre-irradiated levels. The observed rate constant,  $k_{\text{obs}}$ , did not show a dependence on the concentration of  $\text{CO}$ . This behaviour is not consistent with the loss of  $\text{CO}$  being the primary photochemical reaction. The appearance of new bands in the steady-state UV/Vis spectrum monitored throughout the laser experiments give evidence for the formation of a new species. The molar extinction coefficient of the product is similar to that of the parent compound hence there is no evidence of formation of a new species in the laser experiment. In these experiments only depletion of the parent absorption and no transient absorptions are observed. Changes in the IR spectrum recorded after flash photolysis, noted only in the presence of added  $\text{PPh}_3$  or  $\text{C}_5\text{H}_5\text{N}$ , have given evidence for the formation of a monosubstituted derivative  $(\mu_2\text{-C}_6\text{H}_5\text{C}_2\text{H})\text{Co}_2(\text{CO})_5(\text{L})$  ( $\text{L} = \text{PPh}_3$  or  $\text{C}_5\text{H}_5\text{N}$ ). Clearly the photochemical changes observed were the result of excitation by the monitoring lamp rather than the laser output. This result is consistent with the recently published results of matrix isolation studies which demonstrated that irradiation with  $\lambda_{\text{exc}} = 350 \text{ nm}^8$  fails to produce significant photochemistry.

To explain the depletion of the parent absorption observed in these experiments, following laser excitation it is proposed that homolytic cleavage of the cobalt - cobalt bond occurs which rapidly undergoes an efficient recombination. Consequently further time-resolved experiments were conducted using the second and fourth harmonic of the Nd-YAG fundamental wavelength at 532 and 266 nm respectively.

#### 2.2.6 Laser flash photolysis of $(\mu_2\text{-C}_6\text{H}_5\text{C}_2\text{H})\text{Co}_2(\text{CO})_6$ at $\lambda_{\text{exc}} = 266 \text{ nm}$

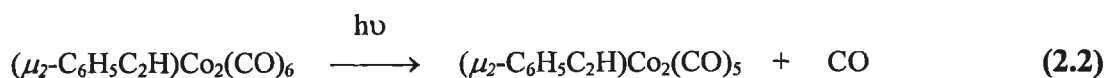
The excitation wavelength of the laser was changed to 266 nm to determine if there was a difference in the behaviour of the system at this excitation wavelength compared to that observed following irradiation with  $\lambda_{\text{exc}} = 355 \text{ nm}$ . Samples were prepared as outlined previously in both acetonitrile and cyclohexane respectively and placed under 1 atmosphere of CO ( $[\text{CO}] = 9 \times 10^{-3} \text{ M}$ ). The monitoring beam was varied from 480 to 350 nm. However no photochemistry was observed following  $\lambda_{\text{exc}} = 266 \text{ nm}$  excitation. The steady-state UV/Vis spectrum showed an overall decrease of parent bands for both solvent systems indicating the degradation of the parent species.

#### 2.2.7 Laser flash photolysis of $(\mu_2\text{-C}_6\text{H}_5\text{C}_2\text{H})\text{Co}_2(\text{CO})_6$ at $\lambda_{\text{exc}} = 532 \text{ nm}$

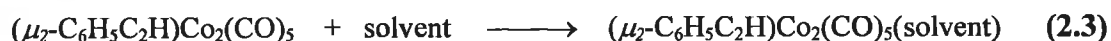
Pulsed photolysis ( $\lambda_{\text{exc}} = 532 \text{ nm}$ ) of a **pachc** sample prepared in pentane containing 10% pyridine resulted in the transient which absorbs with a  $\lambda_{\text{max}}$  at 400 nm as presented in Figure 2.12. This intermediate follows first order kinetics with the rate of recovery ( $k_{\text{obs}}$ ) measured at  $5 \times 10^3 \text{ s}^{-1}$  under 1 atmosphere of argon. Under these conditions the transient signal is not reversible. The signal observed is assigned to the formation of a solvated species  $(\mu_2\text{-C}_6\text{H}_5\text{C}_2\text{H})\text{Co}_2(\text{CO})_5(\text{solvent})$  which reacts with  $\text{C}_5\text{H}_5\text{N}$  to form a long lived species assigned  $(\mu_2\text{-C}_6\text{H}_5\text{C}_2\text{H})\text{Co}_2(\text{CO})_5(\text{C}_5\text{H}_5\text{N})$ . The lifetime of this species depends on the concentration of added pyridine and a second order rate constant for the reaction of  $(\mu_2\text{-C}_6\text{H}_5\text{C}_2\text{H})\text{Co}_2(\text{CO})_5(\text{solvent})$  with pyridine

was determined  $3.0 \times 10^6 \text{ dm}^3 \text{ mol}^{-1} \text{ s}^{-1}$  at 298 K. Experiments conducted in the presence of  $\text{PPh}_3$  showed similar a transient absorption with  $\lambda_{\text{max}}$  at 400 nm.

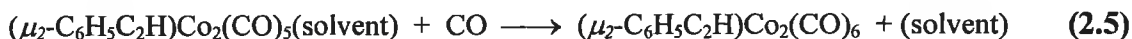
Thus, the primary photoreaction in solution at  $\lambda_{\text{exc}} = 532 \text{ nm}$  is given by the following (reaction 2.2)



As coordinately unsaturated 16 electron intermediates are extremely reactive, and are known to coordinate weakly even to inert gases thus it is assumed that the pentacarbonyl intermediate coordinates to a solvent molecule according to reaction 2.3



In the presence of a ligand (e.g.  $\text{PPh}_3$  or  $\text{C}_5\text{H}_5\text{N}$ ) the solvated intermediate exchanges a solvent molecule for a ligand molecule (reaction 2.4). In the presence of CO the solvent intermediate recombines with CO to regenerate the parent hexacarbonyl according to reaction 2.5.



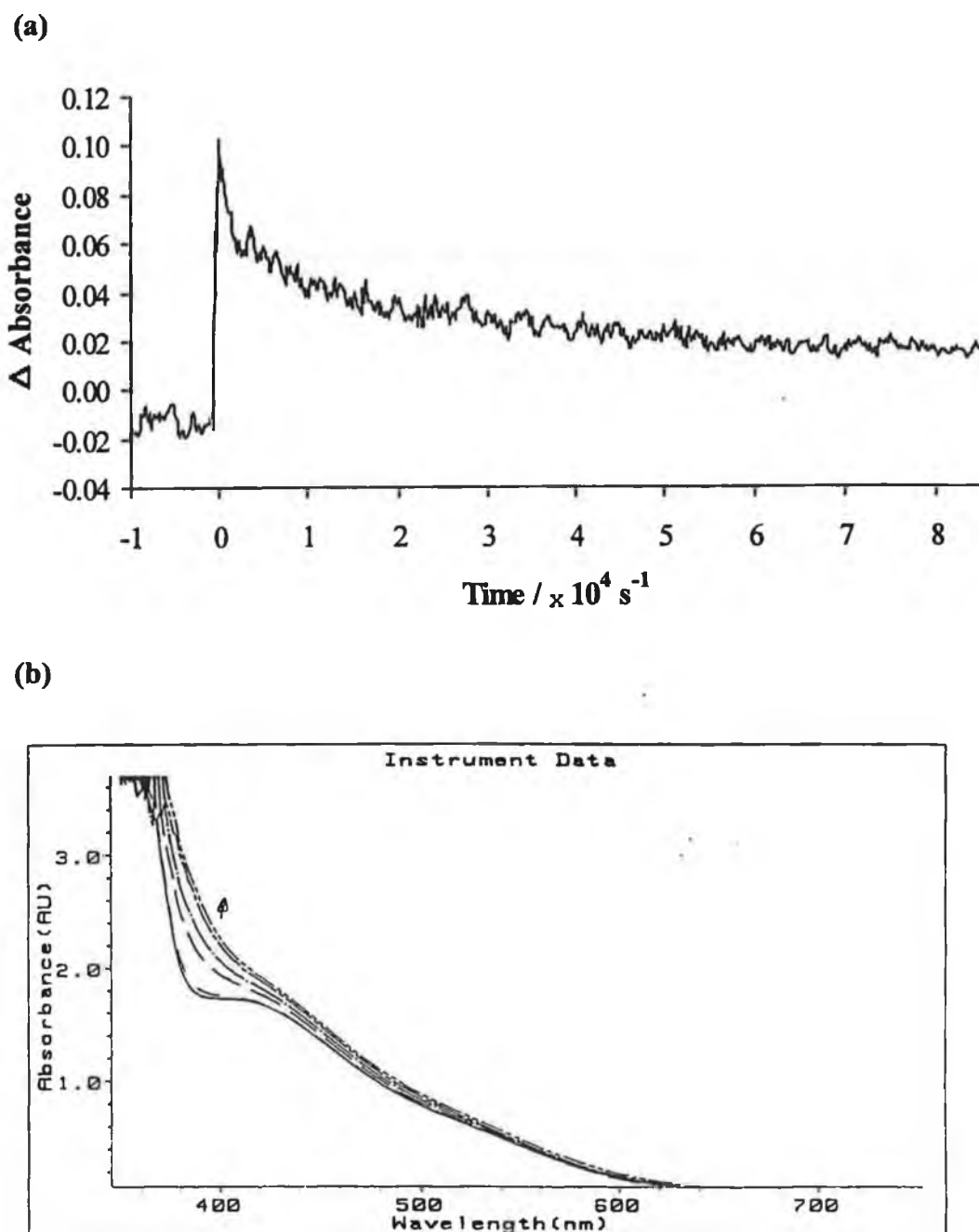


**Figure 2.12** Laser flash photolysis of *pacc* (conc. =  $1.1 \times 10^{-7}$  M) in 10% pyridine under 1 atmosphere of argon; (a) shows the transient decay signal ( $\lambda_{\text{exc}} = 532$  nm) monitored at 390 nm (b) shows the steady-state UV/Vis spectrum obtained throughout flash photolysis; — pre photolysis, - - - after photolysis.

Changes in the steady-state UV/Vis spectrum of the sample were monitored at intervals throughout the experiment. There was an increase in bands in the region  $\lambda > 340$  to 500 nm which indicates the formation of a new species. New bands were observed in the IR spectrum obtained immediately after the flash photolysis experiment. The newly formed species was identified as ( $\mu_2$ - $\text{C}_6\text{H}_5\text{C}_2\text{H}$ ) $\text{Co}_2(\text{CO})_5(\text{C}_5\text{H}_5\text{N})$  on comparison with steady-state photochemical experiments performed earlier. The shift of parent bands to smaller wavenumbers on formation of the product is consistent with the addition of an electron donating substituent.

In the UV/Vis spectral region at  $\lambda < 340$  nm the absorbance of the parent is too intense to observe changes upon photolysis. A more dilute solution was prepared so that any spectral changes in the high energy region of the spectrum could be observed. However, the solutions prepared with an OD = 0.5 A.U. at  $\lambda_{\text{exc}} = 532$  nm failed to produce transient signals in pulsed photolysis experiments. The low energy laser beam is not strong enough to excite any species as the concentration of sample is too low. Flash photolysis was carried out on a solution of **pache** prepared in pentane in the absence of pyridine under 1 atmosphere of CO ( $[\text{CO}] = 9 \times 10^{-3}$  M). Steady-state UV/Vis bands showed no change in absorbance bands while monitoring throughout photolysis, which is expected for reversible reactions in the absence of trapping ligand and is evidence for a reversible CO-loss process. A transient decay such as that in Figure 2.13 was obtained.

This depletion followed by a full recovery to parent species is evidence for the reversible photochemical loss of CO. The  $k_{\text{obs}}$  was linearly dependent on the concentration of CO yielding the second order rate constant ( $k_2 = 1.2 \times 10^6 \text{ dm}^3 \text{ mol}^{-1} \text{ s}^{-1}$  at 298 K) as the slope. While the lifetime of the species was reduced under an atmosphere of CO its yield was not affected - behavior which is typical of CO-loss intermediates. Repeated exposure to the laser radiation did not result in significant changes to the steady-state UV/Vis spectrum of the sample.

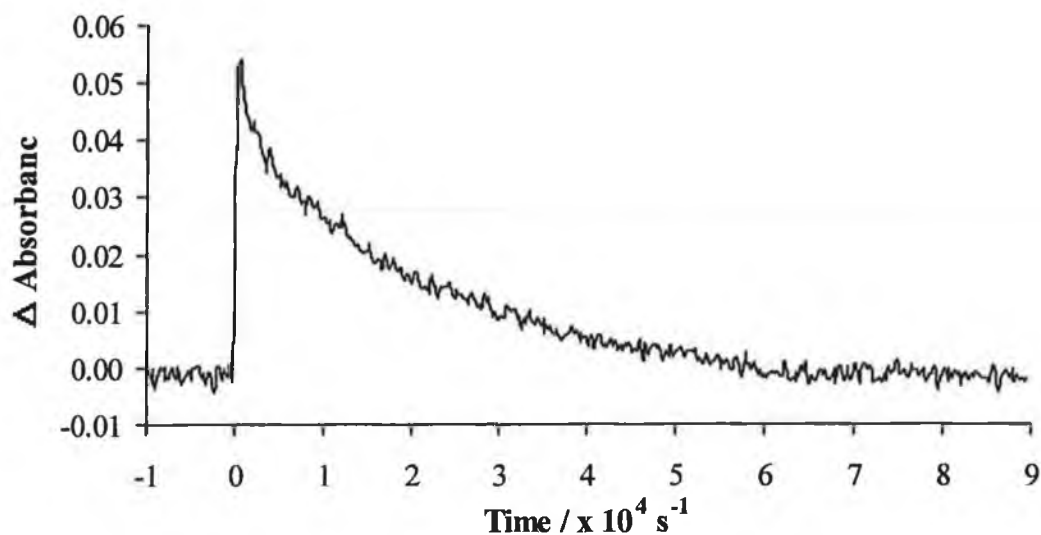
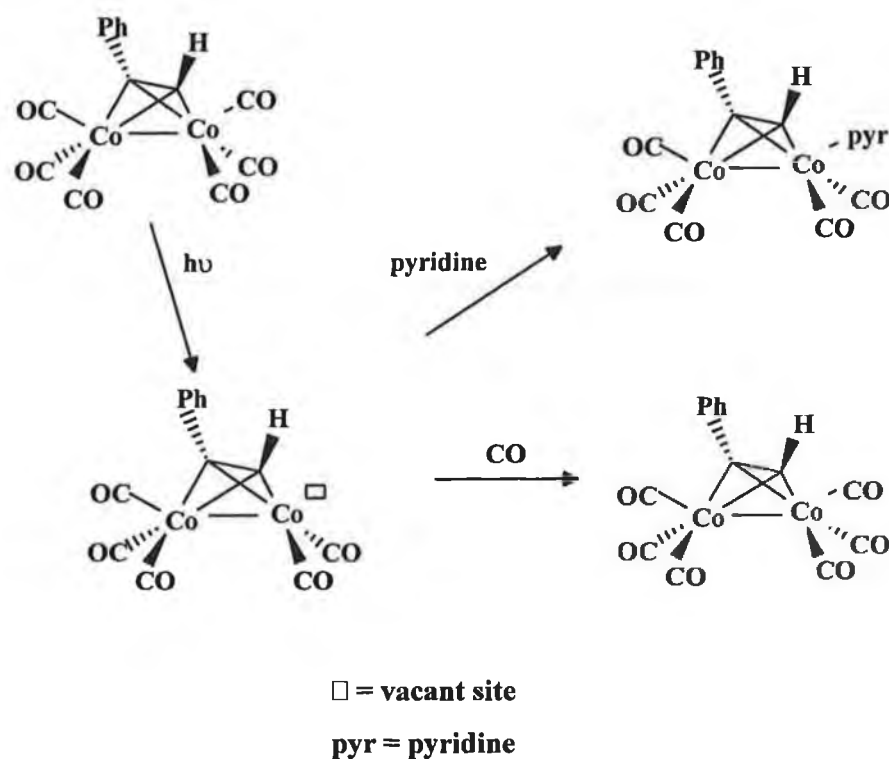


**Figure 2.13** A typical transient signal observed at  $\lambda_{\max} = 400 \text{ nm}$  following laser flash photolysis of *pachc* (conc. =  $1 \times 10^{-7} \text{ M}$ ) in pentane solution with  $\lambda_{\text{exc}} = 532 \text{ nm}$  at 298 K in the presence of 1 atm of CO ( $[\text{CO}] = 9 \times 10^{-3} \text{ M}$ ).

Further experiments in which both CO and pyridine were added to the solution produced a number of transient signals including grow ins and transient decay and recovery. This can be explained by Scheme 2.4. Initially photolysis causes the photodissociation of one CO ligand, the vacant site being occupied by a solvent molecule. The pyridine trapping ligand then competes with free CO in the system to occupy the coordination site.



Scheme 2. 4

### 2.2.8 Steady-state photolysis of $(\mu_2\text{-C}_6\text{H}_5\text{C}_2\text{H})\text{Co}_2(\text{CO})_6$ for $\lambda_{\text{exc}} > 500 \text{ nm}$ .

A sample of **pachc** was dissolved in a pentane solution containing 10% pyridine and flushed with argon for 15 minutes. The spectroscopic changes upon irradiation in front of a xenon arc lamp (275 W) using a visible light filter ( $\lambda_{\text{exc}} > 500 \text{ nm}$ ) were monitored by IR spectroscopy. Depletion of the parent bands were observed at 2093.6, 2056.3, 2028.6(broad) and 2018  $\text{cm}^{-1}$  after monitoring photolysis periodically for 15 minutes. New bands observed at 2069, 2018, 2005, 1994 and 1966  $\text{cm}^{-1}$  are identified as the formation of  $(\mu_2\text{-C}_6\text{H}_5\text{C}_2\text{H})\text{Co}_2(\text{CO})_5(\text{C}_5\text{H}_5\text{N})$ . A band at 1852  $\text{cm}^{-1}$  remains unassigned. Figure 2.14 shows the appearance of new bands and the continual depletion of parent bands. No evidence was found for the formation of the bi-substituted complex in these experiments. Using  $\text{PPh}_3$  as the trapping ligand also resulted in the formation of a monosubstituted pentacarbonyl complex,  $(\mu_2\text{-$

$\text{C}_6\text{H}_5\text{C}_2\text{H})\text{Co}_2(\text{CO})_5(\text{PPh}_3)$ . In general, the photolysis time required was longer, however, when using  $\text{C}_5\text{H}_5\text{N}$  as the trapping ligand.

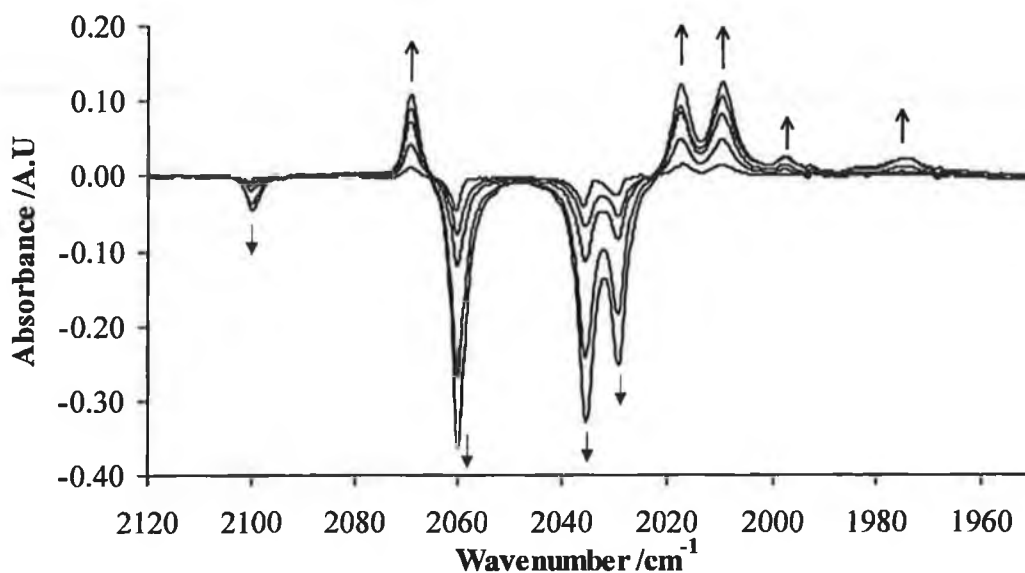


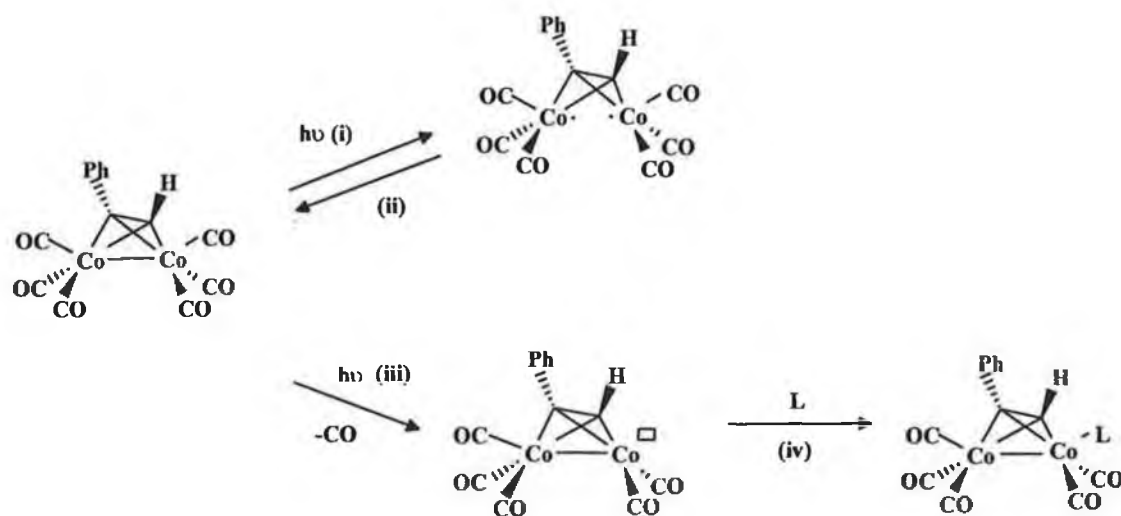
**Figure 2.14** IR spectrum in the CO spectral region observed throughout broad band photolysis of *pachc* in cyclohexane solution at 298 K for  $\lambda_{\text{exc}} > 500 \text{ nm}$  ( $\text{cm}^{-1}$ ,  $\pm 1 \text{ cm}^{-1}$ ).

An experiment monitoring the changes in the steady-state UV/Vis spectrum during steady-state photolysis of *pachc* in the presence of trapping ligand L (L =  $\text{PPh}_3$  or  $\text{C}_5\text{H}_5\text{N}$ ) resulted in featureless spectra. While it is difficult to assign the resulting UV/Vis spectrum in itself, assignment was made based on an IR spectrum run immediately after photolysis. The product was identified as  $(\mu_2\text{-C}_6\text{H}_5\text{C}_2\text{H})\text{Co}_2(\text{CO})_5(\text{L})$ .



2.2.9 Summary for low energy photolysis experiments ( $\lambda_{\text{exc}} = 532 \text{ nm}$ )

While reducing the excitation wavelengths increased the yield of the substituted product, short wavelength photolysis ( $\lambda_{\text{exc}} > 340 \text{ nm}$  or  $> 400 \text{ nm}$ ) also increased the yield of the disubstituted derivatives particularly for  $\text{L} = \text{PPh}_3$ . Upon long wavelength steady-state photolysis ( $\lambda_{\text{exc}} > 500 \text{ nm}$ ) however, only monosubstituted derivatives are observed. Therefore, the cobalt system has been shown for the first time to undergo a wavelength dependent photochemistry. The photolytic method described is very gentle, yields are good and reaction times are faster than with the traditional thermal technique. Long wavelength excitation at  $532 \text{ nm}$  results in the desired CO-loss process and consequently facilitates the next step in the Pauson - Khand reaction. This explains why Livinghouse<sup>2</sup> observed the photochemical promotion of the Pauson - Khand reaction following visible light photolysis. The overall photochemistry is summarised in the following Scheme.



**Scheme 2.5** (i)  $\lambda_{\text{exc}} = 355 \text{ nm}$  in alkane solvent, (ii)  $\tau_{1/2} = 2.5 \times 10^{-8} \text{ s}$  at  $298 \text{ K}$ , (iii)  $\lambda_{\text{exc}} = 500 \text{ nm}$ , (iv)  $k_2 = 1.2 \times 10^6 \text{ dm}^3 \text{ mol}^{-1} \text{ s}^{-1}$  at  $298 \text{ K}$  for  $\text{L} = \text{CO}$  ( $\square$  = vacant site on the cobalt atom).

### 2.3 Photolysis of $(\mu_2\text{-C}_2\text{H}_2)\text{Co}_2(\text{CO})_6$

#### 2.3.1 Molecular modeling of $(\mu_2\text{-C}_2\text{H}_2)\text{Co}_2(\text{CO})_6$

The molecular structure of **achc** is presented in Figure 2.15. While structurally similar to the **pachc** complex discussed earlier, this complex is more symmetrical. The position of the acetylene moiety is such that it sits at right angles to the cobalt - cobalt core. Again the bonding can be described in terms of the acetylene acting as a four electron donor with each cobalt atom receiving two electrons. With no possibility of steric hindrance from the acetylene, the alkene insertion step from a Pauson - Khand cyclisation should be facilitated equally on either face of the cobalt core resulting in equal proportions of cyclopentenone isomers.

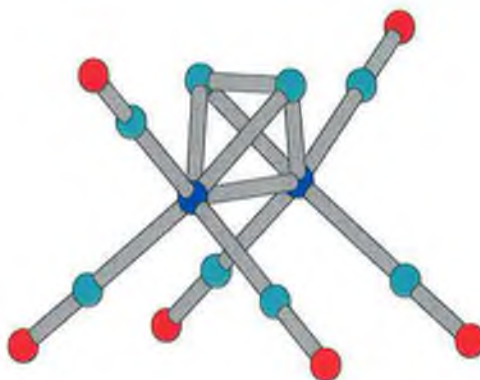


**Figure 2.15** Molecular structure of **achc**

#### 2.3.2 Synthesis and Spectroscopic Characterisation of $(\mu_2\text{-C}_2\text{H}_2)\text{Co}_2(\text{CO})_6$

##### 2.3.2.1 Preparation and IR spectrum of $(\mu_2\text{-C}_2\text{H}_2)\text{Co}_2(\text{CO})_6$

The synthesis of acetylene hexacarbonyldicobalt (**achc**) was carried out by slight modification to the method of Sternberg and Greenfield<sup>10</sup> and proceeds according to reaction 2.6. Since acetylene is a gas it was incorporated into the atmosphere above the  $\text{Co}_2(\text{CO})_8$ . The orange crystalline starting material darkened

ultimately forming a deep red liquid. Formation of the **achc** complex results from simple replacement of the bridging carbonyls in  $\text{Co}_2(\text{CO})_8$ .



The reaction was monitored by IR spectroscopy which indicated the disappearance of parent bands 2095, 2064, 2042, 2032 and 2028, 1867 and 1859  $\text{cm}^{-1}$  as in Figure 2.16. In the product, new terminal CO bands are formed at 2099, 2060, 2035 and 2029  $\text{cm}^{-1}$  with a shoulder at 2018  $\text{cm}^{-1}$ . The product was isolated by vacuum filtration through a plug of silica gel and characterised by IR and  $^1\text{H}$  NMR spectroscopy and elemental analysis.

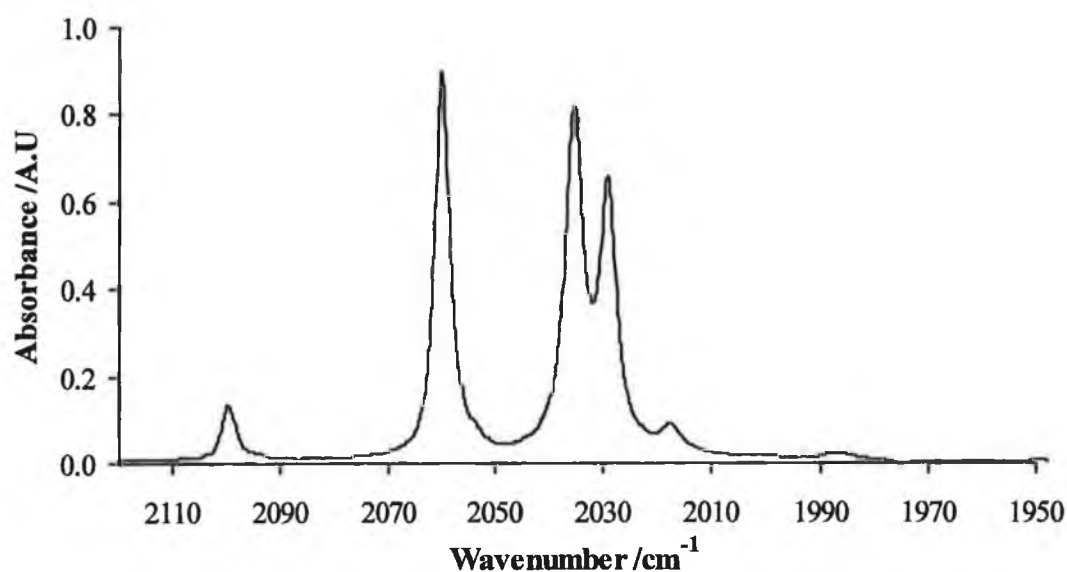


**Figure 2.16** IR spectrum in the CO stretching region of *achc* at 298K in cyclohexane ( $\text{cm}^{-1}$ ,  $\pm 1 \text{ cm}^{-1}$ ).

2.3.2.2. NMR characterisation of  $(\mu_2\text{-C}_2\text{H}_2)\text{Co}_2(\text{CO})_6$ 

The  $^1\text{H}$  NMR spectrum provides evidence for complexation of the acetylene ligand to dicobalt hexacarbonyl moiety in the **achc** complex and is presented in Figure 2.17. An expected shift in the uncoordinated acetylene protons upon complexation was observed. In uncoordinated acetylene a proton resonance appears at 3.4 (s, 2H) ppm while a resonance observed at 6.01 (s, 2H) ppm is assigned to acetylene  $\text{=C-H}$  protons in the **achc** complex. All chemical shifts are measured relative to TMS internal standard.

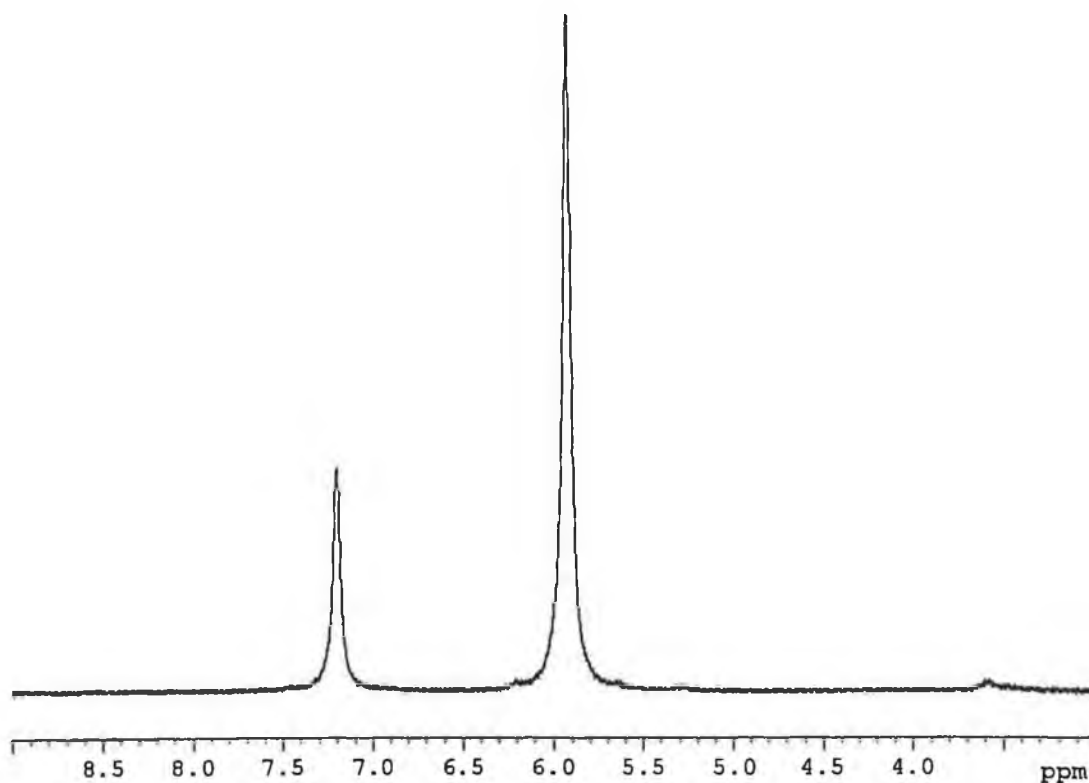
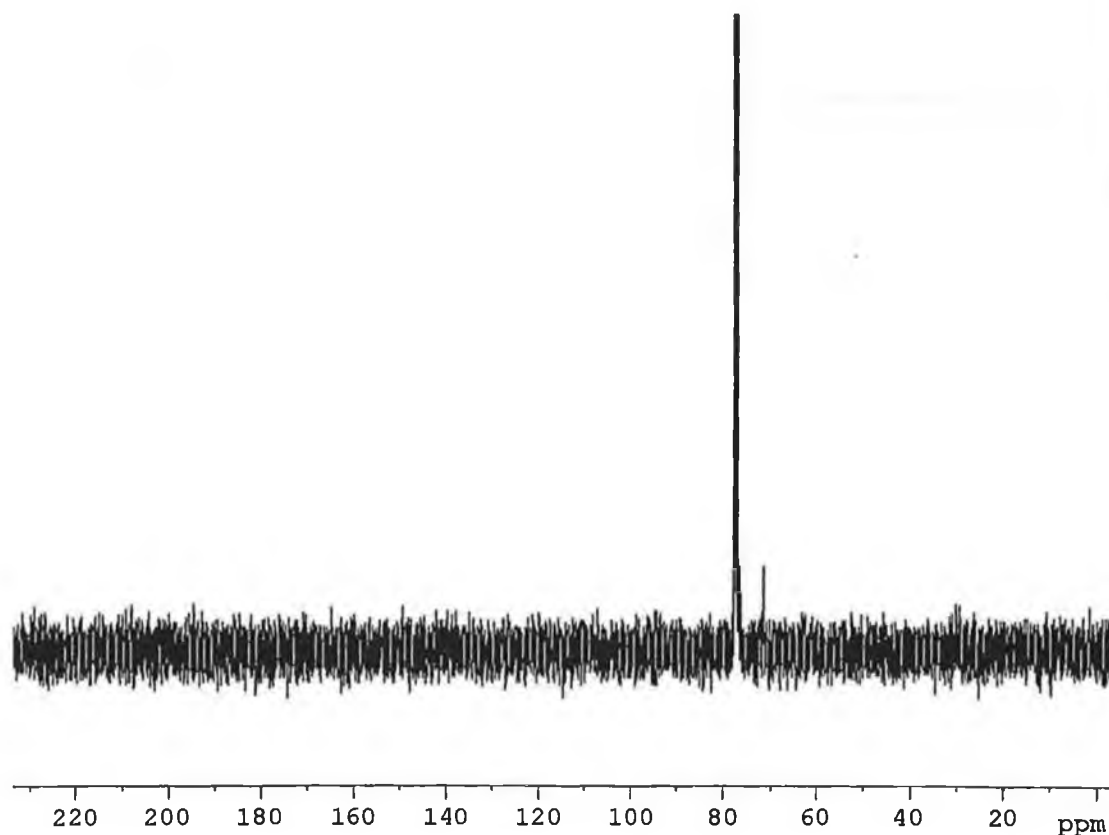


Figure 2.17  $^1\text{H}$  NMR spectrum of **achc** at 298 K in  $\text{CDCl}_3$ .

The  $^{13}\text{C}$  NMR spectrum of **achc** is presented in Figure 2.18. The acetylenic carbon atom which appears at 77.8 ppm in uncoordinated acetylene ( $\text{CDCl}_3$ ) is observed at 71.4 ppm when complexed. The  $\pi$  - electron density of the carbon - carbon bond has decreased and is now localised on the ' $\text{C}_2\text{Co}_2$ ' core. The carbonyl

ligands in the  $(\mu_2\text{-C}_2\text{H}_2)\text{Co}_2(\text{CO})_6$  complex appear as a broad signal at around 199 ppm, suggesting that the carbonyls are rapidly interchanging on an NMR timescale. The triplet resonance at 77 ppm is assigned to  $\text{CDCl}_3$ .



**Figure 2.18**  $^{13}\text{C}$  NMR spectrum of *achc* at 298 K in  $\text{CDCl}_3$ . The triplet at 77 ppm is  $\text{CDCl}_3$

### 2.3.2.3. Electronic absorbance spectrum of $(\mu_2\text{-C}_2\text{H}_2)\text{Co}_2(\text{CO})_6$

The UV/Vis spectrum of **achc** is presented in Figure 2.19. This spectrum resembles that of **pachc** (c.f. Figure 2.5). Bands are observed at 346 ( $\epsilon = 1.33 \times 10^5 \text{ mol}^{-1} \text{ dm}^3 \text{ cm}^{-1}$ ) and 447 nm ( $\epsilon = 2.15 \times 10^4 \text{ mol}^{-1} \text{ dm}^3 \text{ cm}^{-1}$ ). The  $\lambda_{\text{max}}$  at 346 nm has been assigned to a  $\sigma\text{-}\sigma^*$  transition associated with the Co - Co bond<sup>14</sup> while the band at lower energy (447 nm) was assigned to  $\pi\text{-}\pi^*$  transitions. It is worth noting that due

to no conjugation this complex does not absorb as far into the visible region as does the **pachc**. This will become important when choosing the wavelength region for photolysing the sample.

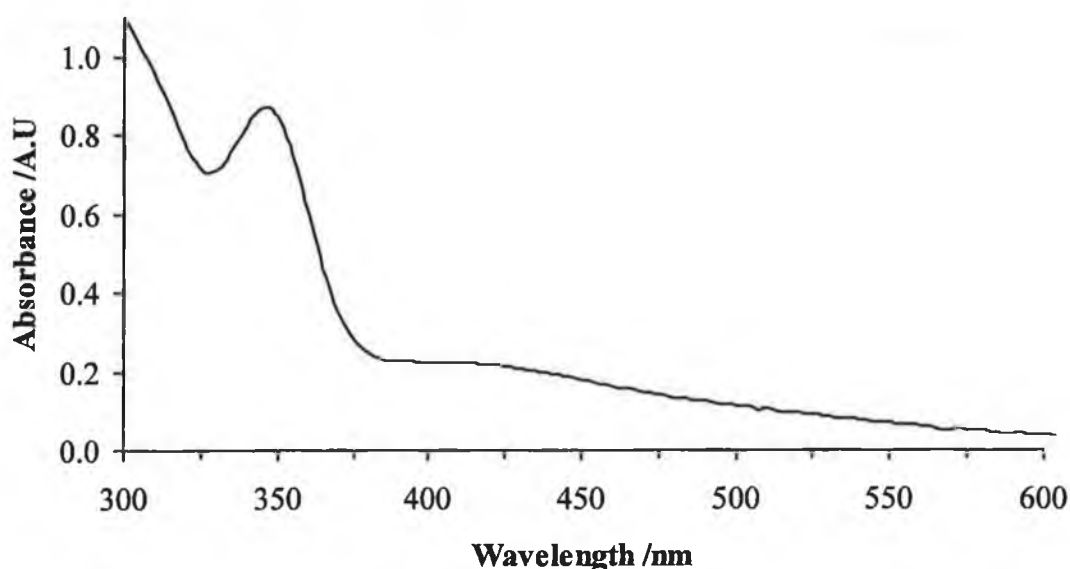


**Figure 2.19** UV/Vis spectrum of **achc** (conc. =  $1.6 \times 10^{-3}$  M) in pentane solution at 298K.

### 2.3.3 Steady-state Photolysis Experiments

#### 2.3.3.1. Photolysis of $(\mu_2\text{-C}_2\text{H}_2)\text{Co}_2(\text{CO})_6$ in the presence of trapping ligands

Irradiation of a cyclohexane solution of **achc** containing a 4-fold excess of pyridine at  $\lambda_{\text{exc}} > 400$  nm resulted in changes to the IR spectrum as outlined in Figure 2.20(a). The negative peaks indicate the depletion of the parent complex upon irradiation. The appearance of new bands is identified as the formation of  $(\mu_2\text{-C}_2\text{H}_2)\text{Co}_2(\text{CO})_5(\text{C}_5\text{H}_5\text{N})$  as well as the further substitution of a second CO ligand with pyridine to form  $(\mu_2\text{-C}_2\text{H}_2)\text{Co}_2(\text{CO})_4(\text{C}_5\text{H}_5\text{N})_2$  (Table 2.4). This latter assignment was based on comparison of the  $\nu_{\text{CO}}$  bands with those of an authentic sample of the species synthesised by thermal methods (see experimental section for

synthesis). The reaction is very clean with two clear isosbestic points observed. The spectrum is shown in Figure 2.20(b). A change in colour from the original deep red to pale yellow was noted. In general the yield of photoproduct was greater when  $\text{PPh}_3$  was used as the trapping ligand.

**Table 2.4** The  $\nu_{\text{CO}}$  band positions observed for steady-state photolysis of **achc**.

Compound	$\nu_{\text{CO}}$
$(\mu_2\text{-C}_2\text{H}_2)\text{Co}_2(\text{CO})_6^{\text{a}}$	2100, 2060, 2035, 2029, 2018(sh)
$(\mu_2\text{-C}_2\text{H}_2)\text{Co}_2(\text{CO})_5(\text{C}_5\text{H}_5\text{N})^{\text{b}}$	2064, 2019, 2002, 1996, 1968
$(\mu_2\text{-C}_2\text{H}_2)\text{Co}_2(\text{CO})_4(\text{C}_5\text{H}_5\text{N})_2^{\text{b}}$	2021, 2004, 1970, 1941
$(\mu_2\text{-C}_2\text{H}_2)\text{Co}_2(\text{CO})_5(\text{PPh}_3)^{\text{b}}$	2069, 2017, 2009, 1998, 1975
$(\mu_2\text{-C}_2\text{H}_2)\text{Co}_2(\text{CO})_4(\text{PPh}_3)_2^{\text{b}}$	2028, 1982, 1965, 1948

*Cyclohexane solution at 298 K ( $\text{cm}^{-1}$ ;  $\pm 1 \text{ cm}^{-1}$ ); <sup>a</sup> complex prepared by a thermal method; <sup>b</sup> complexes generated by steady-state photolysis experiments.*

Irradiation of **achc** in cyclohexane at  $\lambda_{\text{exc}} > 340 \text{ nm}$  with an excess of either pyridine or  $\text{PPh}_3$  also resulted in bands consistent with the formation of the mono and disubstituted complexes. New bands grew during the initial 5 minutes of irradiation.<sup>15</sup> After 5 minutes the parent bands continue to deplete but so do the product bands. However, there was no evidence for further photoproduct formation. A higher yield of photoproduct was observed while comparing irradiation for  $\lambda_{\text{exc}} > 340 \text{ nm}$  with  $\lambda_{\text{exc}} > 400 \text{ nm}$ . This is due to the absorption characteristics of **achc** which has a greater absorption in the region around 340 nm.

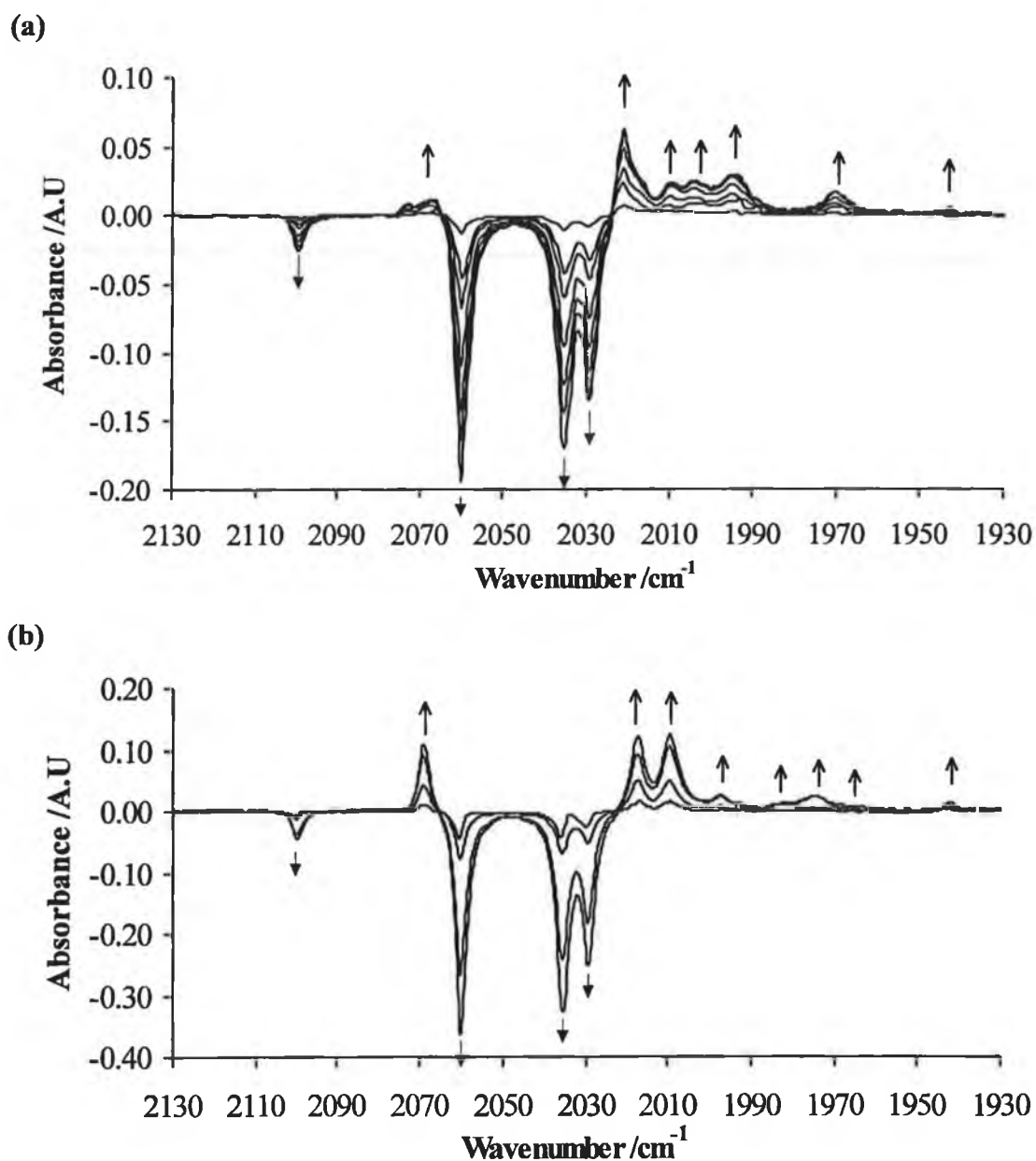


**Figure 2.20** IR spectrum in the CO stretching region following photolysis of *achc* acquired at  $t = 10$  s, 0.5, 1, 5, 10 and 30 minutes irradiation ( $\lambda_{\text{exc}} > 400$  nm) (a) in cyclohexane with added pyridine ( $10^{-4}$  M); the positive bands are identified as  $(\mu_2\text{-C}_2\text{H}_2)\text{Co}_2(\text{CO})_5(\text{C}_5\text{H}_5\text{N})$  and  $(\mu_2\text{-C}_2\text{H}_2)\text{Co}_2(\text{CO})_4(\text{C}_5\text{H}_5\text{N})_2$ ; (b) in pentane with added  $\text{PPh}_3$  ( $10^{-4}$  M); the positive bands are identified as  $(\mu_2\text{-C}_2\text{H}_2)\text{Co}_2(\text{CO})_5(\text{PPh}_3)$  and  $(\mu_2\text{-C}_2\text{H}_2)\text{Co}_2(\text{CO})_4((\text{PPh})_3)_2$ .



### 2.3.3.2. $^1\text{H}$ NMR monitored steady-state photolysis of $(\mu_2\text{-C}_2\text{H}_2)\text{Co}_2(\text{CO})_6$ in $d_5$ - pyridine.

In order to obtain conclusive evidence for the complexation of the trapping ligand upon steady-state photolysis a solution of **achc** was prepared in  $d_5$  - pyridine in a degassable NMR tube. The solution was degassed as outlined in chapter 5. An atmosphere of argon was then placed over the sample and the  $^1\text{H}$  NMR spectrum was obtained at  $t = 0, 5, 10$  minutes and 24 hours after irradiation with  $\lambda_{\text{exc}} > 340$  nm from a xenon arc lamp. The peak positions after photolysis are given in Table 2.5. The peak of the acetylene proton (5.08 ppm) broadened throughout the photolysis experiment and is possibly hidden under the peak at 7.07 ppm after 24 hours. The results indicate that the parent **achc** species was degrading to paramagnetic impurities.

**Table 2.5**  $^1\text{H}$  NMR peak positions following photolysis of **achc** in neat  $d_5$  - pyridine at 298 K.

Time	Peak Positions ( $\delta/\text{ppm}$ )
0	5.08, 7.13, 7.48, 8.71
5 min	5.39, 7.11, 7.46, 8.71
10 min	5.60, 7.11, 7.45, 8.71
24 hrs	-----, 7.07, 7.38, 8.71

$\lambda_{\text{exc}} > 340$  nm.

### 2.3.3.3. UV/Vis monitored steady-state photolysis of **achc** and $(\mu_2\text{-C}_2\text{H}_2)\text{Co}_2(\text{CO})_5(\text{PPh}_3)$

A sample of **achc** prepared in cyclohexane containing a 5 - fold excess of pyridine was irradiated at  $\lambda_{\text{exc}} > 340$  nm. A continual increase in the band at 390 nm was accompanied by a decrease in the bands at 306 and 346 nm for photolysis for  $t =$

40 mins. The spectrum obtained is presented in Figure 2.21. While assignment based on the UV/Vis spectroscopy alone is impossible, an IR spectrum obtained after photolysis gave evidence for the formation of  $(\mu_2\text{-C}_2\text{H}_2)\text{Co}_2(\text{CO})_5(\text{C}_5\text{H}_5\text{N})$ . After 45 minutes irradiation time the new band begins to deplete. Further IR analysis showed that degradation of sample had occurred, possibly caused by continual photolysis with high energy photons.

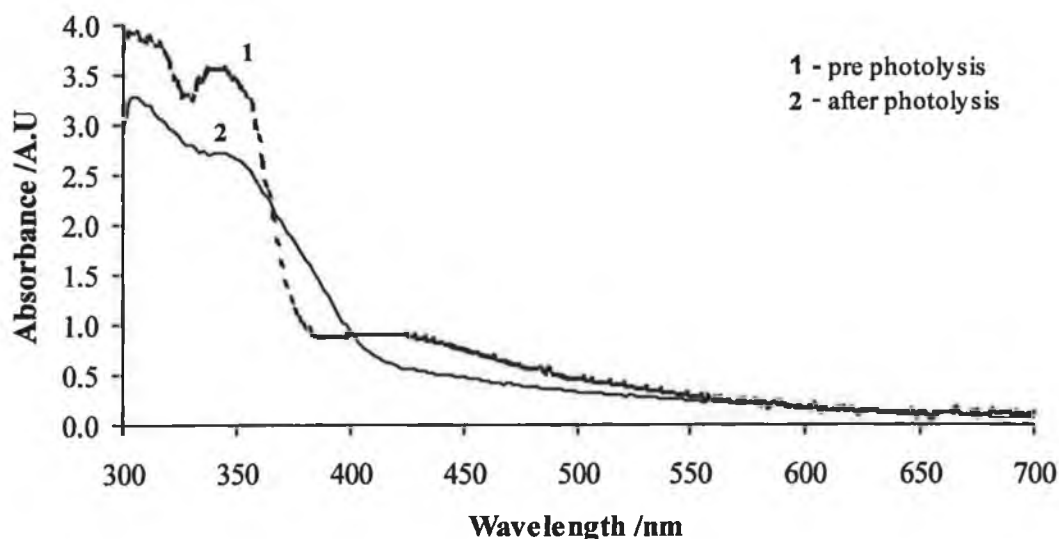


**Figure 2.21** Steady-state UV/Vis spectrum of *achc* containing a 5 fold excess of pyridine in cyclohexane solution at 298 K; — before photolysis, ..... after photolysis;  $\lambda_{\text{exc}} > 340 \text{ nm}$ .

A sample of  $(\mu_2\text{-C}_2\text{H}_2)\text{Co}_2(\text{CO})_5(\text{PPh}_3)$ , prepared previously by thermal methods, was irradiated with  $\lambda_{\text{exc}} > 340 \text{ nm}$  from a xenon arc lamp (275 W). The sample was not degassed. The steady-state UV/Vis monitored spectrum is shown in Figure 2.22. An increase in bands at 222, 276, 282 and  $\sim 500 \text{ nm}$  coincided with a decrease in the band at 324 nm. The photoproduct was identified as  $\text{Co}_2(\text{CO})_8$  based on a change noted for the IR spectrum accompanying UV changes. No further product could be identified.

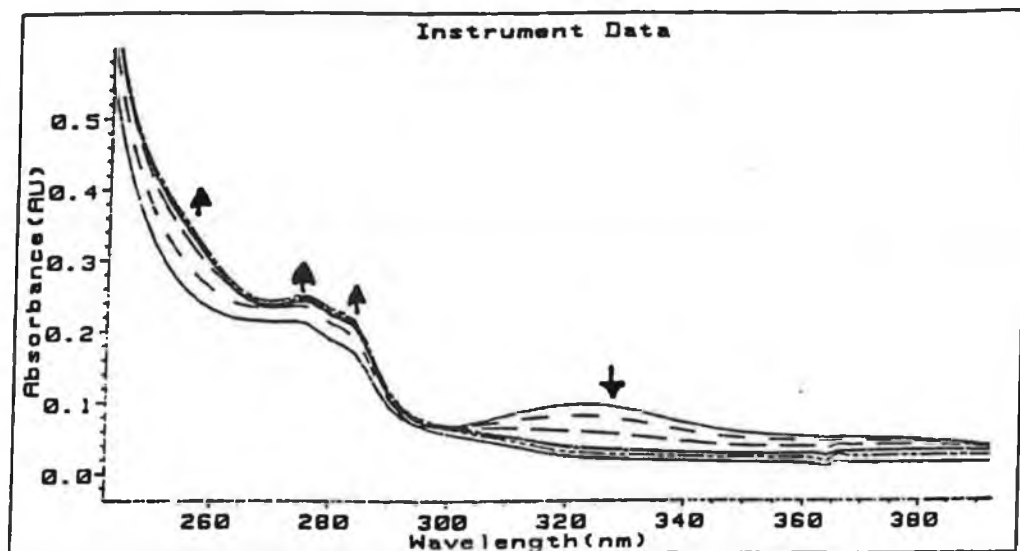


Figure 2.22 Steady-state UV/Vis spectral changes upon photolysis of  $(\mu_2\text{-C}_2\text{H}_2)\text{Co}_2(\text{CO})_5(\text{PPh}_3)$  in cyclohexane solution at 298 K;  $\lambda_{\text{exc}} > 340$  nm; — pre-photolysis, ---- after photolysis.

#### 2.3.3.4. Summary of Results for broad band photolysis experiments ( $\lambda_{\text{exc}} > 340$ and $> 400$ nm)

The results of broad band photolysis of the **achc** complex follows the same trend that was observed with the **pachc** complex studied earlier. Photolysis in degassed hydrocarbon solutions of  $\text{C}_5\text{H}_5\text{N}$  or  $\text{PPh}_3$  resulted in the production of mono- and bi- substituted hexacarbonyl complexes at  $\lambda_{\text{exc}} > 340$  and  $400$  nm. The yield of  $(\mu_2\text{-C}_2\text{H}_2)\text{Co}_2(\text{CO})_5(\text{PPh}_3)$  was greater than the yield of  $(\mu_2\text{-C}_2\text{H}_2)\text{Co}_2(\text{CO})_5(\text{C}_5\text{H}_5\text{N})$ . At  $\lambda_{\text{exc}} > 340$  nm the yield of the appropriate bi - substituted product was again greater than at  $\lambda_{\text{exc}} > 400$  nm. Further investigation into the photolysis of **achc** using monochromatic light sources was carried out.

#### 2.3.4 Laser flash photolysis of $(\mu_2\text{-C}_2\text{H}_2)\text{Co}_2(\text{CO})_6$ at $\lambda_{\text{exc}} = 355 \text{ nm}$

Pulsed photolysis ( $\lambda_{\text{exc}} = 355 \text{ nm}$ ) of **achc**, prepared in pentane containing a 5-fold excess of pyridine, under 1 atmosphere of argon resulted in the transient signal represented in Figure 2.23(a). The transient had maximum intensity while monitoring at 390 nm. The intermediate decayed by first-order kinetics with  $k_{\text{obs}} = 1.7 \times 10^7 \text{ s}^{-1}$  at 298 K. The absorption recovered to pre-irradiated level indicating the reaction is reversible under these conditions. The intensity of the transient absorption increases as the wavelength monitoring beam is decreased. Steady-state UV/Vis spectra were recorded throughout the experiment. An increase in bands at  $\sim 330$  and  $\sim 390 \text{ nm}$  was observed for samples exposed to monitoring beam between 380 - 540 nm. The spectra are given in Figure 2.23(b). At monitoring wavelengths greater than 540 nm no further increase in the steady-state UV/Vis bands was observed. This corresponds with the results from broad band photolysis experiments where very little photoproduct is formed upon irradiation with  $\lambda_{\text{exc}} > 500 \text{ nm}$  (see section 2.36). A closer examination of the UV/Vis spectrum shows that the **achc** does not absorb strongly in the spectral region above 540 nm. The yield of product would therefore be too low to allow any transient signals to be observed at greater than this wavelength. An IR spectrum recorded immediately after flash photolysis confirmed the formation of  $(\mu_2\text{-C}_2\text{H}_2)\text{Co}_2(\text{CO})_5(\text{C}_5\text{H}_5\text{N})$ .

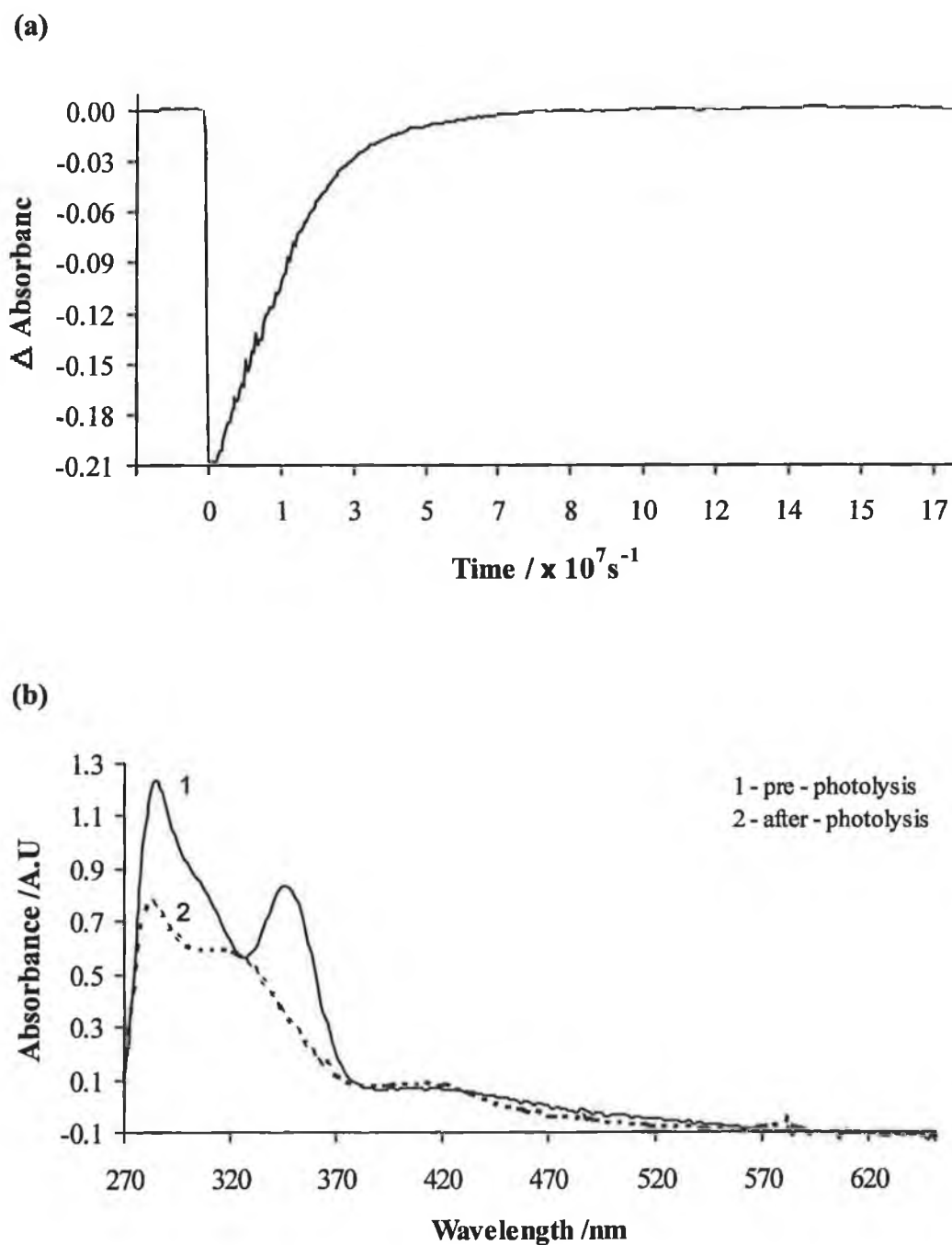


**Figure 2.23** (a) Transient laser signal monitored at 390 nm following laser flash photolysis of *achc* containing a 4 - fold excess of pyridine at  $\lambda_{\text{exc}} = 355$  nm in the presence of 1 atmosphere of argon (b) shows the accompanying UV/Vis spectrum.

Pulsed photolysis ( $\lambda_{\text{exc}} = 355 \text{ nm}$ ) of a solution of **achc** prepared in pentane under 1 atmosphere of CO ( $[\text{CO}] = 9 \times 10^{-3} \text{ M}$ ) resulted in the typical transient signal with a  $\lambda_{\text{max}}$  at 390 nm as depicted in Figure 2.24. Similar signals were obtained across the region of the spectrum where the parent has significant absorbance. The initial bleaching of parent absorption is followed by a recovery to baseline showing the reaction under these conditions to be reversible. The recovery of the depleted absorption followed first order kinetics and this provided an observed rate constant of  $1.8 \times 10^7 \text{ s}^{-1}$  at 298 K. Steady-state UV/Vis spectrum were recorded throughout the experiment. No changes were observed again indicating the reaction to be reversible. Changing the concentration of CO had no effect on the rate of recovery of the parent species (Table 2.6). This is strong evidence that the depletion of the parent absorption was not the result of CO-loss.

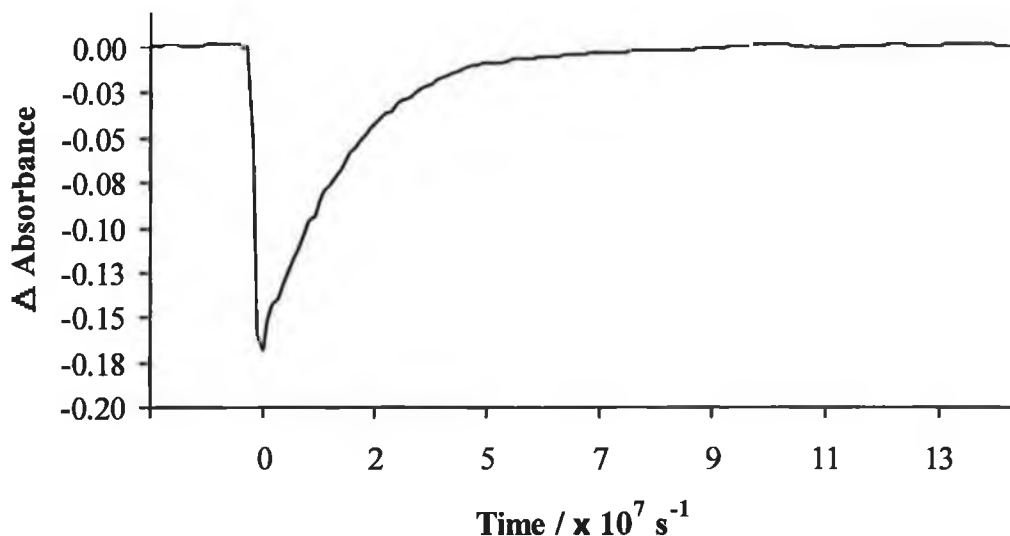


**Figure 2.24** A typical transient laser signal following laser flash photolysis of **achc** in pentane solution at  $\lambda_{\text{exc}} = 355 \text{ nm}$  in the presence of 1 atmosphere of CO ( $[\text{CO}] = 9 \times 10^{-3} \text{ M}$ ). Monitoring wavelength = 390 nm.

**Table 2.6** The observed rate constant ( $\times 10^7 \text{ s}^{-1}$ ) for the reaction of CO with *achc* at various CO concentrations ( $\text{mol dm}^{-3}$ ) at 298 K;  $\lambda_{\text{exc}} = 355 \text{ nm}$ .

[CO]	$k_{\text{obs}}$
0	1.74
$2.25 \times 10^{-3}$	1.84
$4.50 \times 10^{-3}$	1.63
$7.75 \times 10^{-3}$	1.81
$9.00 \times 10^{-3}$	1.82

### 2.3.5 Laser flash photolysis of $(\mu_2\text{-C}_2\text{H}_2)\text{Co}_2(\text{CO})_6$ at $\lambda_{\text{exc}} = 532 \text{ nm}$

In pentane solution containing a 5 - fold excess of  $\text{PPh}_3$ , flash photolysis of **achc** with  $\lambda_{\text{exc}} = 532 \text{ nm}$  in the presence of 1 atmosphere of argon produced a transient signal as shown in Figure 2.25 at a monitoring wavelength of 390 nm. No transient signals were observed above monitoring wavelengths greater than 420 nm. An increase in absorbance was observed between 380 - 420 nm, while above this wavelength no changes were observed. The IR spectrum obtained after flash photolysis give evidence for the formation of a  $\text{PPh}_3$  monosubstituted complex (assignment based on previous work) with new bands appearing at 2069, 2017, 2009, 1998 and  $1975 \text{ cm}^{-1}$ .

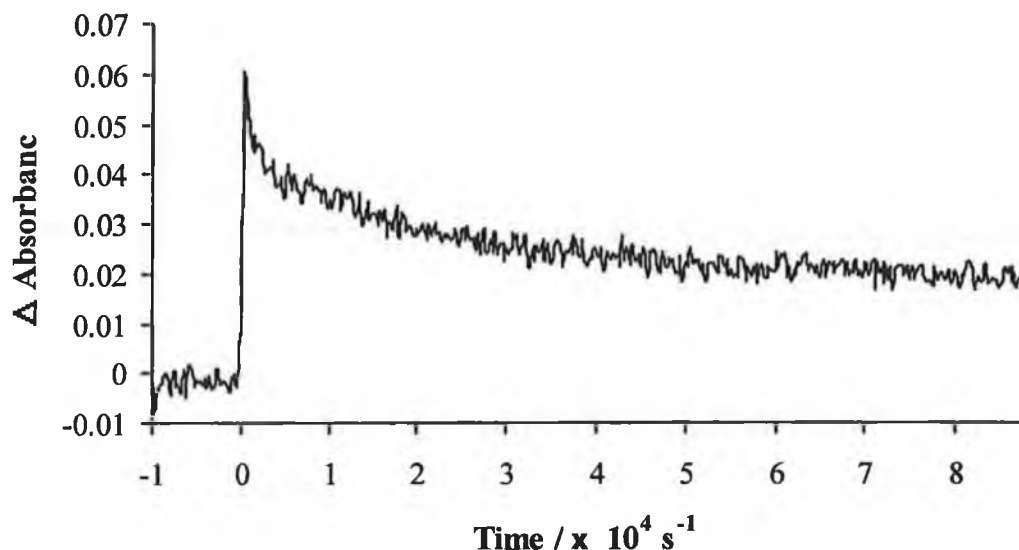


**Figure 2.25** A typical transient signal observed following laser flash photolysis of *achc* in pentane containing  $\text{PPh}_3$  ( $10^{-5}\text{M}$ ) under 1 atmosphere of argon; ( $\lambda_{\text{exc}} = 532\text{ nm}$ ); monitoring wavelength =  $390\text{ nm}$ .

Earlier work by Wrighton and Ginley<sup>14</sup> has shown that the UV/Vis spectrum of dimetal hexacarbonyl complexes shifts to shorter wavelength upon substitution of one CO by  $\text{PPh}_3$ . Since the *achc* parent complex does not absorb as far into the visible as *pachc* it follows that the  $\text{C}_5\text{H}_5\text{N}$  and  $\text{PPh}_3$  substituted complexes would be blue - shifted compared to *pachc* and therefore no transient signals are observed beyond  $420\text{ nm}$ .

The *achc* complex was further irradiated in neat pentane under 1 atmosphere of CO ( $[\text{CO}] = 9 \times 10^{-3}\text{ M}$ ) at  $\lambda_{\text{exc}} = 532\text{ nm}$ . Typical transient signals as shown in Figure 2.26 were observed across the monitoring range where the parent hexacarbonyl has significant absorbance. The transient signal decays following first order kinetics and for all monitoring wavelengths has a decay of  $7.4 \times 10^3 \pm 1.1 \times 10^4\text{ s}^{-1}$  at  $298\text{ K}$ . The transient species in turn produce a long lived species which may be the fast exchange of CO for a solvated species. The IR and steady-state UV/Vis



spectrum taken throughout photolysis show no change in parent bands indicating that the process is reversible.

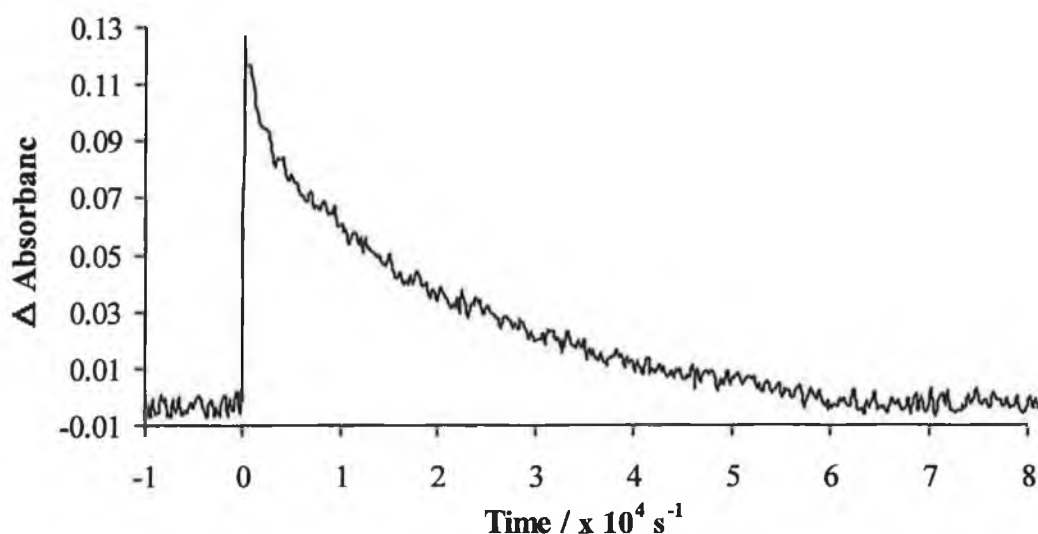


**Figure 2.26** A typical transient signal observed at a monitoring wavelength of 400 nm following laser flash photolysis of **achc** in pentane solution under an atmosphere of CO ( $[\text{CO}] = 9 \times 10^{-3} \text{ M}$ );  $\lambda_{\text{exc}} = 532 \text{ nm}$ .

Addition of CO reduced the lifetime of the transient species while its yield was not affected. The rate of decay of **achc** was found to be directly dependent on CO concentration. This behaviour is typical of the reaction of CO-loss intermediates. The second order rate constant for the reaction of the transient species with CO was calculated to be  $7 \times 10^5 \text{ dm}^3 \text{ mol}^{-1} \text{ s}^{-1}$  at 298 K (Table 2.7).

**Table 2.7** The observed rate constant ( $\text{s}^{-1}$ ) for the reaction of CO with *achc* at various CO concentrations ( $\text{mol dm}^{-3}$ ) at 298 K;  $\lambda_{\text{exc}}$  532 nm.

[CO]	$k_{\text{obs}}$
0	817
$2.25 \times 10^{-3}$	2478
$4.50 \times 10^{-3}$	4536
$7.75 \times 10^{-3}$	6381
$9.00 \times 10^{-3}$	7432

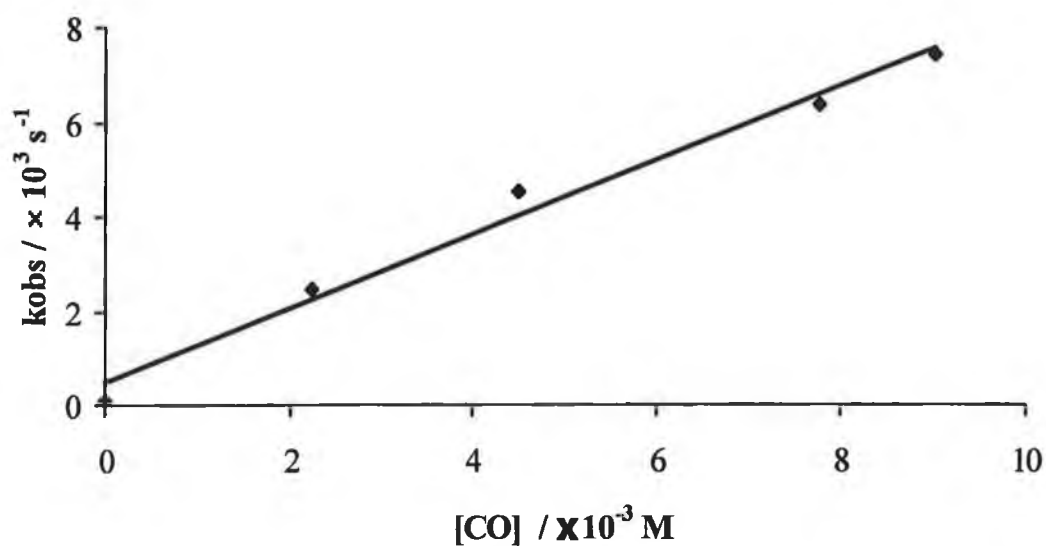


**Figure 2.27** A second order plot of the observed rate constant ( $\text{s}^{-1}$ ) for the reaction of  $(\mu_2\text{-C}_2\text{H}_2)\text{Co}_2(\text{CO})_5$  with CO ( $\text{mol dm}^{-3}$ ) at 298 K.

### 2.3.6 IR monitored steady-state photolysis of $(\mu_2\text{-C}_2\text{H}_2)\text{Co}_2(\text{CO})_6$ for $\lambda_{\text{exc}} > 500 \text{ nm}$

In a cyclohexane solution containing a 5 - fold excess of  $\text{PPh}_3$ , **achc** was irradiated for 20 minutes with  $\lambda_{\text{exc}} > 500 \text{ nm}$ . The spectral changes were monitored by IR spectroscopy. New bands were identified as formation of the monosubstituted acetylene complex  $(\mu_2\text{-C}_2\text{H}_2)\text{Co}_2(\text{CO})_5(\text{PPh}_3)$  (see Table 2.4). The growth of bands for the initial 30 minutes was very slow when compared to the formation of bands when **pachc** was irradiated. Since the absorbance spectrum of **achc** does not absorb far into the visible region the yield would be expected to be quite low.

### 2.3.7 Explanation of results for photolysis of **achc**

Steady-state photolysis of **achc** at  $\lambda_{\text{exc}} > 400 \text{ nm}$  resulted in the formation of both  $(\mu_2\text{-C}_2\text{H}_2)\text{Co}_2(\text{CO})_5(\text{L})$  and  $(\mu_2\text{-C}_2\text{H}_2)\text{Co}_2(\text{CO})_4(\text{L})_2$  substituted complexes where  $\text{L} = \text{PPh}_3$  or  $\text{C}_5\text{H}_5\text{N}$ . Irradiation at shorter wavelength ( $\lambda_{\text{exc}} > 340 \text{ nm}$ ) resulted in a higher yield of substituted products, in particular  $(\mu_2\text{-C}_2\text{H}_2)\text{Co}_2(\text{CO})_4(\text{PPh}_3)_2$ . Laser flash photolysis at  $\lambda_{\text{exc}} = 355 \text{ nm}$  gave transient signals showing depletion of the parent absorption followed by a rapid recovery of this absorbance to pre-irradiated level. The rate of recovery of this absorbance (typically  $1.8 \times 10^7 \text{ s}^{-1}$ ) is too fast to be CO loss, which is a diffusion controlled process. A non-linear dependence of the rate of recovery on the concentration of CO is further evidence that the transient signals observed are not the result of CO-loss species. To explain the depletion of parent absorbance observed in these experiments following laser excitation at  $\lambda_{\text{exc}} = 355 \text{ nm}$  it is proposed that homolytic cleavage of the Co - Co bond occurs which subsequently undergoes rapid recovery.

The steady-state UV/Vis spectra recorded throughout the flash photolysis experiments, however, give evidence for the formation of a new species. While it is impossible to assign this new species from the UV/Vis spectrum alone, the IR spectrum recorded after flash photolysis showed  $\nu_{\text{CO}}$  bands consistent with the

formation of the appropriately substituted  $(\mu_2\text{-C}_2\text{H}_2)\text{Co}_2(\text{CO})_5(\text{L})$  complex. Since the transient signals observed are not the result of CO-loss species, the monitoring beam is therefore causing production of  $(\mu_2\text{-C}_2\text{H}_2)\text{Co}_2(\text{CO})_5(\text{L})$ .

Steady-state experiments performed on **achc** in hydrocarbon solutions containing ligand L at  $\lambda_{\text{exc}} > 500$  nm showed the exclusive formation of  $(\mu_2\text{-C}_2\text{H}_2)\text{Co}_2(\text{CO})_5(\text{L})$  complexes. No bi-substituted complexes were formed in either case. Further time resolved experiments were performed at  $\lambda_{\text{exc}} = 532$  nm. The transient absorption observed is assigned to  $(\mu_2\text{-C}_2\text{H}_2)\text{Co}_2(\text{CO})_5(\text{solvent})$ . The lifetime of this transient species depended on the concentration of added  $\text{PPh}_3$ . Examination of the resulting solution by IR spectroscopy confirmed the presence of  $(\mu_2\text{-C}_2\text{H}_2)\text{Co}_2(\text{CO})_5(\text{PPh}_3)$ . Long wavelength excitation at 532 nm therefore, results in the desired CO-loss process. Thus  $(\mu_2\text{-C}_2\text{H}_2)\text{Co}_2(\text{CO})_6$  exhibits a wavelength dependent photochemistry which closely resembles that observed with  $(\mu_2\text{-C}_6\text{H}_5\text{C}_2\text{H})\text{Co}_2(\text{CO})_6$  studied previously.

## 2.4 Photolysis of $(\mu_2\text{-(C}_6\text{H}_5\text{C)}_2\text{Co}_2(\text{CO})_6$

### 2.4.1 Molecular modeling of $(\mu_2\text{-(C}_6\text{H}_5\text{C)}_2\text{Co}_2(\text{CO})_6$

The molecular structure of **dpachc** is presented in Figure 2.28 which illustrates the general structural similarities to the **achc** complex discussed earlier (Section 2.3.1). The complex is highly symmetrical with the acetylene moiety positioned such that it sits at right angles to the cobalt - cobalt core. Again the bonding can be described in terms of the acetylene acting as a four electron donor with each cobalt atom receiving two electrons. The phenyl groups on the acetylene core are bulky and their presence may hinder coordination to the Co - Co centre, particularly in the case of bulky alkenes.

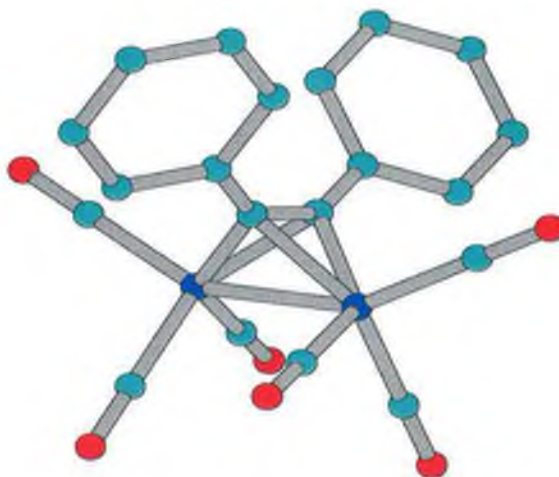


**Figure 2.28** Molecular structure of  $(\mu_2\text{-(C}_6\text{H}_5\text{C)}_2\text{Co}_2(\text{CO})_6$

### 2.4.2 Synthesis and Spectroscopic Characterisation of $(\mu_2\text{-(C}_6\text{H}_5\text{C)}_2\text{Co}_2(\text{CO})_6$

#### 2.4.2.1. Preparation and IR spectrum of $(\mu_2\text{-(C}_6\text{H}_5\text{C)}_2\text{Co}_2(\text{CO})_6$

The synthesis of diphenylacetylene hexacarbonyldicobalt (**dpachc**) proceeds according to Reaction 2.7. Stirring a benzene solution of diphenylacetylene in the presence of dicobalt octacarbonyl under an argon atmosphere at room temperature produces the desired diphenylacetylene hexacarbonyldicobalt in high yield.



The reaction was monitored by IR spectroscopy which indicated the disappearance of parent bands at 2095, 2064, 2042, 2032, 2028, 1867 and 1859  $\text{cm}^{-1}$  while producing new bands at 2091, 2056, 2030, 2027 and 2013(sh)  $\text{cm}^{-1}$  identified as  $(\mu_2\text{-(C}_6\text{H}_5\text{C)}_2)\text{Co}_2(\text{CO})_6$ . The product was purified by flash chromatography on silica gel using pentane as eluent. The  $(\mu_2\text{-(C}_6\text{H}_5\text{C)}_2)\text{Co}_2(\text{CO})_6$  complex was characterised by IR and  $^1\text{H}$  NMR spectroscopy and elemental analysis. The IR spectrum presented in Figure 2.29.

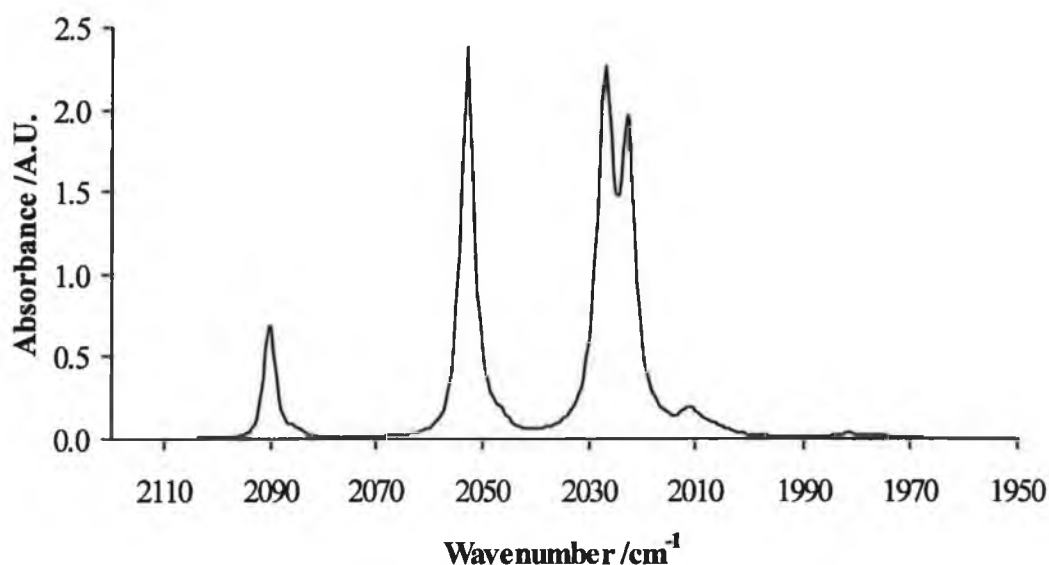


**Figure 2.29** IR spectrum in the CO stretching region of *dpachc* in cyclohexane at 298 K ( $\text{cm}^{-1}$ ,  $\pm 1 \text{ cm}^{-1}$ ).

2.4.2.2. NMR characterisation of  $(\mu_2\text{-(C}_6\text{H}_5\text{C)}_2\text{Co}_2(\text{CO})_6$ 

The  $^1\text{H}$  NMR spectrum in  $\text{CDCl}_3$  of **dpachc** is presented in Figure 2.30. In uncoordinated diphenylacetylene resonances are observed at 7.41 (m, 1H,  $J = 2\text{ Hz}$ ), 7.58 (t, 2H,  $J = 2\text{ Hz}$ ) and 7.60 (m, 2H,  $J = 2\text{ Hz}$ ) ppm while in the complex multiplet resonances observed at 7.19 (s, 1H, Ar C-H), 7.29 (m, 2H, Ar C-H,  $J = 7.2\text{ Hz}$ ), and 7.53 (d, 2H, Ar C-H,  $J = 7.2\text{ Hz}$ ) ppm are respectively assigned to the *para*, *meta* and *ortho* aromatic protons on the phenyl ring. Only one set of phenyl ring protons was observed because of the high degree of symmetry in the complex.

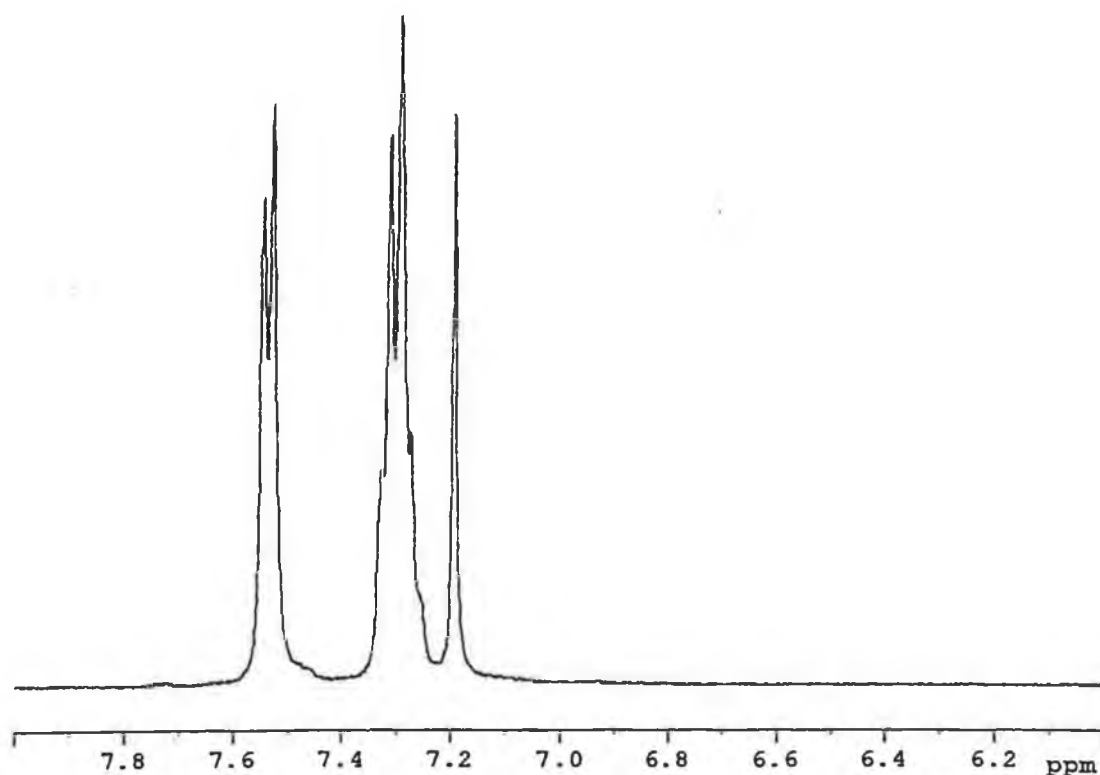
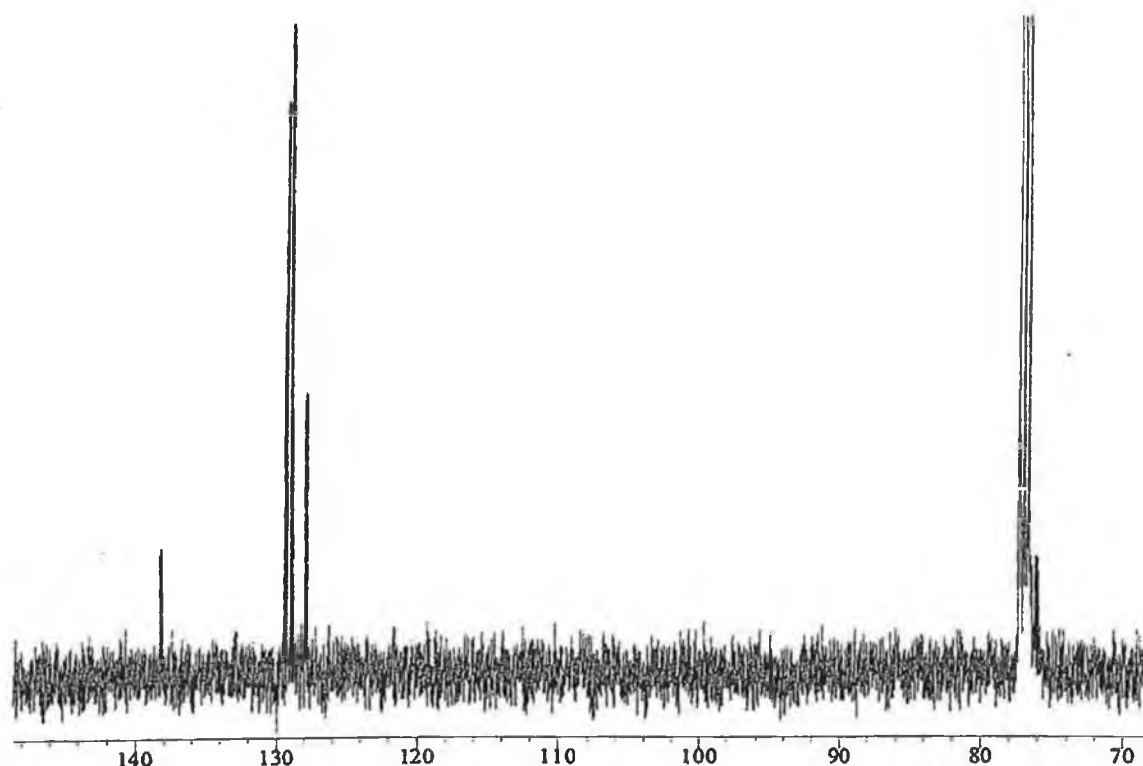


Figure 2.30  $^1\text{H}$  NMR spectrum of **dpachc** at 298 K in  $\text{CDCl}_3$ .

The  $^{13}\text{C}$  NMR spectrum of **dpachc** is presented in Figure 2.31. The acetylenic carbon atom which appears at 84.1 ppm in uncoordinated diphenylacetylene ( $\text{CDCl}_3$ ) is observed at 76.5 ppm when complexed. The carbonyl ligands in the  $(\mu_2\text{-(C}_6\text{H}_5\text{C)}_2\text{Co}_2(\text{CO})_6$  complex appear as a broad signal at 201 ppm. The triplet at 77 ppm is due to  $\text{CDCl}_3$  resonances.



**Figure 2.31**  $^{13}\text{C}$  NMR spectrum of **dpachc** at 298 K in  $\text{CDCl}_3$ . The triplet at 77 ppm is  $\text{CDCl}_3$ .

#### 2.4.2.3. Electronic absorbance spectrum of $(\mu_2\text{-(C}_6\text{H}_5\text{C)}_2\text{Co}_2(\text{CO})_6$

The UV/Vis. spectrum of **dpachc** is presented in Figure 2.32 and this spectrum closely resembles that of **pachc** (Figure 2.5) and **achc** (Figure 2.19). Bands are observed at 330, 360 ( $\epsilon = 2.11 \times 10^5 \text{ mol}^{-1} \text{ dm}^3 \text{ cm}^{-1}$ ), 455 ( $\epsilon = 6.42 \times 10^4 \text{ mol}^{-1} \text{ dm}^3 \text{ cm}^{-1}$ ) and 540 nm ( $\epsilon = 3.43 \times 10^4 \text{ mol}^{-1} \text{ dm}^3 \text{ cm}^{-1}$ ). The  $\lambda_{\text{max}}$  at 360 nm has been assigned as a  $\sigma\text{-}\sigma^*$  transition associated with the M - M bond and the bands at lower



energy to  $\pi\text{-}\pi^*$  transitions.<sup>11</sup> As the complex absorbs into the visible region the wavelength range available for photochemical experiments is considerably extended.

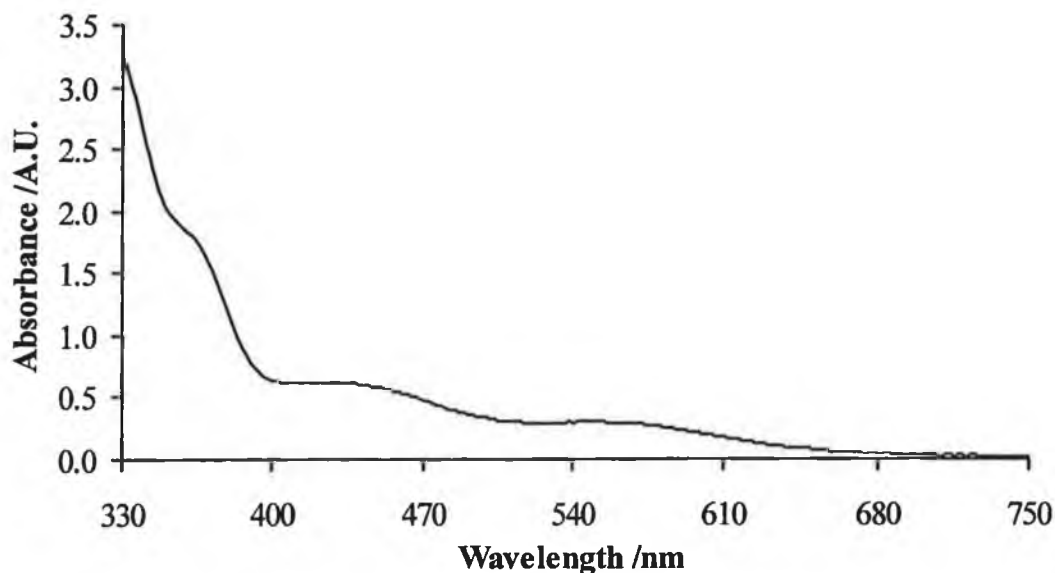


**Figure 2.32** UV/Vis electronic spectrum of *dpachc* in pentane at 298 K; conc. =  $5.7 \times 10^{-5}$  M.

### 2.4.3 Steady-state Photolysis Experiments

#### 2.4.3.1. Photolysis of $(\mu_2\text{-(C}_6\text{H}_5\text{C)}_2\text{Co}_2(\text{CO})_6$ in the presence of trapping ligands

The IR spectroscopic changes in the  $\nu_{\text{CO}}$  region following irradiation of **dpachc** with trapping ligands  $\text{C}_5\text{H}_5\text{N}$  or  $\text{PPh}_3$ , at  $\lambda_{\text{exc}} > 340$ , 400 and 500 nm, are presented in Table 2.8. Surprisingly, broad band photolysis ( $\lambda_{\text{exc}} > 340$  nm) of **dpachc** in cyclohexane containing a 5-fold excess of  $\text{C}_5\text{H}_5\text{N}$  resulted in the substitution of one carbonyl ligand by one  $\text{C}_5\text{H}_5\text{N}$  ligand. Meanwhile irradiation with  $\lambda_{\text{exc}} > 500$  nm resulted in substitution of two carbonyl ligands. Isosbestic points were maintained throughout the course of both experiments indicative that the reactions

were uncomplicated by side reactions. The IR spectra obtained following photolysis at both  $\lambda_{\text{exc}} > 340$  and 400 nm are presented in Figure 2.33 (a) and (b).

**Table 2.8** The  $\nu_{\text{CO}}$  band positions observed for steady state photolysis of *dpachc*.

Compound	$\nu_{\text{CO}}$
$(\mu_2\text{-(C}_6\text{H}_5\text{C)}_2\text{Co}_2(\text{CO})_6)^{\text{a}}$	2091, 2055, 2029, 2026, 2021(sh)
$(\mu_2\text{-(C}_6\text{H}_5\text{C)}_2\text{Co}_2(\text{CO})_5(\text{PPh}_3))^{\text{b}}$	2062, 2016, 2004, 1995, 1970
$(\mu_2\text{-(C}_6\text{H}_5\text{C)}_2\text{Co}_2(\text{CO})_4(\text{PPh}_3)_2)^{\text{b}}$	2022, 1978, 1971, 1944
$(\mu_2\text{-(C}_6\text{H}_5\text{C)}_2\text{Co}_2(\text{CO})_5(\text{C}_5\text{H}_5\text{N}))^{\text{b}}$	2060, 2016, 2003, 1990, 1964
$(\mu_2\text{-(C}_6\text{H}_5\text{C)}_2\text{Co}_2(\text{CO})_4(\text{C}_5\text{H}_5\text{N})_2)^{\text{b}}$	2016, 1966, 1962, 1942

Cyclohexane solution at 298 K ( $\text{cm}^{-1}$ ;  $\pm 1 \text{ cm}^{-1}$ ); <sup>a</sup> complex prepared by thermal methods; <sup>b</sup> generated by steady-state photolytical methods.

Irradiation of **dpachc** at  $\lambda_{\text{exc}} > 500$  nm in the presence of  $\text{C}_5\text{H}_5\text{N}$  showed the growth of bands at 2062, 2016, 2004, 1995 and 1970  $\text{cm}^{-1}$ . These are identified as  $(\mu_2\text{-(C}_6\text{H}_5\text{C)}_2\text{Co}_2(\text{CO})_5(\text{C}_5\text{H}_5\text{N}))$  by comparison with the IR spectrum of an authentic sample. The product bands, at 2016, 1966, 1962  $\text{cm}^{-1}$  and 1942  $\text{cm}^{-1}$ , are identified as  $(\mu_2\text{-(C}_6\text{H}_5\text{C)}_2\text{Co}_2(\text{CO})_4(\text{C}_5\text{H}_5\text{N})_2)$ . The intensity of the monosubstituted product bands was reduced after irradiation for 35 minutes indicating degradation of the complex.<sup>16</sup> However, irradiation of **dpachc** in cyclohexane solution containing  $\text{C}_5\text{H}_5\text{N}$  at  $\lambda_{\text{exc}} > 340$  nm, for 35 minutes, also formed the monosubstituted complex  $(\mu_2\text{-(C}_6\text{H}_5\text{C)}_2\text{Co}_2(\text{CO})_5(\text{C}_5\text{H}_5\text{N}))$ . This product began to decay after 25 minutes irradiation and no further products were observed. No disubstituted complexes were formed either in the presence of  $\text{PPh}_3$  or  $\text{C}_5\text{H}_5\text{N}$ . Irradiation of **dpachc** with  $\lambda_{\text{exc}} > 400$  nm gave similar results, however the yield of  $(\mu_2\text{-(C}_6\text{H}_5\text{C)}_2\text{Co}_2(\text{CO})_5(\text{C}_5\text{H}_5\text{N}))$  was smaller.

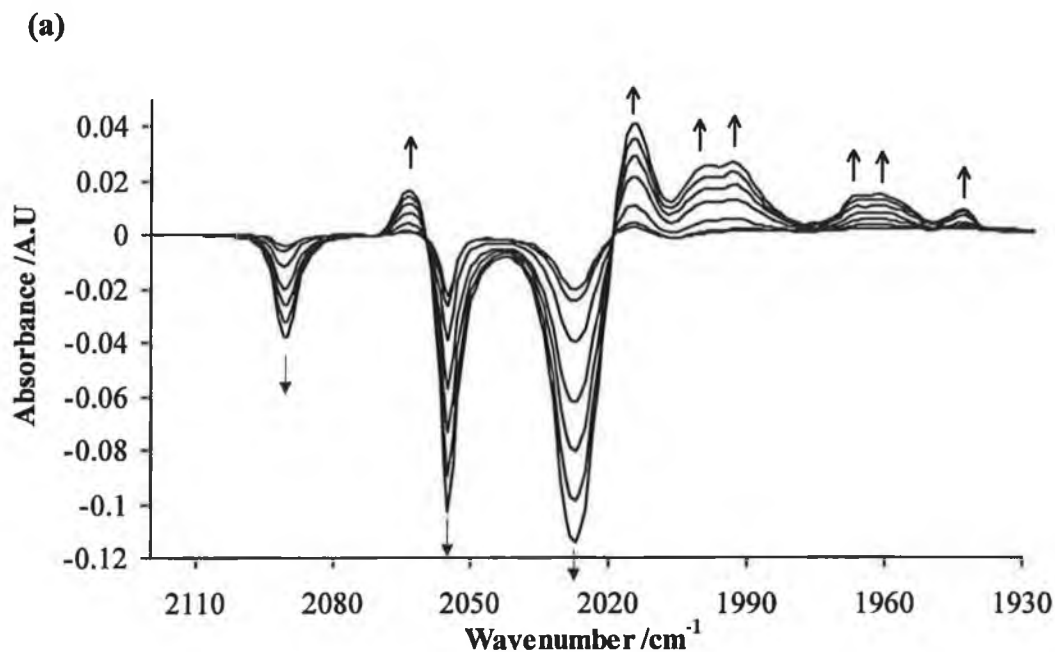


**Figure 2. 33(a)** IR difference spectrum in the CO stretching region following broad band photolysis of *dpachc* in the presence of pyridine ( $\lambda_{\text{exc}} > 500 \text{ nm}$ ). Spectra were acquired at 0.5, 1, 2, 5, 10, 25 and 35 minutes respectively. The positive bands are identified as  $(\mu_2\text{-(C}_6\text{H}_5\text{C)}_2\text{Co}_2(\text{CO})_5(\text{C}_5\text{H}_5\text{N})$  and  $(\mu_2\text{-(C}_6\text{H}_5\text{C)}_2\text{Co}_2(\text{CO})_4(\text{C}_5\text{H}_5\text{N})_2$ .

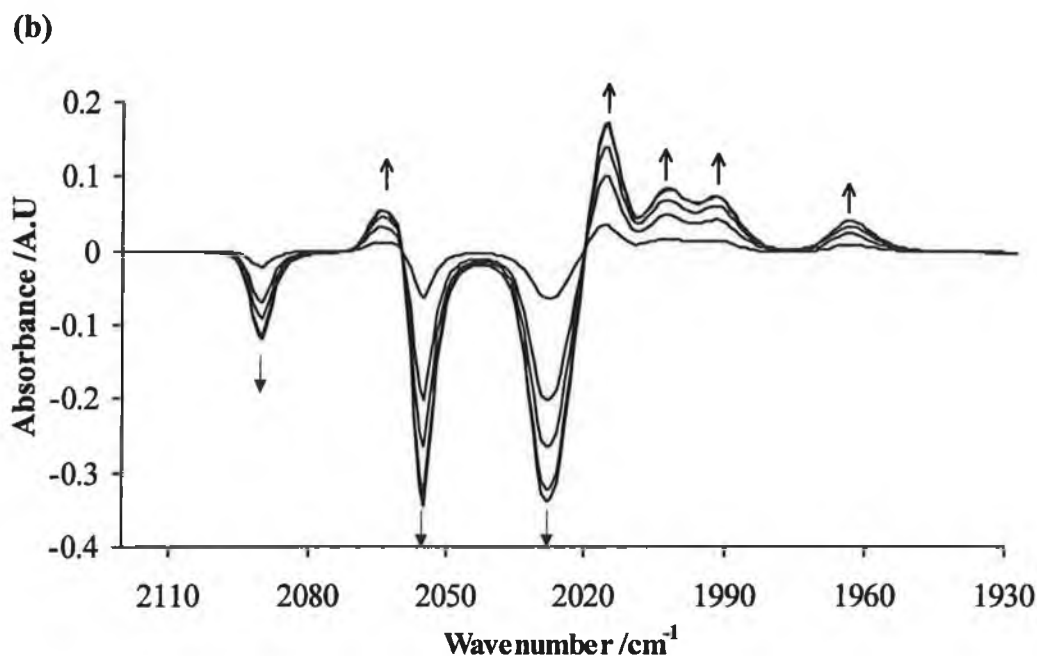


**Figure 2. 33(b)** IR difference spectrum in the CO stretching region following broad band photolysis of **dpachc** in the presence of pyridine ( $\lambda_{\text{exc}} > 340$  nm). Spectra were acquired at 1, 5, 10, 25 and 35 minutes respectively. The positive bands are identified as  $(\mu_2\text{-(C}_6\text{H}_5\text{C)}_2\text{Co}_2(\text{CO})_5(\text{C}_5\text{H}_5\text{N}))$ . The negative bands indicate the depletion of the parent  $(\mu_2\text{-(C}_6\text{H}_5\text{C)}_2\text{Co}_2(\text{CO})_6$  species.

Further broad band photolysis experiments were carried out on **dpachc** using light filters at  $\lambda_{\text{exc}} > 340$ , 400 and 500 nm consecutively, to determine which wavelength region produced the disubstituted tetracarbonyl complex. Initial irradiation of **dpachc** containing  $\text{C}_5\text{H}_5\text{N}$  at  $\lambda_{\text{exc}} > 340$  nm, for 19 minutes, resulted in the growth of new bands identified as the formation of the monosubstituted pentacarbonyl complex  $(\mu_2\text{-(C}_6\text{H}_5\text{C)}_2\text{Co}_2(\text{CO})_5(\text{C}_5\text{H}_5\text{N}))$ . Subsequent irradiation with  $\lambda_{\text{exc}} > 400$  nm ( $t = 19$  to 41 minutes) showed the slow growth of bands of the disubstituted complex  $(\mu_2\text{-(C}_6\text{H}_5\text{C)}_2\text{Co}_2(\text{CO})_4(\text{C}_5\text{H}_5\text{N})_2$ . Finally, irradiation with  $\lambda_{\text{exc}} > 500$  nm ( $t = 41$  to 55 minutes) showed a further increase in the bands of the disubstituted complex (Figure 2.34). Since steady-state photolysis experiments were carried out using broad band irradiation, both mono and bi-substituted complexes are

expected to form during irradiating at  $\lambda_{\text{exc}} > 340$  nm. Note however, the production of *only* the monosubstituted pentacarbonyl complex during irradiation with  $\lambda_{\text{exc}} > 340$  nm and the observation of *both* mono- and di- substituted complexes during irradiation with  $\lambda_{\text{exc}} > 500$  nm is in complete contrast to the results obtained with **achc** and **pachc** (*c.f.* Section 2.2 and 2.3). Scheme 2.6 summarises the steady-state photochemical reactions of **dpachc**.

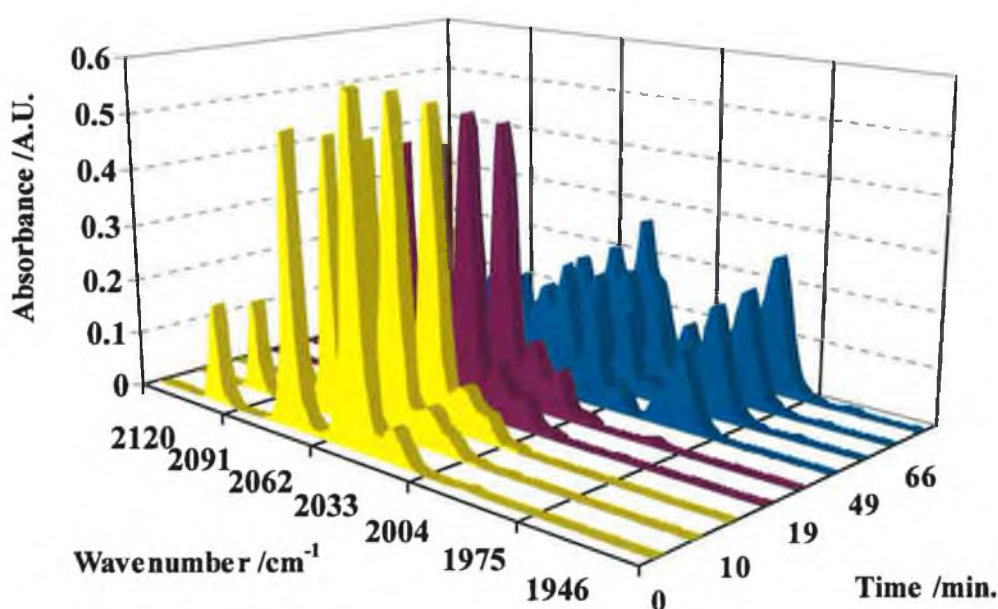
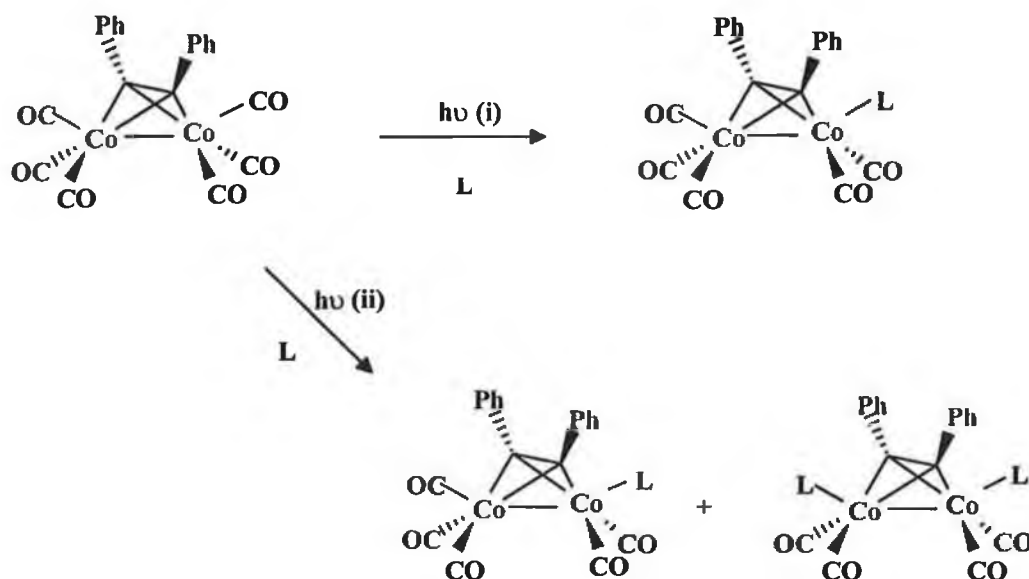


**Figure 2.34** IR spectra in the CO stretching region obtained following broad band photolysis of **dpachc** in the presence of pyridine ( $10^{-4}$  M) using consecutive filters  $\lambda_{\text{exc}} > 340$ , 400 and 500 nm. Spectra were acquired at 1, 5, 15, 19, 24, 44, 50, 55 and 66 minutes respectively (i)  $\lambda_{\text{exc}} > 340$  nm (ii)  $\lambda_{\text{exc}} > 400$  nm, (iii)  $\lambda_{\text{exc}} > 500$  nm.



**Scheme 2.6** (i)  $\lambda_{exc} > 340$  nm in alkane solvent, (ii)  $\lambda_{exc} > 500$  nm in alkane solvent;  $L = \text{PPh}_3$  or  $\text{C}_5\text{H}_5\text{N}$ .

Further studies with bandpass filters at  $320 > \lambda < 390$  nm were carried out to provide further evidence that only the pentacarbonyl complex is formed at  $\lambda < 400$  nm. Irradiation of a solution of **dpachc** in cyclohexane containing  $\text{C}_5\text{H}_5\text{N}$  showed the growth of bands of the monosubstituted complex  $(\mu_2\text{-(C}_6\text{H}_5\text{C)}_2\text{Co}_2(\text{CO})_5(\text{C}_5\text{H}_5\text{N}))$  for  $t = 0$  to 4 minutes. Further photolysis from  $t = 4$  to 20 minutes showed a simultaneous depletion of bands of both the monosubstituted complex and the parent complex. This indicates the degradation of products in the presence of high energy photons.

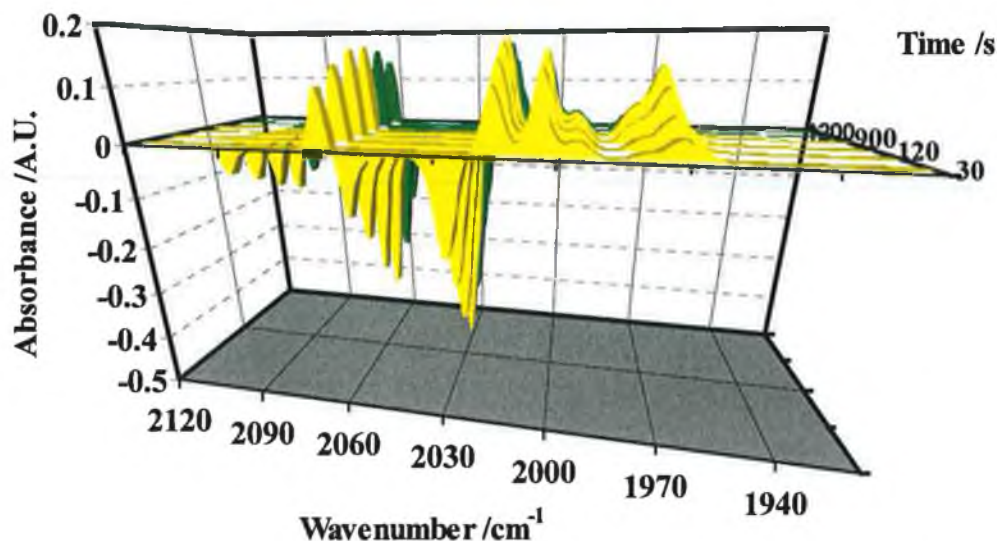


**Figure 2. 35** IR difference spectra in the CO stretching region obtained following broad band photolysis of **dpachc** in the presence of pyridine ( $320 > \lambda_{\text{exc}} < 390$  nm). Spectra were acquired at 0.5, 1, 2, 4, 9, 15 and 20 minutes respectively. The positive bands are identified as the formation of  $(\mu_2\text{-(C}_6\text{H}_5\text{C)}_2\text{Co}_2(\text{CO})_5(\text{C}_5\text{H}_5\text{N})$  (see text). The negative bands are due to the depletion of the parent  $(\mu_2\text{-(C}_6\text{H}_5\text{C)}_2\text{Co}_2(\text{CO})_6$  species.

#### 2.4.4 Laser flash photolysis of $(\mu_2\text{-(C}_6\text{H}_5\text{C)}_2\text{Co}_2(\text{CO})_6$ at $\lambda_{\text{exc}} = 355$ nm

A solution of **dpachc** (conc. =  $5.2 \times 10^{-6}$  M) in pentane containing pyridine (conc. =  $2.1 \times 10^{-5}$  M) was photolysed at  $\lambda_{\text{exc}} = 355$  nm under 1 atmosphere of argon. The resulting transient signal centered at 400 nm is given in Figure 2.36. The absorption increase indicates the formation of a long-lived species. The reaction is therefore not reversible under these conditions. Similar transient signals were obtained across all the spectral region of the parent absorption. The intensity of the transient absorption increased as the monitoring beam wavelength was decreased. The rate of formation of this species could not be measured with the equipment

available. The steady-state UV/Vis spectrum recorded throughout the experiment showed an increase in a band at 400 nm indicating the formation of a new species, however, it is impossible to assign the photoproduct from the UV/Vis spectra alone. An IR spectrum recorded immediately after flash photolysis indicated the formation of  $(\mu_2\text{-(C}_6\text{H}_5\text{C)}_2\text{)Co}_2(\text{CO})_5(\text{C}_5\text{H}_5\text{N})$ . Experiments conducted in pentane solution containing a 5-fold excess of  $\text{PPh}_3$  gave similar transient signals.

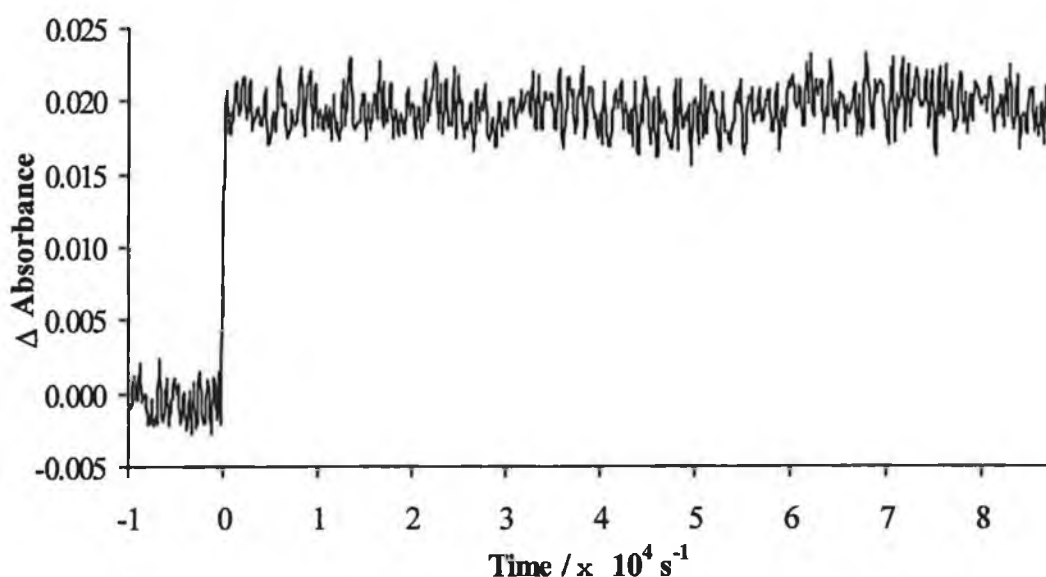


**Figure 2.36** A typical transient signal observed at 400 nm following laser flash photolysis of *dpachc* in pentane solution containing pyridine under 1 atmosphere of argon;  $\lambda_{\text{exc}} = 355 \text{ nm}$ .

Pulsed excitation ( $\lambda_{\text{exc}} = 355 \text{ nm}$ ) of **dpachc** (conc. =  $4.5 \times 10^{-6} \text{ M}$ ) in pentane solution under 1 atmosphere of CO ( $[\text{CO}] = 9 \times 10^{-3} \text{ M}$ ) resulted in the depletion and rapid recovery of the parent absorption as presented in Figure 2.37. The absorption recovered to pre-irradiated level indicating that under these conditions the reaction is reversible. Similar transient signals were obtained across the region of the spectra where the parent has significant absorbance with the intensity of the transient



absorption increasing as the wavelength of monitoring beam is decreased. The intermediate species decayed following first order kinetics with  $k_{\text{obs}} = 5.7 \times 10^6 \text{ s}^{-1}$  at 298 K. Steady-state UV/Vis spectra were recorded throughout the experiment. No changes in the spectrum were observed, again indicating a reversible reaction. Changing the concentration of CO had no effect on the rate of recovery of the transient absorption (Table 2.9).

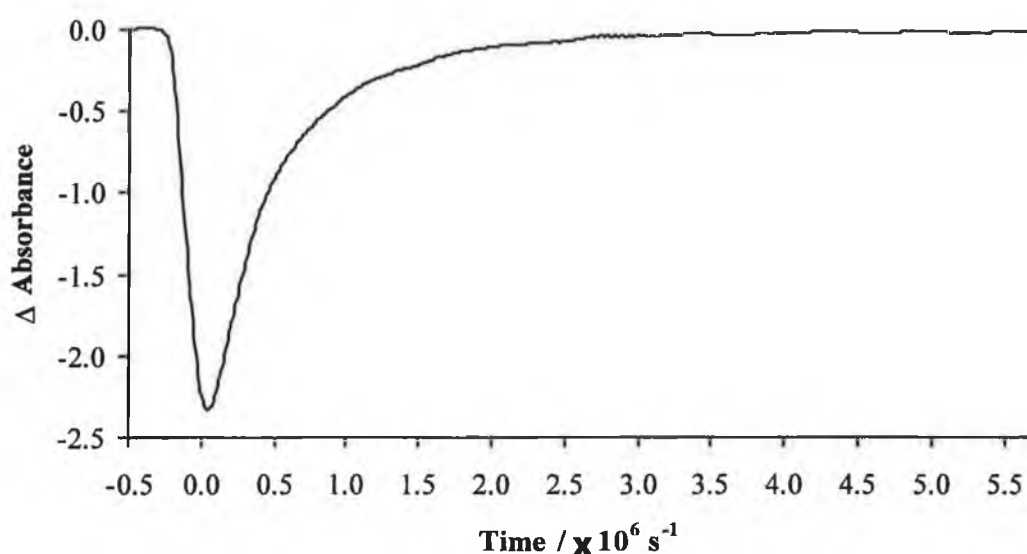


**Figure 2.37** A typical transient signal observed following laser flash photolysis of *dpachc* in pentane solution at  $\lambda_{\text{exc}} = 355 \text{ nm}$  under 1 atmosphere of CO ( $[\text{CO}] = 9 \times 10^{-3} \text{ M}$ ). The measured rate constant  $k_{\text{obs}} = 5.7 \times 10^6 \text{ s}^{-1}$ . Monitoring wavelength = 400 nm.

**Table 2.9** Measured rate constant ( $\text{s}^{-1}$ ) following flash photolysis of *dpachc* ( $\lambda_{\text{exc}} = 355 \text{ nm}$ ) under varying concentrations of CO.

[CO] /M	$k_{\text{obs}} / \times 10^6 \text{ s}^{-1}$
$9.0 \times 10^{-3}$	5.73
$4.45 \times 10^{-3}$	5.82
$2.25 \times 10^{-3}$	5.56

#### 2.4.5 Laser flash photolysis of $(\mu_2\text{-(C}_6\text{H}_5\text{C)}_2)\text{Co}_2(\text{CO})_6$ at $\lambda_{\text{exc}} = 532 \text{ nm}$

Pulsed photolysis of **dpachc** ( $\lambda_{\text{exc}} = 532 \text{ nm}$ ) under 1 atmosphere of argon in pentane solution, containing a 5-fold excess of  $\text{C}_5\text{H}_5\text{N}$ , resulted in the typical transient signal shown in Figure 2.38 at a monitoring wavelength of 400 nm. Under these conditions the reaction is not reversible. The signal shows a depletion of the parent absorption followed by an absorbance grow in indicating the formation of a long-lived species. The intermediate decayed following first order kinetics with  $k_{\text{obs}} = 1.7 \times 10^6 \text{ s}^{-1}$  at 298 K. Similar transient signals were obtained across the region of the spectrum where the parent has significant absorbance. The intensity of the transient absorption increased as the wavelength of the monitoring beam decreased. An increase in the steady-state UV/Vis spectrum was observed throughout the course of the experiment.

Irradiation ( $\lambda_{\text{exc}} = 532 \text{ nm}$ ) of **dpachc** in pentane under 1 atmosphere of CO ( $[\text{CO}] = 9 \times 10^{-3} \text{ M}$ ) resulted in a transient bleaching and recovery of the parent absorption. The transient followed first order kinetics with a  $k_{\text{obs}}$  of  $5.6 \times 10^6 \text{ s}^{-1}$  at 400 nm. The steady-state UV/Vis spectra taken throughout photolysis and the IR spectrum recorded after photolysis show no change in parent bands indicating that under these conditions the process involved is reversible. Reducing the concentration of CO to  $4.5 \times 10^3 \text{ M}$  had no effect on the rate of recovery of the parent absorption

( $k_{\text{obs}} = 5.9 \times 10^6 \text{ s}^{-1}$ ). This behaviour indicates that the transient is not the result of CO-loss from **dpachc**. The measured rate constant ( $k_{\text{obs}}$ ) showed no dependence on varying concentrations of pyridine as shown by Table 2.10. Further experiments using irradiation with monochromatic laser light at the second harmonic of the Nd-YAG fundamental wavelength at 532 nm using IR spectral monitoring were conducted.

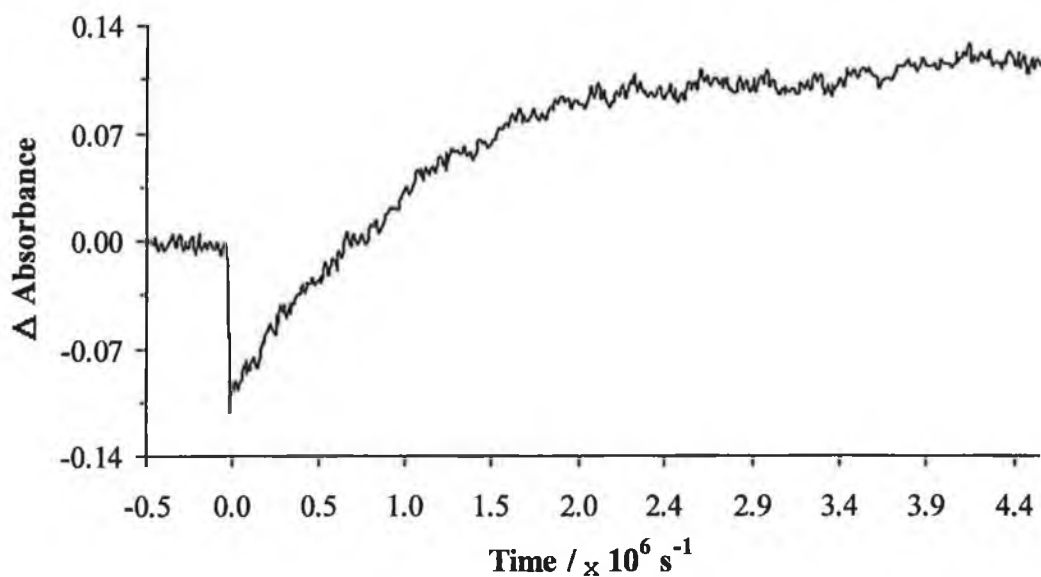


**Figure 2. 38** Transient signal observed for laser flash photolysis of **dpachc** containing a 5 - fold excess of pyridine at  $\lambda_{\text{exc}} = 532 \text{ nm}$  under 1 atmosphere of argon. The measured rate constant  $k_{\text{obs}} = 1.7 \times 10^6 \text{ s}^{-1}$ . Monitoring wavelength = 400 nm.

**Table 2.10** Measured rate constant following photolysis of **dpachc** with varying concentrations of  $\text{C}_5\text{H}_5\text{N}$  under 1 atmosphere of argon;  $\lambda_{\text{exc}} = 532 \text{ nm}$ .

$[\text{C}_5\text{H}_5\text{N}] / \text{M}$	$k_{\text{obs}} / \times 10^6 \text{ s}^{-1}$
$1 \times 10^{-4}$	2.0
$5 \times 10^{-4}$	2.3
$1 \times 10^{-3}$	1.5

#### 2.4.6 Irradiation of $(\mu_2\text{-(C}_6\text{H}_5\text{C)}_2)\text{Co}_2(\text{CO})_6$ with monochromatic light ( $\lambda_{\text{exc}} = 532\text{nm}$ )

Pulsed photolysis ( $\lambda_{\text{exc}} = 532\text{ nm}$ ; typical pulse time = 10ns) of a pentane solution of **dpachc** containing  $\text{PPh}_3$  ( $10^{-4}\text{ M}$ ) produced spectral changes as outlined in Figure 2.39 along with the spectrum of **dpachc** recorded before the photolysis experiment. IR spectra were recorded consecutively after every ten laser shots. The resulting product was assigned as  $(\mu_2\text{-(C}_6\text{H}_5\text{C)}_2)\text{Co}_2(\text{CO})_5(\text{PPh}_3)$  based on comparison of  $\nu_{\text{CO}}$  bands with an authentic sample.

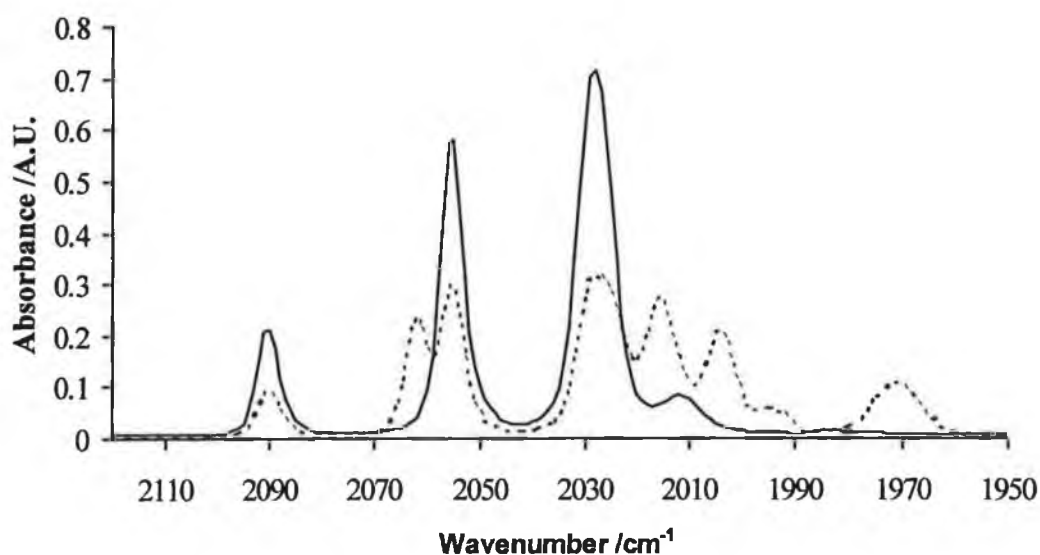


**Figure 2.39** IR spectra in the CO stretching region observed following flash photolysis of **dpachc** in pentane solution containing  $\text{PPh}_3$  ( $10^{-4}\text{ M}$ ) with  $\lambda_{\text{exc}} = 532\text{ nm}$  (a) — pre-photolysis (b) - - - after 300 laser pulses. Bands are identified as  $(\mu_2\text{-(C}_6\text{H}_5\text{C)}_2)\text{Co}_2(\text{CO})_5(\text{PPh}_3)$ .

#### 2.4.7 Laser flash photolysis of $(\mu_2\text{-(C}_6\text{H}_5\text{C)}_2\text{Co}_2(\text{CO})_6$ at $\lambda_{\text{exc}} = 266 \text{ nm}$

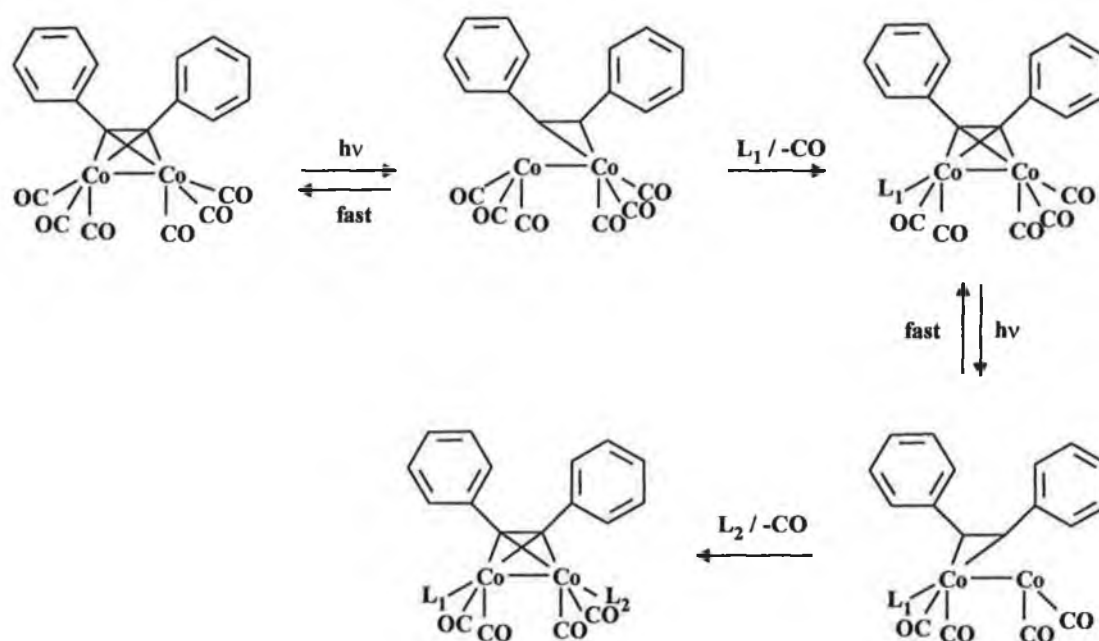
The excitation wavelength of the laser was changed to 266 nm to determine if there was a difference in the behaviour of this system at this excitation wavelength compared to that observed following irradiation with 355 nm. Samples were prepared as outlined previously in both pentane and cyclohexane respectively and placed under 1 atmosphere of CO ( $[\text{CO}] = 9 \times 10^{-3} \text{ M}$ ). The monitoring beam was varied from 580 to 350 nm. No photochemical changes were observed with either solvent. The steady-state UV/Vis spectra monitored throughout the course of the experiment showed no change in parent bands. Repeating the experiments under 1 atmosphere of argon gave similar results.

#### 2.4.8 Discussion of results for photolysis of **dpachc**

The absorption of **dpachc** extends much further into the visible region than that of either **pachc** or **achc** and may help to explain the remarkable difference in photochemical activity observed for these complexes. For **pachc** and **achc** two excited states are accessible, one which gives rise to homolytic Co - Co bond cleavage and a second which results in CO bond dissociation. In the **dpachc** complex the possibility of irradiating into a third state arises. **Dpachc** has an extreme conjugated  $\pi$  - system due to the presence of two phenyl rings and as a consequence the absorbance is extended further into the visible region of the spectrum. A possible explanation for the observed photochemistry is that the extended conjugation of the  $\pi$  system results in a third low lying excited state which when populated alters the coordination mode of the alkyne. We propose that this third excited state results in a hapticity change on the diphenylacetylene moiety and thus gives rise to the observed photochemistry.

In order to explain the formation of both mono- and disubstituted complexes while irradiating at  $\lambda_{\text{exc}} > 500$  nm Scheme 2.7 is proposed. Photon 1 is absorbed by the hexacarbonyl complex resulting in a hapticity change of the acetylene ligand, which now becomes a two electron donor, leaving a vacant site on one of the cobalt centres. There is then competition between the incoming ligand  $\text{L}_1$  ( $\text{L} = (\text{C}_6\text{H}_5\text{N})$  or  $\text{PPh}_3$ ) and the fast reversal reaction in which the acetylene quickly reverts back to a four electron donor.

Absorption of a second photon occurs at the second cobalt centre. Further competition between another molecule of CO or ligand  $\text{L}_2$  results in a second ligand substitution producing the disubstituted  $(\mu_2\text{-(C}_6\text{H}_5\text{C)}_2\text{Co}_2(\text{CO})_4(\text{PPh}_3)_2$  complex. The yield of the monosubstituted complex is dependent on the formation of the hapticity changed complex. However, the rate of reaction of  $(\mu_2\text{-(C}_6\text{H}_5\text{C)}_2\text{Co}_2(\text{CO})_6$  with L is independent of the concentration of L. Laser flash photolysis experiments performed at  $\lambda_{\text{exc}} = 532$  nm showed no dependence of  $k_{\text{obs}}$  on the concentration of either pyridine, or  $\text{PPh}_3$  - the overall rate being dominated by the fast reversal process.



where  $\text{L}_1$  and  $\text{L}_2 = (\text{C}_6\text{H}_5\text{N})$  or  $\text{PPh}_3$

**Scheme 2.7**

The rate constant ( $k_{\text{obs}}$ ) for the reaction of **dpachc** with pyridine with  $\lambda_{\text{exc}} = 355$  nm, under 1 atmosphere of argon, is  $1.7 \times 10^6 \text{ s}^{-1}$  while monitoring at 400 nm. This is an order of magnitude slower than the rate observed with **pachc** and **achc** under the same conditions ( $10^7 \text{ s}^{-1}$ ) and is consistent with a hapticity change. The rate of reaction observed upon irradiation of **dpachc** with  $\lambda_{\text{exc}} = 532$  nm, under 1 atmosphere of CO, is also too fast to be CO loss ( $k_{\text{obs}} = 5.6 \times 10^6 \text{ s}^{-1}$  at 400 nm). Irradiation with monochromatic light was used to probe whether this process results from the absorption of a single photon or is the result of multi-photon absorption. The monosubstituted complex  $(\mu_2\text{-(C}_6\text{H}_5\text{C)}_2\text{Co}_2(\text{CO})_5(\text{PPh}_3))$  was formed predominantly when **dpachc** was irradiated with light at  $\lambda_{\text{exc}} = 532$  nm. This is a consequence of the relative magnitudes of the extinction coefficient,  $\epsilon$ , for the monosubstituted pentacarbonyl and the disubstituted species. The pentacarbonyl complex exhibits a strong absorption band further into the visible which upon broad band irradiation

( $\lambda_{\text{exc}} > 500$  nm) results in a hapticity change and ultimately the production of the disubstituted complex by the reaction with a second molecule of  $\text{PPh}_3$ . This explains the formation of both mono- and disubstituted complexes during irradiation with broad band light ( $\lambda_{\text{exc}} > 500$  nm).

## 2.5 Conclusions

This work demonstrates the importance of correct selection of excitation wavelength in inducing the photochemical decarbonylation of  $(\mu_2\text{-RC}_2\text{H})\text{Co}_2(\text{CO})_6$  complexes. For the **pachc** and **achc** complexes two excited states are accessible. Time resolved behavior upon excitation at 355 nm results in Co - Co bond cleavage followed by a rapid recombination to form parent. There may be some but very little CO-loss. It is possible that the CO-loss that was observed was the result of irradiation by the monitoring lamp and not laser excitation. Long wavelength excitation at 532 nm results exclusively in the desired CO-loss process and consequently facilitates the next step in the Pauson - Khand reaction. This explains why Livinghouse observed the photochemical promotion of the Pauson - Khand reaction following visible light photolysis.

In the case of the **dpachc** complex, the observed photochemistry follows a different pathway. The possibility of irradiating into a third excited state arises. The population of this excited state results in a hapticity change on the diphenylacetylene moiety. Long wavelength excitation at 532 nm results in a hapticity change of the acetylene ligand which ultimately results in a ligand substitution reaction yielding the pentacarbonyl species. Further irradiation of the pentacarbonyl species produces the tetracarbonyl complex by a similar mechanism.



## 2.6 References

---

1. (a) N.E. Schore, *Chem. Rev.*, **88** (1988) 1081; (b) K.M. Nicholas, *Acc. Chem. Res.*, **20** (1987) 207; (c) R.S. Dickson, P. J. Fraser, *Adv. Organomet. Chem.*, **12** (1974) 323.
2. D.B. Belanger, T. Livinghouse, *Tetrahedron Lett.*, **39** (1998) 7641.
3. Krafft, I.L. Scott, R.H. Romero, S. Feilbelmann, C.E. Van Pest, *J. Am. Chem. Soc.*, **115** (1993) 7199.
4. I.S. Chia, W.R. Cullen, M. Franklin, A.R. Manning, *Inorg. Chem.*, **14** (1975) 2521.
5. W.J. Kerr, G.G. Kirk, D. Middlemiss, *J. Organomet. Chem.*, **519** (1996) 93.
6. J.C. Anderson, B.F. Taylor, C. Viney, E.J. Wilson, *J. Organomet. Chem.*, **519** (1996) 103.
7. B.L. Pagenkopf, T. Livinghouse, *J. Am. Chem. Soc.*, **118** (1996) 2285.
8. C.M. Gordon, M. Kiszka, I.R. Dunkin, W.J. Kerr, J.S. Scott, J. Gebicki, *J. Organomet. Chem.*, **554** (1998) 147.
9. Sternberg, H. Greenfield, R.A. Friedel, J. Wotiz, R. Markby, I. Wender, *J. Am. Chem. Soc.*, **76** (1954) 1457.
10. Sternberg, H. Greenfield, R.A. Friedel, J. Wotiz, R. Markby, I. Wender, *J. Am. Chem. Soc.*, **78** (1956) 120.
11. I.S. Chia, W.R. Cullen, M. Franklin, A.R. Manning, *Inorg. Chem.*, **14** (1975) 2521.
12. J.J. Bonnet, R. Mattieu, *Inorg. Chem.*, **17** (1978) 1973.
13. C.J. Breheny, J.M. Kelly, C. Long, S. O' Keeffe, M.T. Pryce, G. Russell, M.M. Walsh, *Organometallics*, **17** (1998) 3690.
14. M.S. Wrighton, D.S. Ginley, *J. Am. Chem. Soc.*, **97** (1965) 2065.
15. Irradiation source was an Applied Photophysics xenon arc lamp (275 W).

- 
16. Degradation studies carried out on **pachc**, **achc** and **dpachc** indicated that **dpachc** is the most unstable of the three complexes. Typically solutions of each complex were prepared in hydrocarbon solvent and IR spectra were recorded each hour for 16 hours.

## **CHAPTER 3**

### **Reactions of $(\mu_2\text{-alkyne})\text{Co}_2(\text{CO})_6$ Complexes with Alkenes**

### 3.1 Introduction

The reported thermal reactions of dicobalt carbonyl complexes with olefins involved the reaction of acetylene hexacarbonyldicobalt complexes with norbornadiene (**nbd**).<sup>1</sup> When the reactions were carried out in aromatic solvents, arenecobalt complexes  $((\text{ArH})\text{Co}_3(\text{CO})_9)$  were formed, while the reaction in dimethoxyethane solvent produced dicarbonylcyclopentadienylcobalt(II). The majority organic products from these reactions are the ketones (Figure 3.1). Stereoisomers are formed in the majority of cases, however, when the products are derived from unsymmetrical acetylenes ( $\text{MeC}\equiv\text{CH}$  or  $\text{PhC}\equiv\text{CH}$ ) the products are regiospecific. The ketone products from these reactions have been shown to derive from the acetylene and a carbonyl group from the hexacarbonyl reagent.<sup>2</sup>

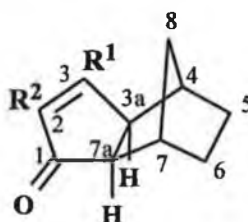


**Figure 3.1** *4,7-methanohexahydroindanone skeleton of ketones derived from dicobalt carbonyl complexes and acetylenes.*

Typically, for PK reactions the alkyne is added to octacarbonyl dicobalt in either stoichiometric amounts or in excess.<sup>3</sup> Alternatively the acetylene hexacarbonyldicobalt complex can be used as the starting material rather than the octacarbonyl dicobalt species. A convenient preparation of these alkyne hexacarbonyls was reported by Perasamy and involves the reduction of  $\text{CoBr}_2$  with Zn in the presence of the alkyne and CO at 1 atmosphere pressure.<sup>4</sup> Phenylacetylene hexacarbonyldicobalt was often used to test the reactivity of diverse simple alkenes in

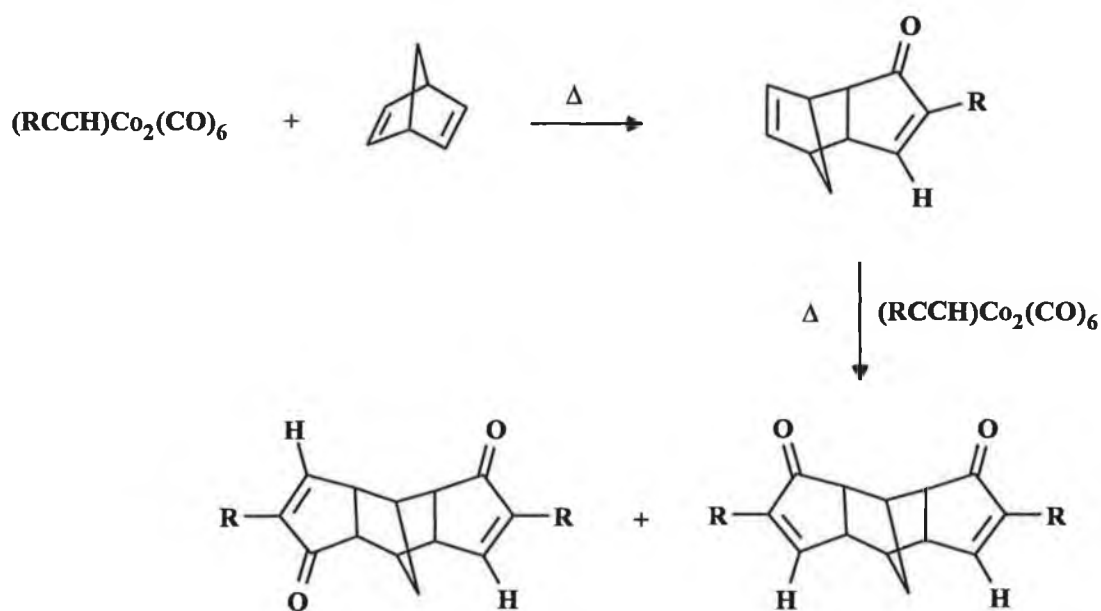
the early work of Pauson and Khand. Table 3.1 lists the typical yields for the reaction of phenylacetylene hexacarbonyldicobalt with a variety of simple alkenes.

Common solvents for the reaction are benzene, heptane, isooctane or toluene. The reactions are usually carried out in an inert atmosphere (argon or  $\text{N}_2$ ) at 60 - 70 °C for strained alkenes or at 80 - 130 °C for less reactive alkenes. Livinghouse has shown that optimum conditions for thermal PK cyclisation is achieved within the temperature region 60 - 70 °C using high purity  $\text{Co}_2(\text{CO})_8$ .<sup>5</sup> Purification of the resulting cyclopentenone can be achieved through flash chromatography by elution with slightly polar mobile phases (hexane/diethyl ether 85:15).

**Table 3.1** Typical yields for reaction of  $(\mu_2\text{-C}_6\text{H}_5\text{C}_2\text{H})\text{Co}_2(\text{CO})_6$  with alkenes reported by Pauson.

Alkene	Reaction Conditions	Yield (%)
bicyclo[2,2,2]octene <sup>6</sup>	60-80 °C, 4-6 hrs	34
cyclohexene <sup>6</sup>	120 °C, 6-7 hrs	3
cycloheptene <sup>6</sup>	120 °C, 6-7 hrs	41
cyclooctene <sup>6</sup>	120 °C, 6-7 hrs	35
cyclopentadiene <sup>7</sup>	120 °C, 5 hrs	60
norbornene <sup>8</sup>	60-70 °C, 4 hrs	59

Alkenes with two double bonds like norbornadiene can undergo two subsequent reactions with acetylene hexacarbonyldicobalt complexes. One molecule can add to the first ene bond to generate cyclopentenone while further reaction at the second ene bond can also occur (Scheme 3.1).

**Scheme 3.1.**

The primary photoinduced reaction of metal carbonyl complexes often involves decarbonylation. Chapter 2 showed that  $(\mu_2\text{-alkyne})\text{Co}_2(\text{CO})_6$  complexes undergo CO-loss at wavelengths greater than 500 nm.  $\text{C}_6\text{H}_5\text{N}$  and  $\text{PPh}_3$  were used as trapping ligands to enable the isolation of these pentacarbonyl complexes. The next stage in the PKR following CO-loss is the attachment of the alkene to the cobalt carbonyl moiety.

In general, complexes of the type  $\text{M}(\text{CO})_5(\text{s})$ , where  $\text{s}$  = solvent and  $\text{M} = \text{Cr}$ ,  $\text{W}$  or  $\text{Mo}$  can be prepared as stable intermediates by conventional photochemical techniques. For weak coordinating solvents like  $n$ -alkanes, benzene, toluene and their fluorinated analogues, the  $\text{M}(\text{CO})_5(\text{s})$  species are short lived and undergo rapid substitution with nucleophiles. In the case of strong coordinating solvent such as THF, it is possible to prepare pure and stable complexes of the type  $\text{M}(\text{CO})_5(\text{THF})$  in solution and in some cases these THF analogues can be isolated. Lewis bases can in turn replace the solvated metal carbonyl species and thus offer a route to normally

inaccessible substituted metal carbonyl complexes. A general mechanism for substitution of initial metal carbonyls *via* the solvated species is detailed in reaction 3.1. The widely studied olefin substituted metal carbonyls of the Group 6 elements are conveniently accessible from the parent  $\text{M}(\text{CO})_6$  complexes ( $\text{M} = \text{Cr}, \text{Mo}, \text{W}$ ) by means of photolytic CO displacement in the presence of the appropriate olefin.



where S = solvent, L = nucleophile. (3.1)

The displacement of THF from photogenerated  $\text{Cr}(\text{CO})_5(\text{THF})$  by alkenes (*cis*-cyclooctene (cco), *trans*-cyclooctene (tco)) to afford  $\text{Cr}(\text{CO})_5(\text{cco})$  and  $\text{Cr}(\text{CO})_5(\text{tco})$  has been investigated by Grevels and Skibbe.<sup>9</sup> Solid  $\text{Cr}(\text{CO})_5(\text{cco})$  is sufficiently stable to be handled at room temperature. However, in solution at temperatures above  $-40^\circ\text{C}$  the complex gradually decomposes forming  $\text{Cr}(\text{CO})_6$  and inorganic chromium species, unless an excess of cco is present. In contrast,  $\text{Cr}(\text{CO})_5(\text{tco})$  is stable in solution and unlike its *cis* analog undergoes further photosubstitution of CO for a second olefinic ligand.

This chapter focuses on the photochemical reactions of ( $\mu_2$ -alkyne) $\text{Co}_2(\text{CO})_6$  complexes (alkyne =  $\text{C}_2\text{H}_2$  or  $\text{C}_6\text{H}_5\text{C}_2\text{H}$ ) with alkenes (Figure 3.2) and outlines attempts to isolate ( $\mu_2$ -alkyne) $\text{Co}_2(\text{CO})_5(\text{alkene})$  type complexes. The thermal reactions of alkenes with dicobalt hexacarbonyl complexes were also carried out in order to aid with identification of products derived under photochemical conditions.

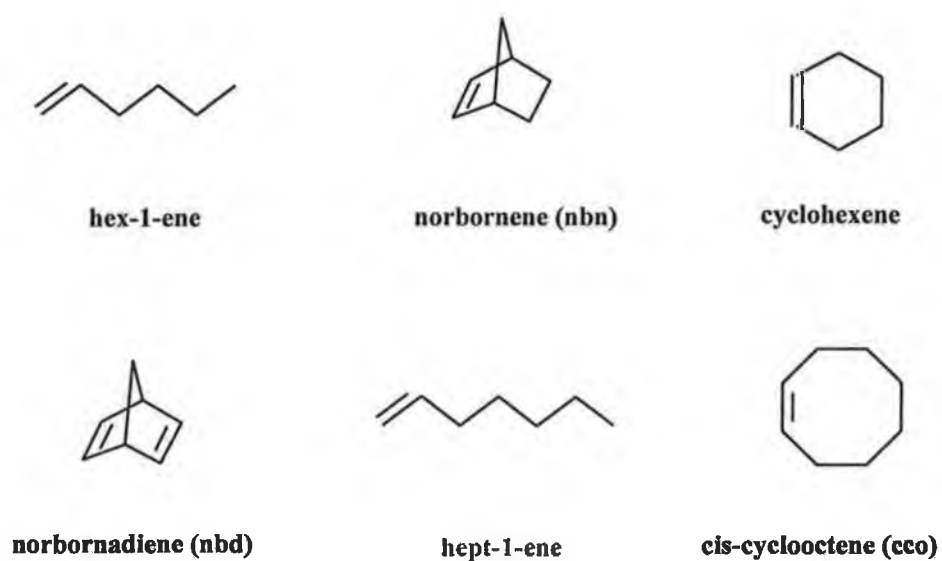
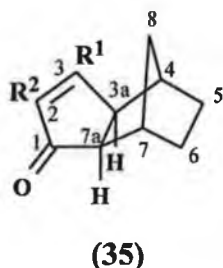


**Figure 3.2** *Alkenes used in this study.*



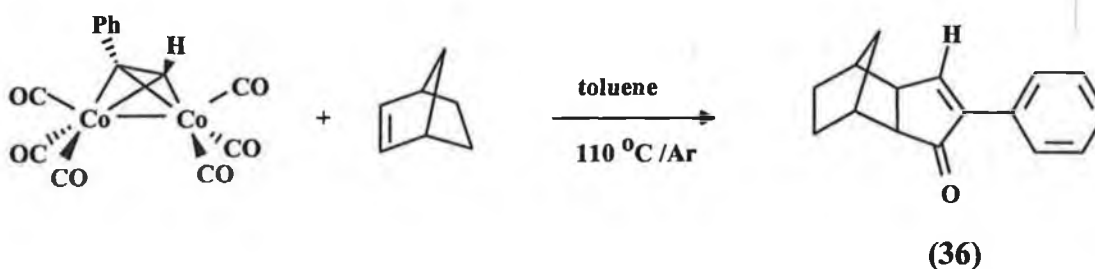
### 3.2 Thermal Preparation of Cyclopentenone Complexes



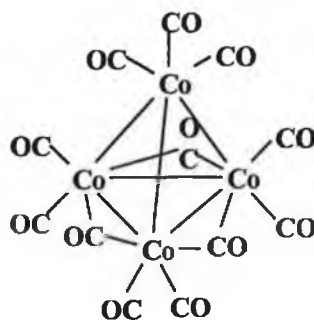
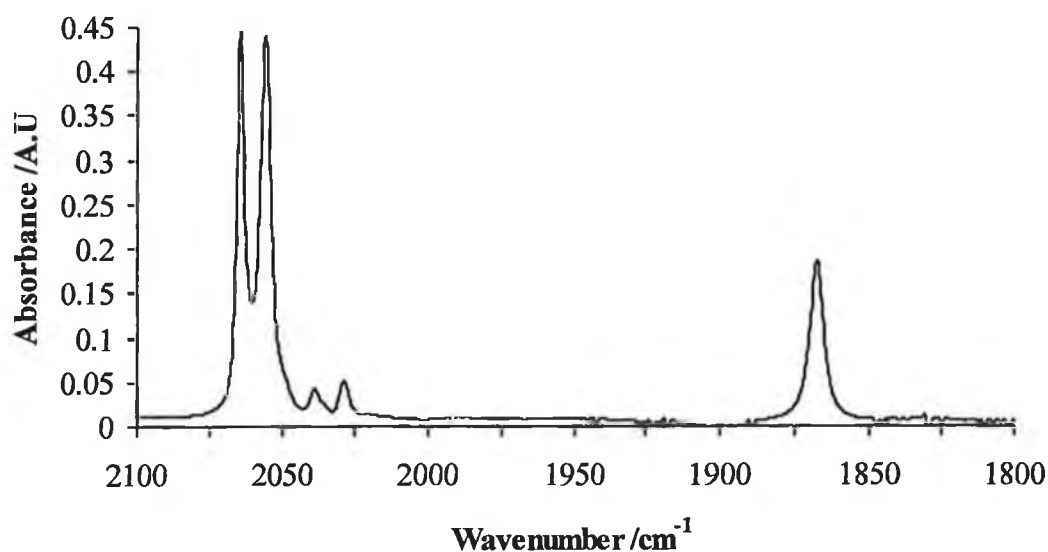
All ketones used in this study are numbered according to (35).

#### 3.2.1 Thermal cyclisation of 2-phenyl-3a,4,5,6,7,7a-hexahydro-4,7-methanoinden-1-one (36)

Thermal cyclisations of  $(\text{alkyne})\text{Co}_2(\text{CO})_6$  complexes with alkenes producing cyclopentenones was carried out in order to enable identification of products produced in photochemical experiments. The cyclisations involved employ two standard methods. The first involves a standard procedure of heating to reflux equimolar amounts of the hexacarbonyl  $(\mu_2\text{-C}_6\text{H}_5\text{C}_2\text{H})\text{Co}_2(\text{CO})_6$  and **nbn** in toluene at 110 °C under an atmosphere of argon for 36 hours (Reaction 3.2).<sup>10</sup> A solution colour change from deep red to pale orange was observed. After the removal of solvent under vacuum the product was purified by flash chromatography on neutral alumina. A hexane:diethyl ether (85:15 v/v) mixture eluted  $\text{Co}_4(\text{CO})_{12}$  (Figure 3.3) as a blue band and finally 2-phenyl-3a,4,5,6,7,7a-hexahydro-4,7-methanoinden-1-one (36) was eluted as a pale yellow band. Crystals were grown from hexane:diethyl ether. The IR spectrum of  $\text{Co}_4(\text{CO})_{12}$  in the  $\nu_{\text{CO}}$  region is presented in Figure 3.4.

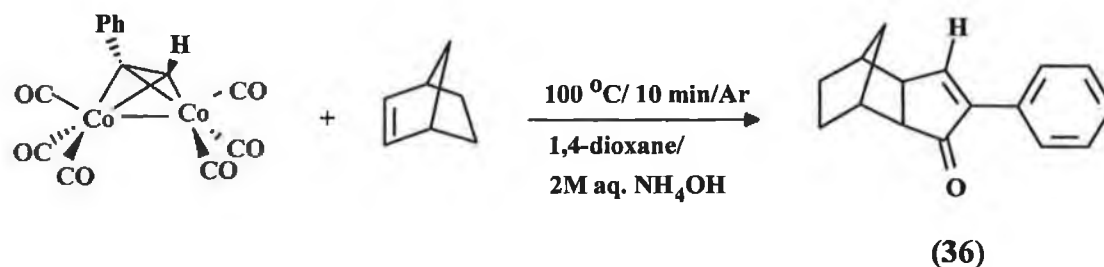


Reaction 3.2

Figure 3.3  $\text{Co}_4(\text{CO})_{12}$ Figure 3.4 IR spectrum in the carbonyl region of  $\text{Co}_4(\text{CO})_{12}$  ( $\text{cm}^{-1}$ ;  $\pm 1\text{cm}^{-1}$ , cyclohexane).

The second method of cyclopentenone synthesis was carried out according to Sugihara *et al*<sup>11</sup> and involves the use of ammonia derivatives to enhance the rate of the Pauson - Khand reaction (Reaction 3.3). Equimolar amounts of the hexacarbonyl  $(\mu_2\text{-C}_6\text{H}_5\text{C}_2\text{H})\text{Co}_2(\text{CO})_6$  and **nbn** were stirred at 100 °C for 10 minutes in a biphasic system of 1,4-dioxane and a 2M aqueous solution of ammonium hydroxide. A simple

extraction workup followed by flash chromatography on silica gel gave the corresponding cyclopentenone. In contrast to published yields of 100 % the yield obtained here was in the range 20 - 25 %. Prolonging the reaction time to 3 hours and employing various reaction temperatures (60, 70 and 110 °C) did not improve yields.



### Reaction 3.3

Cyclopentenone (**36**) was characterised by IR, <sup>1</sup>H-, <sup>13</sup>C-, DEPT 135 and DEPT 45 NMR spectroscopy (Table 3.2). The IR spectrum of the white crystals (Figure 3.5) showed two bands at 1699 and 1677 cm<sup>-1</sup> which have been assigned to the  $\nu_{\text{CO}}$  and  $\nu_{\text{C=C}}$  vibrations of the enone respectively. The <sup>1</sup>H NMR spectrum (Figure 3.6) showed four singlets corresponding to the protons (**3a**, **4**, **7** and **7a**) of the enone. The signal due to one of the tertiary protons **7a** suffers the greatest downfield shift due to its close proximity to the enone carbonyl group. The phenyl protons were observed as multiplets at 7.72 (m, 2H, *ortho* C-H), 7.32 (m, 2H, *meta* C-H) and 7.38 (m, 1H, *para* C-H) ppm. The peak at 7.65 ppm is assigned to the single proton at position **3**. The remaining CH<sub>2</sub> protons **6**, **5**, and **8** were observed at 1.01 (1H), 1.14 (1H), 1.35 (m, 2H), 1.66 (m, 1H) and 1.76 (m, 1H) ppm.

The <sup>13</sup>C spectrum (Figure 3.7) shows two peaks at 160.7 (C-H) and 146.5 (q-C) ppm assigned to the olefinic carbons, the latter being a quaternary carbon which disappears in the DEPT 45 spectrum (Figure 3.8(a)). The carbonyl carbon was observed at 209.5 ppm while signals for the phenyl group were observed at 127.5, 128.8 and 131.9 (q-C) ppm. The peaks at 28.8, 29.5 and 31.7 ppm are assigned to the three CH<sub>2</sub> carbons of the **nbn** component (negative peaks in DEPT 135 (Figure

3.8(b)) while the remaining peaks at 38.7, 39.8, 48.1, 55.4 ppm (all C-H) are assigned to the remaining four tertiary aliphatic carbons.

**Table 3.2**  $^1\text{H}$ -,  $^{13}\text{C}$ -NMR and IR spectral data of (2-phenyl-3a,4,5,6,7,7a-hexahydro-4,7-methanoinden-1-one (36).

$^1\text{H}^a$	1.01(d, 1H, $^2J$ 10Hz), 1.14(d, 1H, $^2J$ 10Hz), 1.35(m, 2H), 1.66(m, 1H), 1.76(m, 1H), 2.28(d, 1H), 2.38(d, 1H), 2.50(d, 1H), 2.71(t, 1H), 7.32(m, 2H), 7.38(m, 1H), 7.72 (m, 2H), 7.65(1H) ppm.
$^{13}\text{C}^a$	28.8, 29.5, 31.7, 38.7, 39.8, 48.1, 55.3, 127.5, 128.8, 131.9(q), 146.5(q), 160.7, 209.5
IR <sup>b</sup>	1699, 1677 $\text{cm}^{-1}$ .

<sup>a</sup> in  $\text{CDCl}_3$ ; <sup>b</sup> in toluene.

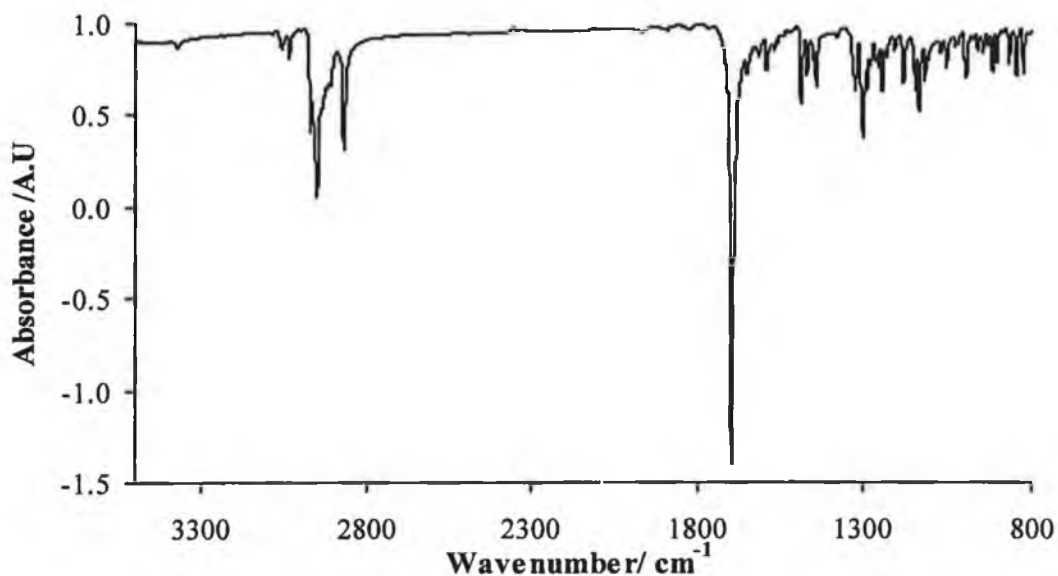


**Figure 3.5** IR spectrum of 2-phenyl-3a,4,5,6,7,7a-hexahydro-4,7-methanoinden-1-one (36) ( $\text{cm}^{-1}$ ;  $\pm 1\text{cm}^{-1}$ , toluene).

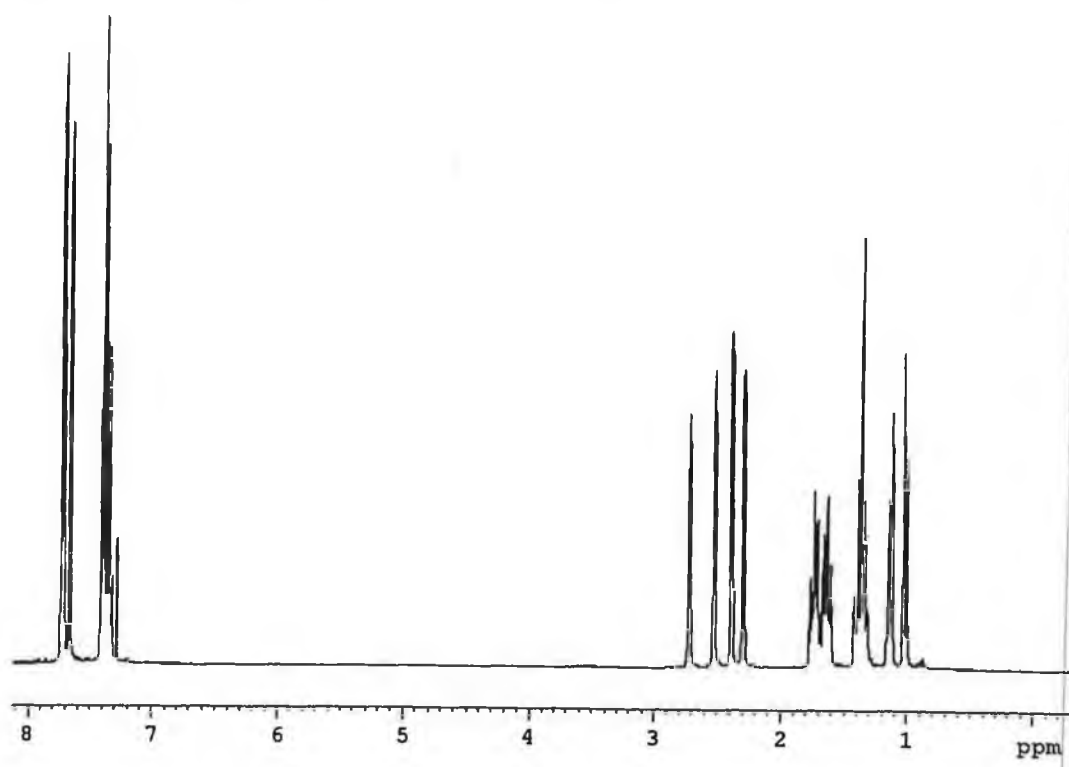


**Figure 3.6**  $^1\text{H}$  NMR spectrum of 2-phenyl-3a,4,5,6,7,7a-hexahydro-4,7-methanoinden-1-one (36) ( $\text{CDCl}_3$ ,  $\delta/\text{ppm}$ , 298 K).

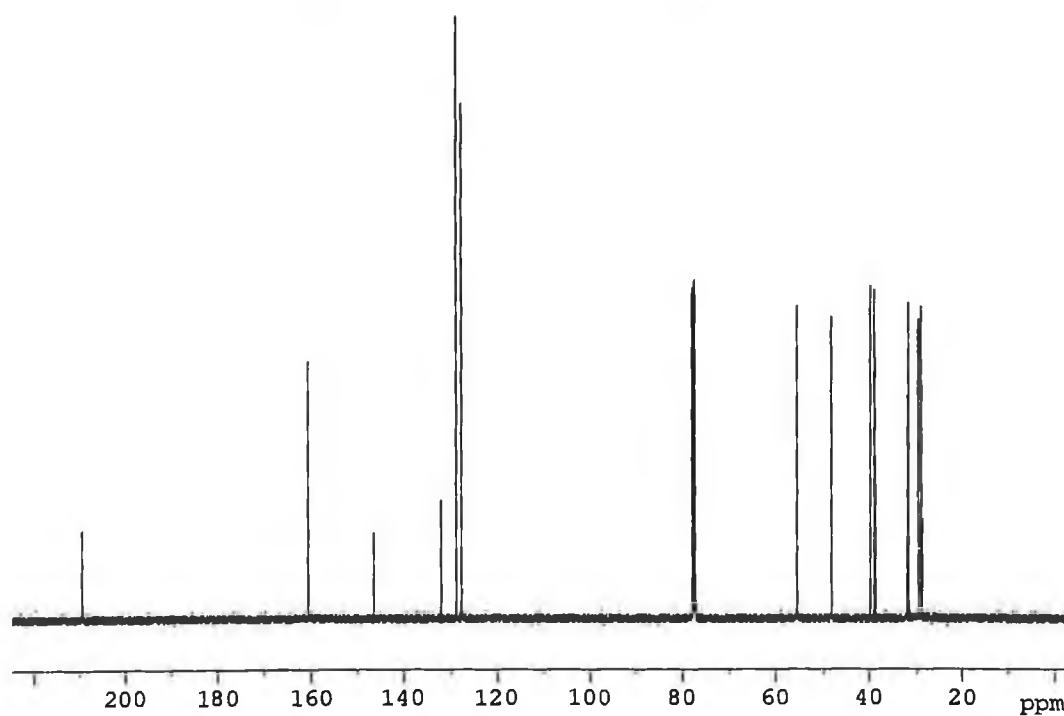


**Figure 3.7**  $^{13}\text{C}$  NMR spectrum of 2-phenyl-3a,4,5,6,7,7a-hexahydro-4,7-methanoinden-1-one (36) ( $\text{CDCl}_3$ ,  $\delta/\text{ppm}$ , 298 K).

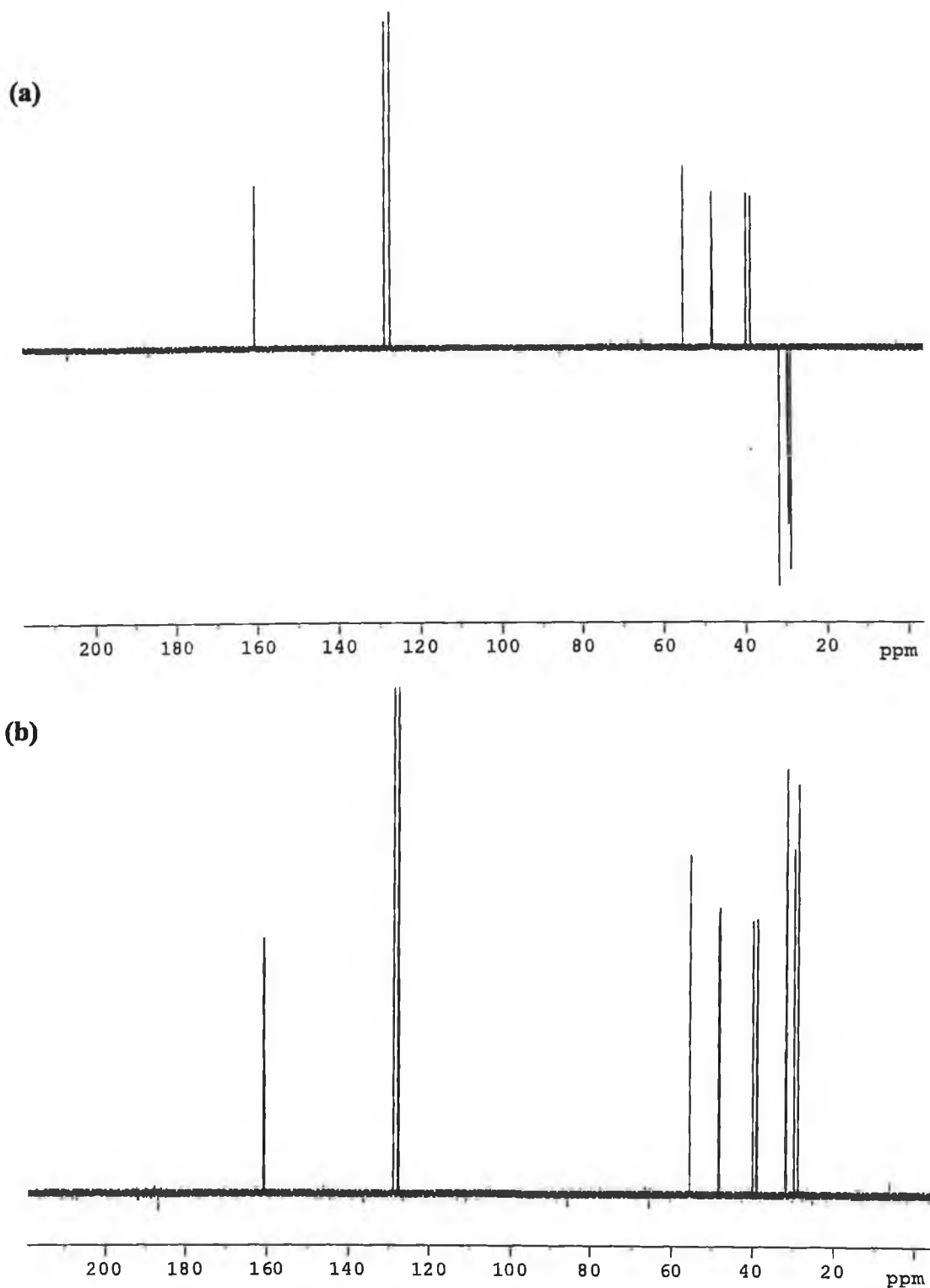


**Figure 3.8** (a) DEPT 45 and (b) DEPT 135 NMR spectra of 2-phenyl-3a,4,5,6,7,7a-hexahydro-4,7-methanoinden-1-one (36) ( $\text{CDCl}_3$ ,  $\delta/\text{ppm}$ , 298 K).

### 3.2.2 Thermal preparation of 2-phenyl-3a,4,5,6,7,7a-hexahydroinden-1-one (37)

The synthesis of 2-phenyl-3a,4,5,6,7,7a-hexahydroinden-1-one (**37**) (Figure 3.9) was carried out by heating the hexacarbonyl ( $\mu_2\text{-C}_6\text{H}_5\text{C}_2\text{H}$ ) $\text{Co}_2(\text{CO})_6$  with a slight excess of cyclohexene (1:1.1) in toluene at 100 °C under an atmosphere of argon for 36 hours.<sup>10</sup> A color change from deep red to pale yellow was observed. After removal of the solvent under vacuum the product was purified by flash chromatography on silica gel. Pentane or hexane eluted any remaining starting complex as a red band. A hexane:diethyl ether (85:15 v/v) mixture then eluted  $\text{Co}_4(\text{CO})_{12}$  as a blue band and finally cyclopentenone (**37**) eluted as a colourless band. It proved difficult to remove the last traces of solvent as the compound was quite volatile.

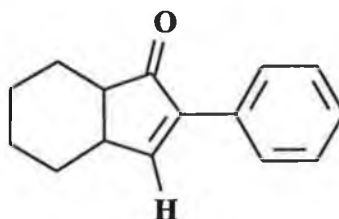


**Figure 3.9** 2-phenyl-3a,4,5,6,7,7a-hexahydroinden-1-one (**37**)

The compound was characterised by IR,  $^1\text{H}$ -,  $^{13}\text{C}$ -, DEPT 135 and DEPT 45 NMR spectroscopy (Table 3.3). The IR spectrum of the white powder showed two bands at 1734 and 1698  $\text{cm}^{-1}$  which have been assigned to the  $\nu_{\text{CO}}$  and  $\nu_{\text{C}=\text{C}}$  vibrations of the enone respectively. The  $^1\text{H}$  NMR spectrum of compound (**37**) closely resembles that of compound (**36**) showing two doublets corresponding to the protons **3a** and **7a** of the enone. The signal due to one of the tertiary protons **7a** suffers the greatest downfield shift due to its close proximity to the enone carbonyl group. The phenyl protons were observed as multiplets at 7.79 (2H, *ortho* C-H) and 7.48 (2H, *meta* C-H) - 7.36 (1H, *para* C-H) ppm. The peak at 7.75 ppm is assigned to the

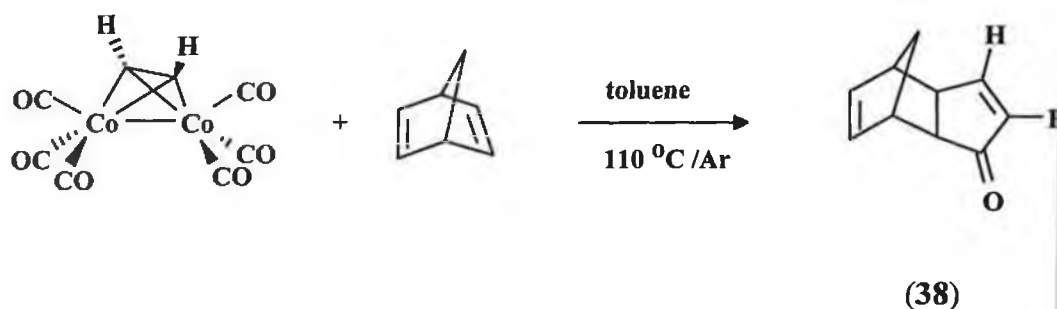
proton at position 3. The remaining  $\text{CH}_2$  protons 4, 5, 6 and 7 were observed as a complex multiplet between 1.12 and 1.66 ppm (8H).

The  $^{13}\text{C}$  spectrum ( $\text{CDCl}_3$ ) shows two peaks at 159.2 (C-H) and 145.1 (q-C) ppm assigned to the olefinic carbons, the latter being a quaternary carbon which disappears in the DEPT 45 spectrum. The carbonyl carbon was observed at 208.1 ppm while signals for the phenyl group were observed at 126.0, 127.7 and 130.5 (q-C) ppm. The peaks at 27.3, 28.1, 28.7 and 30.3 ppm are assigned to the four  $\text{CH}_2$  carbons of the cyclohexane component (negative peaks in DEPT 135) while the remaining peaks at 46.7 and 53.9 ppm (all C-H) are assigned to the remaining two tertiary aliphatic carbons.

### 3.2.3 Thermal synthesis of 3a,4,7,7a-Tetrahydro-4,7-methanoinden-1-one (38)

The thermal synthesis of 3a,4,7,7a-tetrahydro-4,7-methanoinden-1-one (38) was carried out according to Reaction 3.4. Equimolar amounts of **nbd** and **achc** were heated in toluene for 18 hours at 110 °C under an atmosphere of argon. The product was isolated by solvent evaporation at low pressure followed by flash chromatography on neutral alumina. A hexane:diethyl ether (85:15 v/v) mobile phase eluted any unreacted starting complex followed by (38). The product was characterised by  $^1\text{H}$ ,  $^{13}\text{C}$  NMR, and IR spectroscopy. The  $^1\text{H}$  NMR spectrum gave evidence for the cyclopentenone unit showing a set of double doublets at 6.3 and between 7.3-7.5 ppm which are assigned to the diene protons. The spectrum was very complicated in the region between 0.8 and 2.9 ppm because of coupling between the aliphatic protons. The  $^{13}\text{C}$  spectrum however, clearly provided evidence for the cyclopentenone unit, the peak at 210.5 ppm diagnostic of the carbonyl carbon. Olefinic resonances were observed at 163.8 ppm and 137.3 ppm. The remaining resonances are given in Table 3.3.





## Reaction 3.4

**Table 3.3**  $^1\text{H}$ -,  $^{13}\text{C}$ -NMR and IR spectral data of (a) 2-phenyl-3a,4,5,6,7,7a-hexahydro-4,7-methanoinden-1-one (37) and (b) 3a,4,7,7a-tetrahydro-4,7-methanoinden-1-one (38).

<p>(37)</p>	<p><math>^1\text{H}^a</math> 1.12 -1.66 (complex m, 8H, <math>\text{CH}_2</math>), 2.60 (s, 1H, CH), 2.81 (s, 1H, CH), 7.36 (s, 1H), 7.48 (m, 2H), 7.75 (s, 1H), 7.79 (d, 2H) ppm.</p> <p><math>^{13}\text{C}^a</math> 27.3, 28.1, 28.7, 30.3, 46.7, 53.9, 126.0, 127.7, 130.5(q), 145.1(q), 159.3, 208.1 ppm.</p> <p>IR<sup>b</sup> 1734, 1698 <math>\text{cm}^{-1}</math>.</p>
<p>(38)</p>	<p><math>^1\text{H}^a</math> 0.8 (m, 2H, CH), 2.26-2.39 (m, CH, 2H), 2.91 (s, br, 2H), 6.3 (d, 2H, =CH), 7.31 (dd, 1H, =CH), 7.53 (dd, 1H, =CH) ppm.</p> <p><math>^{13}\text{C}^a</math> 24.1, 31.6, 32.7, 37.0, 39.6, 49.5, 52.7, 137.3, 163.8, 210.5 ppm.</p> <p>IR<sup>c</sup> 1701 <math>\text{cm}^{-1}</math>.</p>

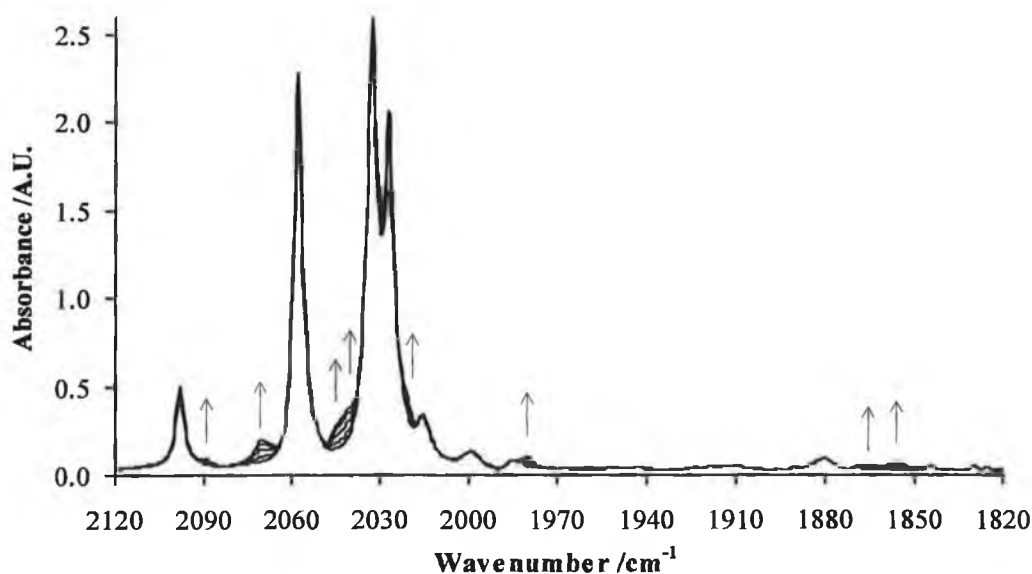
<sup>a</sup> in  $\text{CDCl}_3$ ; <sup>b</sup> in pentane; <sup>c</sup> in toluene.

### 3.3 Steady-state Photolysis Experiments

#### 3.3.1 IR monitored steady-state photolysis of $(\mu_2\text{-C}_2\text{H}_2)\text{Co}_2(\text{CO})_6$ in the presence of alkenes

In order to identify any products which arise as a result of photolysis of  $(\text{alkyne})\text{Co}_2(\text{CO})_6$  complexes in the presence of alkenes irradiation of a cyclohexane solution of **achc** containing cyclohexene was carried out with  $\lambda_{\text{exc}} > 500$  nm. However, the resulting IR spectra recorded at  $t = 0, 0.5, 1, 2, 5, 10, 15, 20, 30$  and  $40$  minutes provided no evidence for photoproduct formation. A similar solution of **achc** was irradiated with  $\lambda_{\text{exc}} > 400$  nm at  $t = 0, 1, 2, 5, 10, 18, 27, 36, 51$  and  $60$  minutes. The resulting spectra are represented in Figure 3.10. The IR combination and difference spectra are shown. Arrows indicate the direction of band increase or decrease. New bands at  $2089, 2071, 2045, 2041, 2021, 1981, 1868, 1857$   $\text{cm}^{-1}$  were identified as  $\text{Co}_2(\text{CO})_8$ . The parent bands of **achc** depleted continuously throughout the experiment.

(a)



(b)

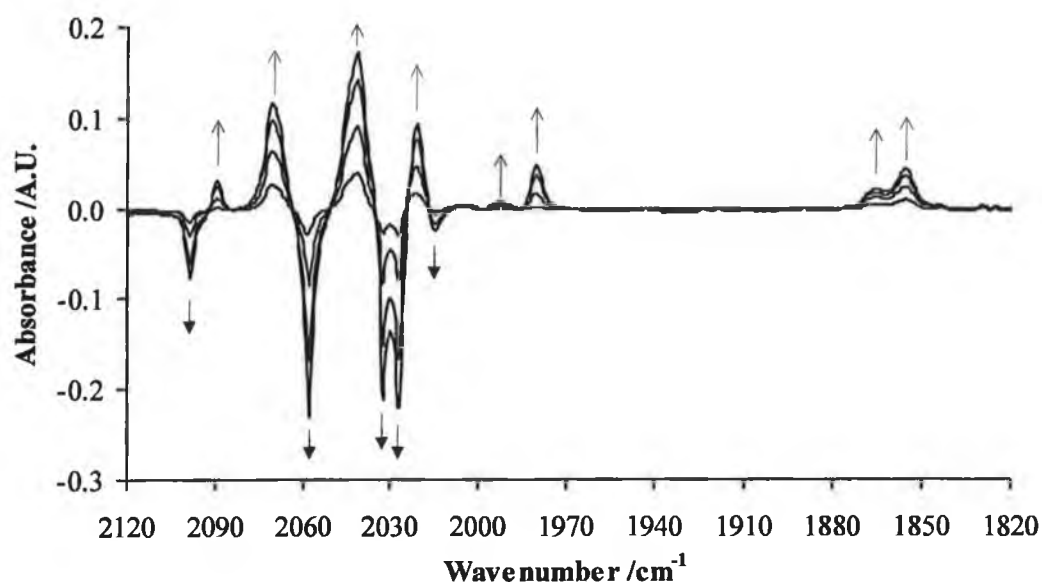


**Figure 3.10** The IR combination and difference spectra following broad band photolysis of *achc* ( $\lambda_{\text{exc}} > 400 \text{ nm}$ ) in the presence of cyclohexene ( $\text{cm}^{-1}$ ;  $\pm 1 \text{ cm}^{-1}$ ). Spectra were acquired at  $t = 0, 18, 27, 51$  and  $60$  minutes; (a) combination spectra showing new photoproduct (indicated by the arrows) and parent bands (b) difference spectrum. The positive bands are identified as  $\text{Co}_2(\text{CO})_8$ . The negative bands are due to parent depletion.

Irradiation of a similar solution of *achc* containing cyclohexene with  $\lambda_{\text{exc}} > 320 \text{ nm}$  from  $t = 0$  to  $60$  minutes resulted in bands at  $1700$  and  $1695 \text{ cm}^{-1}$  corresponding to the  $\nu_{\text{CO}}$  and  $\nu_{\text{C}=\text{C}}$  bands of the resulting ketone. Bands were also observed which were consistent with  $\text{Co}_2(\text{CO})_8$  formation. Further steady-state photolysis experiments with *achc* and hex-1-ene with  $\lambda_{\text{exc}} > 320 \text{ nm}$  resulted in band system which corresponds to a mixture of products (Figure 3.11). The bands at  $2071, 2044, 2001, 1993, 1980, 1870$  and  $1857 \text{ cm}^{-1}$  were subsequently identified as  $\text{Co}_2(\text{CO})_8$ . Following comparison of the  $\nu_{\text{CO}}$  stretching frequencies of  $\text{Co}_4(\text{CO})_{12}$  and  $\text{Co}_2(\text{CO})_8$  in *n*-hexane published by Ungváry and Marko<sup>12</sup> (Table 3.4), the bands at  $2065, 2051$  and  $1866 \text{ cm}^{-1}$  were identified as  $\text{Co}_4(\text{CO})_{12}$  (Figure 3.4), a common

decomposition product of  $\text{Co}_2(\text{CO})_8$ . Note that the excess number of terminal CO bands of  $\text{Co}_2(\text{CO})_8$  is consistent with the existence of at least two isomeric configurations of  $\text{Co}_2(\text{CO})_8$  in solution.

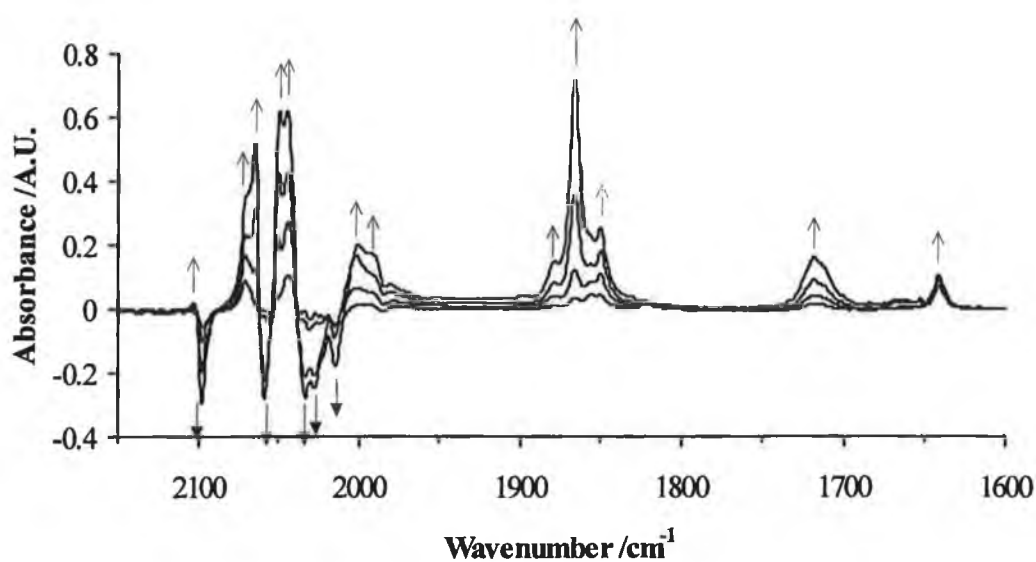


**Figure 3.11** IR difference spectrum in the CO stretching region obtained following broad band photolysis of *achc* containing hex-1-ene ( $\lambda_{\text{exc}} > 320 \text{ nm}$ ,  $\text{cm}^{-1}$ ;  $\pm 1 \text{ cm}^{-1}$ , pentane solvent). Spectra shown were acquired at  $t = 5, 15, 30$  and  $70$  minutes.

Further bands in the spectrum observed at  $1719$  and  $1642 \text{ cm}^{-1}$  are assigned to a ketone carbonyl stretch  $\nu_{\text{CO}}$  and an alkene  $\nu_{\text{C}=\text{C}}$  stretch respectively (in a separate experiment these complexes were prepared and characterised by IR or  $^1\text{H}$  NMR spectroscopy). These results are consistent with the formation of cyclopentenone from the *achc* and hex-1-ene and show that cyclopentenones can be generated photochemically.

**Table 3.4** Carbonyl stretching frequencies and relative band intensities for  $\text{Co}_2(\text{CO})_8$  and  $\text{Co}_4(\text{CO})_{12}$  in *n*-hexane solution.<sup>12</sup>

$\text{Co}_2(\text{CO})_8$		$\text{Co}_4(\text{CO})_{12}$	
$\nu_{\text{CO}}$	Rel. Intensity	$\nu_{\text{CO}}$	Rel. Intensity
2112	~0.5	2104	0.5
2107	~0.3	2063	90
~2071	65	2055	100
2069	73	~2048	-
2059	21	2038	6
~2044	90	2028	8
2042	100	1997	$^{13}\text{CO}$ , ~0.5
2031	49	1898	0.4
2023	81	1867	33
2002	4	~1832	$^{13}\text{CO}$ , ~0.5
~1991	5	~1991	5
1866	3	1857	23
1857	23		
~1822	~0.5		

**Achc** was photolysed in degassed alkane solvents (cyclohexane and pentane respectively) containing **nb**d with  $\lambda_{\text{exc}} > 500$  nm. No changes were observed in the IR spectra monitored at  $t = 0, 0.5, 1, 2, 5, 10, 15, 20$  and 30 minutes with either solvent system. Photolysis of **achc** with  $\lambda_{\text{exc}} > 400$  nm in degassed pentane containing **nb**d for  $t = 0, 0.5, 1, 2, 5, 10, 15, 20$  and 30 minutes produced new bands at 2075, 2024, 2010(br), 1850(s), 1834(br), 1719 and 1716(sh)  $\text{cm}^{-1}$ . The parent hexacarbonyl bands depleted throughout photolysis. The IR combination and difference spectrum for the photoreaction are given in Figure 3.12 for  $t = 15$  minutes. The positive bands represent the product while the negative bands represent the depletion of parent species. A further band observed at 1719  $\text{cm}^{-1}$  provides evidence for a ketone carbonyl in cyclopentenone. A shoulder on this latter band which was observed at

$1716\text{ cm}^{-1}$  is assigned to the  $\nu_{\text{C}=\text{C}}$  stretch of the alkene. The broad band at  $1834\text{ cm}^{-1}$  may reflect a strained carbonyl group (compare the bridging carbonyl stretches of  $\text{Co}_2(\text{CO})_8$  at  $1866$  and  $1856\text{ cm}^{-1}$ ). Ungváry reported similar IR absorptions at  $2081.5$ ,  $2072$ ,  $2024(\text{br})$  and  $1834\text{ cm}^{-1}$  after mixing  $\text{PhC}\equiv\text{CH}$  with  $\text{HCo}(\text{CO})_4$  in heptane for 20 minutes at  $15^\circ\text{C}$ .<sup>13</sup> The suggested structure of the product was the alkenylcobalt carbonyl (**39**). Heck also reported an IR absorption at  $1834\text{ cm}^{-1}$  for the product of the reaction of crotonyl chloride with  $\text{NaCo}(\text{CO})_4$  in ether and was assigned to a  $\pi$ -crotonylcobalt tricarbonyl.<sup>14</sup>

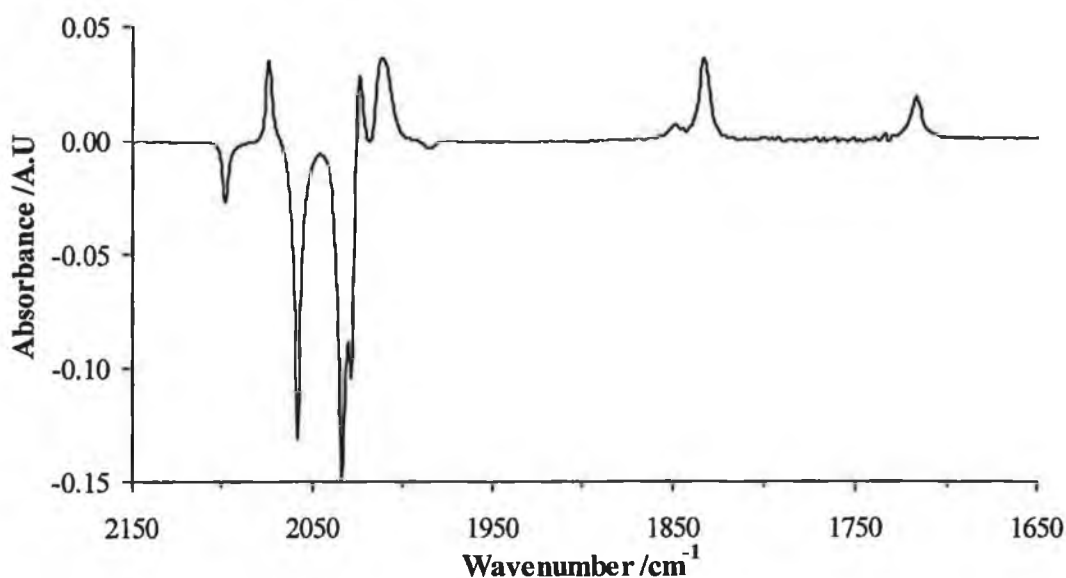
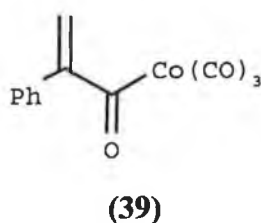


**Figure 3.12** IR difference spectrum in the CO stretching region obtained following broad band photolysis of *achc* after 15 minutes irradiation in the presence of *nb*d ( $\lambda_{\text{exc}} > 400\text{ nm}$ ,  $\text{cm}^{-1}$ ;  $\pm 1\text{ cm}^{-1}$ , pentane solvent).

In order to follow the photochemical reaction of  $(\mu_2\text{-alkyne})\text{dicobalthexacarbonyl}$  complexes with alkenes, NMR monitored photolysis experiments were undertaken on **ache** solutions containing **nbn**. These experiments may also provide evidence for the formation of the  $(\mu_2\text{-alkyne})\text{Co}_2(\text{CO})_5(\text{alkene})$  complex, a proposed intermediate in the PK reaction. The sample solutions were prepared in  $\text{d}_6\text{-cyclohexane}$  solvent in a degassable NMR tube and placed under an atmosphere of CO. The sample was irradiated at  $t = 5, 10$  and  $15$  minutes after which time  $^1\text{H}$  spectra were recorded. After each photolysis step the resulting  $^1\text{H}$  NMR spectrum showed the starting material peaks had broadened considerably. The sample was then heated to  $40^\circ\text{C}$  and another NMR spectrum recorded. Again the spectrum showed considerable peak broadening, possibly obscuring any product peaks. An IR spectrum of this solution obtained immediately following photolysis showed a  $\nu_{\text{CO}}$  band at  $1718\text{ cm}^{-1}$  indicating the formation of a cyclopentenone.

In contrast with the abundance of infrared spectroscopy information on cobalt carbonyl complexes,  $^1\text{H}$  NMR investigations were carried out occasionally to confirm the identity of new compounds, rather than to provide structural information. Mostly the spectra obtained exhibit line-broadening, an effect of the quadrupole moment of  $^{59}\text{Co}$ .<sup>15</sup> More recent investigations, however, suggest that paramagnetic Co(II) impurities generated by accidental oxidation are responsible for poor quality spectra.<sup>16</sup>

### 3.3.2 *UV/Vis. monitored photolysis of $(\mu_2\text{-C}_2\text{H}_2)\text{Co}_2(\text{CO})_6$ and alkenes **nbn** and **nbd***

Steady-state photolysis experiments of  $(\text{alkyne})\text{Co}_2(\text{CO})_6$  complexes (alkyne =  $\text{C}_2\text{H}_2$  and  $\text{C}_6\text{H}_5\text{C}_2\text{H}$ ) with **nbn** and **nbd** were conducted under both an atmosphere of argon and an atmosphere of CO in sealed cells. The solutions were irradiated with  $\lambda_{\text{exc}} > 500\text{ nm}$  for 5 hours. The UV/Vis spectra were monitored at periodic intervals throughout the experiments. After 5 hours irradiation a slight increase in bands at  $\sim 395$  and  $460\text{ nm}$  was observed and was accompanied by a solution colour change

from red to pale yellow. While assignment of the UV/Vis product bands was impossible an IR spectrum recorded following photolysis showed weak features consistent with the formation of  $\text{Co}_2(\text{CO})_8$ . No other product bands were observed. Heating the sealed cell to 50 °C showed further growth of bands in the UV/Vis spectrum. An IR spectrum recorded following heating showed a carbonyl peak at  $1701\text{ cm}^{-1}$  indicating the presence of a ketonic carbonyl. By comparison of product band formation at equivalent time intervals the experiments conducted under an atmosphere of carbon monoxide produced product at a faster rate than those conducted under an atmosphere of argon.

### 3.3.3 IR monitored steady-state photolysis of $(\mu_2\text{-C}_6\text{H}_5\text{C}_2\text{H})\text{Co}_2(\text{CO})_6$ in the presence of alkenes

The reaction of **pachc** with alkenes was monitored by IR spectroscopy. Initially **pachc** was irradiated ( $\lambda_{\text{exc}} > 500\text{ nm}$ ) in an argon flushed cyclohexane solution containing cyclohexene at  $t = 0.5, 1, 2, 5, 10, 15$  and 20 minutes. The parent bands depleted throughout the experiment and while no new bands were observed, a yellow precipitate was produced. Repeating the experiment in toluene solution gave rise to a carbonyl band at  $1701\text{ cm}^{-1}$  which is consistent with the formation of cyclopentenone.<sup>17</sup> Bands were also observed which were consistent with the formation of  $\text{Co}_2(\text{CO})_8$ . Neither the cyclopentenone or  $\text{Co}_2(\text{CO})_8$  are significantly soluble in alkane solvent and this explains the formation of the yellow precipitate observed when the experiment was conducted in cyclohexane solution. Further irradiation of the solution with  $\lambda_{\text{exc}} > 340\text{ nm}$  gave rise to a higher yield of product.

**Pachc** was irradiated ( $\lambda_{\text{exc}} > 500\text{ nm}$ ) in an argon flushed toluene solution containing **nbn** with  $t = 0.5, 1, 3, 8$  and 18 minutes. No changes were observed in the IR spectrum recorded throughout the experiment. Further photolysis of the same solution with  $\lambda_{\text{exc}} > 400\text{ nm}$  and subsequently with  $\lambda_{\text{exc}} > 340\text{ nm}$  ( $t = 23, 30$  and 35



mins.) gave rise to new bands at 2104(vs), 2072, 2046, 2042, 2002, 1856 and 1860  $\text{cm}^{-1}$ . These are consistent with the formation of  $\text{Co}_2(\text{CO})_8$ . Bands were also observed at 1708 and 1380  $\text{cm}^{-1}$  which are consistent with the formation of cyclopentenone. A typical difference IR spectrum observed following photolysis is shown in Figure 3.13.

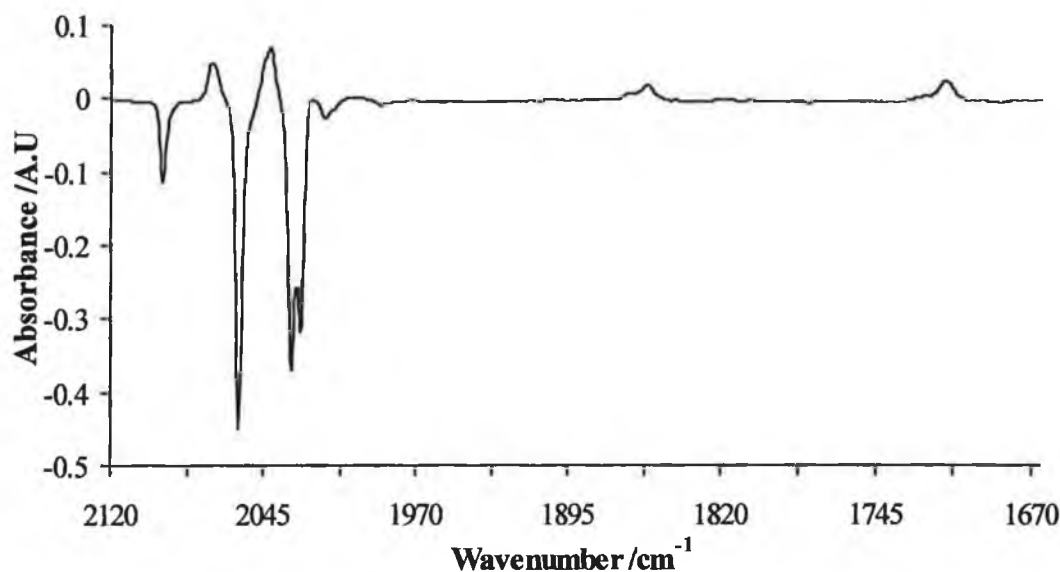


**Figure 3.13** IR difference spectrum in the CO stretching region obtained following broad band photolysis of *pachc* containing *nbn* ( $\lambda_{\text{exc}} > 400 \text{ nm}$ , toluene,  $\text{cm}^{-1}$ ;  $\pm 1 \text{ cm}^{-1}$ ). The spectrum was acquired at  $t = 30$  minutes. The positive bands are due to the formation of  $\text{Co}_2(\text{CO})_8$  and cyclopentenone while the negative bands are due to the depletion of the parent complex.

**Pachc** was irradiated in hept-1-ene solution containing a four fold excess of pyridine. A series of spectra were measured up to an irradiation time of 50 minutes. The spectrum obtained following irradiation with  $\lambda_{\text{exc}} > 500 \text{ nm}$  displayed two isosbestic points with bands observed at 2069, 2018, 2005, 1994 and 1966  $\text{cm}^{-1}$ . These bands were identified as  $(\mu_2\text{-C}_6\text{H}_5\text{C}_2\text{H})\text{Co}_2(\text{CO})_5(\text{C}_6\text{H}_5\text{N})$  based on previous assignment (*c.f.* chapter 2). No evidence for formation of the hept-1-ene substituted

complex  $(\mu_2\text{-C}_6\text{H}_5\text{C}_2\text{H})\text{Co}_2(\text{CO})_5(\text{hept-1-ene})$  was observed indicating the pyridine adduct was more stable.

IR monitored steady-state experiments were also conducted in the presence of the strong donor ligands tetracyanoethylene (tcne) and methanol. The solutions were prepared as previously by dissolving **pachc** in degassed toluene. The respective donor ligands were added and the solutions were irradiated with  $\lambda_{\text{exc}} > 500$  nm. The spectra were measured at  $t = 0, 1, 2, 5, 10$  and  $15$  minutes. No changes were observed in the IR spectra recorded throughout the experiments. The solutions were then subjected to irradiation with  $\lambda_{\text{exc}} > 400$  nm. Again no spectroscopic changes in the IR spectrum were observed. Similar results were obtained for solutions of **pachc** prepared in neat tcne and methanol respectively.

**Pachc** was also irradiated in degassed solutions containing a 4 fold excess of mecn with  $\lambda_{\text{exc}} > 500$  nm. No spectroscopic changes were observed throughout photolysis. When the solution was subsequently irradiated with  $\lambda_{\text{exc}} > 400$  nm new bands were observed at  $1998(\text{vs}), 1894$  and  $1629\text{ cm}^{-1}$ . However, these bands are not consistent with the formation of  $(\mu_2\text{-C}_6\text{H}_5\text{C}_2\text{H})\text{Co}_2(\text{CO})_5(\text{mecn})$ , and the product formed remains unidentified.

### 3.4 Photolytic reaction of (alkyne)dicobalthexacarbonyl complexes with alkenes

#### 3.4.1 Reaction of *pachc* with norbornene

In an attempt to synthesise ( $\mu_2$ -alkyne) $\text{Co}_2(\text{CO})_5(\text{alkene})$  type complexes the hexacarbonyl complexes **pachc** and **achc** were reacted with a slight excess of alkenes under photochemical conditions. Two methods of synthesis were employed. The first involved irradiating a carbon monoxide purged toluene solution of **pachc** with a slight excess of **nbn** by a slide projector lamp<sup>18</sup> (mainly visible) for 24 hours. Samples were removed periodically with a syringe through a septum seal and monitored by IR spectroscopy. During the experiment the solution colour had changed from deep red to pale yellow and a brown precipitate had formed in the reaction flask. After filtration, the solvent was removed under vacuum and the product was purified by chromatography on silica gel (60 mesh) using a hexane:diethyl ether mixture (85:15 v/v) as eluent. The resulting product was identified as 2-phenyl-3a,4,5,6,7,7a-hexahydro-4,7-methanoinden-1-one (**36**) by IR,  $^1\text{H}$  and  $^{13}\text{C}$  NMR spectroscopy (c.f. Table 3.3). No evidence was obtained for the formation of ( $\mu_2$ - $\text{C}_6\text{H}_5\text{C}_2\text{H}$ ) $\text{Co}_2(\text{CO})_5(\text{nbn})$  from the analysis of IR spectral bands taken throughout the experiment.

The second method of photolytic synthesis involved exposing a carbon monoxide purged toluene solution of **pachc** containing a slight excess of **nbn** to natural light for 48 hours. The solution became colourless and a light brown precipitate had formed in the reaction vessel. Workup was carried out as before by filtration to remove the precipitate and the removal of the solvent under vacuum. The product was purified on silica gel (60 mesh) using a hexane:diethyl ether mixture (85:15 v/v) as eluent. IR,  $^1\text{H}$  and  $^{13}\text{C}$  NMR spectroscopic techniques again revealed

the formation of the cyclopentenone (**36**). While no evidence was obtained for the formation of  $(\mu_2\text{-C}_6\text{H}_5\text{C}_2\text{H})\text{Co}_2(\text{CO})_5(\text{nbn})$  from the analysis of IR spectral bands taken throughout the experiment, these experiments do show that irradiation can be used as an alternative energy source for the Pauson - Khand reaction. Similar experiments conducted under an atmosphere of argon also produced the corresponding cyclopentenone as the major product, however, the reaction times required were longer.

#### 3.4.2 Reaction of *pachc* with cyclohexene

A solution of **pachc** was prepared in toluene containing a 4 - fold excess of cyclohexene. The solution was subjected to three freeze - pump - thaw cycles using a dynamic vacuum and then placed under an atmosphere of CO. The flask was then irradiated with natural light for 1 week. Samples were taken daily and monitored by IR spectroscopy. The spectra showed bands consistent with the presence of  $\text{Co}_2(\text{CO})_8$  and a further band at  $1701\text{ cm}^{-1}$  consistent with the presence of a ketonic carbonyl group. An orange/brown precipitate had also formed. Separation by flash chromatography on neutral alumina (hexane/diethyl ether :85/15 v/v) gave rise to three fractions. Fraction one (red) was identified as **pachc**. Fraction two (orange) was identified as  $\text{Co}_2(\text{CO})_8$  while fraction three (yellow) was identified as cyclopentenone.

#### 3.4.3 Reaction of *achc* with norbornadiene

A solution of **achc** containing a 1.5 excess of **nbd** was photolysed under an atmosphere of CO by a slide projector lamp (mainly visible) for 24 hours in toluene solution ( $\lambda_{\text{exc}} > 500\text{ nm}$ ). Bands were observed after 16 hours at 2075, 2069, 2042, 2039, 2033, 2010, 1858 and  $1834\text{ cm}^{-1}$  indicating a mixture of products had formed.

Small scale flash chromatography of this sample under an atmosphere of argon using hexane:diethyl ether (85:15v/v) eluted **achc** as a red solution and  $\text{Co}_4(\text{CO})_{12}$  as an orange solution. A third fraction decomposed on the column. A second sample taken after 24 hours showed bands at 2075, 2014, 2010 and  $1834\text{ cm}^{-1}$ . These product bands have been observed earlier while irradiating **achc** and **nbd** with  $\lambda_{\text{exc}} > 340\text{ nm}$  (*c.f.* section 3.2.1). The band at  $1834\text{ cm}^{-1}$  indicates the presence of a bridging carbonyl group. The identity of this compound is yet unresolved. No further bands for  $\text{Co}_4(\text{CO})_{12}$  were observed probably due to its insolubility in cyclohexane solvent. Removal of solvent after photolysis followed by flash chromatography eluted a sweet smelling yellow product which was identified by its IR  $\nu_{\text{CO}}$  band at  $1700\text{ cm}^{-1}$  as the corresponding norbornadiene cyclopentenone. While the  $^1\text{H}$  NMR spectrum of this compound was complex, two double doublets were observed at 7.31 - 7.53 ppm respectively with matching J - values which are consistent with two alkene protons. Other signals observed at 6.3(d, 2H) provide further evidence for the cyclopentenone.

A solution of **achc** and **nbd** was prepared in toluene as previously under one atmosphere of CO and irradiated with natural light. The reaction was monitored by IR spectroscopy. After 24 hours two bands of equal intensity were observed at 1705 and  $1701\text{ cm}^{-1}$ . These have been identified as the formation of a diketone resulting from two cyclisations of the dicobalthexacarbonyl complex with **nbd**. The initial reaction of **achc** with **nbd** retains a norbornene system which can undergo a second cyclisation producing the diketone, a reaction which has been previously reported.<sup>2b</sup>

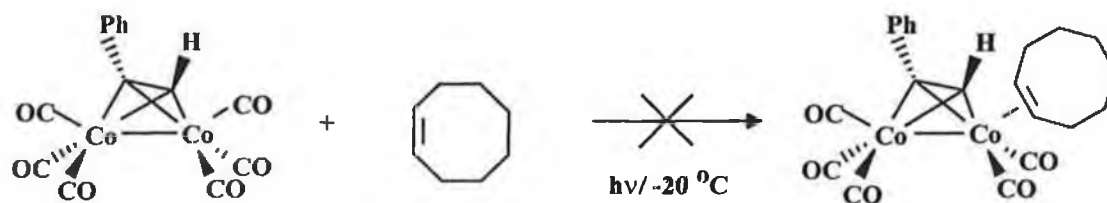
#### 3.4.4 Reaction of **dpachc** with *cis*-cyclooctene (**cco**) and norbornene

Two solutions of **dpachc** were prepared in toluene containing a four - fold excess of the ligands **cco** and **nbn** respectively. The solutions were irradiated with natural light. After 1 week no detectable reaction was observed with **cco**. However, with **nbn** a precipitate had formed in the reaction flask indicating the formation of

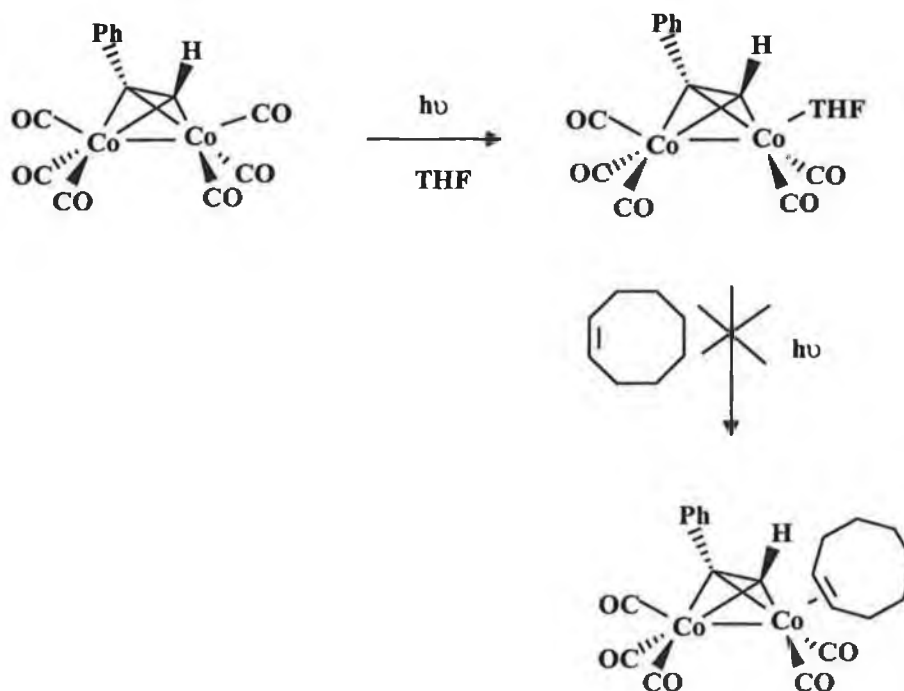
$\text{Co}_2(\text{CO})_8$ . An IR band was observed at  $1705\text{ cm}^{-1}$  indicating the presence of a ketonic carbonyl. Heating the solution to  $40^\circ\text{C}$  gave rise to an increase in yield of the ketonic product. Full characterisation of the corresponding cyclopentenone was not carried out. In the photochemical induced experiments the cyclopentenone compounds were formed *in situ* and thus were identified by the  $\nu_{\text{CO}}$  band without isolating the complexes. As a result of overlap of several of the bands of the complexes not all bands of each complex can be expected to be observed individually and hence peak picking is difficult.

### 3.5 Preparation of $(\mu_2\text{-alkyne})\text{Co}_2(\text{CO})_5(\text{alkene})$ Complexes at Low Temperature

A common method used for the synthesis of olefin substituted metal carbonyls is that of Grevels and Skibbe<sup>9</sup> where an alkane solution of the metal carbonyl and the olefin are photolysed at low temperature. Subsequent exchange of one the carbonyls for alkene follows producing the desired metal pentacarbonyl alkene species. In this work, the attempted synthesis of  $(\mu_2\text{-C}_6\text{H}_5\text{C}_2\text{H})\text{Co}_2(\text{CO})_5(\text{cco})$  was carried out according to Reaction 3.5 by purging a solution of **pachc** and **cco** with argon for 30 minutes. The solution was then irradiated using an apparatus in which the photolysis solution surrounds a medium pressure Xe arc lamp (Applied Photophysics, 400 Watt,  $\lambda_{\text{exc}} > 300\text{ nm}$ ) and is cooled at  $-20^\circ\text{C}$  by circulating ethanol from a low temperature circulator (*c.f.* Figure 4.1, Chapter 4). Samples were extracted periodically throughout the experiment and analysed by IR spectroscopy. No evidence was obtained for formation of the desired pentacarbonyl species  $(\mu_2\text{-C}_6\text{H}_5\text{C}_2\text{H})\text{Co}_2(\text{CO})_5(\text{cco})$  in these experiments.

**Reaction 3.5**

Another attempt at synthesising the  $(\mu_2\text{-C}_6\text{H}_5\text{C}_2\text{H})\text{Co}_2(\text{CO})_5(\text{cco})$  complex involved first preparing  $(\mu_2\text{-C}_6\text{H}_5\text{C}_2\text{H})\text{Co}_2(\text{CO})_5(\text{THF})$  and then reacting this complex with **cco** at low temperature (Scheme 3.2). However, no evidence was obtained in the IR for formation of the pentacarbonyl  $(\mu_2\text{-C}_6\text{H}_5\text{C}_2\text{H})\text{Co}_2(\text{CO})_5(\text{THF})$  species. Continuation of the experiment by addition of **cco** and subjecting the solution to further irradiation was carried out in the case that the THF substituted pentacarbonyl complex may not be observed in the IR spectrum. However, no pentacarbonyl species was formed in either case.

**Scheme 3.2**

Another attempted method of synthesis of the ( $\mu_2$ - $\text{C}_6\text{H}_5\text{C}_2\text{H}$ ) $\text{Co}_2(\text{CO})_5(\text{alkene})$  complex involved irradiating ( $\mu_2$ - $\text{C}_6\text{H}_5\text{C}_2\text{H}$ ) $\text{Co}_2(\text{CO})_6$  in pentane solution with hex-1-ene with  $\lambda_{\text{exc}} > 500$  nm in order to achieve the CO-loss product. The solution was prepared in a degassable cell and was placed under an atmosphere of argon. Subsequent heating of this solution to 40 °C resulted in a solution colour change from deep red to orange. Samples were extracted from the cell at periodic intervals and after which the solution was once again placed under an atmosphere of argon and the experiment was continued. However, no evidence was obtained for formation of the pentacarbonyl species ( $\mu_2$ - $\text{C}_6\text{H}_5\text{C}_2\text{H}$ ) $\text{Co}_2(\text{CO})_5(\text{hex-1-ene})$ . This reaction was repeated with the alkenes cyclohexene, hept-1-ene, **nbn** and **nbd**. Again no pentacarbonyl product resulted. In the case of **nbn** and cyclohexene workup of the product solutions by flash chromatography on neutral alumina using diethyl ether: hexane 15:85% v/v as eluent gave rise to the corresponding cyclopentenone.

### 3.6 Conclusions

Large scale synthesis of cyclopentenones derived from the reaction of the ( $\mu_2$ -alkyne) $\text{Co}_2(\text{CO})_6$  complex with the alkenes **nbn**, **nbd**, and cyclohexene was achieved by published thermal methods in order to enable identification of products derived from similar photochemical reactions. Broad band photolysis ( $\lambda_{\text{exc}} > 400$  nm) of ( $\mu_2$ -alkyne) $\text{Co}_2(\text{CO})_6$  complexes in the presence of various alkenes (hept-1-ene, **nbn**, **nbd**, cyclohexene) results in the *in situ* formation of the corresponding cyclopentenones instead of the anticipated ( $\mu_2$ -alkyne) $\text{Co}_2(\text{CO})_5(\text{alkene})$  complex.  $\text{Co}_2(\text{CO})_8$ , which is generated catalytically in the Pauson - Khand reaction, was identified as a by product of these reactions. Low energy photolysis of ( $\mu_2$ -alkyne) $\text{Co}_2(\text{CO})_6$  complexes in the presence of cyclohexene and **nbn**, with  $\lambda_{\text{exc}} > 500$  nm, results in no detectable photoreaction. In general, the yield of cyclopentenone is higher when high energy irradiation ( $\lambda_{\text{exc}} > 340$  nm) is used. Employing strong donor



ligands **tcne**, ethanol and **mecn** in broad band photolysis experiments failed to give rise to the appropriately substituted pentacarbonyldicobalt complex.

In an attempt to isolate  $(\mu_2\text{-alkyne})\text{Co}_2(\text{CO})_5(\text{alkene})$  type complexes by photochemical means toluene solutions of  $(\mu_2\text{-alkyne})\text{Co}_2(\text{CO})_6$  were irradiated with **nbn** under an atmosphere of CO by (a) natural light and (b) by slide projector lamp (mainly visible) giving rise to the corresponding **nbn** derived cyclopentenone. Under similar conditions cyclohexene and **nbd** derived cyclopentenones were prepared. Most importantly, cyclopentenone production was achieved without applying any heat to the photolytic system. In addition to the ketone products from these reactions, the ligand bridged complex  $\text{Co}_4(\text{CO})_{12}$  was isolated. The formation of  $\text{Co}_4(\text{CO})_{12}$  is not unexpected while irradiating with  $\lambda_{\text{exc}} > 320$  nm as the high energy involved would push for decomposition of  $\text{Co}_2(\text{CO})_8$ .

The first stage in the PK reaction involves CO-loss. The next step which involves alkene coordination to the cobalt carbonyl moiety cannot be achieved by irradiation at  $\lambda_{\text{exc}} > 500$  nm. It may be possible that the  $(\mu_2\text{-alkyne})\text{Co}_2(\text{CO})_5(\text{alkene})$  complex is formed but is highly unstable and rapidly converts back to the  $(\mu_2\text{-alkyne})\text{Co}_2(\text{CO})_6$  complex. Subsequently synthesis of  $(\mu_2\text{-alkyne})\text{Co}_2(\text{CO})_5(\text{alkene})$  complexes was attempted under low temperature photochemical conditions. However, various attempts to isolate  $(\mu_2\text{-alkyne})\text{Co}_2(\text{CO})_5(\text{cco})$  and  $(\mu_2\text{-alkyne})\text{Co}_2(\text{CO})_5(\text{nbn})$  complexes in a low temperature reaction vessel failed. In the latter case, instead of the formation of the anticipated alkene coordinated pentacarbonyl complexes, the **nbn** derived cyclopentenone complex was isolated. The  $(\mu_2\text{-alkyne})\text{Co}_2(\text{CO})_5(\text{THF})$  analogues also, could not be isolated under low temperature photochemical conditions.

It appears that the energy barrier on going from  $(\mu_2\text{-alkyne})\text{Co}_2(\text{CO})_6$  to  $(\mu_2\text{-alkyne})\text{Co}_2(\text{CO})_5(\text{alkene})$  is low so that instead of isolation of the pentacarbonyl intermediate, conversion into cyclopentenone occurs. The identification of

cyclopentenones formed from the reaction of  $(\mu_2\text{-alkyne})\text{Co}_2(\text{CO})_6$  complexes with alkenes was based on previous examples of norbornene cyclopentenones. We have shown however, that irradiation can be used as an alternative energy source for Khand reactions.

### 3.7 References

---

1. I.U. Khand, G.R. Knox, P. L. Pauson, *Chem. Commun.*, (1971) 36.
2. (a) I.U. Khand, G.R. Knox, P. L. Pauson, W.E. Watts, M.I. Foreman, *Chem. Commun.*, (1973) 977; (b) I.U. Khand, G.R. Knox, P. L. Pauson, W.E. Watts, *Chem. Commun.*, (1973) 975.
3. (a) O. Geis, H.G. Schmalz, *Angew. Chem. Int. Ed.*, **37** (1998) 911; (b) P.L. Pauson in 'Organometallics in Organic Synthesis 2', A. de Meijere, H. tom Dieck, Eds.; Springer -Verlag Berlin Hiedelberg (1987) 234; (c) P.L. Pauson, *Tetrahedron*, **41** (1985) 5855; (d) N.E. Schore in 'Organic Reactions', L.A. Paquette Ed. **Vol. 40** (1991); (e) P.L. Pauson, I.U. Khand, *Ann. N. Y. Acad. Sci.*, **295** (1977) 2; (f) F.L. Bowden, A.B.P. Lever, *Organomet. Chem. Rev.*, **3** (1968) 227; (g) M.E. Krafft, I.L. Scott, R.H. Romero, S. Feilbelmann, C.E. Van Pelt, *J. Am. Chem. Soc.*, **115** (1993) 7199.
4. M. Perasamy, M. Rama Reddy, A. Deva Sagayaraj, *Tetrahedron*, **50** (1994) 6955.
5. T. Livinghouse, L. Pagenkopft, *J. Amer. Chem. Soc.*, **118** (1996) 2285.
6. I.U. Khand, P.L. Pauson, *J. Chem. Res. (M)*, (1977) 168.
7. I.U. Khand, P.L. Pauson, *J. Chem. Res. (M)*, (1977) 4418.
8. I.U. Khand, G.R. Knox, P.L. Pauson, W.E. Watts. M.I. Foreman *J. Chem. Soc. Perkin Trans.* (1973) 977.
9. F. W. Grevels, V. Skibbe, *J. Chem. Soc. Chem. Commun.*, (1984) 681.
10. N.E. Schore in 'Organic Reactions', L.A. Paquette Ed., **40** (1991).
11. T. Sugihara, M. Yamada, H. Ban, M. Yamaguchi, C. Kaneko, *Angew. Chem. Int. Ed. Engl.* **36** (1997) 2801.
12. L. Ungváry, I. Marko, *Inorg. Chim. Acta*, **4** (1970) 324.
13. T.M. Bockman, J.F. Garst, F. Ungváry, *J. Organomet. Chem.*, **586** (1999) 41.
14. R.F. Heck, *J. Am. Chem. Soc.*, **85** (1963) 3381.

- 
15. J. Somlyai-Haász, F. Haász, V. Galamb, A. Benedetti, C. Zucchi, G. Pályi, *J. Organomet. Chem.*, 419 (1991) 205.
  16. I. Kovács, G. Szalontai, F. Ungváry, *J. Organomet. Chem.*, **24** (1996) 115.
  17. The cyclopentenones derived from **pachc** were synthesised on larger scale by thermal methods and characterised by IR,  $^1\text{H}$  and  $^{13}\text{C}$  NMR spectroscopy.
  18. Lamp model = Kodex Carousel S-Av2020.

## **CHAPTER 4**

### **Experimental Procedures**

## 4. Experimental

### 4.1 Reagents

$\text{Co}_2(\text{CO})_8$  (Fluka Chemicals), the alkynes phenylacetylene, diphenylacetylene (Aldrich Chemical Co.) and acetylene gas (Air Products), triphenylphosphine (Aldrich Chemical Co.), pyridine, cyclohexane, hept-1-ene, and pentane (Spectroscopy Grade - Aldrich Chemical Co.) were used as received. All manipulations involving  $\text{Co}_2(\text{CO})_8$ , were conducted under an argon atmosphere.

### 4.2 Equipment

Infrared spectra were recorded on a Perkin Elmer 2000 FTIR spectrometer, solution cells were fitted with NaCl windows ( $d = 0.1\text{mm}$ ), and spectroscopic grade cyclohexane or pentane were used.  $^1\text{H}$  and  $^{13}\text{C}$  NMR spectra were obtained using a Brüker model Avance DPX spectrometer in appropriate deuterated solutions and were calibrated with respect to the residual proton resonances of the solvent or with an external TMS standard. UV/Vis spectra were recorded using a Hewlett Packard 8453A photodiode array spectrometer using 1 cm quartz cells. Photolysis was performed using an Applied Photophysics medium-pressure Xe arc lamp (275W) (Figure 4.1). Wavelength selection was achieved using Corning cut-off filters.

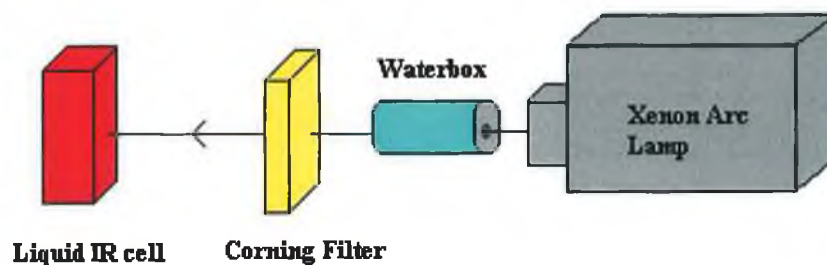


**Figure 4.1** *Apparatus for steady - state photolysis experiments*

The laser system used was a pulsed Nd:YAG laser capable of generating the second, third, or fourth harmonic at 532, 355 or 266 nm as required, with typical energies of 150, 30 and 45 mJ per pulse respectively. The pulse duration is approximately 10 ns. The excitation and monitoring beams are arranged in a cross-beam configuration.<sup>1</sup> The apparatus has been described in chapter 1.

### **4.3 *Sample preparation for Laser Flash Photolysis Experiments***

All samples were prepared for laser flash photolysis in a degassing bulb attached to a fluorescence cell and protected from light by aluminum foil. Samples were prepared in the dark by dissolution in the appropriate spectroscopy grade solvent. The concentration of solution was adjusted so that the absorbance at  $\lambda_{\text{exc}}$  (266, 355 or 532 nm) was between 0.8 and 1.2 AU. The solutions were subjected to degassing by three cycles of a freeze-pump-thaw procedure to  $10^{-2}$  Torr. The solution at room temperature, was then subjected to a dynamic vacuum (liquid pumping), a process which has been shown to remove traces of water.<sup>2</sup>

The atmosphere of interest (Ar or CO) was placed over the sample solution. The concentration of gas permitted over the sample was controlled by a pressure gauge. On flashing the sample over a range of 650 - 270 nm the filters for  $\lambda > 340$ , 400 and 500 nm were employed to ensure selective irradiation of the sample. The UV/Vis spectral changes before and after degassing the sample were recorded as well as periodic monitoring of spectra throughout the photolysis experiment.

#### 4.4 *General Experimental Details for the Preparation of Acetylene Cobalt carbonyl complexes*

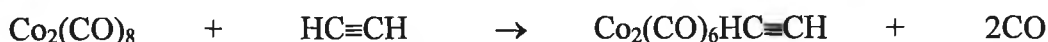
The preparation of acetylene cobalt carbonyl complexes was carried out in conventional glassware consisting of three-necked flask equipped with gas inlet, reflux condenser and mercury check valve; distilled or spectroscopic grade pentane was used as a solvent under an argon atmosphere. Typically the starting components were allowed to react at room temperature with continuous magnetic stirring overnight in hydrocarbon solvent. The reaction solutions were filtered and their volume reduced under low pressure; the products were isolated by flash chromatography (Kieselgel B.F. Merck) with mixtures of light petroleum (40 - 60°) and diethyl ether as eluents (1:1). The products were crystallised at 4 °C. In the case of acetylene, products exist as an oil at room temperature. All products were stored at low temperatures under an Ar atmosphere in sealed containers.

#### 4.5 *Synthesis of ( $\mu_2$ -alkyne)hexacarbonyldicobalt Complexes. Reaction of $\text{Co}_2(\text{CO})_8$ with alkynes*

The ( $\mu_2$ -alkyne) $\text{Co}_2(\text{CO})_6$  complexes were prepared by the standard method which involves the slow addition of the alkyne to a degassed solution of  $\text{Co}_2(\text{CO})_8$  in pentane.<sup>3</sup> The solution was stirred overnight at room temperature following which the solvent was removed under reduced pressure yielding the dark red products. Details of synthesis for each alkyne are given below.

##### 4.5.1 *( $\mu_2$ -C<sub>2</sub>H<sub>2</sub>)Co<sub>2</sub>(CO)<sub>6</sub> - Acetylene hexacarbonyldicobalt(0)*<sup>4</sup>

( $\mu_2$ -C<sub>2</sub>H<sub>2</sub>)Co<sub>2</sub>(CO)<sub>6</sub> was prepared by treating  $\text{Co}_2(\text{CO})_8$  with acetylene gas according to





Bright orange crystals of cobalt carbonyl (1 g, 2.9 mmol) was weighed under Ar in a glove bag, added to a three-necked round bottom flask, protected from sunlight, and flushed with Ar. The flask was charged with acetylene gas displacing the Ar. A mercury bubbler allowed the emission of CO gas and maintained a positive pressure of acetylene. The reaction was stirred overnight. The orange crystalline starting material turned dark brown and liquefied with evolution of CO. The reaction flask was flushed periodically with acetylene to keep a positive atmosphere of acetylene in the gas phase. A deep red liquid obtained was first vacuum filtered, to remove an unidentifiable brown solid (5 %, m.p. > 300 °C, insoluble), and then transferred to a distilling flask and distilled under reduced pressure with temperatures not exceeding 30 °C yielding the dark red product.

Spectroscopic and analytical data for  $(\mu_2\text{-C}_2\text{H}_2)\text{Co}_2(\text{CO})_6$ :-  $^1\text{H}$  NMR ( $\text{CDCl}_3$ ,  $\delta/\text{ppm}$ ) 6.01(s, 2H,  $\equiv\text{C-H}$ );  $^{13}\text{C}$  NMR ( $\text{CDCl}_3$ ,  $\delta/\text{ppm}$ ) 71.4 (C-H), 198.99 (C-O); IR  $\nu_{\text{CO}}$  (pentane) 2099, 2059, 2035, 2029, 2018(sh)  $\text{cm}^{-1}$ ; UV/Vis (pentane) 308 (sh), 346, 447 nm; M.p. 13 -13.5 °C; yield 95 %; Anal. Calc. C 30.80 %, H 0.65 %, Found C 31.07 %, H 0.65 %.

#### 4.5.2 $(\mu_2\text{-C}_6\text{H}_5\text{C}_2\text{H})\text{Co}_2(\text{CO})_6$ - Phenylacetylene hexacarbonyldicobalt(0)<sup>4a,5</sup>

A three-necked flask was fitted with a gas inlet and a mercury bubbler to permit the escape of CO gas and Ar flushing gas. Dicobalt octacarbonyl (1.5 g, 44 mmol) was weighed as previously and added to pentane (12  $\text{cm}^3$ ). Phenylacetylene (490  $\text{cm}^3$ , 44 mmol) was added stepwise using a pressure equalising addition funnel. The flask was kept under a positive pressure of Ar and left to stir overnight. A deep red solution had formed. The solution was filtered through a glass sintered funnel filled with silica gel (60 mesh) wetted with pentane. 3 x 30  $\text{cm}^3$  aliquots of pentane were used. The first fraction eluted  $(\mu_2\text{-C}_6\text{H}_5\text{C}_2\text{H})\text{Co}_2(\text{CO})_6$  which was identified by IR. The second fraction eluted unreacted phenylacetylene.

Spectroscopic and analytical data for  $(\mu_2-(C_6H_5)C_2H)Co_2(CO)_6$ :-  $^1H$  NMR ( $CD_3CN$ ,  $\delta/ppm$ ) 6.3 (1H, s, =C-H), 7.19 (1H, s, Ar CH), 7.25 (2H, d, Ar CH,  $J = 6.2$  Hz), 7.45 (2H, d, Ar CH,  $J = 6.2$  Hz);  $^{13}C$  NMR ( $CDCl_3$ ,  $\delta/ppm$ ) 132(s), 128.7(s), 128.6(s), 123.6(s) ( $C_6H_5$ ), 89.7(s,  $C\equiv C$ ); IR  $\nu_{CO}$  (pentane) 2094, 2056, 2032, 2029, 2018(sh)  $cm^{-1}$ ; UV/Vis (pentane) 352, 422, 536 nm; M.p. 52-53 °C, Anal. Calc. C 43.33 %, H 1.56 %, Found C 43.06 %, H 1.65 %.

#### 4.5.3 $(\mu_2-(C_6H_5C)_2)Co_2(CO)_6$ - Diphenylacetylene hexacarbonyldicobalt(0)

A three-necked flask was fitted with an Ar inlet and a mercury bubbler to permit the escape of CO gas and Ar flushing gas. Dicobalt octacarbonyl (1.5 g, 44 mmol) was weighed out as previously and added to pentane (12  $cm^3$ ). A diphenylacetylene (7.8 g, 44 mmol) solution (pentane 3  $cm^3$ ) was added stepwise using a pressure equalising addition funnel. The flask was kept under a positive pressure of Ar and left to stir overnight. A deep red solution had formed. The solution was chromatographed on silica gel (60 mesh). The first fraction eluted with pentane gave  $(\mu_2-(C_6H_5C)_2)Co_2(CO)_6$  which was identified by IR spectroscopy. The second fraction eluted unreacted diphenylacetylene. Typical yields were in the range 90 - 95 %.

Spectroscopic and analytical data for  $(\mu_2-(C_6H_5C)_2)Co_2(CO)_6$ :-  $^1H$  NMR ( $CD_3Cl_3$ ,  $\delta/ppm$ ) 7.53 (2H, d, Ar C-H,  $J = 7.2$  Hz), 7.29 (2H, m, Ar C-H,  $J = 7.2$  Hz), 7.19 (1H, s, Ar C-H);  $^{13}C$  NMR ( $CDCl_3$ ) 138 (q-C), 129.2(s), 128.9(s), 127.8(s), ( $C_6H_5$ ), 76.5 (s,  $C\equiv C$ ), 76.1 (s,  $\equiv C-H$ ) ppm; IR  $\nu_{CO}$  (pentane) 2091, 2055, 2029, 2026 and 2021(sh)  $cm^{-1}$ ; UV/Vis (pentane) 330, 360, 455 and 540 nm; Calc. C 51.75 %, H 2.17 %, Found C 51.64 %, H 2.46 %.

#### 4.6 *Synthesis of the Ligand Substituted Pentacarbonyl Complexes. Reaction of ( $\mu_2$ -alkyne) $\text{Co}_2(\text{CO})_6$ with ligands triphenylphosphine and pyridine*

##### 4.6.1 *Thermal Synthesis of ( $\mu_2$ - $\text{RC}_2\text{R}'$ ) $\text{Co}_2(\text{CO})_5(\text{PPh}_3)$ - Alkyne dicobalt pentacarbonyltriphenylphosphine complexes*

The thermal synthesis of ( $\mu_2$ - $\text{RC}_2\text{R}'$ ) $\text{Co}_2(\text{CO})_5(\text{PPh}_3)$  complexes was carried out according to the method of Manning.<sup>6</sup> Typically ( $\mu_2$ - $\text{C}_2\text{H}_2$ ) $\text{Co}_2(\text{CO})_6$  (15 mg,  $4.9 \times 10^{-5}$  moles) was added to equimolar  $\text{PPh}_3$  (128.5 mg,  $4.9 \times 10^{-5}$  moles) in benzene (5  $\text{cm}^3$ ), previously dried over  $\text{CaCl}_2$ , and distilled under Ar. The mixture was heated to reflux temperature (75 °C) under Ar after which time the solvent was removed under reduced pressure. The residual dark red oil was dissolved in a minimum volume of DCM and chromatographed on silica gel (60 mesh). The unreacted starting material ( $\mu_2$ - $\text{C}_2\text{H}_2$ ) $\text{Co}_2(\text{CO})_6$  was removed by elution with petroleum ether. The product was eluted by diethyl ether-petroleum ether (1:1 v/v). Evaporation of the solvent in an Ar stream yielded the crystalline product. Identification was determined by IR and UV/vis spectroscopy. Typical yield was in the range 90 - 95%.

Spectroscopic and analytical data for ( $\mu_2$ - $\text{C}_2\text{H}_2$ ) $\text{Co}_2(\text{CO})_5(\text{PPh}_3)$ :- IR  $\nu_{\text{CO}}$  (pentane): 2069, 2017, 2009, 1997, 1975 (vs)  $\text{cm}^{-1}$ ; UV/Vis (pentane):  $\lambda_{\text{max}}$  323 and 376 nm; M.p. 123 °C;

Spectroscopic and analytical data for ( $\mu_2$ - $\text{C}_6\text{H}_5\text{C}_2\text{H}$ ) $\text{Co}_2(\text{CO})_5(\text{PPh}_3)$ :- IR  $\nu_{\text{CO}}$  (pentane): 2065, 2016, 2006, 1997, 1972(vs)  $\text{cm}^{-1}$ ; UV/Vis (pentane):  $\lambda_{\text{max}}$  328 and 346 and 382 nm; M.p. 104 °C;

Spectroscopic and analytical data for ( $\mu_2$ - $\text{C}_2(\text{C}_6\text{H}_5)_2$ ) $\text{Co}_2(\text{CO})_5(\text{PPh}_3)$ :- IR  $\nu_{\text{CO}}$  (pentane): 2062, 2016, 2004, 1995, 1970(vs)  $\text{cm}^{-1}$ ; UV/Vis (pentane):  $\lambda_{\text{max}}$  352 and 392, 482 and 526 nm; M.p. 230 °C dec.

#### 4.6.2 Thermal Synthesis of $(\mu_2\text{-RC}_2\text{H})\text{Co}_2(\text{CO})_5(\text{C}_6\text{H}_5\text{N})$ - Alkyne dicobalt pentacarbonyl pyridine complexes

Synthesis of the  $(\mu_2\text{-RC}_2\text{R}')\text{Co}_2(\text{CO})_5(\text{C}_6\text{H}_5\text{N})$  complexes was carried out in the same manner as above using an equimolar amount of pyridine. Typically  $(\mu_2\text{-C}_2\text{H}_2)\text{Co}_2(\text{CO})_6$  (20 mg,  $6.5 \times 10^{-5}$  moles) was added to  $\text{C}_5\text{H}_5\text{N}$  (67  $\mu\text{L}$ ,  $6.5 \times 10^{-5}$  moles) in benzene (5  $\text{cm}^3$ ), previously dried over  $\text{CaCl}_2$ , and distilled under Ar. The mixture was heated to reflux temperature under Ar after which time the solvent was removed under reduced pressure. The residual dark red oil was dissolved in a minimum volume of DCM and chromatographed on silica gel (60 mesh). The unreacted starting material  $(\mu_2\text{-C}_2\text{H}_2)\text{Co}_2(\text{CO})_6$  was removed by elution with petroleum ether. The product was eluted by diethyl ether-petroleum ether (1:1 v/v). Evaporation of the solvent in an Ar stream yielded the crystalline product. Identification was determined by IR and UV/Vis spectroscopy. In general longer reactions times were necessary for pyridine substitution to occur. Typical yields were in the range 85 - 90 %.

Spectroscopic data for  $(\mu_2\text{-C}_2\text{H}_2)\text{Co}_2(\text{CO})_5(\text{C}_6\text{H}_5\text{N})$ :- IR (pentane):  $\nu_{\text{CO}}$  2064, 2014, 2002, 1996, 1968  $\text{cm}^{-1}$ ; UV/Vis (pentane) :  $\lambda_{\text{max}}$  324, 342 and 416 nm;

Spectroscopic data for  $(\mu_2\text{-(C}_6\text{H}_5\text{)C}_2\text{H})\text{Co}_2(\text{CO})_5(\text{C}_6\text{H}_5\text{N})$ :- IR (pentane):  $\nu_{\text{CO}}$  2069, 2018, 2005, 1994, 1966  $\text{cm}^{-1}$ ; UV/Vis (pentane):  $\lambda_{\text{max}}$  322, 352 and 396 nm;

Spectroscopic data for  $(\mu_2\text{-(C}_6\text{H}_5)_2\text{C}_2)\text{Co}_2(\text{CO})_5(\text{C}_6\text{H}_5\text{N})$ :- IR (pentane):  $\nu_{\text{CO}}$  2060, 2016, 2003, 1990, 1964,  $\text{cm}^{-1}$ ; UV/Vis (pentane) :  $\lambda_{\text{max}}$  354, 423 and 506 nm

#### 4.7 *Synthesis of the $(\mu_2\text{-R}_2\text{C}_2\text{H})\text{Co}_2(\text{CO})_4(\text{L})_2$ Tetracarbonyl Complexes ( $\text{L} = \text{C}_5\text{H}_5\text{N}$ or $\text{PPh}_3$ ).*

##### 4.7.1 *Synthesis of $(\mu_2\text{-R}_2\text{C}_2\text{H})\text{Co}_2(\text{CO})_4(\text{C}_5\text{H}_5\text{N})_2$ complexes*

The thermal synthesis of  $(\mu_2\text{-R}_2\text{C}_2\text{H})\text{Co}_2(\text{CO})_4(\text{C}_5\text{H}_5\text{N})_2$  was carried out according to a method reported by Manning for the preparation of similar complexes.<sup>6</sup> Typically  $(\mu_2\text{-C}_2\text{H}_2)\text{Co}_2(\text{CO})_5(\text{C}_5\text{H}_5\text{N})$  (20 mg,  $17.8 \times 10^{-3}$  moles) was added to equimolar  $\text{C}_5\text{H}_5\text{N}$  (45.5  $\mu\text{L}$ ,  $17.8 \times 10^{-3}$  moles) in dry benzene (10  $\text{cm}^3$ ). The mixture was allowed to reflux under Ar for 4 hours at 80 °C after which time the solvent was removed under reduced pressure. The residual dark red oil was dissolved in a minimum volume of DCM and chromatographed on silica gel (60 mesh). Evaporation of the solvent in an Ar stream yielded the crystalline product. Identification was determined by IR and UV/Vis spectroscopy. Typical yield was in the range 90 - 95 %.

Spectroscopic data for  $(\mu_2\text{-(C}_2\text{H}_2))\text{Co}_2(\text{CO})_4(\text{C}_6\text{H}_5\text{N})_2$ :- IR  $\nu_{\text{CO}}$  ( $\text{C}_5\text{H}_{12}$ ): 2021, 2004, 1970, 1941  $\text{cm}^{-1}$ ;

Spectroscopic for  $(\mu_2\text{-(C}_6\text{H}_5)\text{C}_2\text{H})\text{Co}_2(\text{CO})_4(\text{C}_6\text{H}_5\text{N})_2$ :- IR  $\nu_{\text{CO}}$  ( $\text{C}_5\text{H}_{12}$ ): 2018, 2002, 1967, 1942  $\text{cm}^{-1}$ ;

Spectroscopic data for  $(\mu_2\text{-(C}_6\text{H}_5)_2\text{C}_2)\text{Co}_2(\text{CO})_4(\text{C}_6\text{H}_5\text{N})_2$ :- IR  $\nu_{\text{CO}}$  ( $\text{C}_5\text{H}_{12}$ ): 2016, 1966, 1962, 1942  $\text{cm}^{-1}$ .

#### 4.7.2 *Synthesis of $(\mu_2\text{-R}_2\text{C}_2\text{H})\text{Co}_2(\text{CO})_4(\text{PPh}_3)_2$ complexes*

The thermal synthesis of  $(\mu_2\text{-R}_2\text{C}_2\text{H})\text{Co}_2(\text{CO})_4(\text{PPh}_3)_2$  was carried out according to the method of Manning.<sup>6</sup> Typically  $(\mu_2\text{-C}_2\text{H}_2)\text{Co}_2(\text{CO})_5(\text{PPh}_3)$  (20 mg,  $17.8 \times 10^{-3}$  moles) was added to equimolar  $\text{PPh}_3$  (4.66 mg,  $17.8 \times 10^{-3}$  moles) in dry benzene (10  $\text{cm}^3$ ), and distilled under Ar. The mixture was allowed to reflux under Ar for 4 hours at 80 °C after which time the solvent was removed under reduced pressure. The residual dark red oil was dissolved in a minimum volume of DCM and chromatographed on silica gel (60 mesh). Evaporation of the solvent in an Ar stream yielded the crystalline product. Identification was determined by IR spectroscopy. Typical yield was in the range 90 - 95 %.

Spectroscopic data for  $(\mu_2\text{-(C}_2\text{H}_2)\text{Co}_2(\text{CO})_4(\text{PPh}_3)_2$ :- IR  $\nu_{\text{CO}}$  ( $\text{C}_5\text{H}_{12}$ ): 2027, 1982, 1965, 1950  $\text{cm}^{-1}$ ;

Spectroscopic and analytical data for  $(\mu_2\text{-(C}_6\text{H}_5)\text{C}_2\text{H})\text{Co}_2(\text{CO})_4(\text{PPh}_3)_2$ :- IR  $\nu_{\text{CO}}$  ( $\text{C}_5\text{H}_{12}$ ): 2021, 2004, 1972, 1942  $\text{cm}^{-1}$ ; M.p. 200 °C;

Spectroscopic and analytical data for  $(\mu_2\text{-(C}_6\text{H}_5\text{C})_2)\text{Co}_2(\text{CO})_4(\text{PPh}_3)_2$ :- IR  $\nu_{\text{CO}}$  ( $\text{C}_5\text{H}_{12}$ ): 2022, 1978, 1971.3, 1944  $\text{cm}^{-1}$ ; M.p. 200 °C dec.;

#### 4.8 *Steady-state photochemical experiments. Photochemical synthesis of $(\mu_2\text{-RC}_2\text{H})\text{Co}_2(\text{CO})_5(\text{L})$ ( $\text{L} = \text{C}_5\text{H}_5\text{N}$ or $\text{PPh}_3$ )*

##### 4.8.1 *Photochemical synthesis of $(\mu_2\text{-RC}_2\text{H})\text{Co}_2(\text{CO})_5(\text{C}_5\text{H}_5\text{N})$ complexes*

The relevant alkyne was dissolved in either cyclohexane or pentane with a 4-fold excess of ( $\text{C}_5\text{H}_5\text{N}$ ). The solution was flushed with Ar gas for 20 minutes before being transferred to NaCl IR solution cells for irradiation in front of a Xenon arc lamp. Corning filters were used to select light at  $\lambda > 340$ , 400 and 500 nm. Typically

solutions were irradiated for 0.5, 1, 2, 5, 10, 15, 20 and 30 minutes. In most cases spectra were recorded in absorbance mode. The spectrum of the solvent/pyridine mixture was recorded before addition of the hexacarbonyl complex. This spectrum was then subtracted from all sample spectra in order to eliminate any solvent peaks appearing in the region of interest. Subtraction of a spectrum of prephotolysed sample from the photolysed spectra gave the difference spectra with increasing bands showing the appearance of newly formed species while the negative spectra indicate the depletion of parent material. IR  $\nu_{\text{CO}}$  data for these compounds are provided in Chapter 2.

#### 4.8.2 Photochemical synthesis of $(\mu_2\text{-RC}_2\text{H})\text{Co}_2(\text{CO})_5(\text{PPh}_3)$ complexes

The relevant alkyne was dissolved in either cyclohexane or pentane with a 4-fold excess of  $(\text{PPh}_3)$ . The solution was flushed with Ar gas for 20 minutes before being transferred to NaCl IR solution cells for irradiation in front of a Xenon arc lamp. Corning filters were used to select light at  $\lambda > 340$ , 400 and 500 nm. Typically solutions were irradiated for 0.5, 1, 2, 5, 10, 15, 20 and 30 minutes. In most cases spectra were recorded in absorbance mode. The spectrum of the solvent/pyridine mixture was recorded before addition of the hexacarbonyl complex. This spectrum was then subtracted from all sample spectra in order to eliminate any solvent peaks appearing in the region of interest. Subtraction of a spectrum of prephotolysed sample from the photolysed spectra gave the difference spectra with increasing bands showing the appearance of newly formed species while the negative spectra indicate the depletion of parent material. IR  $\nu_{\text{CO}}$  data for these compounds are provided in Chapter 2.

#### 4.9 Preparation of $(\mu_2\text{-C}_2\text{H}_2)\text{Co}_2(\text{CO})_6$ for $^1\text{H}$ NMR monitored Steady-state Photolysis

A sample of **achc** was dissolved in  $\text{d}_5$ -pyridine, filtered through a plug of cotton wool and placed in a degassable NMR tube. The solution was subjected to three cycles of freeze-pump-thawing using an acetone : liquid  $\text{N}_2$  mixture to bring the temperature down to  $-35^\circ\text{C}$  (the temperature of liquid  $\text{N}_2$  is too low and would crack the degassable tube). 1 atm of Ar was placed over the sample. A  $^1\text{H}$  NMR spectrum was recorded before photolysis. The sample was then photolysed in front of the Xe arc lamp with  $\lambda > 340\text{ nm}$  for 5 minutes, an NMR recorded and then photolysed for a further 5 minutes and another NMR recorded.

Spectroscopic data for  $(\mu_2\text{-C}_2\text{H}_2)\text{Co}_2(\text{CO})_6$  :-  $^1\text{H}$  NMR (d-pyridine,  $\delta/\text{ppm}$ )

t = 0 mins : 5.08 (s, 1H,  $\equiv\text{CH}$ ), 7.13 (s, 2H, ortho H), 7.48 (s, 1H), 8.71 (s, 2H);

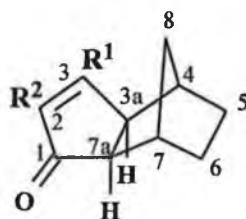
t = 5 mins : 5.39 (s, 1H,  $\equiv\text{CH}$  broad), 7.11 (s, 2H), 7.46 (s, 1H), 8.70 (s, 2H);

t = 10 mins: 5.6(s, 1H,  $\equiv\text{CH}$ , v. broad), 7.11 (s, 2H), 7.45, (s, 1H), 8.71 (s, 2H);

t = 24 hrs : no  $\equiv\text{CH}$ , 7.07 (s, 2H), 7.38 (s, 1H), 8.71 (s, 2H);



#### 4.10 Cyclopentenone Synthesis



##### *4,7-methanohexahydroindanone skeleton of ketones*

##### 4.10.1 Thermal synthesis of 2-Phenyl-3a,4,5,6,7,7a-Hexahydro-4,7-methanoinden-1-one (36)

###### **Method A**

Norbornene (178 mg, 1.90 mmol) was added to a three-necked RBF containing ( $\mu_2$ -C<sub>6</sub>H<sub>5</sub>C<sub>2</sub>H)Co<sub>2</sub>(CO)<sub>6</sub> (0.5 g, 1.3 mmol) in spectroscopic grade *n*-hexane (30 cm<sup>3</sup>). The mixture was heated to reflux temperature for 48 hours at 100 °C under Ar after which time the solution colour had changed from deep red to orange. Solvent was removed under vacuum and the product was columned on silica gel (60 mesh). Hexane:diethyl ether (85:15 v/v) eluted ( $\mu_2$ -C<sub>6</sub>H<sub>5</sub>C<sub>2</sub>H)Co<sub>2</sub>(CO)<sub>6</sub> (15 %) as a red band, followed by Co<sub>4</sub>(CO)<sub>12</sub> (30 %) as a blue band and finally cyclopentenone (50 %) as a yellow band. Spectroscopic and analytical data for 2-Phenyl-3a,4,5,6,7,7a-Hexahydro-4,7-methanoinden-1-one:- M.p. 95 °C, <sup>1</sup>H NMR (CDCl<sub>3</sub>,  $\delta$ /ppm): 1.01 (d, 1H, <sup>2</sup>J 10Hz), 1.14 (d, 1H, <sup>2</sup>J 10Hz), 1.35 (m, 2H), 1.66 (m, 1H), 1.76 (m, 1H), 2.28 (d, 1H), 2.38 (d, 1H), 2.50 (d, 1H), 2.71 (t, 1H), 7.32 (m, 2H), 7.38 (m, 1H), 7.65 (d, 1H), 7.72 (m, 2H); <sup>13</sup>C NMR (CDCl<sub>3</sub>,  $\delta$ /ppm) 208.1, 159.3, 145.1 (q), 103.5 (q), 127.7, 126.0, 53.9, 46.7, 38.4, 37.3, 30.3, 28.7, 28.1, 27.3; IR (CHCl<sub>3</sub>):  $\nu_{CO}$  : 1699, 1677 cm<sup>-1</sup>; UV/Vis (pentane) 290, 332 nm.

**Method B**

The second method of cyclopentenone synthesis was carried out according to Sugihara *et al.*<sup>7</sup> Typically a solution of  $(\mu_2\text{-C}_6\text{H}_5\text{C}_2\text{H})\text{Co}_2(\text{CO})_6$  (442 mg, 1.13 mmol) and norbornene (168 mg, 1.71 mmol) in 1,4-dioxane (3.0 cm<sup>3</sup>) and 2 M aqueous solution of  $\text{NH}_4\text{OH}$  (9.0 cm<sup>3</sup>) was stirred at 100 °C for 10 min. After cooling, diethyl ether was added, and the resulting suspension was filtered. The filtrate was washed successively with  $\text{H}_2\text{O}$ , 5 % aqueous  $\text{HCl}$ , and saturated aqueous  $\text{NaHCO}_3$ , dried over  $\text{MgSO}_4$ , and concentrated in vacuo. The product was columned on silica gel (60 mesh) with diethyl ether:hexane (15:85 v/v). Yield 40 %.

Spectroscopic and analytical data :- M.p. 95-96 °C,  $^1\text{H}$  NMR ( $\text{CDCl}_3$ ,  $\delta/\text{ppm}$ ): 1.01 (d, 1H,  $^2\text{J}$  10Hz), 1.14 (d, 1H,  $^2\text{J}$  10Hz), 1.35 (m, 2H), 1.66 (m, 1H), 1.76 (m, 1H), 2.28 (d, 1H), 2.38 (d, 1H), 2.50 (d, 1H), 2.71 (t, 1H), 7.32 (m, 2H), 7.38 (m, 1H), 7.65 (d, 1H), 7.72 (m, 2H);  $^{13}\text{C}$  NMR ( $\text{CDCl}_3$ ,  $\delta/\text{ppm}$ ) 208.1, 159.3, 145.1(q), 103.5(q), 127.7, 126.0, 53.9, 46.7, 38.4, 37.3, 30.3, 28.7, 28.1, 27.3; IR ( $\text{CHCl}_3$ ):  $\nu_{\text{CO}}$  : 1699, 1677 cm<sup>-1</sup>; UV/Vis (pentane) 290, 332 nm.

#### 4.10.2 Thermal synthesis of 2-Phenyl-3a,4,5,6,7,7a-hexahydroinden-1-one (37)

Cyclohexene (195 cm<sup>3</sup>, 1.9 mmol) was added to a three-necked RBF containing  $(\mu_2\text{-C}_6\text{H}_5\text{C}_2\text{H})\text{Co}_2(\text{CO})_6$  (0.5 g, 1.3 mmol) in spectroscopic grade *n*-hexane (30 cm<sup>3</sup>). The mixture was heated to reflux temperature for 48 hours under Ar after which time the solution colour had changed from deep red to red/brown. Solvent was removed under vacuum and the product was columned on silica gel (60 mesh). Hexane:diethyl ether (85:15 v/v) eluted  $(\mu_2\text{-C}_6\text{H}_5\text{C}_2\text{H})\text{Co}_2(\text{CO})_6$  (15 %) as a red band, followed by  $\text{Co}_4(\text{CO})_{12}$  (30 %) as a blue band and finally cyclopentenone (50 %) as a yellow band. Spectroscopic and analytical data for 2-phenyl-3a,4,5,6,7,7a-hexahydroindene-1-one :-  $^1\text{H}$  NMR ( $\text{CDCl}_3$ ,  $\delta/\text{ppm}$ ): 1.12 -1.66 (complex m, 8H,  $\text{CH}_2$ ), 1.82 (m, 1H), 2.60 (s, 1H), 2.81 (s, 1H), 7.36 (s, 1H), 7.48 (m, 2H), 7.75 (s, 1H), 7.79 (d, 2H);  $^{13}\text{C}$  NMR

(CDCl<sub>3</sub>,  $\delta$ /ppm) 27.3, 28.1, 30.3, 28.7, 46.7, 53.9, 126.0, 127.7, 130.5(q), 145.1(q), 159.3, 208.1; IR (CHCl<sub>3</sub>):  $\nu_{\text{CO}}$ : 1734, 1698 cm<sup>-1</sup>.

#### 4.10.3 Thermal synthesis of 3a,4,7,7a-Tetrahydro-4,7-methanoinden-1-one (38)

Norbornadiene (34.5  $\mu$ L, 320 mmol) was added to a three-necked RBF containing ( $\mu_2$ -C<sub>2</sub>H<sub>2</sub>)Co<sub>2</sub>(CO)<sub>6</sub> (105 mg, 320 mmol) in spectroscopic grade toluene (30 cm<sup>3</sup>). The mixture was stirred for 18 hours at 110 °C under Ar after which time the solution colour had changed from deep red to dark orange. The solution was filtered to remove a light brown precipitate. Solvent was removed under vacuum and the product was columned on silica gel (60 mesh). Hexane:diethyl ether (85:15 v/v) eluted ( $\mu_2$ -C<sub>2</sub>H<sub>2</sub>)Co<sub>2</sub>(CO)<sub>6</sub> as a red band and was followed by cyclopentenone as a yellow band. Spectroscopic and analytical data for 3a,4,7,7a-Tetrahydro-4,7-methanoinden-1-one:- <sup>1</sup>H NMR (CDCl<sub>3</sub>,  $\delta$ /ppm): 0.8 (m, 2H, CH), 2.26-2.39 (m, CH, 2H), 2.91 (s, br, 2H), 6.3 (d, 2H), 7.31 (dd, 1H, =CH), 7.53 (dd, 1H, =CH); <sup>13</sup>C NMR (CDCl<sub>3</sub>,  $\delta$ /ppm): 24.1, 31.6, 32.7, 37.0, 39.6, 49.5, 52.7, 137.3, 163.8, 210.5; IR (toluene):  $\nu_{\text{CO}}$ : 1701 cm<sup>-1</sup>.

#### 4.10.4 Thermal synthesis of 3a,4,5,6,7a-Hexahydro-4,7-methanoinden-1-one

Norbornene (0.68 g, mmol) was added to a solution of ( $\mu_2$ -C<sub>2</sub>H<sub>2</sub>)Co<sub>2</sub>(CO)<sub>6</sub> (150 mg, 0.48 mmol) in degassed toluene (20 cm<sup>3</sup>) in a three-necked RBF fitted with a gas inlet and a bubbler to permit the escape of CO gas. The mixture was stirred for 16 hours at 70 °C under Ar after which time the solution colour had changed from deep red to orange. Solvent was removed under vacuum and the product was columned on silica gel (60 mesh) using hexane:diethyl ether (85:15 v/v) as eluent. The cyclopentenone was eluted as a pale yellow band.

Spectroscopic and analytical data for 3a,4,5,6,7a-Hexahydro-4,7-methanoinden-1-one:- <sup>1</sup>H NMR (CDCl<sub>3</sub>,  $\delta$ /ppm): 1.0 (m, 2H, CH<sub>2</sub>), 1.23-1.73 (m, 4H, 2  $\times$  CH<sub>2</sub>), 2.16

(m, 2H, CH), 2.38 (broad s, 1H, CH), 2.69 (m, 1H, CH), 6.3 (d,  $2 \times 1\text{H}$ , =CH), 7.52 (dd, 1H); IR (toluene):  $\nu_{\text{CO}}$ :  $1701\text{ cm}^{-1}$ .

#### 4.11 Photochemical synthesis of Norbornene derived Cyclopentenones

##### 4.11.1. Reaction of phenylacetylene dicobalthexacarbonyl with norbornene

###### Method A

$(\mu_2\text{-C}_6\text{H}_5\text{C}_2\text{H})\text{Co}_2(\text{CO})_6$  (0.2 g, 0.43 mmol) and norbornene (81 mg, 0.86 mmol) were added to a two-necked RBF containing spectroscopic grade *n*-hexane ( $25\text{ cm}^3$ ). The solution was purged with carbon monoxide for 20 minutes. A blank sample was obtained by withdrawing  $2\text{ cm}^3$  of the solution through a syringe and placed in a covered sealed container and kept under a carbon monoxide atmosphere. The flask was then placed 15 cm in front of a Kodex Carousel S-Av2020 slide projector and left exposed to the beam for 24 hours after which time the solution colour had changed from deep red to pale yellow. Solvent was removed under vacuum and the product was columned on silica gel (60 mesh) using a hexane:diethyl ether mixture (85:15 v/v) as eluent. The resulting cyclopentenone (**36**) was eluted as a colourless fraction and was characterised by IR,  $^1\text{H}$  and  $^{13}\text{C}$  NMR spectroscopy.

###### Method B

$(\mu_2\text{-C}_6\text{H}_5\text{C}_2\text{H})\text{Co}_2(\text{CO})_6$  (0.2 g, 0.43 mmol) and norbornene (85 mg, 0.90 mmol) were added to a two-necked RBF containing spectroscopic grade toluene ( $25\text{ cm}^3$ ) giving a deep red solution. The solution was purged with carbon monoxide for 20 minutes. The flask was then placed on a window and exposed to natural light for 48 hours after which time the solution had become colourless and a light brown precipitate had formed. After filtration to remove the precipitate the solvent was removed under vacuum and the product was columned on silica gel (60 mesh) using a hexane:diethyl

ether mixture (85:15 v/v) as eluent. The resulting cyclopentenone (**36**) was eluted as a colourless fraction and was characterised by IR,  $^1\text{H}$  and  $^{13}\text{C}$  NMR spectroscopy.

#### 4.11.2 *Reaction of phenylacetylene dicobalthexacarbonyl with cyclohexene*

$(\mu_2\text{-C}_6\text{H}_5\text{C}_2\text{H})\text{Co}_2(\text{CO})_6$  (0.2 g, 0.43 mmol) and cyclohexene (212  $\text{cm}^3$ , 1.72 mmol) were added to a two-necked RBF containing spectroscopic grade cyclohexane (25  $\text{cm}^3$ ) giving a deep red solution. The solution was purged with carbon monoxide for 20 minutes. The flask was then placed on a window and exposed to natural light for 48 hours. The solution had changed to pale orange colour and a light brown precipitate had formed. After filtration to remove the precipitate the solvent was removed under vacuum and the product was columned on silica gel (60 mesh) using a hexane:diethyl ether mixture (85:15 v/v) as eluent. The resulting cyclopentenone (**37**) was eluted as a pale yellow fraction and was characterised by IR,  $^1\text{H}$  and  $^{13}\text{C}$  NMR spectroscopy.

#### 4.11.3 *Reaction of phenylacetylene dicobalthexacarbonyl with norbornadiene*

$(\mu_2\text{-C}_6\text{H}_5\text{C}_2\text{H})\text{Co}_2(\text{CO})_6$  (0.2 g, 0.51 mmol) and norbornadiene (205  $\mu\text{L}$ , 2.04 mmol) were added to a two-necked RBF containing spectroscopic grade cyclohexane (30  $\text{cm}^3$ ) giving a deep red solution. The solution was purged with carbon monoxide for 20 minutes. The flask was then placed on a window and exposed to natural light for 48 hours after which time the solution had become dark orange and a light brown precipitate had formed. After filtration to remove the precipitate the solvent was removed under vacuum and the product was columned on silica gel (60 mesh) using a hexane:diethyl ether mixture (85:15 v/v) as eluent. The resulting cyclopentenone (**38**) was eluted as a pale yellow fraction and was characterised by IR,  $^1\text{H}$  and  $^{13}\text{C}$  NMR spectroscopy.

#### 4.11.4 *Reaction of phenylacetylene dicobalthexacarbonyl with hept-1-ene*

$(\mu_2\text{-C}_6\text{H}_5\text{C}_2\text{H})\text{Co}_2(\text{CO})_6$  (0.2 g, 0.51 mmol) and hept-1-ene (194  $\mu\text{L}$ , 2.1 mmol) were added to a two-necked RBF containing spectroscopic grade cyclohexane (25  $\text{cm}^3$ ) giving a deep red solution. The solution was purged with carbon monoxide for 20 minutes. The flask was then placed on a window and exposed to natural light for 48 hours after which time the solution had become colourless and a light brown precipitate had formed.

#### 4.11.5 *Reaction of phenylacetylene dicobalthexacarbonyl with cis-cyclooctene (cco)*

$(\mu_2\text{-C}_6\text{H}_5\text{C}_2\text{H})\text{Co}_2(\text{CO})_6$  (0.25 g, 0.64 mmol) and cco (0.28  $\text{cm}^3$ , 2.16 mmol) were added to a two-necked RBF containing spectroscopic grade cyclohexane (25  $\text{cm}^3$ ) giving a deep red solution. The solution was purged with carbon monoxide for 20 minutes. The flask was then placed on a window and exposed to natural light for 96 hours. No visible reaction was detected.

#### 4.12 Photolytic synthesis of Olefin Substituted ( $\mu_2$ -alkyne)dicobaltcarbonyl Complexes

##### 4.12.1 Photolysis apparatus

The apparatus employed in the preparation of the substitution complexes is depicted in Figure 4.2. It consists of a double-walled pyrex glass vessel containing a medium pressure mercury arc lamp (400 Watt). Cooling is achieved by means of a low temperature circular containing ethanol (-20 °C) and thus maintains a low reaction temperature inside the photolysis apparatus. The solutions to be photolysed are placed in the external vessel and are left stirring throughout the photolysis. The immersion-well is very effective in capturing the lamp's output. Argon purging ensures deaeration and removes carbon monoxide liberated during the reaction. Samples can be extracted at any time throughout the experiment through a tap at the base of the vessel. The products were isolated by removing the solvent under reduced pressure and purified by flash chromatography. Identification was achieved using IR and NMR spectroscopy.

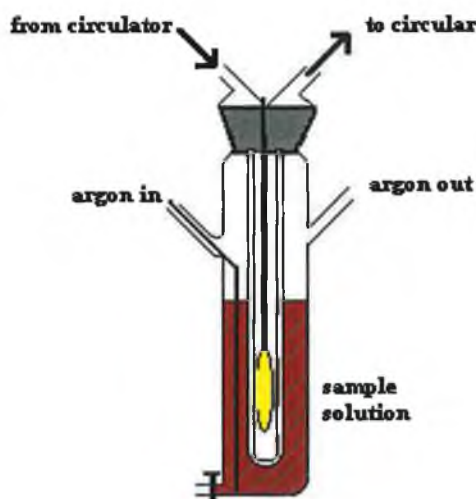


**Figure 4.2** Low temperature photolysis apparatus

#### 4.12.2 *Attempted synthesis of $(\mu_2\text{-C}_6\text{H}_5\text{C}_2\text{H})\text{Co}_2(\text{CO})_5(\text{cis-cyclooctene})$*

The attempted synthesis of  $(\mu_2\text{-C}_6\text{H}_5\text{C}_2\text{H})\text{Co}_2(\text{CO})_5(\text{cco})$  was carried out according to the method of Grevels and Skibbe<sup>8</sup> for the preparation of similar olefin substituted species.  $(\mu_2\text{-C}_6\text{H}_5\text{C}_2\text{H})\text{Co}_2(\text{CO})_6$  (385 mg, 0.99 mmol) was dissolved in pentane (250 cm<sup>3</sup>) and purged with argon for 30 minutes. *Cis*-cyclooctene (1.03 cm<sup>3</sup>, 7.94 mmol) was added and the solution was irradiated with a 400 watt medium pressure Xe arc lamp (Applied Photophysics,  $\lambda_{\text{exc}} > 300$  nm) at -20 °C for 5 hours under argon in the dark. Samples were extracted periodically and analysed by IR spectroscopy. No evidence was obtained for formation of the pentacarbonyl species  $(\mu_2\text{-C}_6\text{H}_5\text{C}_2\text{H})\text{Co}_2(\text{CO})_5(\text{cco})$ .

#### 4.12.3 *Attempted synthesis of $(\mu_2\text{-C}_6\text{H}_5\text{C}_2\text{H})\text{Co}_2(\text{CO})_5(\text{THF})$*

$(\mu_2\text{-C}_6\text{H}_5\text{C}_2\text{H})\text{Co}_2(\text{CO})_5(\text{THF})$  was synthesised according to the method of Grevels and Skibbe.<sup>8</sup>  $(\mu_2\text{-C}_6\text{H}_5\text{C}_2\text{H})\text{Co}_2(\text{CO})_6$  (200 mg, 0.51 mmol) was dissolved in THF (250 cm<sup>3</sup>) and purged with argon for 30 minutes prior to irradiation with a 400 watt medium pressure Xe arc lamp (Applied Photophysics). The solution was continuously stirred at -20 °C for 5 hours under argon in the dark. Samples were extracted periodically and analysed by IR spectroscopy. No evidence was obtained for formation of the pentacarbonyl species  $(\mu_2\text{-C}_6\text{H}_5\text{C}_2\text{H})\text{Co}_2(\text{CO})_5(\text{THF})$ .

### 4.13 *Purification Procedures*

#### 4.13.1 *Purification of Norbornadiene (nbd)*

Norbornadiene (nbd) is likely to polymerise when stored over long periods therefore purification before use is important. Nbd was placed in a round bottom flask containing activated alumina. The mixture was heated to reflux temperature. The



solvent was distilled using a short path distillation apparatus into a collecting flask and used immediately.  $^1\text{H}$  NMR was used to confirm purity.

Spectroscopic data for nbd :-  $^1\text{H}$  NMR ( $\text{CDCl}_3$ ,  $\delta/\text{ppm}$ ):- 2.1 (m, 1H, CH), 3.7 (t, 2H,  $\text{CH}_2$ ), 6.85 (t, 1H, =CH);  $^{13}\text{C}$  NMR ( $\text{CDCl}_3$ ,  $\delta/\text{ppm}$ ):- 51 (q-C), 76 ( $\text{CH}_2$ ), 144 (=CH).

#### 4.13.2 Purification of Hept-1-ene

Sodium was placed in a round bottom flask containing spectroscopic grade hept-1-ene. The mixture was heated to reflux temperature with the RBF attached to an insulated Vigro column. The solvent was distilled into a collecting flask and used immediately.  $^1\text{H}$  NMR was used to confirm purity.

Spectroscopic data for hept-1-ene:-  $^1\text{H}$  NMR (d-acetone,  $\delta/\text{ppm}$ ):- 0.82 (t, 3H,  $\text{CH}_3$ ), 1.27 (m, 4H,  $2 \times \text{CH}_2$ ), 1.34 (m, 2H,  $\text{CH}_2$ ), 1.96 (q, 2H,  $\text{CH}_2$ ), 4.88 (m, 2H,  $\text{C}=\underline{\text{CH}}_2$ ), 5.73 (m, 1H,  $\underline{\text{CH}}=\text{CH}_2$ );  $^{13}\text{C}$  NMR ( $\text{CDCl}_3$ ,  $\delta/\text{ppm}$ ):- 14.19, 22.6, 31.5, 31.5, 33.9, 114.3 and 139.4.

#### 4.13.3 Purification of Hex-1-ene

Sodium was placed in a round bottom flask containing spectroscopic grade hex-1-ene. The mixture was heated to reflux temperature with the RBF attached to an insulated Vigro column. The solvent was distilled into a collecting flask and used immediately.  $^1\text{H}$  and  $^{13}\text{C}$  NMR was used to confirm purity.

Spectroscopic data for hex-1-ene:-  $^1\text{H}$  NMR ( $\text{CDCl}_3$ ,  $\delta/\text{ppm}$ ):- 0.91 (q,  $\text{CH}_3$ ), 1.34 (m,  $\text{CH}_2$ ), 1.36 (m,  $\text{CH}_2$ ), 2.06 (q,  $\text{CH}_2$ ), 4.9 (dd,  $=\text{CHCH}_2$ ).

#### 4.13.4 Purification of Tetrahydrofuran (THF)

Freshly cut sodium and benzophenone were added to a RBF containing spectroscopic grade THF. The mixture was heated to reflux temperature until a colour change from yellow to blue was observed. Solvent was distilled into a collecting flask, discarding the first 10% and used immediately.  $^1\text{H}$  NMR was used to confirm purity.

Spectroscopic data for THF :-  $^{13}\text{H}$  NMR (d-acetone,  $\delta/\text{ppm}$ ):- 1.85 (CH) and 3.74 (OCH).

#### 4.14 References

---

1. B.S. Creaven, M.W. George, A.G. Ginsburg, C. Hughes, J.M. Kelly, C. Long, I. McGrath, M.T. Pryce, *Organometallics*, **12** (1993) 3127.
2. C.J. Breheny, J.M. Kelly, C. Long, S.O'Keefe, M.T. Pryce, G. Russell, M.M. Walsh, *Organometallics*, **17** (1998) 3690.
3. (a) V. Vargheuse, M. Saha, N. Nicholas, *Org. Synth.*, **67** (1988) 141; (b) H.W. Sternberg, H. Greenfield, R.A. Friedel, J. Wotiz, I. Wender, *J. Am. Chem. Soc.*, **7** (1954) 1457.
4. (a) G. Bor, *Chem. Ber.*, **96** (1963) 2644; (b) G. Bor, *J. Organomet. Chem.*, **94** (1975) 1.
5. G. Bor, S.F.A. Kettle, P.L. Strangellini, *Inorg. Chim. Acta*, **18** (1976) L18.
6. L.S. Chia, W.R. Cullen, M. Franklin, A.R. Manning, *Inorg. Chem.*, **14** (1975) 2521.
7. T. Sugihara, M. Yamada, H. Ban, M. Yamaguchi, C. Kaneko, *Angew. Chem. Int. Ed. Engl.*, **36** (1997) 2801.
8. F.W. Grevels, V. J. Skibbe, *J. Chem. Soc. Chem. Commun.*, (1984) 681.

## **CHAPTER 5**

### **Conclusions**

## 5.0 Conclusions

The scope of this thesis is the application of photochemical reactions to the synthesis of organic molecules with the aim of finding a more useful, convenient, or new synthetic route to known molecules, or of establishing new syntheses of previous unattainable and often complicated molecules.

In this work, the synthesis and photochemistry of a number of ( $\mu_2$ -alkyne) $\text{Co}_2(\text{CO})_6$  complexes is described. The ( $\mu_2$ -alkyne) $\text{Co}_2(\text{CO})_6$  complexes were prepared by published thermal means and characterisation was achieved by IR, NMR, UV/Vis spectroscopy and elemental analysis. The photochemical reactions of ( $\mu_2$ -alkyne) $\text{Co}_2(\text{CO})_6$  complexes (alkyne =  $\text{C}_2\text{H}_2$ ,  $\text{C}_6\text{H}_5\text{C}_2\text{H}$  or  $(\text{C}_6\text{H}_5\text{C})_2$ ) with ligands  $\text{C}_5\text{H}_5\text{N}$  and  $\text{PPh}_3$  was described in Chapter 2. The ( $\mu_2$ -alkyne) $\text{Co}_2(\text{CO})_6$  complexes (where alkyne =  $\text{C}_6\text{H}_5\text{C}_2\text{H}$  or  $\text{C}_2\text{H}_2$ ) undergo CO-loss at wavelengths greater than 500 nm.  $\text{C}_6\text{H}_5\text{N}$  and  $\text{PPh}_3$  were used as trapping ligands (L) to enable the isolation of these pentacarbonyl complexes. These ( $\mu_2$ -alkyne) $\text{Co}_2(\text{CO})_5(\text{L})$  complexes were prepared both by thermal and photochemical means.

The photochemistry of the ( $\mu_2$ -( $\text{C}_6\text{H}_5\text{C})_2$ ) $\text{Co}_2(\text{CO})_6$  complex was shown to follow a different reaction pathway. Excitation at  $\lambda_{\text{exc}} = 532$  nm resulted in a hapticity change of the acetylene ligand. Ultimately a ligand substitution reaction results producing ( $\mu_2$ -( $\text{C}_6\text{H}_5\text{C})_2$ ) $\text{Co}_2(\text{CO})_5(\text{L})$ . Further irradiation of this pentacarbonyl species produces the tetracarbonyl ( $\mu_2$ -( $\text{C}_6\text{H}_5\text{C})_2$ ) $\text{Co}_2(\text{CO})_4(\text{L})_2$  complex in a similar reaction. It would be interesting to prepare complexes with different alkyne ligands on the  $\{\text{Co}_2(\text{CO})_6\}$  moiety. The photochemistry of such complexes could be studied with regard to looking at similarities between (a) symmetrical and unsymmetrical complex behaviour (b) the effect of the extent of alkyne substitution and (c) the effect of differing functional groups on the alkyne moiety.

The photochemical reactions of  $(\mu_2\text{-alkyne})\text{Co}_2(\text{CO})_6$  complexes (alkyne =  $\text{C}_2\text{H}_2$  or  $\text{C}_6\text{H}_5\text{C}_2\text{H}$ ) with alkenes was described and attempts to isolate  $(\mu_2\text{-alkyne})\text{Co}_2(\text{CO})_5(\text{alkene})$  type complexes were outlined. The resulting complexes were identified by IR spectroscopy. The synthesis of  $(\mu_2\text{-alkyne})\text{Co}_2(\text{CO})_5(\text{alkene})$  complexes proved more complicated than the corresponding  $(\mu_2\text{-alkyne})\text{Co}_2(\text{CO})_5(\text{L})$  complexes (where  $\text{L} = \text{C}_5\text{H}_5\text{N}$  or  $\text{PPh}_3$ ). The thermal reactions of alkenes with dicobalt hexacarbonyl complexes were also carried out in order to aid with identification of products derived by photochemical means. The cyclopentenones resulting from these reactions, typical Pauson - Khand adducts, were characterised by IR and NMR spectroscopy.

Cyclopentenones were generated by photochemical means using one or both of two synthetic routes. The first method involved subjecting a solution of the  $(\mu_2\text{-alkyne})\text{Co}_2(\text{CO})_6$  complex - alkene mixture to visible irradiation (natural light) under an atmosphere of carbon monoxide. The second route involved subjecting a similar solution to irradiation by a Kodex Carousel lamp under an atmosphere of carbon monoxide. Similar experiments conducted under an atmosphere of argon produced a lower yield of cyclopentenone.

As a result of this study, the photochemistry of a series of cobalt carbonyl complexes with varying alkyne ligands was described and is a basis for a more in-depth study into the photochemical reactions of related  $(\mu_2\text{-alkyne})$ cobalt carbonyl complexes. From this work develops new projects which are necessary in completing the study of the role of photochemistry in the Pauson - Khand reaction. Some of the concepts are as follows:-

- a) Further studies into the preparation of  $(\mu_2\text{-alkyne})\text{Co}_2(\text{CO})_5(\text{alkene})$  type complexes.

- b) Studies on the photochemistry of  $(\mu_2\text{-alkyne})\text{Co}_2(\text{CO})_5(\text{alkene})$  complexes with  $\lambda_{\text{exc}} > 320, 400$  and  $500$  nm with the ultimate goal of tuning the PK reaction to be carried out photochemically.
- c) Matrix studies on  $(\mu_2\text{-alkyne})\text{Co}_2(\text{CO})_5(\text{L})$  complexes where  $\text{L} = \text{C}_5\text{H}_5\text{N}$  and  $\text{PPh}_3$  with  $\lambda_{\text{exc}} > 500$  nm.
- d) Matrix studies on  $(\mu_2\text{-alkyne})\text{Co}_2(\text{CO})_5(\text{alkene})$  complexes with  $\lambda_{\text{exc}} > 320, 400$  and  $500$  nm.
- e) Studies on mixed metal complexes including the preparation of alkyne mixed metal hexacarbonyl complexes containing varying alkyne substituents followed by studies of the photochemistry of such complexes.

## **Appendix A**

-----

### **Presentations and Publications**



## **Presentations and Publications**

**Poster Presentations:-** 'Can Photochemistry promote the Pauson - Khand Reaction?'

1. The Fiftieth Irish Universities Chemistry Research Colloquium, National University of Ireland Galway, May 1998.
2. European Photochemistry Association (EPA) Summer school, Noordwijk, The Netherlands, June 1998.

**Publications:-** The Photochemistry of  $(\mu_2\text{-RC}_2\text{H})\text{Co}_2(\text{CO})_6$  Species (R = H or  $\text{C}_6\text{H}_5$ ), Important Intermediates in the Pauson - Khand Reaction, S.M. Draper, C. Long, B. M. Myers *J. Organomet. Chem.*, 588 (1999) 195.

## **Appendix B**

-----

### **Paper**

# The photochemistry of $(\mu_2\text{-RC}_2\text{H})\text{Co}_2(\text{CO})_6$ species ( $\text{R} = \text{H}$ or $\text{C}_6\text{H}_5$ ), important intermediates in the Pauson–Khand reaction

Sylvia M. Draper <sup>a</sup>, Conor Long <sup>b,\*</sup>, Bronagh M. Myers <sup>b</sup>

<sup>a</sup> Department of Chemistry, University of Dublin, Trinity College, Dublin 2, Ireland

<sup>b</sup> Inorganic Photochemistry Centre, Dublin City University, Dublin 9, Ireland

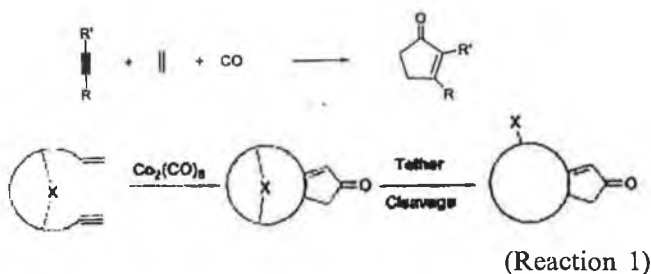
## Abstract

The photochemistry of  $(\mu_2\text{-RC}_2\text{H})\text{Co}_2(\text{CO})_6$  ( $\text{R} = \text{H}$  or  $\text{C}_6\text{H}_5$ ) has been investigated by both time-resolved and steady-state techniques. Pulsed excitation in cyclohexane solution with  $\lambda_{\text{exc}} = 355$  nm causes Co–Co bond homolysis while photolysis at  $\lambda_{\text{exc}} = 532$  nm results in CO loss. Steady-state photolysis ( $\lambda_{\text{exc}} > 500$  nm) in the presence of suitable trapping ligands (L) produced the monosubstituted complexes  $(\mu_2\text{-RC}_2\text{H})\text{Co}_2(\text{CO})_5(\text{L})$  ( $\text{L} = \text{C}_5\text{H}_5\text{N}$  or  $\text{PPh}_3$ ) in high yields. © 1999 Elsevier Science S.A. All rights reserved.

**Keywords:** Cobalt; Carbonyl; Photochemistry; Flash photolysis; Pauson–Khand

## 1. Introduction

We are currently interested in investigating the possibility of using photochemical techniques to promote the Pauson–Khand reaction [1], i.e. the cycloaddition of an alkyne, an alkene and carbon monoxide (Reaction 1). The products of the Pauson–Khand reaction can be highly regio- and stereo-chemically pure, explaining its enormous potential in the synthesis of biologically important molecules such as hirsutic acid [2], prostaglandins [3], *trans*-dihydrojasmonate [4], ste-modin [5], and  $(\pm)$ -pentalene [6], amongst others.



However, the high temperatures required for the Pauson–Khand process is a considerable disadvantage,

particularly if the olefin substrates undergo thermally induced rearrangements. Consequently, techniques that reduce the thermal demands of this process will significantly expand the range of its application.

The carbonyl functionality of the product enone is usually supplied by a metal carbonyl fragment, generally derived from dicobalt octacarbonyl, although alternative sources such as tungsten [7], and iron [8] carbonyl compounds have also been successfully used. Many reactions to date require that the metal carbonyl fragment be supplied in stoichiometric amounts, which is undoubtedly a significant problem for commercialisation of the Pauson–Khand process. Consequently, there is growing interest in the development of systems which use only catalytic amounts of the metal carbonyl compound [9]. Recently it has been shown that visible light effectively promotes catalytic Pauson–Khand reactions [10], however the precise role the photon plays in the reaction remains uncertain.

In the case of the cobalt system, and based on studies of the regio- and stereo-chemical control of the products, it has been proposed that decarbonylation of an initially formed  $(\mu_2\text{-alkyne})\text{Co}_2(\text{CO})_6$  species, is a prerequisite to the overall reaction sequence. Confirmation of this comes from the work of Krafft and co-workers [11] who have successfully trapped such a CO-loss species by a sulphur atom of a thio-substituent on the alkyne,

\* Corresponding author. Tel.: +353-1-7048001; fax: +353-1-7048002.

E-mail address: conor.long@dcu.ie (C. Long)

Table 1

The  $\nu_{\text{CO}}$  band positions ( $\text{cm}^{-1}$ ;  $\pm 1 \text{ cm}^{-1}$ ) in pentane solution for the dicobalt carbonyl compounds in this investigation

Compound	$\nu_{\text{CO}}$
$(\mu_2\text{-C}_6\text{H}_5\text{C}_2\text{H})\text{Co}_2(\text{CO})_6$	2094, 2056, 2033, 2029, 2014(sh)
$(\mu_2\text{-C}_2\text{H}_2)\text{Co}_2(\text{CO})_6$	2100, 2060, 2035, 2029, 2018(sh)
$(\mu_2\text{-C}_6\text{H}_5\text{C}_2\text{H})\text{Co}_2(\text{CO})_5$	2069, 2018, 2005, 1994, 1966,
(pyridine)	
$(\mu_2\text{-C}_6\text{H}_5\text{C}_2\text{H})\text{Co}_2(\text{CO})_5(\text{PPh}_3)$	2065, 2016, 2006, 1997, 1972
$(\mu_2\text{-C}_6\text{H}_5\text{C}_2\text{H})\text{Co}_2(\text{CO})_4(\text{PPh}_3)_2$	2021, 2004, 1972, 1949
$(\mu_2\text{-C}_6\text{H}_5\text{C}_2\text{H})\text{Co}_2(\text{CO})_4$	2018, 2002, 1967, 1942
(pyridine) <sub>2</sub>	
$(\mu_2\text{-C}_2\text{H}_2)\text{Co}_2(\text{CO})_5(\text{pyridine})$	2064, 2019, 2002, 1996, 1968
$(\mu_2\text{-C}_2\text{H}_2)\text{Co}_2(\text{CO})_4(\text{pyridine})_2$	2021, 2004, 1970, 1941
$(\mu_2\text{-C}_2\text{H}_2)\text{Co}_2(\text{CO})_5(\text{PPh}_3)$	2069, 2017, 2009, 1998, 1975
$(\mu_2\text{-C}_2\text{H}_2)\text{Co}_2(\text{CO})_4(\text{PPh}_3)_2$	2028, 1982, 1965, 1948

yielding an isolable pentacarbonyl complex amenable to spectroscopic and structural analyses.

Conveniently, the  $(\mu_2\text{-alkyne})\text{Co}_2(\text{CO})_6$  intermediates are readily isolated, and while their thermal chemistry is well known [12], few detailed studies of their photochemical properties have appeared to date [13]. Of particular importance, in this regard, is a recent matrix isolation study, which demonstrated that CO-loss occurs following short-wavelength ( $\lambda_{\text{exc}} = 250 \text{ nm}$ ) photolysis of  $(\mu_2\text{-alkyne})\text{Co}_2(\text{CO})_6$  [14]. This work demonstrated that  $(\mu_2\text{-alkyne})\text{Co}_2(\text{CO})_6$  is photochemically inert when irradiated with  $\lambda_{\text{exc}} = 350 \text{ nm}$ . However, it would not be feasible to use photons of wavelengths less than  $300 \text{ nm}$  in the Pauson–Khand reaction because of the risk of photochemical damage to the unsaturated substrates.

A fuller investigation, in particular of the wavelength-dependent nature of the photochemistry of  $(\mu_2\text{-alkyne})\text{Co}_2(\text{CO})_6$  compounds, might provide both further evidence for the importance of the CO-loss process to the Pauson–Khand reaction, and present an alternative and more attractive means of promoting the

reaction particularly when thermally sensitive substrates are required.

This paper reports the results of our investigation into the photochemistry of a range of  $(\mu_2\text{-alkyne})\text{Co}_2(\text{CO})_6$  compounds by both steady-state and laser flash photolysis techniques and demonstrates the importance of correct selection of excitation wavelengths in promoting the desired CO-loss process.

## 2. Results and discussion

Table 1 contains the band positions in the carbonyl stretching region for the compounds used in this study. Typical UV–vis spectra for the dicobalt hexacarbonyl compounds are presented in Fig. 1. In general these compounds absorb across a broad range of wavelengths up to  $630 \text{ nm}$  providing the photochemist with a wide choice of excitation wavelengths. Preliminary experiments were conducted using broad-band photolysis techniques in order to identify which spectral region produced the desired CO-loss process.

### 2.1. Steady-state photolysis of $(\mu_2\text{-C}_6\text{H}_5\text{C}_2\text{H})\text{Co}_2(\text{CO})_6$ in the presence of trapping ligands

Broad-band photolysis of  $(\mu_2\text{-C}_6\text{H}_5\text{C}_2\text{H})\text{Co}_2(\text{CO})_6$  with  $\lambda_{\text{exc}} > 340 \text{ nm}$  in the presence of a trapping ligand L ( $\text{L} = \text{C}_5\text{H}_5\text{N}$  or  $\text{PPh}_3$ ) produced the monosubstituted  $(\mu_2\text{-C}_6\text{H}_5\text{C}_2\text{H})\text{Co}_2(\text{CO})_5(\text{L})$  species. Product assignment in each case was based on a comparison of the  $\nu_{\text{CO}}$  bands with those of authentic samples of the appropriate monosubstituted hexacarbonyl species (cf. Table 1). Prolonged photolysis of  $(\mu_2\text{-C}_6\text{H}_5\text{C}_2\text{H})\text{Co}_2(\text{CO})_5(\text{PPh}_3)$  however, also produced the disubstituted species  $(\mu_2\text{-C}_6\text{H}_5\text{C}_2\text{H})\text{Co}_2(\text{CO})_4(\text{PPh}_3)_2$ . Qualitatively similar results were obtained in experiments using  $\lambda_{\text{exc}} > 400 \text{ nm}$ , however, in general the photolysis times required were longer under similar experimental conditions owing to the lower optical density of the parent hexacarbonyl compound within this spectral range. These results clearly demonstrate that CO-loss can be achieved under photochemical conditions, and these results prompted a fuller investigation of this system using monochromatic light sources.

### 2.2. Laser flash photolysis of $(\mu_2\text{-C}_6\text{H}_5\text{C}_2\text{H})\text{Co}_2(\text{CO})_6$ in cyclohexane solution ( $\lambda_{\text{exc}} = 355 \text{ nm}$ )

Pulsed photolysis ( $\lambda_{\text{exc}} = 355 \text{ nm}$ ) of  $(\mu_2\text{-RC}_2\text{H})\text{Co}_2(\text{CO})_6$  ( $\text{R} = \text{C}_6\text{H}_5$  or  $\text{H}$ ) in cyclohexane solution results in a depletion of the absorption of the hexacarbonyl compound within the rise-time of the monitoring system ( $\sim 20 \text{ ns}$ ). The depletion is followed by a rapid recovery of the absorption to the pre-irradiation level. This behaviour is observed at all monitoring

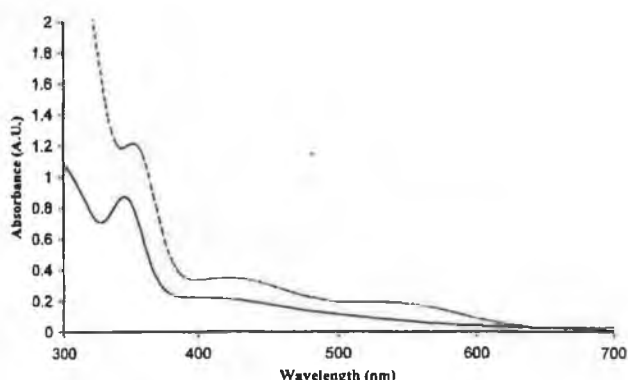


Fig. 1. The UV–vis spectra of  $(\mu_2\text{-RC}_2\text{H})\text{Co}_2(\text{CO})_6$  ( $\text{R} = \text{H}$ , —, conc. =  $1.6 \times 10^{-3} \text{ M}$ ;  $\text{R} = \text{C}_6\text{H}_5$ , ----, conc. =  $3.2 \times 10^{-4} \text{ M}$ ) in pentane solution at room temperature.

wavelengths where the parent hexacarbonyl has significant absorbance.

The recovery of the depleted absorption followed first-order kinetics, and this provided an observed first-order rate constant of  $4 \times 10^7 \text{ s}^{-1}$  at 298 K. Addition of CO to the solution had no effect on the rate of recovery of the depleted absorption. This is strong evidence that the depletion of the parent absorption was not the result of CO-loss. No transient absorption signals were detected out to monitoring wavelengths of 600 nm, indicating that the photoproduct has a lower extinction across the entire accessible spectral range when compared to that of the parent compound. Such observations have precedence in the literature [15].

A series of experiments was conducted in which a trapping ligand ( $\text{C}_5\text{H}_5\text{N}$ ) was added to the photolysis solution in a 20-fold excess over the parent carbonyl compound (typical concentration of parent compound =  $1 \times 10^{-5} \text{ M}$ ). Again the only spectral change observed was depletion of the parent hexacarbonyl which recovered with an observed rate constant identical to that measured in the presence of CO. This demonstrated that the intermediate produced does not react with pyridine. However, an IR spectrum recorded after flash photolysis experiments confirmed the presence of  $(\mu_2\text{-RC}_2\text{H})\text{Co}_2(\text{CO})_5(\text{C}_5\text{H}_5\text{N})$ . Clearly the photochemical changes observed were the result of excitation by the monitoring lamp rather than the laser output. This result is consistent with the recently published results of matrix isolation studies, which demonstrated that no photochemistry results from irradiation with  $\lambda_{\text{exc}} = 350 \text{ nm}$  [14].

To explain the depletion of the parent absorption observed in these experiments, following laser excitation, without resulting photochemical change, we propose that homolytic cleavage of the cobalt–cobalt bond occurs, which rapidly undergoes efficient recombination. Consequently further time-resolved experiments were conducted using the second harmonic of the Nd-YAG fundamental at 532 nm.

### 2.3. Laser flash photolysis of $(\mu_2\text{-RC}_2\text{H})\text{Co}_2(\text{CO})_6$ in cyclohexane solution with $\lambda_{\text{exc}} = 532 \text{ nm}$

Pulsed photolysis of  $(\mu_2\text{-RC}_2\text{H})\text{Co}_2(\text{CO})_6$  ( $\text{R} = \text{C}_6\text{H}_5$  or  $\text{H}$ ) with  $\lambda_{\text{exc}} = 532 \text{ nm}$  resulted in the formation of a transient species which absorbs with a  $\lambda_{\text{max}}$  at 400 nm. The position of this absorption compared well to that observed in matrix isolation experiments on the same system [14]. Addition of CO ( $[\text{CO}] = 9 \times 10^{-3} \text{ M}$ ) reduced the lifetime of the transient species while its yield was not affected. A typical transient signal is presented in Fig. 2. This behaviour is typical of the reaction of CO-loss intermediates. Under these conditions the system is fully reversible i.e. repeated exposure to the laser radiation did not result in the build-up of high concen-

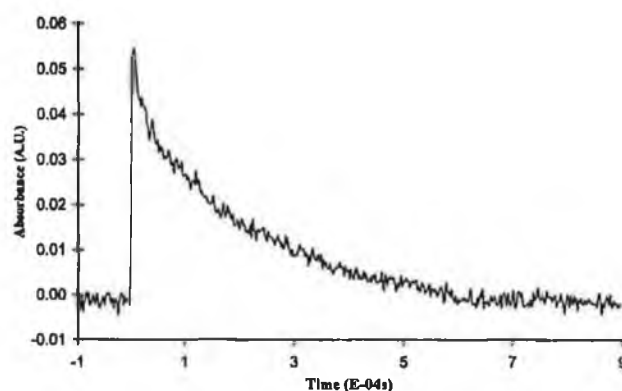


Fig. 2. A typical transient absorption signal observed at 400 nm following pulsed photolysis of  $(\mu_2\text{-C}_6\text{H}_5\text{C}_2\text{H})\text{Co}_2(\text{CO})_6$  in pentane solution with  $\lambda_{\text{exc}} = 532 \text{ nm}$  at 298 K in the presence of CO (conc. =  $9 \times 10^{-3} \text{ M}$ ).

trations of photoproducts. The  $k_{\text{obs}}$  was linearly dependent on the concentration of CO, yielding the second-order rate constant ( $k_2 = 1.2 \times 10^6 \text{ dm}^3 \text{ mol}^{-1} \text{ s}^{-1}$  at 298 K) as the slope.

Experiments were then conducted in the presence of a trapping ligand ( $\text{PPh}_3$ ). Again a transient absorption was observed with  $\lambda_{\text{max}}$  at 400 nm assigned to  $(\mu_2\text{-C}_6\text{H}_5\text{C}_2\text{H})\text{Co}_2(\text{CO})_5(\text{solvent})$ . The lifetime of this transient species depended on the concentration of added  $\text{PPh}_3$ , and again the analysis of this dependence yields an estimate of the second order rate constant for the reaction of  $(\mu_2\text{-C}_6\text{H}_5\text{C}_2\text{H})\text{Co}_2(\text{CO})_5(\text{solvent})$  with  $\text{PPh}_3$  of  $3.0 \times 10^6 \text{ dm}^3 \text{ mol}^{-1} \text{ s}^{-1}$  at 298 K. Examination of the resulting solution by IR spectroscopy confirmed the presence of  $(\mu_2\text{-C}_6\text{H}_5\text{C}_2\text{H})\text{Co}_2(\text{CO})_5(\text{PPh}_3)$ .

### 2.4. Steady-state photolysis of $(\mu_2\text{-RC}_2\text{H})\text{Co}_2(\text{CO})_6$ ( $\text{R} = \text{C}_6\text{H}_5$ or $\text{H}$ ) in alkane solution

Steady-state experiments using visible light ( $\lambda_{\text{exc}} > 500 \text{ nm}$ ) in the presence of a trapping ligand (L) gave

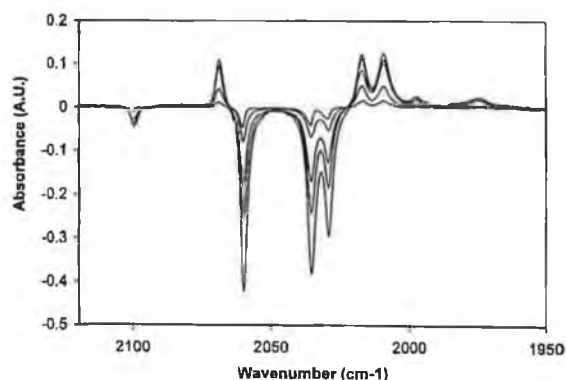
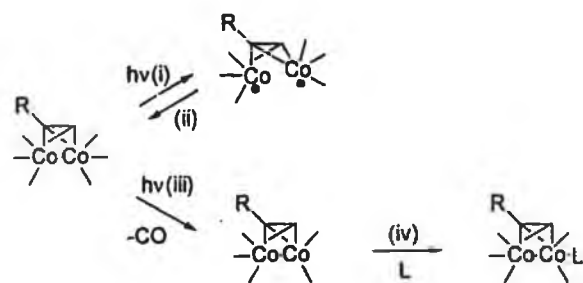


Fig. 3. Difference IR spectra obtained following broad-band photolysis ( $\lambda_{\text{exc}} > 500 \text{ nm}$ ) of  $(\mu_2\text{-C}_2\text{H}_3)\text{Co}_2(\text{CO})_6$  in cyclohexane, acquired at 10, 30, 120, 300 and 600 s, respectively. The negative bands, indicate depletion of the parent absorptions; while the positive bands are assigned to  $(\mu_2\text{-C}_2\text{H}_3)\text{Co}_2(\text{CO})_5(\text{PPh}_3)$  (see text).



Scheme 1. (i)  $\lambda_{\text{exc}} = 350$  nm in alkane solvent, (ii)  $\tau_1 = 2.5 \times 10^{-8}$  s at 298 K, (iii)  $\lambda_{\text{exc}} > 400$  nm, (iv)  $k_2 = 1.2 \times 10^6$  dm<sup>3</sup> mol<sup>-1</sup> s<sup>-1</sup> at 298 K for L = CO (carbonyl ligands are indicated thus — for clarity).

rise exclusively to the monosubstituted pentacarbonyl complexes  $(\mu_2\text{-RC}_2\text{H})\text{Co}_2(\text{CO})_5(\text{L})$  (L = C<sub>5</sub>H<sub>5</sub>N or PPh<sub>3</sub>). Fig. 3 shows the appearance of new bands and the continual depletion of parent bands upon photolysis of  $(\mu_2\text{-RC}_2\text{H})\text{Co}_2(\text{CO})_6$  in the presence of PPh<sub>3</sub>. While reducing the excitation wavelengths ( $\lambda_{\text{exc}} > 340$  nm) increased the yield of the substituted product, short wavelength photolysis also increased the yield of the disubstituted derivatives particularly for L = PPh<sub>3</sub>.

### 3. Summary and conclusions

This work demonstrates the importance of the correct selection of excitation wavelength in inducing the photochemical decarbonylation of  $(\mu_2\text{-RC}_2\text{H})\text{Co}_2(\text{CO})_6$  complexes. Excitation at 355 nm does not result in CO-loss and the time resolved behaviour can be interpreted in terms of a Co–Co bond cleavage followed by a rapid reformation. In this respect, the compound acts as a 'photon sink' in this region of the spectrum. Long-wavelength excitation at 532 nm results in the desired CO-loss process and consequently facilitates the next step in the Pauson–Khand reaction. This explains why Livinghouse et al. [10] observed the photochemical promotion of the Pauson–Khand reaction following visible light photolysis.

The overall photochemistry is summarised in Scheme 1.

## 4. Experimental

### 4.1. Reagents

$\text{Co}_2(\text{CO})_8$  (Fluka Chemicals), the alkynes phenylacetylene (Aldrich Chemical) and acetylene gas (Air Products), triphenylphosphine (Aldrich Chemical), pyridine, cyclohexane, hept-1-ene, and pentane (spectroscopic grade, Aldrich Chemical) were used as received. All manipulations involving  $\text{Co}_2(\text{CO})_8$  were conducted under an argon atmosphere.

### 4.2. Equipment

IR spectra were recorded on a Perkin–Elmer 2000 FTIR spectrometer, solution cells were fitted with NaCl windows ( $d = 0.1$  mm), and spectroscopic grade cyclohexane or pentane was used. <sup>1</sup>H- and <sup>13</sup>C-NMR spectra were obtained using a Bruker model AC400 spectrometer and were calibrated with respect to the residual proton resonances of the solvent or with an internal TMS standard. UV spectra were measured on a Hewlett–Packard 8453A photodiode array spectrometer using 1 cm quartz cells. Photolysis was performed using an Applied Photophysics medium-pressure Xe arc lamp (275 W). Wavelength selection was achieved using Corning cut-off filters.

The laser system used was a pulsed Nd:YAG laser capable of generating the second, third or fourth harmonic at 532, 355 or 266 nm as required, with typical energies of 150, 30, and 45 mJ per pulse, respectively. The pulse duration was approximately 10 ns. The apparatus has been described in detail elsewhere with the excitation and monitoring beams arranged in a cross-beam configuration [16]. All samples were prepared for laser flash photolysis in a degassing bulb attached to a fluorescent cell and protected from light. The solutions were subjected to three cycles of a freeze–pump–thaw procedure to  $10^{-2}$  torr. The solution, at room temperature, was then subjected to a dynamic vacuum, a process which has been shown to remove traces of water [17]. The required atmosphere of Ar or CO was then admitted to the sample cell.

### 4.3. Synthesis of $(\mu^2\text{-alkyne})\text{hexacarbonyldicobalt}$ complexes

The  $(\mu_2\text{-alkyne})\text{Co}_2(\text{CO})_6$  complexes were prepared by the standard method, which involves the slow addition of the alkyne to a degassed solution of  $\text{Co}_2(\text{CO})_8$  in pentane [18]. The solution was stirred overnight at room temperature, following which the solvent was removed under reduced pressure yielding the dark red products.

Spectroscopic and analytical data for  $(\mu_2\text{-C}_2\text{H}_2)\text{Co}_2(\text{CO})_6$ : <sup>1</sup>H-NMR (CDCl<sub>3</sub>): 6.01(s, 2H, C–H) ppm. <sup>13</sup>C-NMR (CDCl<sub>3</sub>): 59.358 (C–H), 198.99 (C–O) ppm. UV(C<sub>5</sub>H<sub>12</sub>): 346, 447 nm. M.p. 13–13.5°C. Yield 95%. Anal. Calc. C 30.80%, H 0.65%. Found C 31.07%, H 0.65%. The  $\nu_{\text{CO}}$  data are presented in Table 1. Spectroscopic and analytical data for  $(\mu_2\text{-C}_6\text{H}_5\text{C}_2\text{H})\text{Co}_2(\text{CO})_6$ : <sup>1</sup>H-NMR (CD<sub>3</sub>CN): 6.66(1H, s, =C–H), 7.36–7.59(5H, m, Ar CH) ppm. <sup>13</sup>C-NMR (CDCl<sub>3</sub>): 128.1(s), 128.85(s), 130.21(s), (C<sub>6</sub>H<sub>5</sub>) ppm. UV(C<sub>5</sub>H<sub>12</sub>): 352, 422, 536 nm. M.p. 52–53°C. Anal. Calc. C 43.33%, H 1.56%. Found C 43.06%, H 1.65%. The  $\nu_{\text{CO}}$  data are presented in Table 1.

#### 4.4. Synthesis of $(\mu_2\text{-RC}_2\text{H})\text{Co}_2(\text{CO})_5(\text{C}_5\text{H}_5\text{N})$ and $(\mu_2\text{-RC}_2\text{H})\text{Co}_2(\text{CO})_5(\text{PPh}_3)$

The thermal syntheses of  $(\mu_2\text{-RC}_2\text{H})\text{Co}_2(\text{CO})_5(\text{L})$  complexes where  $\text{L} = \text{PPh}_3$  or pyridine were carried out according to the method of Manning and co-workers [19]. Equimolar amounts of the desired ligand and  $(\mu_2\text{-RC}_2\text{H})\text{Co}_2(\text{CO})_6$  were added to benzene (5 cm<sup>3</sup>) and brought to reflux temperature for 4 h yielding dark red solutions. The solvent was then removed under reduced pressure, followed by chromatography on silica gel. The unreacted starting materials were removed by elution with petroleum ether. The products were eluted by diethylether–petroleum ether (1:1 v/v). Evaporation of the solvent in an Ar stream yielded the crystalline products. Typical yields were in the range 90–95%. IR  $\nu_{\text{CO}}$  data for these compounds are provided in Table 1. UV  $(\mu_2\text{-C}_2\text{H}_2)\text{Co}_2(\text{CO})_5(\text{PPh}_3)$  ( $\text{C}_5\text{H}_5\text{N}$ ):  $\lambda_{\text{max}}$  322, 376, and 506 nm.

#### 4.5. Steady-state photochemical experiments: photochemical synthesis of $(\mu_2\text{-RC}_2\text{H})\text{Co}_2(\text{CO})_5(\text{L})$ ( $\text{L} = \text{C}_5\text{H}_5\text{N}$ or $\text{PPh}_3$ )

The relevant alkyne compound was dissolved in cyclohexane together with a four-fold excess of the desired trapping ligand  $\text{L}$ . The solution was purged with argon gas for 15 min, before being transferred to an IR solution cell for irradiation with light of selected wavelengths. The reaction was then followed by IR spectroscopy

#### Acknowledgements

The authors would like to thank Enterprise Ireland (formally Forbairt) for financial assistance.

#### References

- [1] (a) I. Ojima, M. Tzamarioudaki, Z. Li, J. Donovan, *Chem. Rev.* 96 (1996) 635. (b) N.E. Schore, in: L.A. Paquette (Ed.), *Organic Reactions*, vol. 40, 1991. (c) N.E. Schore, in: P.M. Trost (Ed.), *Comprehensive Organic Synthesis*, vol. 5, Pergamon, Oxford, 1991, p. 1037. (d) P.L. Pauson, *Organometallics* in: A. de Meijere, H. von Dieck (Eds.), *Organic Synthesis 2*, Springer-Verlag, Berlin, 1987, p. 234. (e) P.L. Pauson, *Tetrahedron* 41 (1985) 5855. (f) P.L. Pauson, I.U. Khand, *Ann. N.Y. Acad. Sci.* 2 (1977) 295. (g) F.L. Bowden, A.B.P. Lever, *Organomet. Chem. Rev.* 3 (1968) 227.
- [2] (a) P. Magnus, C. Exon, P. Albough-Robertson, *Tetrahedron* 41 (1985) 5861. (b) P. Magnus, L. Principle, *Tetrahedron Lett.* 26 (1985) 4851. (c) C. Exon, P. Magnus, *J. Am. Chem. Soc.* 105 (1983) 2477.
- [3] (a) L. Daalman, R.F. Newton, P.L. Pauson, R.G. Taylor, A. Wadsworth, *J. Chem. Res. (S)* (1984) 344. (b) H.J. Jeffer, P.L. Pauson, *J. Chem. Res. (M)* (1983) 2201.
- [4] V. Rautenshlauch, P. Megard, J. Conesa, W. Küster, *Angew. Chem. Int. Ed. Engl.* 29 (1990) 1413.
- [5] J. Germanas, C. Aubert, K.P.C. Vollhardt, *J. Am. Chem. Soc.* 113 (1991) 4006.
- [6] N.E. Shore, E.G. Rowley, *J. Am. Chem. Soc.* 110 (1988) 5224.
- [7] (a) T.R. Hoyer, J.A. Suriano, *J. Am. Chem. Soc.* 115 (1993) 1154. (b) T.R. Hoyer, J.A. Suriano, *Organometallics* 11 (1992) 2044.
- [8] (a) A.J. Pearson, R.A. Dubbert, *J. Chem. Soc. Chem. Commun.* (1991) 202. (b) A.J. Pearson, R.A. Dubbert, *Organometallics* 13 (1994) 578. (c) A.J. Pearson, R.A. Dubbert, *Organometallics* 13 (1994) 1656.
- [9] (a) N.Y. Lee, Y.K. Chung, *Tetrahedron Lett.* 37 (1996) 3145. (b) S.C. Berk, R.B. Grassman, S.L. Buckwald, *J. Am. Chem. Soc.* 116 (1994) 8593. (c) B.M. Trost, *Science* 254 (1991) 1471. (d) B.M. Trost, *Angew. Chem. Int. Ed. Engl.* 34 (1995) 259. (e) N. Jeong, S.H. Hwang, Y.W. Lee, Y.S. Lim, *J. Am. Chem. Soc.* 119 (1997) 10549. (f) N. Yeong, S.H. Hwang, Y.W. Lee, Y.K. Chung, *J. Am. Chem. Soc.* 116 (1994) 3159. (g) B.Y. Lee, Y.K. Chung, N. Leong, Y. Lee, S.H. Hwang, *J. Am. Chem. Soc.* 116 (1994) 8793.
- [10] B.L. Pagenkopt, T. Livinghouse, *J. Am. Chem. Soc.* 118 (1996) 2285.
- [11] E. Krafft, I.L. Scott, R.H. Romero, S. Feilbelmann, C.E. Van Pest, *J. Am. Chem. Soc.* 115 (1993) 7199.
- [12] (a) I.S. Chia, W.R. Cullen, M. Franklin, A.R. Manning, *Inorg. Chem.* 14 (1975) 2521. (b) R.F. Heck, *J. Am. Chem. Soc.* 85 (1963) 657. (c) J.J. Bonnet, R. Mathieu, *Inorg. Chem.* 17 (1978) 1973. (d) M. Arewgoda, B.H. Robinson, J. Simpson, *J. Am. Chem. Soc.* 105 (1983) 1893. (e) A. Avey, G.F. Nieckaez, D.R. Tyler, *Organometallics* 14 (1995) 2790. (f) G. Varadi, A. Vizi-Orosz, S. Vastag, G. Palyi, *J. Organomet. Chem.* 108 (1976) 225. (g) M.E. Krafft, *Tetrahedron Lett.* 29 (1988) 999. (h) W.G. Sly, *Inorg. Chem.* 81 (1959) 18. (i) L.M. Bower, R. Mathieu, *Inorg. Chem.* 17 (1978) 1973.
- [13] J.C. Anderson, B.F. Taylor, C. Viney, E.J. Wilson, *J. Organomet. Chem.* 519 (1996) 103.
- [14] C.M. Gordon, M. Kiszka, I.R. Dunkin, W.J. Kerr, J.S. Scott, J. Gebicki, *J. Organomet. Chem.* 554 (1998) 147.
- [15] J.R. Knorr, T.L. Brown, *J. Am. Chem. Soc.* 115 (1993) 4087.
- [16] B.S. Creaven, M.W. George, A.G. Ginsburg, C. Hughes, J.M. Kelly, C. Long, I. McGrath, M.T. Pryce, *Organometallics* 12 (1993) 3127.
- [17] C.J. Breheny, J.M. Kelly, C. Long, S. O'Keeffe, M.T. Pryce, G. Russell, M.M. Walsh, *Organometallics* 17 (1998) 3690.
- [18] (a) V. Varghese, M. Saha, N. Nicholas, *Org. Synth.* 67 (1988) 141. (b) H.W. Sternberg, H. Greenfield, R.A. Friedel, J. Wotiz, R. Markby, I. Wender, *J. Am. Chem. Soc.* 76 (1954) 1457.
- [19] L.S. Chia, W.R. Cullen, M. Franklin, A.R. Manning, *Inorg. Chem.* 14 (1975) 2521.

## **Appendix C**

---

**Calculations for determination of extinction coefficients.**

**Peakfit Analysis of UV spectra.**

**Calculated rate of reaction from rate equations.**



### **1.1. Determination of extinction coefficients**

In order to calculate the concentration of the metal carbonyl complex in solution, knowing the absorbance at a particular wavelength, and utilising the Beer-Lambert law (eq. A1), the molar extinction coefficient in that solvent at that particular wavelength must be known. The Beer Lambert Law is given by :-

$$A = \epsilon c l \quad (A1)$$

where  $A$  = absorbance at a particular wavelength (AU)

$\epsilon$  = molar extinction coefficient ( $\text{dm}^3 \text{mol}^{-1} \text{cm}^{-1}$ )

$c$  = concentration ( $\text{mol dm}^{-3}$ )

$l$  = pathlength of the cell (cm)

The data used in the determination of the extinction coefficients is given in Appendix D.

### **1.2. Peakfit Analysis of UV/vis Spectra**

Although a peak may be just discernible in a UV/vis spectrum it may not produce a local maxima in the data stream. A Jandel scientific peakfit package was employed to observe low intensity overlapped absorptions. Initially a smoothing algorithm is applied to the spectrum, the Savitsky- Golay procedure was employed in this study. The algorithm is based on least squared quatic polynomial fitting across a moving window within the data. The line-shape of the spectra are Voigt in nature, a convolution of Gaussian and Lorentzian line shape. The Lorentzian line shape is the 'natural' shape for spectra consisting of energy absorption or emission due to a transition between energy states. The line broadening is attributed to the lifetimes of

the energy stated and the Heisenberg principle. The Gaussian line broadening originates from instrument optical and electrical effects, and is often referred to as the spread function. The spectral lines are deconvoluted during the peakfitting to yield the Lorentzian and instrument response width. In this study a residual method was employed to elucidate 'hidden' peaks in the UV/vis spectra of some compounds. A residual may be defined as the difference in Y - values between a data point and the sum of component peaks evaluated at the data points X - value. The peaks are then arranged in such a way that their total area equals the area of the data, and so 'hidden' peaks are revealed by residues.

### ***1.3. Calculated rate of reaction from rate equations***

Calculation of  $k_2$

$$k_{\text{obs}} / [\text{CO}] = k_2 \quad (\text{dm}^3 \text{ mol}^{-1} \text{ s}^{-1}) \text{ at } 298 \text{ K.}$$

where

$$\begin{aligned} k_{\text{obs}} &= \text{the observed rate constant,} \\ 1 \text{ atm } [\text{CO}] &= 9 \times 10^{-3} \text{ M,} \\ 1/2 \text{ atm } [\text{CO}] &= 4.5 \times 10^{-3} \text{ M} \end{aligned}$$

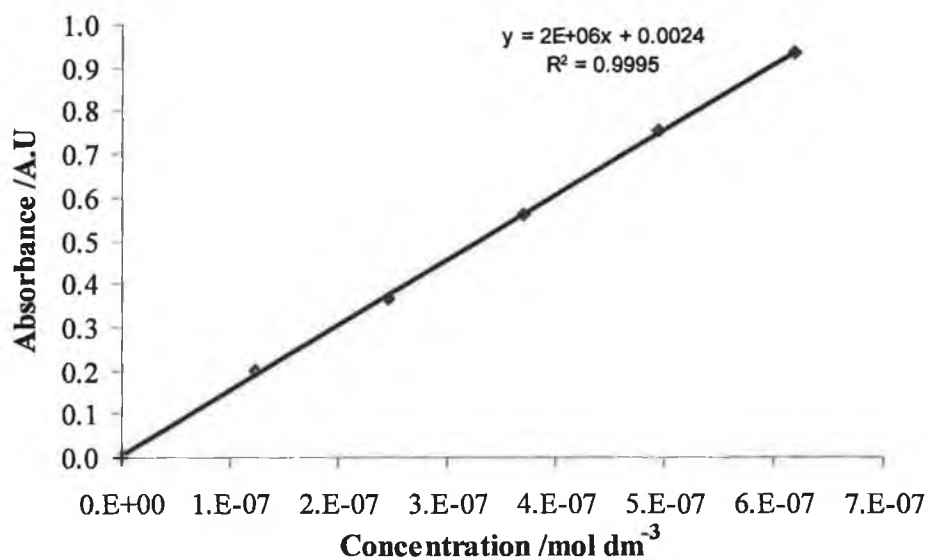
## **Appendix D**

---

### **Data for the determination of extinction coefficients**

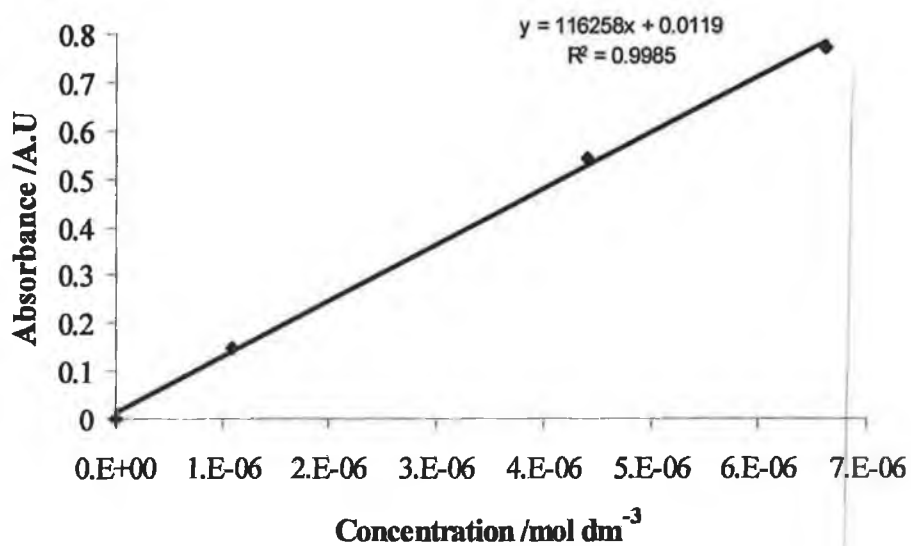
- (a) Data for extinction coefficient of  $(C_2H_2)Co_2(CO)_6$  in cyclohexane at 354 nm

$[(C_2H_2)Co_2(CO)_6]$ (mol dm <sup>-3</sup> )	O.D @ 354 nm (AU)
0.0	0.000
6.19 E-07	0.933
4.95 E-07	0.755
3.71 E-07	0.558
2.47 E-07	0.364
1.24 E-07	0.199



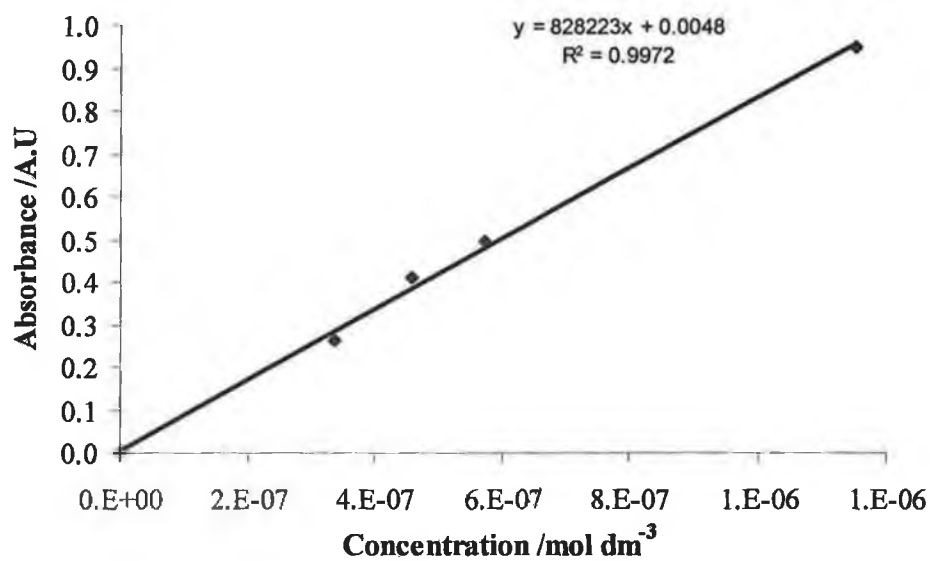
- (b) Data for extinction coefficient of  $(\text{C}_6\text{H}_5\text{C}_2\text{H})\text{Co}_2(\text{CO})_6$  in cyclohexane at 354 nm

$[(\text{C}_6\text{H}_5\text{C}_2\text{H})\text{Co}_2(\text{CO})_6]$ (mol dm <sup>-3</sup> )	O.D @ 354 nm (AU)
0.0	0.000
4.8 E-08	0.358
9.6 E-08	0.728
7.7 E-08	0.599



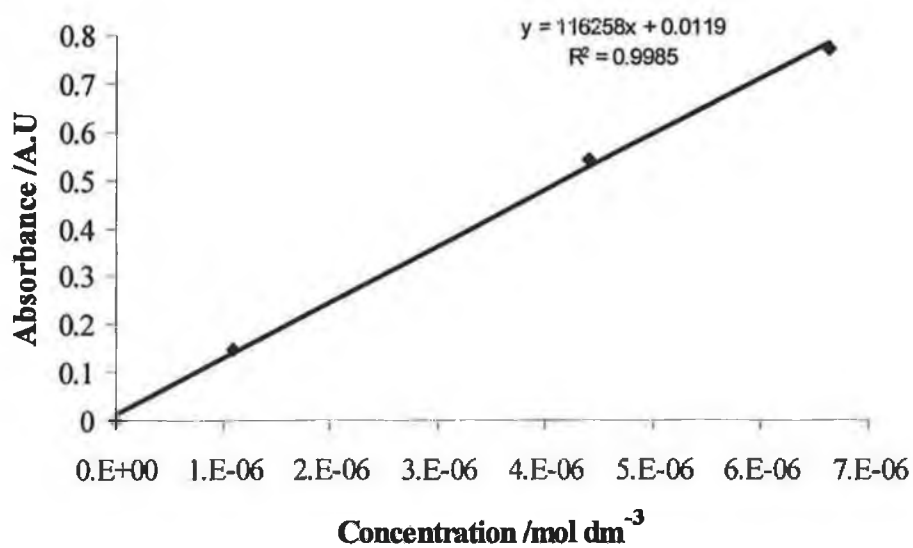
- c) Data for extinction coefficient of  $((\text{C}_6\text{H}_5)_2\text{C}_2\text{H})\text{Co}_2(\text{CO})_6$  in cyclohexane at 354 nm

$[(\text{C}_6\text{H}_5)_2\text{C}_2\text{H})\text{Co}_2(\text{CO})_6]$ (mol dm <sup>-3</sup> )	O.D @ 354 nm (AU)
0.0	0.000
3.39 E-07	0.263
4.59 E-07	0.408
5.74 E-07	0.494
1.15 E-06	0.948



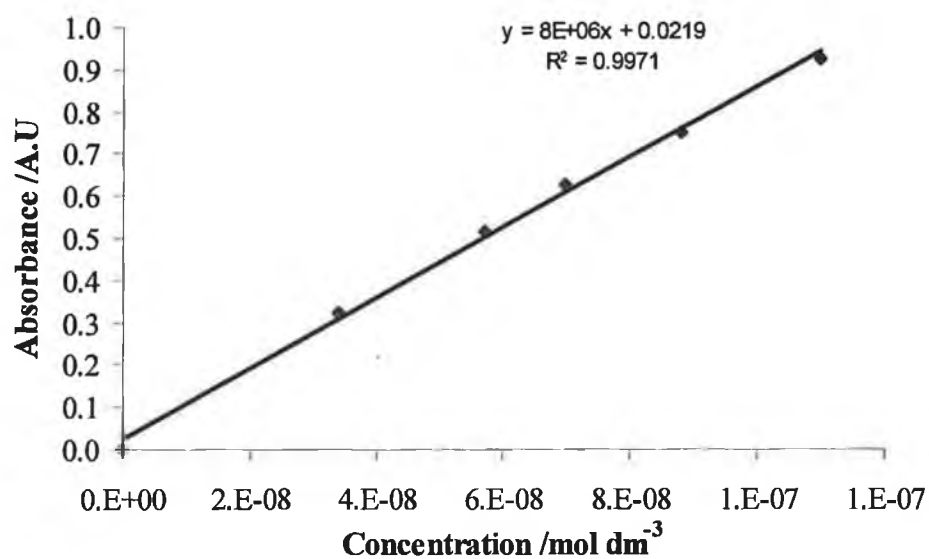
(d) Data for extinction coefficient of  $(\text{C}_2\text{H}_2)\text{Co}_2(\text{CO})_6$  in pentane at 354 nm

$[(\text{C}_2\text{H}_2)\text{Co}_2(\text{CO})_6]$ (mol dm <sup>-3</sup> )	O.D @ 354 nm (AU)
0.0	0.000
6.62 E-06	0.770
4.42 E-06	0.541
1.10 E-06	0.148



- (e) Data for extinction coefficient of  $(\text{C}_6\text{H}_5\text{C}_2\text{H})\text{Co}_2(\text{CO})_6$  in pentane at 354 nm

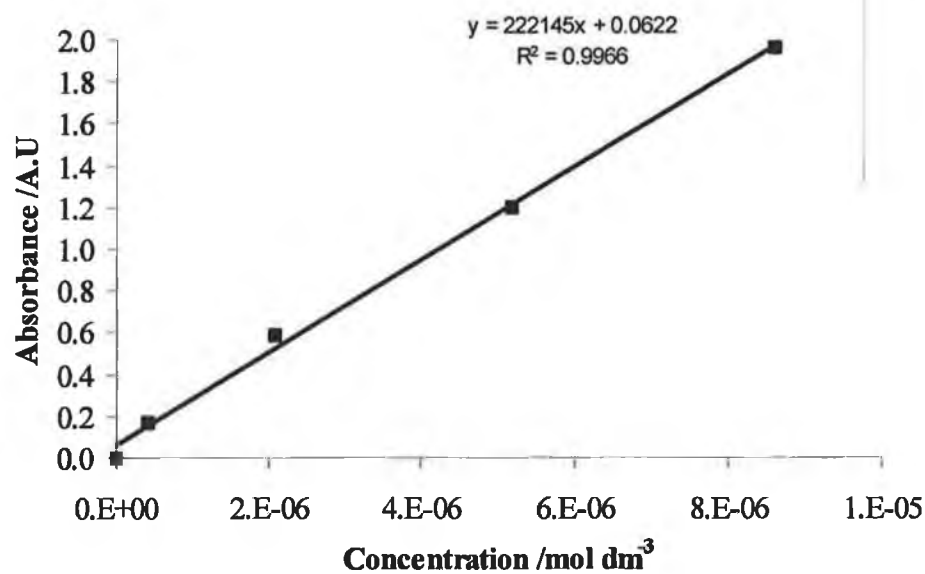
$[(\text{C}_6\text{H}_5\text{C}_2\text{H})\text{Co}_2(\text{CO})_6]$ (mol dm <sup>-3</sup> )	O.D @ 354 nm (AU)
0.0	0.000
1.1 E-07	0.925
8.8 E-08	0.752
7.0 E-08	0.626
5.7 E-08	0.513
3.4 E-08	0.321





- (f) Data for extinction coefficient of  $((C_6H_5)_2C_2H)Co_2(CO)_6$  in pentane at 354nm

$[(C_6H_5)_2C_2H)Co_2(CO)_6]$ (mol dm <sup>-3</sup> )	O.D @ 354 nm (AU)
0.0	0.000
8.6 E-06	1.964
5.17 E-06	1.197
2.07 E-06	0.589
4.14 E-07	0.172



- (g) Data for extinction coefficient of  $((C_6H_5C_2H)Co_2(CO)_5(PPh_3))$  in pentane at 354 nm

$[(C_6H_5C_2H)Co_2(CO)_5(PPh_3)]$ (mol dm <sup>-3</sup> )	O.D @ 354 nm (AU)
0.0	0.000
1.2 E-08	0.09978
2.4 E-08	0.26091
4.8 E-08	0.59854
8.03E-08	1.0535

